INVESTIGATION OF THE ROLE OF NEUTROPHILS IN THE PRODUCTION OF AUTOANTIGENS IN PATIENTS WITH RHEUMATOID ARTHRITIS

by

JULIA SPENGLER

A thesis submitted to
The University of Birmingham
For the degree of
DOCTOR OF PHILOSOPHY

School of Immunity and Infection
College of Medical and Dental Sciences
The University of Birmingham

October 2015

Abstract

In most patients with rheumatoid arthritis (RA), citrullinated autoantigens are targeted by autoantibodies (ACPA). However, the process leading to protein citrullination by peptidylarginine deiminases (PADs) in the joint remains unclear. In this thesis, I tested the hypothesis that generation of neutrophil extracellular traps (NETosis), can contribute to release of enzymatically active PADs and citrullinated autoantigens in inflamed joints.

I have shown that *in vitro* induced NETosis leads to release of citrullinated proteins and enzymatically active PADs both attached to NETs and free in the supernatant. In the SF from RA patients DNA levels correlated with neutrophil concentrations, and DNA levels and PAD activity were found to be increased compared with OA patients. Finally, I demonstrated the antigenicity of *in vitro* generated NETs and identified citrullinated histone H3 as a NET-component recognised by ACPA and RA sera.

Based on the findings in this thesis release of active PADs into SF by neutrophil cell death is a plausible explanation for the generation of citrullinated extracellular autoantigens. In ACPA positive RA patients the continuous production of these autoantigens combined with pre-existing ACPA may result in the formation of immune complexes and perpetuation of the inflammatory response.

“The point is that, whenever we propose a solution to a problem, we ought to try as hard as we can to overthrow our solution, rather than defend it. Few of us, unfortunately, practice this precept; but other people, fortunately, will supply the criticism for us if we fail to supply it ourselves.” – Karl Raimund Popper

To my family

Acknowledgements

I want to thank my supervisor Dr Dagmar Scheel-Toellner for all her support throughout my PhD, for the many opportunities to present and discuss my research in front of an international audience, for all the inspiring discussions about the exciting world of immunology, for giving me independence and teaching me a scientific approach to my reasoning, for her patience with me, for believing in me and encouraging me to believe in myself.

I owe many thanks to my co-supervisors Prof Paul Cooper and Dr Mike Milward for all the discussions and advice, and for pain-stakingly proof-reading my thesis. I am also very grateful to Prof Karim Raza for his invaluable support and advice and, of course, for providing countless clinical samples. I would also like to thank Dr Andrew Filer for supplying clinical samples and sharing his medical and statistical knowledge, and whose involvement has been much appreciated. This work would not have been possible without the generosity of the patients and all the staff involved in collecting clinical samples, especially Jacqueline Cobb. I will also be eternally grateful to my faithful blood donors.

Many thanks to Prof Chris Buckley, Dr Stephen Young and Dr Graham Wallace for their advice, support and encouraging words.

I would also like to gratefully acknowledge the European Community's Collaborative project FP7-HEALTH-2010-261460 "Gums&Jonts" for funding this research project and for the collaboration with Prof Iain Chapple at the Dental School, University of Birmingham, UK.

Many thanks also to my collaborators Prof Karin Lundberg and Dr Jimmy Ytterberg at the Karolinska Institutet in Stockholm for providing purified ACPA, for the mass spectrometry analyses and for their help with the peptide ELISA.

I owe many thanks to members of the Scheel-Toellner Group, both past and present, whose help has been invaluable, especially Bozo Lugonja for introducing me into the work with the delicate neutrophils and for his sense of

humour, and to Dr Farrah Ali, Nichola Adlard, Dr Lorraine Yeo and Dr Elizabeth Clay for their technical support.

A owe huge thanks to the entire RRG for all the support and advice over the years and for making the lab a fun and very pleasant place to work. Especially, I would like to thank the world's best technician Holly Adams for feeding me with chocolate for my "late nights" and "bad days", for the forest trip and the roast dinner. Thank you also to Dr Guillaume Desanti for sharing his expertise, for his sense of humour and for all his advice (I will do my best to become a multi-resistant bacterium!!) and thank you very much to Saba, Joana and Dominika for all their encouraging words, for their support, their friendship, for the dinners and all the fun that we have had.

Thank you very much to all my friends and colleagues in Germany and to Prof Heiko Mühl for his time, support, advice and belief in me throughout my career.

Finally, I would like to thank my family and my dear best friend Thomas for all your endless patience, love and support, and to my grandfather who taught me diligence and perseverance. I am very lucky to have learned from you and cannot thank you enough.

Table of contents

List of figures

List of tables

Abbreviations

ACR	American College of Rheumatology
ACPA	Anti-citrullinated protein antibodies
AFU	Arbitrary fluorescence units
AMC	Anti-modified citrulline
ANCA	Anti-neutrophil cytoplasmic antibodies
APCs	Antigen presenting cells
BCR	B cell receptor
BM	Bone marrow
CAIA	Collagen antibody-induced arthritis
CCP	Cyclic citrullinated peptide
CDRs	Complementarity determining regions
CIA	Collagen-induced arthritis
CGD	Chronic Granulomatous Disease
CRP	C-reactive protein
DMARDs	Disease modifying anti-rheumatic drugs
ESR	Erythrocyte sedimentation rate
EULAR	ACR//European League Against Rheumatism
FDCs	Follicular dendritic cells
FcγR	Fc-gamma receptor
FLS	Fibroblast-like synoviocytes
f-MLP	N-formyl-methionine-leucine-phenylalanine
FS	Felty's syndrome
G-CSF	Granulocyte colony-stimulating factor
GM-CSF	Granulocyte-macrophage colony-stimulating factor
GWAS	Genome- wide association studies
H_2O_2	Hydrogen peroxide
HLA	Human leucocyte antigen
HMGB1	High-Mobility-Group-Protein B1
HRP	Horseradish peroxidase
ICs	Immune complexes
ICAM	Intercellular adhesion molecule
Ig	Immunoglobulin
IFN	Interferon
IL	Interleukin
IQR	Inter-quartile range
LFA-1	Lymphocyte function-associated antigen 1
LPS	Lipopolysaccharide
Mac-1	Macrophage-1 antigen
MCP	Metacarpophalangeal joints
MHC	Major histocompatibility complex
MMPs	Matrix metalloproteinases
MPO	Myeloperoxidase

MRI	Magnetic resolution imaging
MS	Mass spectrometry
NADPH	Nicotinamide adenine dinucleotide phosphate
NE	Neutrophil elastase
NETs	Neutrophil extracellular traps
NSAIDs	Non-steroidal anti-inflammatory drugs
OA	Osteoarthritis
PADs	Peptidylarginine deiminases
PAD1,2,3,4	Peptidylarginine deiminase 1,2,3,4
PB	Peripheral blood
PD	Periodontitis
pDCs	Plasmacytoid dendritic cells
PEG	Polyethylene glycol
PKC	Protein kinase C
PMA	Phorbol-12-myristat-13-acetate
PMN	Polymorphonuclear leukocytes
PR3	Proteinase 3
PRRs	Pattern recognition receptors
PSGL-1	P-selectin glycoprotein ligand-1
PsA	Psoriatic arthritis
PTM	Post-translational modification
PVDF	Polyvinylidene difluoride
RA	Rheumatoid arthritis
Rac2	Ras-related C3 botulinum toxin substrate 2
ReA	Reactive arthritis
RF	Rheumatoid factor
ROS	Reactive oxygen species
RT	Room temperature
SCID	Severe combined immunodeficiency
SF	Synovial fluid
s.d.	Standard deviation
SLE	Systemic lupus erythematosus
SN	Supernatant
ST	Synovial tissue
SVV	Small-vessel vasculitis
TCA	Trichloroacetic acid
TCR	T cell receptor
TNF	Tumor necrosis factor
UK	United Kingdom
VAS	Visual analogue score
VEGF	Vascular endothelial growth factor

1 Introduction

1.1 Neutrophils

Neutrophils are the most abundant leukocyte population in human blood and are the first cells which arrive at a site of inflammation. Historically they have been seen as simple phagocytes of the innate immune system playing only a limited role in the immune response. However over the past 10-20 years, research has revealed that neutrophils have complex and sophisticated mechanisms by which they locate and eliminate pathogens, and subsequently orchestrate the inflammatory responses. Importantly, many of these studies and concepts are still novel and need further scrutinisation before they are finally accepted by the scientific community. Nevertheless, the literature has highlighted a much more diverse role of these cells than previously appreciated which provides an important basis for further research.

1.1.1 Neutrophil maturation

Neutrophils are derived from hematopoietic stem cells within the bone marrow (BM) and develop in a process termed "granulopoiesis". On a daily basis, around 10^{11} neutrophils are generated in a normal adult human (1). Granulocyte-colony-stimulating factor (G-CSF) levels control the production of neutrophils in the BM and maintain neutrophil counts under homeostatic conditions or increase neutrophil numbers during infection (2). Aged neutrophils die by constitutive apoptosis in circulation and in the absence of activating stimuli (3). They can finally be ingested by macrophages to prevent the release of their cytotoxic components into the local tissue environment (4).

The release and retention of neutrophils from the BM is tightly regulated by the expression of two chemokine receptors on neutrophils and their respective ligands on stromal cells of the BM. During neutrophil maturation the chemokine receptor CXCR4 is gradually down-regulated while CXCR2 increases in abundance leading to the egress of neutrophils from the BM (5). Depletion of both receptors subsequently results in constitutive release of neutrophils into the blood circulation, suggesting a dominant role for CXCR4 (6). Interestingly, G-CSF has been demonstrated to stimulate neutrophil release both directly and by down-regulating expression of CXCL12, the ligand of CXCR4, in BM stromal cells (7,8).

The BM is also the site where neutrophil granules, the hallmark of granulocytes, are formed sequentially during granulopoiesis (8). Primary (or azurophilic) granules are the earliest-formed granules. Their main components include myeloperoxidase (MPO), antimicrobial peptides, such as defensins, and three predominant serine proteinases: cathepsin G, elastase, and proteinase 3, which enable their main functional role of killing and digestion of microbes (9). The secondary (or specific) granules, which are formed after the primary granules, help limit free radical reactions. Their characteristic constituent is the glycoprotein lactoferrin, which binds and sequesters iron and copper, lysozyme and lipocalin. The smallest tertiary (or gelatinase) granules are formed at a late stage of neutrophil maturation and contain only few antimicrobials. Instead, they hold a number of metalloproteases such as gelatinase, which are able to degrade many extracellular matrix proteins (10). In addition, neutrophils also have a fourth set of storage organelles, the so-called secretory vesicles. They are formed through endocytosis and their membrane serves as a reservoir for

membrane-bound molecules employed during neutrophil migration (8,11). Importantly, the distinction between these types of granules reflects differences in granule contents and their mobilisation. Nevertheless, this nomenclature is too rigid, since considerable overlap exists in the cargo of these granules, depending on the time-point at which they are produced (11–13).

1.1.2 Neutrophil recruitment

After being released from the BM neutrophils continuously and randomly survey blood vessel walls on their way through the circulation in search of endothelial inflammatory signals. In order to arrive at the site of the inflamed tissue they first need to traverse the blood vessel walls. This process largely takes place in post-capillary venules and typically involves the following steps of: tethering, rolling, adhesion, crawling and transmigration (8,14). Initial attachment of neutrophils is enabled by their constitutive expression of the glycoprotein PSGL-1 and L-selectin. These molecules interact with their ligands on activated endothelial cells, P- and E-selectins, resulting in the tethering of neutrophils to the surface of the endothelium as they roll along it. During the process of “rolling”, interaction with selectins, chemoattractants and cytokines leads to activation and clustering of the β2 integrins LFA-1 and Mac-1 on the surface of neutrophils resulting in rolling arrest and firm adhesion (11,15). Neutrophils subsequently begin to crawl in a process dependent on integrins and ICAMs along the vessel wall until they find a site for transmigration. Once they have passed the endothelium, neutrophils follow chemotactic gradients, such as host-produced cytokines or pathogen-derived chemoattractants, to the site of

inflammation and/or infection (11). Interestingly, neutrophil recruitment does not always involve the steps described above and varies substantially in different organs, such as in the lung and the liver (16).

Importantly, whereas migration of neutrophils through activated endothelium is dependent on β2 integrins, long-distance migration of neutrophils in tissue distant from the site of injury was recently revealed not to be (5). Using two-photon intravital microscopy Lämmermann and colleagues demonstrated that neutrophils recruited to a focus of inflammation drive a second wave of neutrophil recruitment and clustering in the form of "swarms" (17). "Neutrophil swarming" was found to be initiated through release of chemoattractants from dead cells in developing neutrophil clusters, with a key role of leukotriene B4 as communication signal between neutrophils identified (17).

1.1.3 Neutrophil activation and antimicrobial strategies

Neutrophil activation has been shown to be a multi-step process. Initially, they can be primed by cytokines, such as TNF-α, GM-CSF, IL-8 and IFN-γ or bacterial products (18). This can result in the rapid transport of pre-formed receptors to the cell surface via mobilisation of intracellular granules and the partial assembly of the NADPH oxidase. Additionally, activation of transcription factors can trigger *de novo* expression of molecules such as cytokines or receptors enhancing neutrophil function or prolonging their lifespan (18). The second stage of activation occurs after their recruitment to the site of inflammation. Here, neutrophils apply several different mechanisms to kill pathogens including phagocytosis, degranulation and the generation of

neutrophil extracellular traps (NETs). Phagocytosis is an active, receptor-mediated process by which particles are taken up by the neutrophil and are internalised into a vacuole known as a phagosome (2). The interaction between neutrophils and microorganisms can either be direct (through pattern-recognition receptors (PRRs)), or opsonin-mediated (through FcγR-mediated phagocytosis of IgG-opsonised particles or through complement receptor-mediated phagocytosis) (11,19). Following engulfment, phagosome maturation initiates fusion of granules to the phagosome so that antimicrobial molecules can enter the phagosomal lumen. After fusion, the NADPH oxidase complex assembles on the phagosomal membrane and begins ROS production by reducing molecular oxygen to superoxide (11). Spontaneous dismutation of superoxide or dismutation catalysed by the enzyme superoxide dismutase (SOD) yields hydrogen peroxide (H_2O_2) (20). In addition, myeloperoxidase (MPO) can react with H_2O_2 and lead to the generation of highly reactive products including hypohalous acids, the major molecule of which is hypochlorous acid (HOCl). These mechanisms create an environment which is highly toxic to most pathogens (11,19).

The process of degranulation involves mobilisation of the previously described neutrophil granules, with those granules formed last during neutrophil maturation, released first. Granules can fuse either with the plasma membrane to release their contents into the extracellular space, or with the phagosome. Although many studies have shown that degranulation into tissue could contribute to the antimicrobial milieu during an immune response against microorganisms, most data were generated *in vitro* and have therefore to be interpreted with caution (9,11).

Finally, a further antimicrobial strategy and, simultaneously, a novel form of cell death of neutrophils was reported by Brinkmann and his team in 2004 (21). The formation of NETs was revealed to be part of an active form of cell death that leads to the release of highly decondensed chromatin structures into the extracellular space. Although NETs were primarily described not only to entrap and immobilise microorganisms but also to kill them, the killing capacity was recently been questioned (22) and requires further examination. Due to the significance of NET formation for this thesis, this antimicrobial mechanism will be discussed in more detail in the following section.

1.1.4 NETosis

Initially, the formation of NETs was described as a distinct form of active cell death and was therefore termed “NETosis” to distinguish it from apoptosis and necrosis (23). In contrast to apoptotic cells, no internucleosomal DNA fragmentation and exposure of phosphatidylserine or activation of caspases have been observed. Also, neutrophils undergoing NETosis do not appear to show morphological characteristics typical of necrotic cells (24). *In vitro,* activated neutrophils flatten, lose their characteristic lobular nuclear form and decondense their chromatin (23,25). Subsequently, the nuclei and granules begin to lose their integrity during the first hour of activation and the nuclear membrane fragments into vesicles. This process results in mixing of decondensed chromatin with the granule contents which is followed by cell membrane rupture and release of NETs into the extracellular compartment.

Although alternative models of NET formation (such as the release of mitochondrial DNA from intact neutrophils (26) or the presence of anuclear viable neutrophils after NET formation (27)) have recently been described, these mechanisms are not discussed in more detail in this thesis. In the following, the term "NET formation" will therefore only be used to describe the lytic cell death process of "NETosis" which has been characterised in the original publication by Brinkmann et al. (21) and also underpins the majority of publications in this area.

1.1.4.1 Signalling mechanisms leading to NETosis

To date, very little is known about the cellular processes leading to NET formation (23). Since the discovery of NETs, there have been a number of studies published which found that the formation of extracellular traps does not appear to be restricted to neutrophils. Indeed other cell types, such as eosinophils and mast cells, have been shown to release extracellular DNA complexed with antimicrobial proteins (26,28). In addition, the list of synthetic and physiological molecules, as well as microorganisms able to induce NETs is growing. Indeed NETs have been found to be induced by Gram-positive and Gram-negative bacteria, by fungi, viruses, parasites, LPS, IL-8 and antibodies (21,24,29–33) (Table 1-1).

Additionally, NETs can also be induced by artificial chemical stimuli such as Phorbol-12-myristat-13-acetate (PMA), which actives protein kinase C (PKC), or the ionophore A23187 (34). The high diversity of stimuli found to induce NET formation so far, complicates investigation of shared signalling pathways.

Additionally, signalling molecules such as ROS are known to participate in several cell death programmes in the same cell (35) further adding to the complexity of the process. Currently, the vast majority of stimuli described to induce NETosis are dependent on ROS generation by NADPH oxidase. Thus, neutrophils from patients with Chronic Granulomatous Disease (CGD), who lack this enzyme are not able to form NETs (36). When neutrophils of CGD patients are treated with H_2O_2, however, the pathway downstream of the NADPH oxidase is rescued enabling NET formation (24). In addition, MPO which converts H_2O_2 and generates hypohalous acids, was also shown to be essential for NET formation (37). Accordingly, hypochlorous acid, one of the products generated by MPO, is also able to induce NET release (38).

Moreover, MPO together with neutrophil elastase (NE), was recently shown to be involved in the chromatin decondensation observed during NETosis. Both proteins have been shown to enter the nucleus, via as yet an undescribed mechanism, whereby NE degrades histones and synergises with MPO driving chromatin decondensation independent of its known enzymatic activity (39). Furthermore, the autophagy pathway has been proposed to be required for NETosis since neutrophils upon stimulation with PMA, develop large vacuoles that are reminiscent of autophagosomes (40). This, however, has only been shown using a broad range inhibitor of autophagy and has yet to be confirmed in further studies (23).

With regard to signalling pathways upstream of the NADPH oxidase, it has been proposed that the Raf-MEK-ERK pathway is implicated in NET formation (41) as is Rac2 (42). These observations may be explained by the finding that Rac2-

deficient cells cannot form a functional NADPH oxidase complex to generate ROS.

BACTERIA	*Echerichia coli*	Grinberg et al. 2008
	Shigella flexneri	Brinkmann et al. 2004
	Staphylococcus aureus	Fuchs et al. 2007
		Plisczek et al. 2010
		Berends et al. 2010
	Streptococcus pyogenes	Mori et al. 2012
		Buchanan et al. 2006
VIRUSES	HIV-1	Saitoh et al 2012
	Influenza viruses	Narasaraju et al. 2011
		Hemmers et al. 2011
FUNGI	*Candida albicans*	Urban et al. 2009
		Papayannopoulos et al. 2010
	Aspergillus fumigatus	Bruns et al. 2010
PARASITES	*Leishmania spp*.	Guimaraes-Costa et al. 2009
		Gabriel et al. 2010
	Plasmodium falciparum	Baker et al. 2010
OTHERS	PMA	Brinkmann et al. 2004
	H_2O_2, IL-8, LPS	Fuchs et al. 2007
	MSU christals	Mitroulis et al. 2011
	ANCA antibodies	Kessenbrock et al. 2009

Table 1-1 Examples showing the range of stimuli known to induce NETosis

1.1.4.2 The role of PAD4 in NET formation

Several studies have demonstrated that NETosis also involves activation of the enzyme peptidylarginine deiminase 4 (PAD4) (34,43,44). PAD4 belongs to a family of five PAD isoforms, whose enzymatic activity leads to citrullination of the arginine side chains of proteins. This enzymatic reaction is discussed in more detail in chapter 1.3.2.

PAD4 is the only PAD enzyme with a nuclear localisation signal sequence (45) and the importance of this enzyme in NETosis is underlined by the observation that neutrophils in PAD4-deficient mice cannot generate NETs (46). Initially it was assumed that citrullination was induced by elevated calcium concentrations during apoptosis, however this view has now been revised (34). Instead, PAD4 is known to catalyse the citrullination of histones during NETosis and this mechanism is now proposed as an important step in the decondensation of the nuclear DNA. Whereas increased supraphysiological calcium concentrations are known to be required for full PAD4 activity (47–49), the exact mechanism inducing intracellular PAD4 activity still remains to be elucidated.

Citrullination was initially implicated in an epigenetic form of gene regulation in the human HL-60 granulocyte cell line (23,50). Latterly, Neeli et al. were able to show citrullinated histone H3 within NET structures in LPS-stimulated neutrophils using confocal microscopy (34). In this report, it was demonstrated that citrullination of histones H2A, H3 and H4 in neutrophils forming NETs, but not during apoptosis, represents a response to inflammatory stimuli. This was also confirmed by Wang and coworkers who demonstrated that histone hypercitrullination mediates chromatin decondensation and NET formation (44). In this study it was proposed that the conversion of certain arginine residues to

citrullines by PAD4 leads to a loss of their positive charge and thereby weakens the interaction between histones and DNA (23). The elimination of these positive charges may enable the unwinding of chromatin and thus, the formation of NETs. PAD4 inhibitors, such as Cl-amidine, in contrast, significantly reduced histone decondensation and NET formation in response to either Ionomycin or *Shigella flexneri* (44). Moreover, neutrophils from PAD4$^{-/-}$ mice were shown to be incapable of forming NETs upon activation by different stimuli, and furthermore no hypercitrullination of histone H3 was detectable (46). *In vivo*, these mice exhibited more severe bacterial infections than wildtype mice and developed larger lesions when challenged with a *S. pyogenes* infection (23).

Citrullination of histone H3 can be induced by a number of bacterial and pro-inflammatory signalling molecules, including LPS, TNF, f-MLP, lipoteichoic acid (LTA), and H_2O_2 (34,46,51). Importantly, however, not all stimuli discovered to induce NETs so far have been clearly demonstrated to also induce histone citrullination. The significance of the stimulus PMA for histone citrullination, which is also utilised in this thesis, for example, is currently under debate. While a very recent publication by Neeli and colleagues has questioned as to whether PMA induces histone citrullination (52), several other studies (including those presented in this thesis) have observed the opposite (46,53) suggesting that factors such as the stimulation time or concentration of PMA, which differed between studies, may be important factors. Since the generation of ROS is also required for NETosis, it is likely that ROS may also be involved in the initiation of PAD4 activation. Indeed, H_2O_2, for example, is reportedly able to induce PAD4-dependent histone citrullination in neutrophils (34). Also, when neutrophils are pre-incubated with the NADPH oxidase inhibitor apocynin, LPS-

induced citrullination of histone H4 is decreased (51). Furthermore, since NE was recently found to cleave histones to drive chromatin decondensation during NET formation, as described previously (see 1.1.4.1), and PAD4 is known to promote relaxation of the chromatin structure, the interaction of both these enzymes and their exact role in the chromatin decondensation during NETosis remains to be clarified. All proposed mechanisms upstream of PAD4 activation are summarised in Figure 1-1.

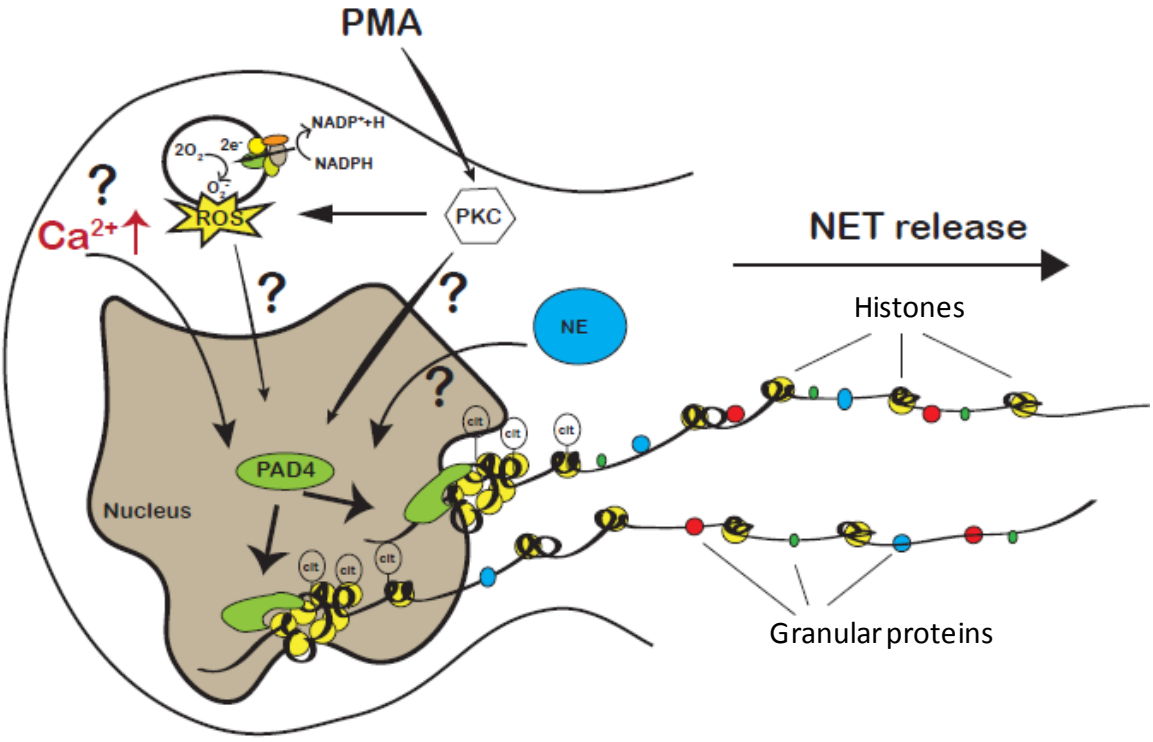

Figure 1-1 Role of PAD4 signalling in NETosis

Decondensation of chromatin during NETosis has been shown to require PAD4 activity (44). However, the cellular pathways involved in PAD4 activation and whether they converge upon the chromatin decondensation process is currently unknown. Thus far, there are several lines of evidence implicating signalling involvement of elevated calcium levels (Ca^{2+}), activation of PKC, ROS generation and cleavage of histones by neutrophil elastase (NE).

1.1.4.3 NETs and autoimmunity

Whereas initially NET formation was regarded mainly as an additional defence mechanism against extracellular microorganisms, recent work suggests that these structures could also serve as putative sources of immuno-stimulatory proteins with the potential of inducing autoimmunity and tissue damage (23). Indeed neutrophil components are well established as a source of autoantigens in a number of autoimmune conditions, primarily in small-vessel vasculitides (SVV) and SLE (Figure 1-2). For example, MPO and PR3 were discovered as the predominant autoantigens recognised by anti-neutrophil cytoplasmic antibodies (ANCA) in SVV (54). Interestingly, ANCA were also shown to activate neutrophils *in vitro* (55), and are able to induce vasculitis in animal models (56,57).

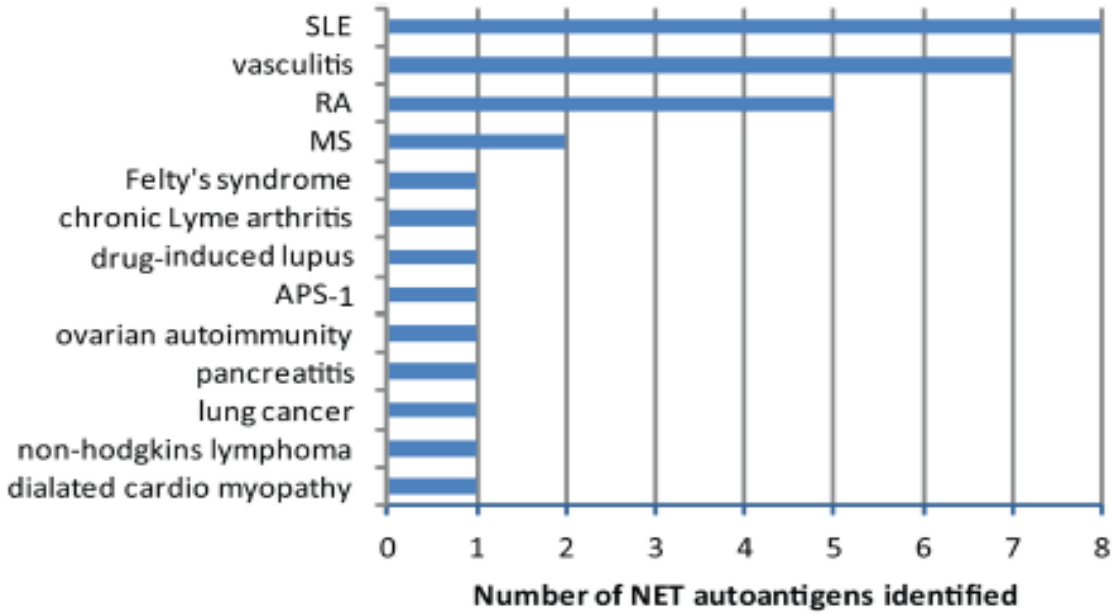

Figure 1-2 Autoantigens present in NETs

The number of NET proteins reported to be autoantigens in various diseases is quantified and reveals that NET autoimmunity is most common in patients with vasculitis, SLE, and RA (Darrah et al., 2013).

In SLE, an autoimmune syndrome that is characterised by immune complex deposition, inflammation and organ damage (58), autoantibodies are primarily directed against nucleosomes, but also against neutrophil components such as NE, MPO and LL-37 (23,59). In addition, elevated plasma levels of defensins (60) and HMGB1 (61) can be detected in SLE patients.

Thus, neutrophil-associated proteins appear to be targets for autoantibodies in patients with systemic autoimmunity, however, the reason why these cells are targeted still remains unclear. One possible explanation could be related to neutrophil death at sites of inflammation. However, neutrophil death by apoptosis generally does not lead to release of intracellular constituents unless the mechanisms involved in uptake and removal of these cells are compromised (23).

In this context, the discovery of NETs has provided a new perspective for neutrophil research in the above-described autoimmune diseases. Not only, because a large proportion of NET components have been found to serve as autoantigens in systemic autoimmune diseases, but also because of their potential to induce tissue damage. For example, low density granulocytes (LDGs), have been isolated from SLE patients and characterised for their pathogenic role in endothelial damage and abnormal endothelial differentiation leading to accelerated atherosclerosis in SLE (59,62). Furthermore, impaired serological DNase-I activity has been reported in 36.1% of patients with SLE, leading to impaired degradation of NETs and more active disease (63,64) .

In vivo, neutrophils releasing NETs have also been identified in kidney biopsies from patients with ANCA-positive vasculitis (33). Increased NET formation has also been reported in SLE (65). Lande et al. recently described a mechanism by

which antimicrobial peptides, such as LL-37, were able to protect self-DNA in SLE patients from degradation by nucleases, and, as such, stimulated self-DNA-induced triggering of TLR9 signalling in plasmacytoid dendritic cells (pDCs) (66). In this study, these DNA-protein-complexes induced enhanced IFN-alpha synthesis by pDCs, which is in agreement with current models of lupus pathogenesis, in which an activation of the type I IFN pathway lowers the threshold for autoreactivity of both antigen-presenting and antibody-producing cells (23,67,68).

1.2 Rheumatoid Arthritis

Rheumatoid Arthritis (RA) is an inflammatory disease of unknown aetiology with a prevalence of 0.5-1.0 % within the adult population worldwide (69,70). Median age at disease onset is around 50 years and approximately 2.5 times more women are affected than men (71). Although the joints are the main affected location in the body, many organs can be involved so RA is generally considered a systemic disease. The aetiology and pathogenesis is complex and a combination of different genetic, environmental or other factors are known to play a role. Monozygotic twins exhibit a concordance rate of 12-30% (72,73) and while this provides evidence of the genetic component it also indicates that other environmental factors are involved in disease pathogenesis. In recent years several studies have shown that early and aggressive treatment with disease-modifying anti-rheumatic drugs (DMARDs) and biologic therapies can be effective in controlling inflammation and joint destruction (69). Nevertheless,

disease control is still insufficient in many RA patients and drug-free remission still remains a key future goal (74).

1.2.1 Clinical features and classification

The classic predominant clinical features of RA include bilaterally symmetric painful swelling of the metacarpophalangeal or proximal interphalangeal joints of the hands and the wrists (72,75). Many patients develop chronic inflammation eventually involving several joints which leads to cartilage damage and bone erosion, if not treated aggressively. Several classification criteria for RA were described by the American College of Rheumatology (ACR) in 1956 and were later revised in 1987 (76). Although these criteria are not used for the diagnosis of individual cases in clinical practice, they were developed to select patients for clinical trials and also serve as guidance for physicians. Since the criteria from 1987 were developed based on data from patients with established RA, they were not suitable to diagnose patients with early disease who can present with very few or even no swollen or tender joints (69). New criteria were therefore published in 2010 by the ACR//European League Against Rheumatism (EULAR) (77), which were more adapted for early diagnosis and placed greater emphasis on serological markers such as the so-called anti-cyclic citrullinated peptide (anti-CCP) antibodies (also referred to as anti-citrullinated peptide/protein antibodies (ACPA) and are further described in Chapter 1.3.1).

1.2.2 Phases of RA

Rheumatoid Arthritis appears to develop in several phases (78–80) (Figure 1-3), beginning with a pre-clinical phase during which genetic susceptibility and environmental factors can lead to the breakdown of tolerance and appearance of autoantibodies such as ACPA (see section 1.3.1). These antibodies can be detected up to 14 years prior to the onset of disease symptoms (81). Additionally, other biomarkers, such as CRP or cytokines (82,83) associated with systemic inflammation, have been reported to be abnormal prior to disease onset. With regard to the local inflammation in joints during this pre-clinical phase, some studies, using a range of imaging techniques, have reported subclinical inflammation in a small number of patients with serum ACPA and 'arthralgia' but no clinically-evident synovitis (84–86). However the specificity of these techniques is not clear, but most current studies agree on the fact that individuals who have RA-specific autoantibodies and joint pain but no clinically apparent joint swelling show no signs of synovial inflammation (histologically and by imaging) (87,88). Subsequently it has been proposed that autoimmunity is more likely to be initiated outside the joint.

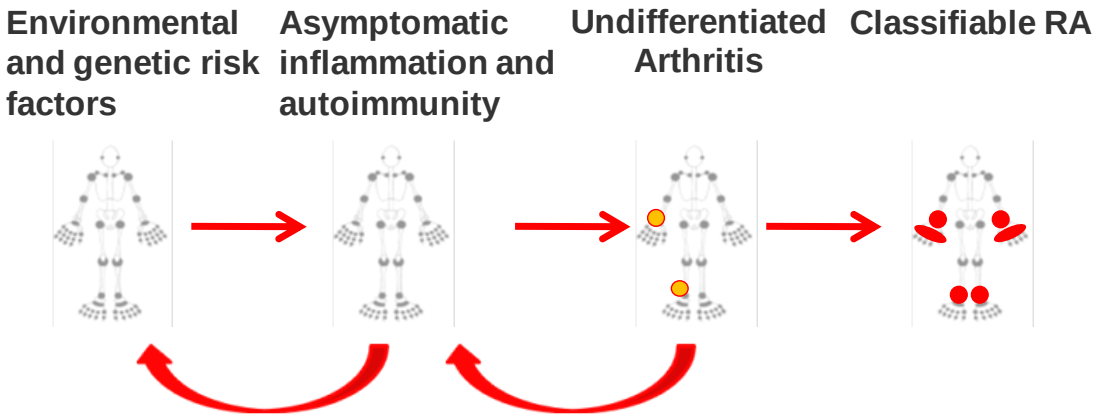

Figure 1-3 Rheumatoid Arthritis develops in several phases

The first phase of RA development is characterised by the influence of environmental and genetic risk factors and is followed by non-clinically apparent inflammation and appearance of autoantibodies. Following these two pre-clinical phases initial symptoms of inflammatory arthritis develop (undifferentiated arthritis) and may further progress to the phase of classifiable RA. Importantly, not all individuals at risk progress through all of these phases and there are also subjects who show resolution of inflammatory arthritis, autoimmunity or inflammation (indicated by the return arrows).

Disease progression from the preclinical phase to RA often involves a phase of undifferentiated arthritis. During this phase synovitis either resolves or becomes persistent. If joint inflammation becomes chronic the disease often fulfils the classification criteria for RA as is described in chapter 1.2.1. Importantly, while each of the above described phases are well recognised, the mechanisms of transition between these phases are far less well understood. Moreover, not all individuals who are at risk of developing RA will progress through all of these phases and ultimately develop RA so that the term 'preclinical RA', needs to be used with caution (79,89).

1.2.3 Synovial biology and pathology

The primary site of inflammation in RA patients is the synovial membrane, which lines the cavity of synovial joints. It consists of an inner intimal lining layer and an outer synovial sublining layer, which mostly consists of connective tissue and merges with the joint capsule. The intimal lining layer in healthy individuals is composed of one or two cell layers of synoviocytes. This layer consists of macrophage-like (type A) and fibroblast-like synoviocytes (FLS) (type B) and lacks a definite basement membrane and tight junctions (72). Additionally, fenestrated capillaries are present through which blood plasma is ultra-filtrated to form an interstitial fluid. This fluid, together with additional constituents secreted by synoviocytes, forms the synovial fluid (SF). Nutrients and oxygen can diffuse through the SF and nourish the avascular cartilage.

In patients with RA, an increase in synoviocyte numbers and SF volume can be observed, and the sublining layer is infiltrated by mononuclear cells including macrophages and lymphocytes (predominantly T cells) (4). Type A synoviocytes in RA secrete pro-inflammatory cytokines and growth factors, which can induce FLS to produce cytokines such as IL-6 and matrix metalloproteinases (MMPs) (90). RA FLS show aggressive tumour-like features such as loss of contact inhibition and anchorage independence, and can play a role in cartilage destruction (91). The lymphocyte infiltration shows different patterns of distribution, which varies from a diffuse infiltrate to discrete focal aggregates, particularly around blood vessels (Figure 1-4). Sometimes these focal aggregates contain clusters of follicular dendritic cells (FDCs) within structures resembling germinal centres (92), and synovial-vessel endothelial cells, which are transformed into high endothelial venules. Although focal

lymphoid aggregates seem to be associated with a more severe synovial and systemic inflammation in some studies, the function of these structures and the relation to a specific clinical phenotype is currently the subject of debate (93–96).

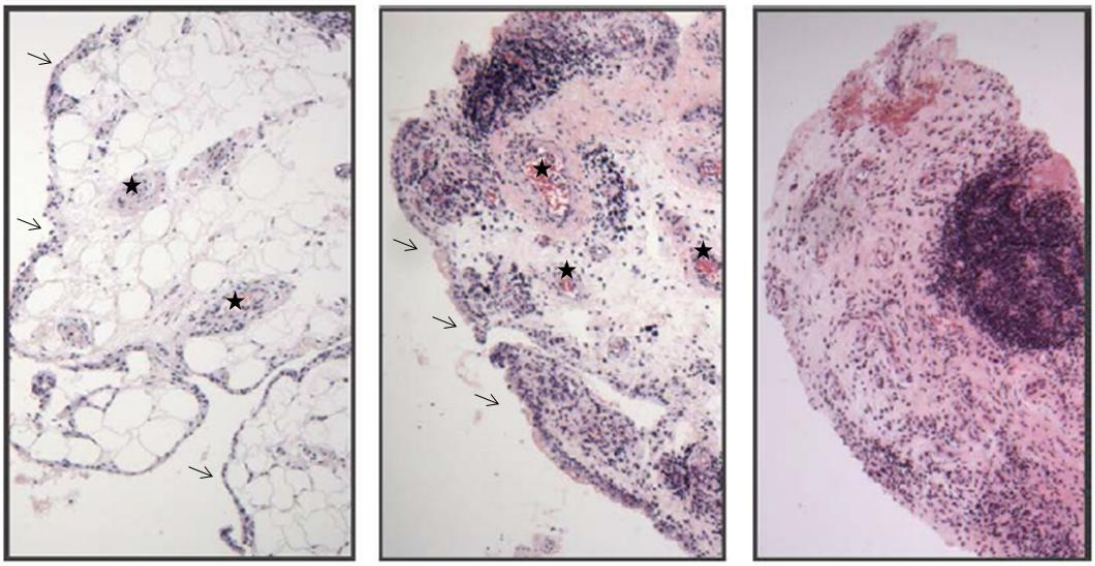

Figure 1-4 Histopathologic appearance of the RA synovium

Different patterns of leukocyte infiltration in the RA synovium can be observed, ranging from scarce infiltration (left), diffuse infiltration (centre) to the formation of focal lymphocytic aggregates (right). Arrows indicate thickened synovial lining layer and stars indicate blood vessels in the sublining layer. Images courtesy of Dr. Dagmar Scheel-Toellner (University of Birmingham).

Importantly, the histological changes of the synovium described above are not specific for RA but can also be observed in other forms of persistent inflammatory arthritides irrespective of the diagnosis (97). In early RA, however, it has been proposed that the degree and pattern of vascularity may be used to distinguish RA from other inflammatory arthritides (97,98). Additionally, the formation of a destructive synovial tissue at the cartilage-bone interface, the so-called pannus, is regarded as a characteristic feature of erosive RA (71,97).

The pannus consists of mostly fibroblasts, macrophages and osteoclasts, which express high levels of proteases and invade cartilage and bone (99). At the pannus-cartilage junction, the site of active tissue damage, an accumulation of polymorphonuclear granulocytes (PMNs) can be seen, suggesting a role in tissue destruction (see chapter 1.2.4).

1.2.4 Role of neutrophils in RA

The early stages of most inflammatory responses are characterised by the influx of neutrophils into the tissue in which the response is triggered (23). Although in a very small sample of RA patients has it been suggested, that in the earliest stages of synovial inflammation, neutrophils may predominate the infiltrate (100). Furthermore only relatively low numbers of these cells can be found in the chronically inflamed synovium of RA patients (23,101). Primarily, neutrophils are present in the SF but can also be observed at the pannus/cartilage interface (102,103). To understand the role of neutrophils in the complex microenvironment of the inflamed joint, it is important to consider the different dynamics which regulate the cell pool of neutrophils and allow the accumulation of these cells in the inflamed joints at different phases of inflammation. Mature neutrophils are considered to be terminally differentiated cells, hence they do not divide and show only a low level of *de novo* protein synthesis. After their recruitment into the joints of RA patients, neutrophils can be removed from the joints through different cell death mechanisms such as apoptosis (35). On the other hand, neutrophils can contribute to the enlargement of the cell pool in the joints by their prolonged survival (Figure

1-5A). In patients with early RA, synovial neutrophils show significantly lower levels of apoptosis compared with patients with other persistent forms of arthritis or a self-limited disease course (104). This may relate to high levels of anti-apoptotic cytokines such as GM-CSF and G-CSF (105). Additionally, neutrophils are also able to secrete IL-8, which creates a "feed-forward" response that drives further recruitment of neutrophils from the circulation. Interestingly, recent *in vitro* (106) and *in vivo* studies using mouse (107) and zebrafish models (108) have shown that neutrophils may be able to migrate from peripheral organs back into the bloodstream through "reverse migration". Although the relevance of this mechanism in humans, and particularly in inflamed joints, would need to be determined, it represents one possible mechanism for neutrophils to escape cell death within the joints and thus an additional factor how the neutrophil cell pool in the inflamed joint may be regulated and inflammation modulated (Figure 1-5A).

Once neutrophils have been recruited to the joints, they can interact with other immune cells and regulate inflammation in the joints in several ways (Figure 1-5B). Neutrophils from the peripheral blood of RA patients are primed for the generation of ROS (109) and neutrophils isolated from RA SF show evidence of enhanced intracellular ROS production *in vivo* (110). Due to the presence of aggregates of immunoglobulins such as RF in the SF or on the surface of the joint, neutrophils can be activated through the engagement of Fcγ receptors on the surface of the neutrophil (Figure 1-5B). Whereas soluble immune complexes from RA SF were shown to induce extracellular secretion of ROS and proteases through FcγRIIIb, generation of intracellular ROS is mediated

through FcγRIIa (111,112). In addition to ROS, neutrophils are able to release other substances with cytotoxic potential. Neutrophil granular enzymes such as gelatinase (113,114) and NE (115) are likely to promote cartilage damage, however, no *in situ* demonstration of direct neutrophil attack on cartilage has yet been demonstrated (72). Granule proteases cannot only activate or deactivate cytokines (116) but also cleave complement proteins and generate chemotactic activity (72). High levels of these neutrophil proteases could overwhelm the antiprotease protective mechanisms and also lead to tissue damage.

RA SF neutrophils have also been demonstrated to release a range of cytokines. Aside from IL-8, neutrophils can shed the B cell stimulating cytokine BLyS or BAFF from their surface following stimulation with TNF-α (117). Additionally, neutrophils express many of the cytokines produced by macrophages such as IFN-α and BAFF (118). Since neutrophils vastly outnumber macrophages in the RA synovial fluid, it is likely that they considerably contribute to the cytokines present in the SF. Interestingly, neutrophils isolated from RA SF have also been demonstrated to be able to transdifferentiate into MHC class II-expressing antigen presenting cells (APCs) (119). These cells can present antigens to T cells in an MHC class II restricted manner (18,119). Since neutrophils express different proteases compared with other APCs it is possible that MHC-II+ neutrophils could play a particular role in antigen presentation in the RA SF. Recently, it has also been demonstrated that neutrophils from the peripheral blood and SF of RA patients show enhanced rate of NETosis compared with neutrophils from healthy individuals and that NETs produced by activated neutrophils can augment inflammatory responses

in fibroblasts. These data suggest they may play an important role in the perpetuation of pathogenic mechanisms (120).

Although data from animal models of RA are difficult to extrapolate they may provide an important insight into the mechanisms of human disease pathogenesis. Both in the Collagen-induced arthritis (CIA) model and in the K/BxN murine autoantibody-mediated model of arthritis (described in more detail in Chapter 1.3.5.4) neutrophils are required for full expression of the disease (72). Depletion of neutrophils in these models results either in a significantly decreased severity or a complete abrogation of arthritis (121,122). Additionally, antibody blockade or knockout of key neutrophil signalling receptors such as the C5aR (123), FcγR (124) or leukotriene B_4 receptors (125) can prevent initiation and propagation of inflammation in K/BxN mice.

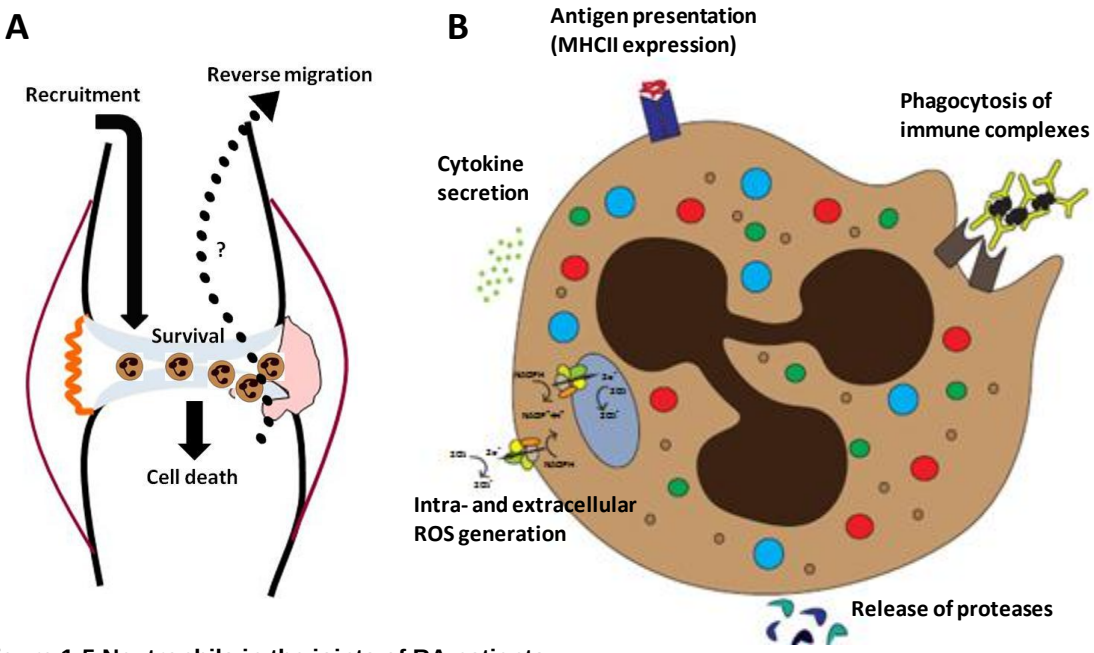

Figure 1-5 Neutrophils in the joints of RA patients

(A) Regulation of the neutrophil cell pool in RA joints by mechanisms including neutrophil recruitment, cell death, prolonged survival and possible exit through reverse migration. Cell numbers may alter over time depending on the phase of the inflammatory response. **(B)** Neutrophils can modulate inflammation in several ways. Secretion of cytokines is important for the recruitment of other inflammatory cells into the joints as well as activation of other immune cells. Release of granule enzymes can activate or deactivate cytokines but can also lead to tissue destruction. Generation of reactive oxygen species (ROS) can, for example, occur following stimulation by immune complexes, which are taken up through Fc receptors. Finally, increased expression of MHC class II molecules on SF neutrophils may enable presentation of antigens to T cells further propagating inflammation.

1.3 Autoimmunity in Rheumatoid Arthritis

At the turn of the 20th century Paul Ehrlich proposed the threat of an organism´s uncontrolled immune system, potentially causing a condition called “horror autotoxicus” in which an immune response is evoked against self (126). Approximately 50 years later, studies by Rose and Roitt for the first time demonstrated the presence of an autoimmune component in Hashimoto’s thyroiditis (127,128) and Frank McFarlane Burnet published his hypothesis regarding “the forbidden clone” in 1949 (129), in which he proposed that autoimmune diseases develop from the escape of self-reactive lymphocyte clones which should have been deleted through normal immune tolerance mechanisms. Further research followed and finally laid the foundation for the current, more complex, understanding that autoreactivity is indeed present even in a healthy organism and is essential for the establishment of normal immune system homeostasis during lymphocyte selection. According to this view autoreactive T and B cells are negatively selected and deleted in primary lymphoid organs during maturation while lymphocytes that are non-reactive to self survive (central tolerance) (130). Autoreactive lymphocytes, which escape deletion in primary lymphoid organs, can still be suppressed in the periphery by mechanisms of peripheral tolerance. Importantly, tolerance mechanisms are mediated through the engagement of antigenic receptors (BCR and TCR) and co-stimulatory signals (largely provided by cells of the innate immune system) and are controlled by the developmental stage of lymphocytes as well as additional modulating factors including cytokines (131). It is therefore rather the

transformation from subclinical self-reactivity to pathogenic autoimmunity that is believed to play an important role in clinical practice (132).

There are over 80 autoimmune diseases known to date which affect about 6% of the world population (133) and a wide range of these conditions are encompassed by the medical subspecialty of rheumatology. Although the prevalence of autoimmune diseases in general is low, their effects on mortality and morbidity are high and the incidence for some of these conditions is reported to be increasing (134–137). Altogether, autoimmune diseases are currently the third-largest clinical burden after cardiovascular diseases and cancer (138).

There are currently no universally accepted criteria for the classification of autoimmune diseases. One possibility is to categorise them based on the site-specificity of their clinicopathology (131). According to this categorisation diseases such as Hashimoto´s thyroiditis, idiopathic thrombocytopenic purpura or Multiple Sclerosis are termed organ-specific and are characterised by an immune response against specific cells or tissues. End-organ damage in organ-specific autoimmune diseases can be mediated by antibodies and/or T cells. In comparison, diseases such as RA, SLE or primary Sjögren´s syndrome belong to the systemic category where the immune system targets ubiquitously expressed autoantigens. This type of condition typically leads to tissue destruction mediated by autoantibodies and, less commonly, by T cells (132).

Additionally, autoimmune diseases can share symptoms with so-called auto-inflammatory syndromes. Although autoinflammatory syndromes are typically only mediated through the innate arm of the immune system and are in most

cases rare monogenic disorders, they could also be considered as one end of a broader definition of autoimmunity. In this context, McGonagle and McDermott proposed in 2006 that the disease categories “autoimmune” and “autoinflammatory” should not be seen as completely separate (139). Instead, they should be regarded as a part of a broad spectrum of diseases, ranging from autoimmune to autoinflammatory. Based on this idea the place on the spectrum of a particular disorder would therefore depend on the relative importance of the innate versus the adaptive immune system in disease pathogenesis (140).

In general, autoimmune diseases are defined by the presence of autoreactive B and T cells, which leads to tissue injury. However, not only has autoreactivity been found to play a role in autoimmune diseases but also target-organ vulnerability (141,142). It is thought that genetic factors governing specific organ vulnerability differ from those governing autoreactivity (141–143). This means that individuals may present with different autoimmune diseases despite sharing the same pathways promoting autoreactivity. For example, while nephritis in the two diseases SLE and Goodpasture syndrome differs in the nature of the inciting antibodies and the localisation of the immune deposits, animal models of the diseases have shown that a significant fraction of the differentially expressed genes that distinguish the nephritis-sensitive strains from the control strains belong to the kallikrein gene family (142). Kallikreins are involved in the regulation of inflammation, apoptosis, redox balance, fibrosis and local blood pressure within the kidneys and possibly impact both diseases concordantly in humans (144).

The clustering of autoimmune disorders in families suggests that the genetic background has an influence on the development of autoimmunity. Genome-wide association studies (GWAS) have recently identified a large number of genetic associations with human autoimmune diseases. In particular, variations in the MHC locus are linked to most autoimmune diseases studied so far (130). In addition, monogenic primary immunodeficiencies, some of which are associated with autoimmunity (145), and animal models, have been useful in exploring a wide range of defects in tolerance mechanisms (131). One example of a defect in central tolerance leading to autoimmunity, is the mutation of the transcription factor AIRE (autoimmune regulator), which causes a rare disease in humans, the autoimmune polyendocrinopathy-candidiasis-ectodermal dystrophy (APECED) and leads to the destruction of multiple endocrine organs (146). Another very common primary immunodeficiency is selective IgA deficiency, which not only results in an increased number of infections in affected individuals but is also associated with several autoimmune diseases (147). Nevertheless, the aetiology of most autoimmune diseases is believed to be more complex. Current evidence suggests that the breakdown of central and/or peripheral tolerance is influenced not only by genetic but also environmental and gender-specific factors.

In the following sections, the mechanisms of autoimmunity in RA patients will be described with a particular emphasis on autoimmunity against antigens which have been post-translationally modified by citrullination. Additionally, unresolved questions will be explored and discussed in the context of other autoimmune conditions.

1.3.1 Autoantibodies in RA

Throughout history, Rheumatoid Arthritis has been considered to be a chronic inflammatory disease. The discovery of autoantibodies in 1940 demonstrated an autoimmune component in RA pathogenesis. Eric Waaler initially observed that sera from patients with RA are able to agglutinate sheep red blood cells sensitised by subagglutinating doses of rabbit antibodies (148) and this phenomenon led to the discovery of autoantibodies now known as rheumatoid factor (RF), and their specificity for the Fc fragment of the IgG heavy chain.

Rheumatoid factor can be detected in up to 50% of patients with early RA, however, sensitivity increases with long-standing disease to between 60–80% (149). These antibodies can be of any isotype, but IgM-RF is not only the most frequently identified isotype but also the one exhibiting the highest sensitivity subsequent to disease onset (150). Prior to disease onset, IgA-RF has been shown to have the highest sensitivity of the rheumatoid factors (151). RFs are not specific for RA and can also be detected in up to 15% of healthy individuals and in patients with other autoimmune conditions (152). IgM-RFs in healthy individuals have been shown to be produced by natural CD5-expressing B cells and these antibodies are polyreactive, at low titre and of low affinity (153,154). Interestingly, whereas IgM-RF levels increase with age, IgG-RF levels decline in the elderly (155). IgM-RFs in healthy individuals also exhibit a low ratio of replacement to silent mutations in their complementarity determining regions (CDRs) (156) suggesting mechanisms preventing affinity maturation. Potentially

beneficial effects of RFs in healthy individuals include binding to immune complexes (ICs), leading to complement fixation and an enhanced clearance of ICs (157,158). Nevertheless, the presence of RF in healthy individuals is associated with up to 26-fold higher risk of developing RA (159). In RA patients RFs can undergo somatic hypermutation and isotype switching (160), however, at the same time also highly conserved IgM-RFs are present (161). It therefore remains unclear as to how exactly RF antibodies from RA patients differ from RFs produced in healthy individuals and whether or not they depend on T cell help (162). Interestingly, IgM-RFs can be detected before the onset of RA and, at relatively high levels, are associated with more severe joint damage (81,163). Conversely, RF levels were shown to decrease with effective therapy (164). RF has therefore remained a component of the classification criteria for RA (77) and RF titres are part of routine clinical assessment (165).

In addition to RFs a variety of other autoantibodies exist in RA patients, however, most of them are not specific for RA (166) and some are directed against nuclear antigens. For example, anti-heterogeneous nuclear ribonucleoprotein (hnRNP) A2 (anti-RA33) is detected in 30-40% of RA patients and may have a diagnostic potential in early inflammatory joint disease (167). Other types of autoantibodies in RA are the anticollagen antibodies, which appear to play a more important role in experimental arthritis models rather than in human RA (165,166).

In the past two decades, the anti-citrullinated protein antibodies (ACPA), a new group of autoantibodies has received a considerable amount of attention. These autoantibodies were demonstrated to be more specific for RA than RF (168–

170). In contrast to RF, ACPA only exist in about 2% of healthy individuals and are also very rare in other inflammatory conditions (171). Originally, these antibodies were described as “anti-perinuclear factor antibodies” or “anti-keratin antibodies” by Guy Serre’s group in France and the target of these antibodies was initially shown to be filaggrin (170,172). At that time, however, it was not known that these antibodies recognise specifically citrulline residues. Notably in 1998, did Walther van Venrooij’s group in the Netherlands demonstrate that antibodies in the sera of RA patients recognise filaggrin-derived peptides, which have been citrullinated at their arginine residues (169). In the following years, it was soon understood that ACPA display strong cross-reactivity and react not only with one specific target antigen but with a wide range of citrullinated autoantigens, of which vimentin (173), α-enolase (174), fibrinogen (175,176) and type II collagen (177) are the best characterised. Assays to determine the ACPA status of patients in clinical practice were therefore developed by screening libraries of citrulline-containing peptides for reactivity with RA sera to identify those yielding the highest sensitivity and specificity (178). Soon after the development of the first assay using artificial cyclic citrullinated peptides (CCP), the first commercial version of this test, the CCP2 assay, became available in 2002 and was followed by the third-generation CCP3 assay in 2010 (179). The CCP assay was included in the 2010 revised classification criteria for RA (77). All of these assays slightly differ in terms of specificity and sensitivity, and although the identity of the peptides used in these assays remains a commercial secret, it is likely that they are of non-physiologic origin (178). For this reason, despite their usefulness in clinical practice, CCP assays do not provide insight into real physiologic antigenic targets of ACPA. Future studies

are needed to study the immune response against citrullinated proteins in more detail to be able to understand the fine specificity of the anti-citrulline autoimmune response in RA patients. Current knowledge regarding ACPA fine specificity, the citrullinated targets and the role that ACPA may play in the pathogenesis of RA patients will be discussed in the subsequent sections.

Recently an additional autoantibody system, the so-called anti-carbamylated (anti-CarP) antibodies, has been discovered (180). Carbamylated proteins are generated through post-translational modification (PTM) of lysine residues into homocitrulline. Interestingly, the structure of homocitrulline highly resembles that of the citrulline residue. Surprisingly, however, it was reported that most ACPA do not react with homocitrulline residues (181,182) and reactivity can be detected in both ACPA positive and ACPA negative RA patients with 13-20% of ACPA negative RA patient sera reacting with carbamylated proteins (180,182). Interestingly, anti-CarP antibodies are associated with a higher rate of joint damage, which was most prominent in ACPA negative patients (181). This new antibody system may therefore represent an additional disease entity and could potentially be used to better characterise ACPA-negative patients. Nevertheless, many questions with regard to the anti-CarP response in RA patients still remain to be answered in order to understand the relevance of this autoimmune response.

1.3.2 Citrullination and ACPA generation

1.3.2.1 Physiological role of citrullination

ACPA in RA patients are directed against protein post-translational modifications termed citrullination (or deimination). This process is a hydrolytic enzymatic reaction catalysed by Ca^{2+}- dependent peptidylarginine deiminases (PADs) and leads to the conversion of the positively charged peptidylarginine into the neutral peptidylcitrulline with ammonia released as a reaction by-product (Figure 1-6). The enzymatic reaction results in an increase in molecular mass of less than 1 Da (183). Importantly, the loss of a positive charge per citrulline also reduces the net charge of the protein and thus has consequences on the protein structure (184,185).

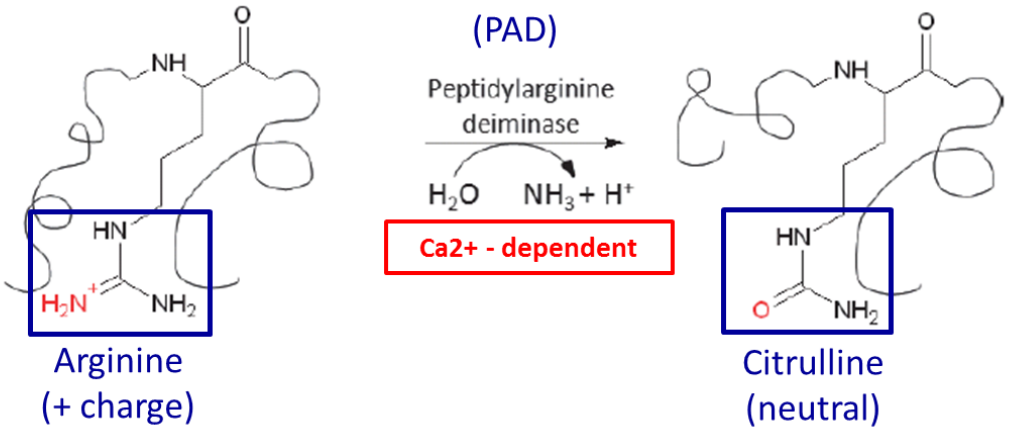

Figure 1-6 Enzymatic conversion of peptidylarginine into peptidylcitrulline

Citrullination is catalysed by the family of peptidylarginine deiminase enzymes (PADs). The guanidino group of the positively charged arginine residue is hydrolysed yielding a neutral ureido group and ammonia. Modified from Wegner et al. (70).

Citrullination is implicated in several physiologic processes such as gene regulation or the terminal differentiation of keratinocytes in the skin. There are five mammalian isoenzymes of PADs that are highly homologous and functionally similar, but differ in their expression pattern throughout organ systems and cell types (23,185,186). Whereas PADs 1, 3, and 6 are primarily expressed in the skin and female reproductive organs (185,187), PAD2 expression can be detected in a wide range of tissues including the central nervous system and skeletal muscle (185). PAD4 expression is found in granulocytes, as well as in some cancerous cell lines and tumours (187,188). The human PAD4 gene was originally named PAD5, but when the close similarity to murine PAD4 was observed, it was renamed PAD4. Subsequently there is no human PAD5 isoform, and when another PAD isoform was identified it was named PAD6 to avoid confusion with this previous work (185,186,189). Since PADs 1, 2, and 4 are the only PADs expressed in cells of the hematopoietic lineage, they are of special immunological interest.

Importantly, several *in vitro* studies suggest that theoretically all arginine residues can be citrullinated. Nevertheless, different kinetic parameters were determined depending on the primary and secondary structure of the substrates (184). Interestingly, *in vitro* studies have shown that a high degree of citrullination (over 10% of arginine residues in a given protein) can denature proteins (190). Whether this also takes place *in vivo*, is not yet known. It can be assumed that citrullination causes changes in the protein structure which results in a looser, more open configuration (190). In the skin, for example, it was shown that citrullination of (pro)filaggrin is essential for its degradation by the

protease calpain, which enables aggregation of keratin filaments into an organised matrix (184,185). Further citrullination is also believed to facilitate degradation of filaggrin to free amino acids (191), which are a component of the so-called ‘Natural Moisturising Factor’ responsible for the hydration of the stratum corneum (192). Thus citrullination is believed to change the protein structure in a way that makes it more susceptible to proteolysis, a process that was also recently shown to play a role in the degradation of the myelin basic protein (MBP) by cathepsin D in the brain (185,193). Here citrullination was shown to open up the structure of MBP so that Phe-Phe peptide bonds within the protein could be exposed and targeted by cathepsin D five-times faster than the native form of the protein (184).

Another process in healthy individuals where citrullination plays an important role is gene regulation. Cuthbert and colleagues proposed a model in which citrullination of arginines in histones antagonises arginine methylation and thereby represses transcription (194). Since PADs cannot only convert arginine residues but also monomethylated arginine residues into citrulline (50), only dimethylation of arginine residues was shown to prevent citrullination and maintain transcriptional activation.

1.3.2.2 Regulation of PAD activity

PADs require high calcium concentrations for their activity (184) and treatment of cells with calcium ionophores can therefore induce the generation of citrullinated residues in proteins (195,196). Nevertheless, little is known about the physiologic stimuli capable of inducing calcium-dependent PAD activity

(186). Interestingly, *in vitro* enzymatic assays measuring PAD activity have demonstrated that calcium concentrations that are required for half maximal activity, are between 0.15-0.5 mM (48,197,198), which is much higher than physiological calcium concentrations. This therefore suggests there must be an additional regulatory mechanism present *in vivo* to either raise calcium levels to above normal levels or lower the calcium dependence of PADs.

Research into the mechanism of regulation of PAD4 activity revealed that PADs also auto-citrullinate upon activation by calcium. Although Andrade et al. reported that citrullination of a cluster of arginines around the active site cleft can lead to inactivation of the enzyme (199), subsequent studies from Thompson and colleagues argued that auto-citrullination does not affect its enzymatic activity (200).

On activation, binding of Ca^{2+} moves the key catalytic thiolate anion C645 residue to the enzyme active site (47), which is essential for PAD4 activity (201). Since PADs may represent potential therapeutic targets for a variety of inflammatory diseases including RA, inhibitors are being developed to prevent PAD activity. For example, F- and Cl-amidine covalently bind to C645 and act as irreversible PAD inhibitors (201). The efficacy of Cl-amidine *in vivo* has been demonstrated in the CIA model in rodents as it was able to significantly reduce disease severity, by up to 55% (202). Interestingly, however, it did not show any effect in the collagen antibody-induced arthritis (CAIA), which is a model generally used to study the effector phase of RA pathogenesis (202).

Furthermore, a recent study suggests that different PAD isoenzymes have different substrate specificities (203), which may be essential for the pathogenesis of the inflammatory conditions mentioned above including RA,

since only one of the PAD enzymes could be essential for the citrullination of target proteins. The development of PAD-selective inhibitors may therefore prove to be more useful than pan-PAD inhibitors in the future for disease treatment.

1.3.3 Variability in clinical observations in RA

RA is a complex and heterogeneous disease. Patients often vary in disease course, have diverse extra-articular manifestations, experience different patterns of disease flares, remissions, and response to treatment. Nevertheless, in recent years research of the anti-citrulline immune response in RA patients has provided a more comprehensive picture regarding the role of possible environmental triggers and susceptibility genes in this disease compared to many other autoimmune diseases. Based on the presence of ACPA it has been proposed to divide RA into separate subsets of disease: ACPA positive and ACPA negative RA (168). Clinically, ACPA positive patients generally develop a considerably more severe disease course with more radiological joint damage than ACPA negative patients, irrespective of treatment provided (204,205). Also, ACPA positive RA patients were demonstrated to show differences in disease risk factors. Most of the HLA-DR alleles that confer susceptibility to RA (particularly HLA-DRB1*) have a common amino acid motif – named the shared epitope (SE) – at positions 70–74 in the third hypervariable region of the DRβ1 chain of the HLA-DR molecule (206). According to the SE hypothesis the SE motif (QKRAA, QRRAA, or RRRAA) allows the presentation of an arthritogenic peptide to T cells and is thus directly involved in the RA pathogenesis (206).

The second most important susceptibility gene, PTPN22, identified in 2005 (207), codes for a tyrosine phosphatase. A single nucleotide polymorphism in this gene was shown to be involved in deregulation of T cell and B cell signalling in RA and also in other autoimmune diseases (207–209). Interestingly, both the above mentioned risk alleles are associated with the ACPA positive but not the ACPA negative RA subset (210,211). APCA negative RA, in contrast, is associated with other genes such as HLA-DRB1*03 (212,213).

Among autoimmune diseases, RA is well-known for the thorough characterisation of the role of smoking as an environmental risk factor and constitutes as a risk factor for the ACPA positive RA subset (214). Furthermore, several studies have shown that this risk factor interacts with the HLA-DR SE genes (209,214,215) supporting the possible nature of an MHC class II-dependent immune response. In this context, using the large case-controlled Swedish Epidemiological Investigation of Rheumatoid Arthritis (EIRA) cohort, Lundberg and colleagues have recently demonstrated that HLA-DRB1 SE, PTPN22 and smoking are associated with the presence of specific ACPA reactivities rather than overall anti-CCP levels (216). The strongest association of HLA-DRB1 SE, PTPN22 and smoking was identified for the RA subset which was defined by the combined presence of antibodies to citrullinated autoantigens α-enolase and vimentin.

On the basis of these studies on environmental and genetic associations, it is therefore considered that the two forms of ACPA positive and ACPA negative RA are likely to exhibit overlapping but individually distinctive pathogenic mechanisms (217).

1.3.4 T and B cell responses to citrullinated proteins

The current view of the critical role of both T and B cells in the pathogenesis of RA is supported by the observations that i) the ST of RA patients is strongly infiltrated by T and B cells, ii) defined HLA-DR alleles are associated with disease, and iii) in many patients disease specific circulating autoantibodies can be detected.

In RA synovium predominantly CD45RO+ expressing $CD4^+$ as well as $CD8^+$ T cells cells with characteristics of memory T cells can be detected (218,219). Although T cells have long been thought to be major drivers of disease, their relevance and contribution to RA pathogenesis has recently been challenged (220). In RA, T cells generally display an activated phenotype with relatively high expression of HLA-DR, CD27, CD69 and CD28, their proliferation and cytokine secretion in synovial T cells are usually less pronounced compared with autologous peripheral blood T cells from the same patient (72). In this context it has also been suggested that synovial T cells functionally resemble resting T cells that have been activated by cytokines rather than by antigen (221). Furthermore, the memory cell phenotype of synovial T cells suggests the presence of already mature T cells that have been previously stimulated elsewhere and recruited to the joints as opposed to the stimulation and maturation of these cells inside the joints (72).

Synovial T cells have been shown to have a restricted T cell repertoire in ACPA positive RA patients compared with OA and SpA patients (222). In a recent study using peptide:TCR tetramers and looking at proliferative responses, Snir

and colleagues demonstrated enhanced reactivity to a citrullinated vimentin peptide in HLA-DRB1*0401 SE positive patients compared with healthy controls (223). The binding of this HLA-DR*0401 tetramer loaded with an autoantigenic citrullinated vimentin demonstrated the presence of autoreactive $CD4^+$ T cells both in RA patients and healthy controls but with the difference that RA patients had significantly increased pro-inflammatory responses following stimulation. In a more recent study, crystal structures and peptide elution experiments demonstrated that whereas citrullinated peptides can be bound by RA-predisposing HLA-DRB1 proteins and RA non-associated HLA-DRB1*04:02 protein, only RA-predisposing HLA-DRB1 molecules could not accommodate arginine peptide side chains in the P4 pocket of the molecules (224). These data therefore suggest that the absence of presentation of non-citrullinated peptides may be critical in RA pathogenesis and suggest a possible altered negative selection of T cells in the thymus dependent on the DR4 allotype. Nevertheless, many questions regarding the importance of autoreactive T cells in RA still remain to be answered. For example, despite extensive research it is still not clear whether the high numbers of T cells in the synovium are a result of clonal expansion to a specific antigen (225,226). Furthermore, limited efficacy of T cell-depleting therapies (227) may reflect the need to look at different T cell subsets in RA in more detail to avoid simultaneous deletion of both effector T cells as well as immune-suppressing regulatory T cells.

To better understand the development of autoimmunity in RA, it is important to also investigate the role of B cells. B cells and plasma cells constitute only about 5% of cells in most RA synovia compared with 30-50% T cells (72) and

different studies investigating the significance of B cell infiltration with regard to disease prognosis have reported conflicting results (95,228,229). Nevertheless, the success of the B cell depleting therapy using anti-CD20 antibody (rituximab), has focussed much attention on the contribution of B cells to RA pathogenesis. In particular, autoantibody production and differentiation into plasma cells have been intensely studied. As described in section 1.3.1, a growing number of autoantibodies generated towards a variety of antigens have been identified in recent years. Importantly, however, mechanisms that initiate and maintain autoantibodies may not only be different from antibody responses against recall antigens (for instance following vaccination) but may also differ between different autoantibody systems in RA (179). Rheumatoid factor, for example, which consists predominantly of non-switched IgM antibodies, is suggested to be generated outside of germinal centres upon TLR signalling and, at least initially, independent of T cell help (230). At the same time, however, some RF clones from RA patients have been identified to be somatically mutated compared with those from healthy subjects (161). Since there is only minimal evidence for extrafollicular responses in human autoimmune disease (231), T cell dependent germinal centre responses are more likely to be involved in the generation of pathogenic autoantibodies (232). Nevertheless, the role of T cells for the induction of RFs still remains unclear and differences between RA patients and healthy individuals cannot be excluded.

In contrast with RF, ACPA are strongly associated with HLA-DR alleles (216) and there is a growing body of data showing immune reactions against citrullinated autoantigens and other antigens locally inside joints of RA patients

(73,233). In comparison with ACPA negative RA patients (234), the ST architecture of ACPA positive RA patients is primarily characterised by a generally higher lymphocyte infiltrate and lower degree of fibrosis (234). Furthermore, it has been demonstrated that variable region genes coding for ACPA in joint-derived B cells are hyper-mutated. If these mutations were reverted back to the corresponding germline sequences autoantibody binding was nullified (235) suggesting that B cells producing these antibodies were most likely driven toward differentiation by local T cells in germinal centres. Given these data, however, it still remains elusive why ACPA IgG show a much lower avidity when compared with normal protective antibody responses against pathogens in the same patients (236). If B cells undergo affinity maturation and isotype switching in germinal centres, the avidity of immunoglobulins expressed by these B cell clones would normally be expected to increase due to the competition for antigens bound on the surface of FDCs. ACPA avidity in individual RA patients, therefore suggests different regulation mechanisms of autoantibody responses, which still remain to be elucidated (179).

In addition to antibody production, it should not be overlooked that B cells are efficient APCs and also able to release cytokines during immune responses. For example, Flores-Borja and colleagues have shown that $CD19^{+}CD24^{hi}CD38^{hi}$ regulatory B cells in healthy individuals can inhibit naïve T cell differentiation into Th1 and Th17 effector T cells *in vitro* while converting $CD4^{+}CD25^{-}$ into regulatory T cells, in part through the production of IL-10 (237). In RA patients, numbers of regulatory B cells were found to be reduced in the peripheral blood and no suppressive Treg cells could be induced by these regulatory B cells. This study therefore indicates that $CD19^{+}CD24^{hi}CD38^{hi}$

regulatory B cells in RA patients may fail to prevent autoreactive responses, which could finally result in autoimmunity (237).

Furthermore, work from our group has shown that B cells in the RA synovium are capable of producing pro-inflammatory and bone-destructive cytokines including RANKL (118). RANKL-producing B cells in RA synovial tissue and fluid were identified as belonging to a distinct subset of B cells defined by expression of the transmembrane protein FcRL4 (238) suggesting that FcRL4+ B cells are likely to represent a pathogenic B cell subset in RA.

1.3.5 Role of ACPA in the pathogenesis of RA

Recent data have contributed considerably to our understanding of APCA in the pathogenesis of RA. Nevertheless, the sequence of events involved in the different stages of disease pathogenesis still remains unclear. Several currently discussed concepts are detailed below:

1.3.5.1 The 'second hit' hypothesis

As previously described, citrullination is a physiological process of post-translational modification of proteins, but hyper- or hypo-citrullination can also play a role in pathobiological settings distinct from RA. An increased amount of MBP or histone H3 protein citrullination has been observed in the brain of patients with Multiple Sclerosis (193,239,240) or Alzheimer's disease (241), while a reduced amount of citrullination of cytokeratin K1 in the epidermis was reported to be pathological in Psoriasis (242). Furthermore, citrullination of proteins such as α-enolase (243) and PAD4 overexpression (244) were observed in a number of different tumours. In RA, the presence of citrullinated

proteins was initially considered to be specific to the synovium (245) and generated a great deal of interest in this PTM. In this context, Suzuki and colleagues also found that one haplotype of PAD4 was associated with increased susceptibility for RA due to increased PAD4 mRNA stability (246), which could explain a possible increased citrullination of proteins. However, thus far these findings have not been repeated in Caucasian populations.

The presence of PAD isoenzymes and citrullinated proteins in the inflamed ST and SF of RA patients has been well characterised (175,247–249). PAD2 and PAD4 expression in the synovium was found in close proximity to citrullinated fibrin deposits and correlated with the inflammatory cell infiltration (250). However, soon after it was recognised that citrullination is an inflammation-dependent process and also present in non-rheumatoid arthritis (251,252), attention focussed on the role of the highly specific ACPA antibodies which can be detected in approximately 60-70% of RA patients (168,171,253). ACPA levels are elevated in SF compared with the peripheral blood, and ACPA production was described in the inflamed RA joint (254) suggesting a local, antigen-driven B cell response at the site of inflammation. Similar to autoantibodies in many other autoimmune diseases, ACPA emerge several years before the onset of disease (81,151) and very few RA patients develop ACPA after the start of their symptoms (204,255). As several studies also suggest the absence of synovial inflammation in ACPA positive individuals with no clinically apparent joint swelling, the concept has been proposed that the initiating event leading to ACPA production is more likely to be located outside the joint and that another, “second hit” (for example, infection or trauma) needs to take place in ACPA positive individuals that causes joint inflammation and

generation of citrullinated proteins which are then targeted by the already present ACPA (168). Currently, there are several lines of evidence suggesting that RA-related autoimmunity may be generated at mucosal surfaces such as the gingiva, lungs or gut. As described in section 1.3.3, smoking represents the most established environmental risk factor for RA. The lung was therefore suggested to be one of the possible sites where anticitrulline immunity could be triggered (168). Despite this association, however, recent studies have demonstrated that increased expression of citrullinated proteins can be found not only in smokers, but also in ACPA positive non-smokers (256). Furthermore, only one-third of ACPA-positive RA cases can be attributed to smoking (257). It can therefore be assumed that other environmental triggers are involved. For example, it has been reported that airway exposures like coal dust (258), silica dust (259) or air pollution from traffic (260) could play a role. Additionally, in support of the notion that autoimmunity might originate at mucosal sites, ACPA are enriched in both bronchoalveolar fluid of early untreated RA patients and even in induced sputum of arthritis-free individuals at risk of developing RA (256,261). Finally, several species of microorganisms at mucosal sites have been implicated in RA pathogenesis, notably overexpansion of *Prevotella copri* in the gut (262) or *Porphyromonas gingivalis* of the oral microbiome (discussed in section 1.3.5.3).

1.3.5.2 Fine specificity of ACPA and epitope spreading

Another possible mechanism by which ACPA may be involved in RA pathogenesis may be related to the process of 'epitope spreading', which

enables the diversification of the immune response from a single epitope to many epitopes on the same molecule (intramolecular epitope spreading) or from one molecule to other molecules (intermolecular epitope spreading). Essential for this mechanism to occur is a need for the ability of B cells to take up antigens, process them intracellularly, load a limited number of peptides from the antigens on MHC class II molecules, and present them on the cell surface to T cells. Intriguingly, although a large number of peptides can theoretically be presented, only a few 'immunodominant' peptides will be selected (263). As shown in Figure 1-7, following T cell dependent or -independent activation of a B cell that is specific for one epitope of an antigen, the same B cell can activate and receive help from T cells that are specific for other epitopes of the antigen (Figure 1-7A). In turn, T cells that are specific for a certain epitope of an antigen, can trigger different B cell specificities (Figure 1-7B) (264). By expanding the number of antigenic epitopes that are recognised, the immune system can thus optimise the immune response to the antigen and this is believed to contribute to the efficient clearance of pathogens (265,266). In many autoimmune diseases, however, this mechanism may contribute to the propagation of disease.

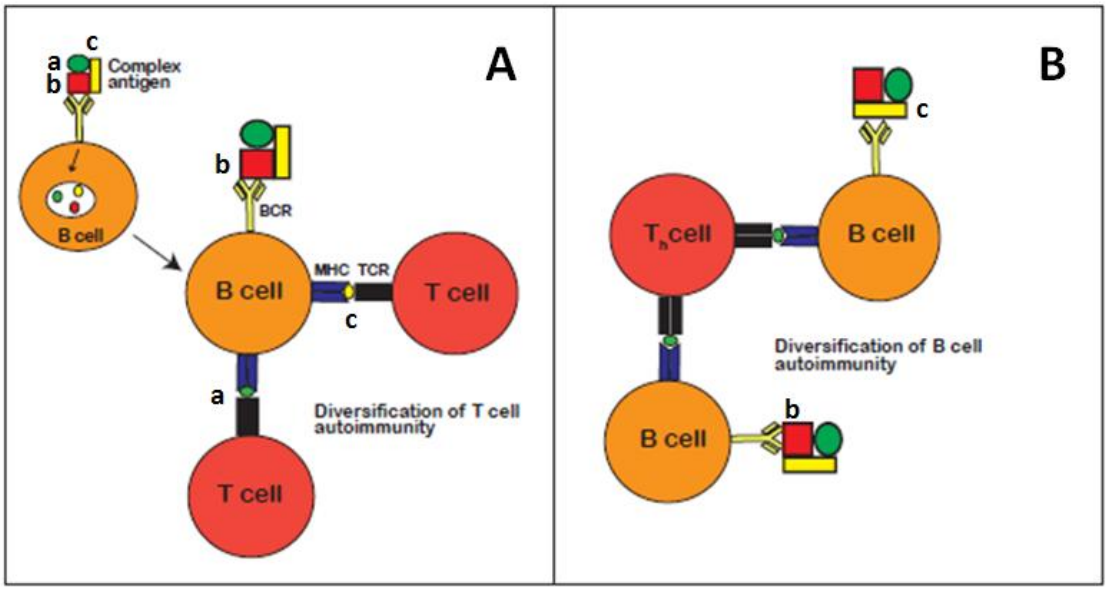

Figure 1-7 Mechanisms of epitope spreading

(A) A B cell, specific for the epitope 'b', takes up through its B cell receptor (BCR) a complex antigen, which consists of multiple epitopes ('a-c'). These multiple T cell-antigenic determinants, all arising from one initial complex antigen, are processed by the B cell and presented in the context of major histocompatiblily complex (MHC) class II. This way, the anti-b-specific B cell can activate, and receive help from, several T cells with different specificities. **(B)** An activated, a-specific T_h cell can, in turn, provide help to B cells that can recognise the same determinants but are specific for other accessible epitopes of the complex. This can finally lead to generation of anti-b and anti-c antibodies.

As mentioned earlier, ACPA in RA patients can be detected several years before the first symptoms of the disease appear. Interestingly, closer to the onset of disease (within 6-12 months), antibody characteristics of ACPA change into higher titres, higher number of specificities and an increase in the number of isotypes used (267–271). Altogether, these data suggest that progressive intra- and intermolecular epitope spreading (as observed by the targeting of additional citrullinated epitopes) together with the emergence of subclinical inflammation (as evidenced by increases in blood cytokine levels (267)) may

play a central role in the progression of individuals from preclinical to clinical RA (256). This notion finds support in other autoimmune conditions like pemphigus (272) or SLE (273) where a similar shift in the antigen recognition profile prior to clinical onset can be observed. Based on these considerations and examples from other autoimmune conditions the hypothesis was therefore made that ACPA may initially be non-pathogenic during the preclinical phase and only gain arthritogenic properties after the above described changes in antibody characteristics (256).

1.3.5.3 Molecular mimicry –link between RA and periodontitis

It has long been suspected that there may be a link between infections and the generation of autoimmune diseases. In 1964, R.T. Damian initially coined the term “molecular mimicry” to describe antigen sharing between host and parasite and thus provided a mechanistic explanation for this association (274). According to the molecular mimicry hypothesis an immune response can be caused by a pathogen that shares an immunodominant epitope with a self-antigen. The conformational structure of the epitope from the self-antigen can then be recognised by B cells or linear peptide sequences recognised by T cells in the context of MHC molecules. This process is referred to as cross-reactivity. The autoimmune reaction against the self-antigen will persist even if the cross-reacting microorganism has already been eliminated from the body (275).

There have been several epidemiological and experimental studies demonstrating a positive association between RA and periodontitis (PD) (276–280). PD is a chronic inflammatory disease of the gingiva and underlying

connective tissues and affects almost half of the adult population in the UK (281). It can cause tooth loss but can also lead to, or associate with, several systemic complications (277,282). Historically, it has been considered that three main bacterial species are closely associated with disease pathogenesis, namely *P.gingivalis, T.denticola and T.forsynthia* (283). However it is suggested that disease is rather caused by an imbalance in the microbial community of the biofilm around the gingival margin accompanied by a dysregulation of the host immune system. In line with this model, it was demonstrated that *P.gingivalis* was one of the pathogens closely associated with periodontitis in susceptible individuals, resulting in inflammatory bone loss (284–286).

In general, the published association studies regarding the link between PD and RA indicate that chronic periodontitis is more prevalent in individuals with RA and *vice versa*. Interestingly, PD and RA share similar pathobiology (278) and risk factors such as smoking (287). One explanation for the association between these diseases is based on the fact that *P.gingivalis* has the unique capability of expressing a bacterial peptidylarginine deiminase (PPAD) (288). In 2004, Rosenstein et al. first proposed that citrullinated proteins generated by PPAD might become systemic autoantigens in the inflammatory context of PD, and ultimately cause autoimmunity in RA (278). This notion was further extended by Wegener and colleagues who found that PPAD is not only able to citrullinate its own proteins but also host proteins such as human fibrinogen and human α-enolase, which are known autoantigens in RA (279). Furthermore, they discovered that the immunodominant peptide CEP-1 of the human protein α-enolase shows 82% sequence identity with the region corresponding to CEP-1 of the bacterial enolase (289). Intriguingly, antibodies to CEP-1 from RA

patients also cross-react with *in vitro* citrullinated enolase from *P.gingivalis*, which suggests a link between the bacterium *P.gingivalis* and RA based on the mechanism of molecular mimicry (290). Interestingly, the link between *P.gingivalis* and RA was supported by two recent and independent animal studies: In CIA, but also in CAIA, it was shown that the ability of *P.gingivalis* to exacerbate disease strictly depends on PPAD expression, as mutants lacking this enzyme fail to influence disease outcome (291,292).

Nevertheless, further studies are needed to investigate the link between *P.gingivalis* and/or PD with ACPA-positive RA, since compelling evidence of exact molecular mechanisms by which *P.gingivalis* may induce the loss of tolerance to citrullinated proteins is still lacking and a subject of significant debate (293–296).

1.3.5.4 Possible effector mechanisms of ACPA

In order for antibodies to be effective during immune responses, they must in general not only bind to their corresponding antigen but also induce immune effector mechanisms through the activation of the complement system and the engagement of Fc receptors. Depending on the endogenous or exogenous nature and location of the antigen, and on the type of immune response responsible for the tissue damage, such effector mechanisms in immune-mediated processes such as allergy and autoimmunity were historically categorised into different types of so-called hypersensitivity reactions (297,298).

One of the most extensively studied murine models of RA to unravel the role of antibody induced joint inflammation is the K/BxN mouse model which results

from crossing KRN-TCR transgenic mice with NOD mice (23). Notably the F1 K/BxN offspring develop spontaneous arthritis (299). The antigen recognised by the KRN TCR in the context of MHC-II I-Ag7 has been identified as glucose-6-phosphate isomerase (GPI) a glycolytic enzyme that is widely expressed (300). Sera from these mice contain GPI specific antibodies and transferring these into healthy as well as in lymphocyte deficient mice, induces joint inflammation. Intriguingly, systemic presence of immune complexes together with participants of the innate immune system like complement, FcγRIII, mast cells and neutrophils induce an inflammatory response reminiscent of the type III hypersensitivity (or 'Arthus') reaction, which can theoretically manifest at many sites in the body. Why this is manifested particularly in the joints of these mice, however, is not well understood. Possibilities discussed include the effect of hydrostatic pressure, regionally distinct vascular properties (301) or further mechanisms leading to a lack of clearance of ICs from the inflamed joint. In the K/BxN model, GPI and associated antibodies have been shown associated with the cartilage surface. Similarly, in ACPA positive RA patients, precipitates of RA and their immunoglobulin antigens are found on the surface of the cartilage (302). The presence of citrullinated proteins has also been observed in precipitates on the surface of the synovial lining of RA patients, suggesting that these may also involve formation of ICs (248). When immune complexes were purified from plasma (303) and the SF of RA patients (304), and analysed for the antigens involved, citrullinated proteins were detected. Importantly, these ICs may play a critical role, because they can activate macrophages to produce cytokines such as TNF-α, which is the driving force in the chronicity of RA (305). Interestingly, this TNF-α secretion can even be increased, if RF IgM are

incorporated into ICs already containing ACPA, and likely depends on an increase in the number of IgG-engaged FcγR (306). An interaction between ACPA and RF has also been suggested due to the fact that RFs preferentially interact with hypoglycosylated IgG and that ACPA are hypoglycosylated compared with total IgG (179). Experiments using mice deficient in individual immunoglobulin receptors revealed that ICs binding to FcγRIII but not to FcγRII were necessary for arthritis development (307,308). Furthermore it has been shown that the inflammatory response depends on the presence of neutrophils, macrophages and the alternative and classical complement pathway (309). *In vivo* inhibition of the CXCR2 receptor led to significant reduction in RA, reflecting its important role in neutrophil recruitment (310). In addition, a recent report has also shown that expression of Syk, a kinase downstream of the Fcγ receptor, specifically in neutrophils is necessary for development of arthritis (23,311).

Finally, in addition to the effector mechanisms described above, the pathogenic role for the anticitrulline response was recently supported by a study demonstrating that ACPA can also affect bone destruction through the activation of osteoclasts (312). If these findings are confirmed they would imply that ACPA have functional properties in the initiation of RA and may be directly pathogenic in contrast to the possibility of just simply enhancing a pre-existing inflammation. Additional investigations are therefore needed to elucidate the exact mechanisms of ACPA contribution to RA pathogenesis.

1.4 Aims

Neutrophils can enter a novel form of cell death known as NETosis, which depends on the enzymatic activity of PAD4. The overarching aim of the work described in this thesis was to test the hypothesis that enzymatically active PADs during NETosis are involved in the generation of citrullinated autoantigens in the inflamed joint, and that these antigens are targeted by anti-citrullinated protein antibodies (ACPA) in RA patients.

In particular, the objectives of this project were:

- To investigate evidence for NETosis in the joints of patients with arthritides.
- To develop a suitable assay to study the release of PADs and citrullinated proteins from neutrophils going into NETosis.
- To relate findings of *in vitro* NETosis to the *in vivo* situation in the joints of RA patients by measuring PAD activity in the synovial fluid and by investigating the composition of proteins in NETs isolated from the synovial fluid.
- To assess the presence of known and novel citrullinated antigens in NETs.
- To examine the antigenicity of NET-associated citrullinated proteins in ACPA positive RA patients.

2 Materials and Methods

2.1 Antibodies

The following antibodies shown in Tables 2.1-2.3 were used for immunofluorescence staining and Western Blotting.

Table 2.1 Details of conjugated primary antibodies used

Immunofluorescence						
antibody	**concentr.* [µg/ml]**	**species**	**isotype**	**supplier**	**clone**	**product number**
anti-PAD4	10.1	mouse	IgG2a	Abcam	4H5	ab128086
anti-PAD2	5	rabbit	IgG	Abcam	-	ab50257
anti-CD68	5	mouse	IgG2b	BD Pharmingen	Y1/82A	556059
anti-CD15	10	mouse	IgM	Immunotools	MEM-158	21270151
anti-neutrophil elastase	12.5	rabbit	IgG	Abcam	-	ab21595
Western Blotting						
anti-PAD4	1	mouse	IgG2b	Novus biologicals	4D8	H00023569-M01
anti-PAD4	3.2	mouse	IgG2a	Abcam	4H5	ab128086
anti-PAD2	25	rabbit	IgG	Abcam	-	ab50257
anti-neutrophil elastase	0.15	mouse	IgG1	SantaCruz	NP57	53388
anti-modified citrulline (AMC)	2	human	IgG1	ModiQuest	clone C4	MQR2.601-100
anti-histone H3	0.08	rabbit	IgG	Abcam	-	ab1791
anti-citrullinated histone H3	1.33	rabbit	IgG	Abcam	-	ab5103

**end concentration (concentr.)*

Table 2.2 Isotype control antibodies used

isotype	**concentration [µg/ml]**	**species**	**supplier**	**product number**
IgG1	*	mouse	DAKO	X0931
IgG2a	*	mouse	DAKO	X0943
IgG2b	*	mouse	DAKO	X0944
IgG	*	rabbit	DAKO	X0936
IgM	*	mouse	DAKO	X0942

**Isotype control antibodies were isotype-, concentration- and species-matched to primary antibodies*

Table 2.3 Conjugated antibodies used

conjugate	description	dilution	supplier	product number
Cy5	goat anti-mouse IgG2b	1:250	Jackson ImmunoResearch	115-175-207
DyLight 488	donkey anti-mouse IgM	1:100	Jackson ImmunoResearch	715-486-020
AlexaFluor 488	donkey anti-rabbit IgG	1:100	Life technologies	A21206
AlexaFluor 647	goat anti-rabbit IgG	1:400	Jackson ImmunoResearch	111-605-047
Biotin	goat anti-mouse IgG2a	1:50	Southern Biotechnology	1080-08
Streptavidin-AlexaFluor 488	-	1:100	Jackson ImmunoResearch	016-540-084
HRP	goat anti-human IgG	1:10000	Jackson ImmunoResearch	109-036-008
HRP	donkey anti-rabbit IgG	1:10000	Amersham	NA934
HRP	sheep anti-mouse IgG	1:10000	Amersham	NA931

2.2 Quantification of extracellular DNA in SF samples (untreated or cell-free)

Untreated synovial fluid samples were used immediately following aseptic aspiration from the joints (see section 2.9) and were diluted with PBS to 1:10, 1:100 and 1:1000. Levels of free DNA were assessed using SYTOX Green as described in section 2.6.1.2. DNA concentrations were calculated using a standard curve of purified DNA (placental DNA, Sigma-Aldrich, D4642). To obtain cell-free SF, samples were centrifuged for 10 min at 300 x g, the supernatants were carefully aspirated away from the cell pellets and used to assay DNA concentration.

2.3 Quantification of cells in SF samples

Untreated SF samples were obtained immediately after joint aspiration. The total cell count and proportion of neutrophils and macrophages within the synovial infiltrate was determined using a Neubauer hemocytometer and

cytospin preparations after a modified Giemsa staining (Diff-Quick™, Gamidor Technical Services, Didcot, UK). To generate cytospins SF cells were re-suspended in MACS buffer (0.5% BSA and 2mM EDTA in PBS) and 1 x 10^5 cells were transferred onto a clean glass slide using a cytocentrifuge, stained with modified a Giemsa stain (Diff-Quick, Gamidor Technical Services, Didcot, UK) and examined by light microscopy (Axiocam, Ero5S, Zeiss). For this purpose slides were fixed for 10 min in methanol (Sigma) and then stained according to manufacturer's instructions. Neutrophils and macrophages were identified by their characteristic morphology. Giemsa staining of neutrophils showed cells with a multilobed blue-violet nucleus and a pale pink granular cytoplasm while macrophages were identified as cells with an irregular amoeboid shape and a pale blue and vacuolated cytoplasm (Figure 2-1). The ratio of neutrophils or macrophages compared with the total cell number was determined in five microscopic fields (40 x 10 original magnification) with a total minimum cell number of 200 cells per sample. Finally, the concentration was calculated using the ratios and the total cell count in the infiltrate. Other cells such as lymphocytes with their high nucleus:cytoplasm ratio or synoviocytes, which were usually found in the form of aggregates, were not considered for the differential leukocyte count.

Figure 2-1 Example image of neutrophils and macrophages in the synovial fluid infiltrate used for cell characterisation and quantification

Cytospin preparation of SF cells from an RA patient stained with Diff-Quick^{TM}. The dashed arrow indicates an example of a neutrophil and the solid arrow a macrophage (40 x 10 original magnification).

2.4 Isolation of neutrophils from peripheral blood

Peripheral blood from healthy donors was anti-coagulated with EDTA (Sigma-Aldrich, E7889) at a final concentration of 1.5 mM and 1 ml of 0.04 mM Dextran T-500 (Sigma-Aldrich, 31392) was added per 6 ml blood to sediment erythrocytes. The supernatant without erythrocytes was then layered on top of a discontinuous Percoll (Sigma-Aldrich, Poole, UK) gradient of 56% Percoll over a layer of 80% Percoll and finally centrifuged at 190 x g for 20 minutes at RT with the centrifugal brake turned off. Neutrophils were collected at the interface between both Percoll layers using a Pasteur pipette and transferred into RPMI 1640 medium (Sigma-Aldrich) containing 2 mM L-glutamine, 100 U/ml penicillin and 100 µg/ml streptomycin (Sigma-Aldrich). The cells were washed by centrifugation at 300 x g for 10 min and resuspended in RPMI. Purity of

neutrophil isolation was determined by Diff-Quick™ staining of cytospins and light microscopy (as described above). Routinely >97% of neutrophils were obtained in preparations, with eosinophils being the main contaminating cell. Cells were counted using a Neubauer hemocytometer.

2.5 Induction of necrotic cell death in neutrophils

Neutrophils were pipetted into 2 ml polypropylene tubes at a cell concentration of 1 x 10^6 ml^{-1} in 1 ml and subjected to 5 freeze-thaw cycles as has previously been described elsewhere (313). After the final freeze-thaw cycle samples were centrifuged for 10 min at 300 x g to remove intact cells, supernatants were transferred to fresh tubes and centrifuged a second time for 10 min at 16000 x g to remove cell debris. The supernatants of unstimulated neutrophils and NETotic neutrophils (generated as described in section 2.6) of the same donors after 4 h of incubation without or with PMA, respectively, were used as controls. Finally, DNA concentration (section 2.6.1.2) and PAD activity (section 2.10) in the supernatants was determined.

2.6 Isolation of NETs

2.6.1 Isolation of NETs from neutrophils stimulated with PMA (*in vitro*)

Isolated neutrophils from healthy donors were seeded in 12-well tissue culture plates at a density of 1 x 10^6 ml^{-1} (1.7 x 10^6 cells per well) and were induced to form NETs using 25 nM phorbol myristate acetate (PMA) for 4 h at 37°C in a

5% CO_2 atmosphere (314). To ensure appropriate stimulation of the cells, cell morphology was checked following stimulation under light microscopy. Unstimulated neutrophils demonstrated a typical rounded shape while neutrophils stimulated with PMA became flattened and exhibited a loss of cell membrane integrity (Figure 2-2). Supernatants from stimulated (SN) and unstimulated neutrophils (SN (unst.)) were harvested and wells were washed three times by removing the supernatant and carefully adding 500 µl of fresh pre-warmed RPMI into the well. Each wash was incubated for 20 min at 37°C. This process was undertaken to remove proteins that do not bind firmly to NETs as is previously described (315).

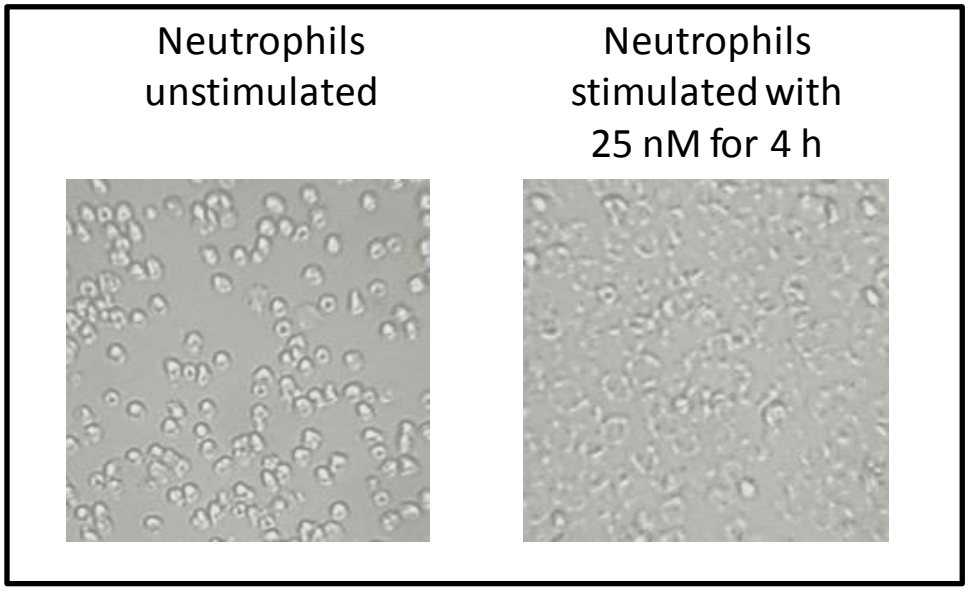

Figure 2-2 Example images of cell morphology of unstimulated and PMA-stimulated neutrophils (25 nM PMA) after 4h cell culture (20 x 10 original magnification)

Cell-associated NETs were solubilised with 10 U/ml DNase-I (Ambion AM2235, Applied Biosystems) for 20 min in 500 µl RPMI and protease inhibitor cocktail (Sigma-Aldrich, P8340) at a dilution of 1:200 (Sigma-Aldrich, P8340) and the

reaction was stopped using a final concentration of 5 mM EDTA. Supernatants from all washing steps (W1-3), DNase-I treated NET fraction (+DNase-I) and control fractions were collected. The supernatants were centrifuged for 10 min at 300 x g to remove intact cells and then centrifuged for 10 min at 16000 x g to remove cell debris (Figure 2-3).

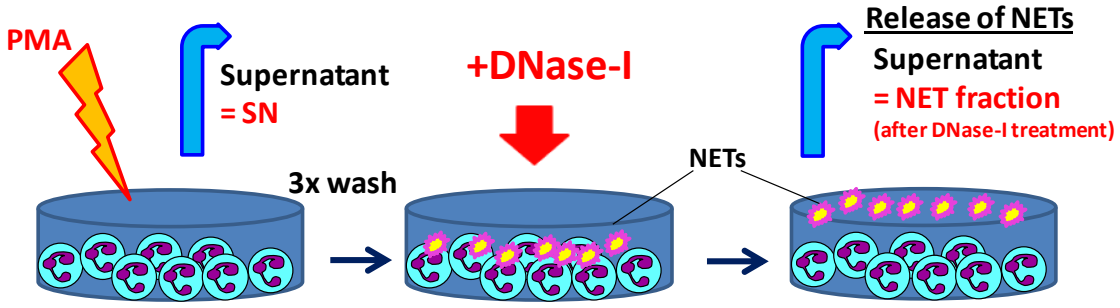

Figure 2-3 The steps in the process used for the isolation of NETs using DNase-I

2.6.1.1 Precipitation of proteins using trichloroacetic acid (TCA)

Proteins in the supernatants of neutrophils (including the NET fraction) were precipitated using a final concentration of 15% w/v trichloroacetic acid (TCA) (T6399, Sigma-Aldrich) for 20 min on ice and centrifuged for 10 min at 16000 x g. Pellets were washed twice with 500 µl ice-cold acetone (Sigma) and then alllowed to air dry on ice. Finally, all protein pellets were solubilised in equal volume of SDS loading buffer or prepared for MS identification as described in section 2.14.

2.6.1.2 Measurement of DNA concentration in supernatants of neutrophils

To quantify DNA, 90 µl of each supernatant was incubated with 10 µl of 10 µM SYTOX Green (Invitrogen) at a final concentration of 1 µM in a black 96-well assay plate (Corning) and incubated for 10 min at RT. Readings were obtained at a wavelength of 530 nm using a plate reader (BioTek-Synergy 2). Values obtained were compared with a standard curve of purified DNA (placental DNA, Sigma-Aldrich, D4642). Differences in volumes were accounted for in the calculation of the final DNA concentration.

2.6.2 Isolation of NETs from synovial fluid of RA patients *(ex vivo)*

For isolation of NETs from SF samples a modified version of the protocol described in section 2.6.1 was applied. Undiluted synovial fluid containing infiltrating cells was seeded on poly-L-lysine (Sigma) coated 12-well plates at 300 µl per well, centrifuged at 300 x g at room temperature to sediment the cells and incubated at 37°C in a 5% CO_2 atmosphere for 30 min. After removing the supernatant 500 µl pre-warmed RPMI were added into each well to gently wash the cells eight times so that proteins are removed which are not firmly attached to NETs. Each wash was incubated for 10 min at 37°C and the supernatants from 1 plate of the last washing step were collected as washing step 8 (W8). Subsequently NET-bound proteins from 1 plate were solubilised for 20 min in 500 µl RPMI with 10 U/ml DNase-I (Ambion AM2235, Applied Biosystems) and protease inhibitor cocktail (Sigma-Aldrich) at a dilution 1:200 (+DNase-I). Importantly, EDTA at a final concentration of 5 mM, was used to stop the activity of DNase-I directly after incubation. A further plate was used as a control with RPMI alone and without DNase-I (-DNase-I) to ensure the

specificity of NET release. The supernatants were then centrifuged for 10 min at 300 x g to remove intact cells and again for 10 min at 16000 x g to remove cell fdebris. Finally, proteins from each fraction (W8, +DNase-I and -DNase-I) were precipitated with TCA (as described in section 2.6.1.1), pellets were dissolved in SDS buffer and loaded onto an acrylamide gel (see below). In parallel, DNA levels in all supernatants were tracked using SYTOX Green as described in section 2.6.1.2.

2.7 SDS-PAGE (Sodium Dodecyl Sulfate-Polyacrylamide Gel-Electrophoresis) and Western Blotting

Acrylamide gels were prepared at 12% or 15% for the resolving gel and 5% for the stacking gel. Gels were placed in a electrophoresis chamber and immersed in running buffer (Geneflow). Protein precipitates were solubilised in SDS loading buffer (0.35 mM SDS, 2.74 mM Glycerol, 0.04% β-Mercaptoethanol, Bromophenol blue powder, 0.1 M Tris, pH 6.8), boiled at 95ºC for 5 min, separated on SDS-PAGE gels using tris-glycine SDS-PAGE Tank Buffer (Geneflow). Samples were transferred to polyvinylidene difluoride (PVDF) membranes (345774, GE Healthcare, Amersham) using Electroblotting Buffer Tris-glycin (Geneflow). After blocking with 5% milk powder (Marvel powder) in TBS with 0.05% Tween-20 (Fisher BioReagents), membranes were incubated overnight at 4°C with primary antibody and developed with HRP conjugated secondary antibody and ECL Plus or ECL Prime (GE Healthcare, Amersham).

2.7.1 Sample preparation

Precipitated proteins from pooled supernatants of 4 wells of PMA-stimulated neutrophils or from pooled supernatants of 12 wells of synovial fluid cells were solubilised in 25 µl SDS buffer prior to loading on a polyacrylamide gel. Intact neutrophils and human skeletal muscle tissue were lysed in RIPA-buffer (Sigma-Aldrich, R0278) in combination with protease inhibitor cocktail (Sigma-Aldrich, P8340) first and the protein concentration was determined using the BCA protein assay kit (Thermo Scientific) according to the manufacturer's instructions. The samples were diluted with 5 x SDS loading buffer prior to loading on a polyacrylamide gel.

2.7.2 Depletion of albumin from the synovial fluid

Frozen and cell-free SF samples were thawed and albumin was removed from supernatants using the ProteoExtract Albumin/IgG Removal Kit, Maxi (Calbiochem). Protein concentrations of the eluate were determined using the BCA protein assay kit (Thermo Scientific) according to the manufacturer's instructions. Twelve µg of each sample was diluted with 5 x SDS loading buffer prior to analysis by SDS-PAGE and Western Blotting (section 2.7).

2.7.3 Relative quantification of protein signal

Images were captured with the ChemiDoc MP imaging system (Bio-Rad) and analysed using Image Lab 4.0 software (Bio-Rad) in the ‘manual band quantification’ mode and the ‘Identify Bands’ tool was used to detect individual bands. By default, the bands were labelled by band number. The ‘assign quantity’ tool was used to assign the brightest or reference band a value of 1.

All other band intensities were subsequently given values between 0-1 relative to this reference band. An example is shown in Figure 2-4.

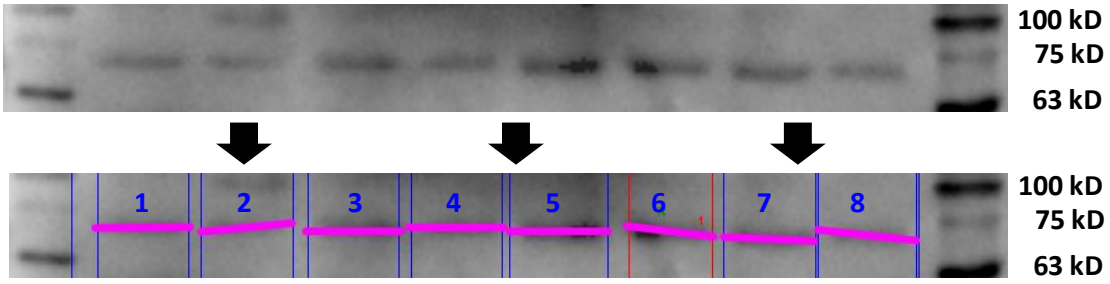

Figure 2-4 Relative quantification of protein bands using Image Lab 4.0 software

Relative quantification of western blot signals was performed using the Image Lab 4.0 software by Bio-Rad. In this example 8 bands were automatically detected by the programme and band 6 was identified as the reference band (in red) with the value 1.0. The signals of the other bands were calculated in relation to this reference band.

2.7.4 Detection of citrulline modifications using the AMC-kit

Citrullinated residues in proteins from neutrophil supernatants blotted on PVDF membranes were modified for assay using the protocol described by Senshu et al. (316). Briefly, membranes were incubated overnight at 37°C with an end concentration of 0.77 mM $FeCl_3$, 1.47 M H_3PO_4 and 2.25 M H_2SO_4 in combination with 0.25 M $C_2H_4O_2$, 25 mM 2,3-butanedione monoxime and 6.64 mM antipyrine. After rinsing with dH_2O and blocking with 5% milk powder in TBS with 0.05% Tween-20 next day, membranes were probed overnight at 4°C with a monoclonal human anti-modified citrulline (AMC) antibody (ModiQuest, clone C4) and developed with HRP conjugated goat anti-human antibody (Jackson ImmunoResearch Laboratories) and ECL Prime (GE Healthcare, Amersham).

2.7.5 Staining of SDS-PAGE gels or PVDF membranes with Coomassie Blue

Gels were prefixed in 50% methanol (MeOH), 10% acetic acid (HOAc) and 40% H_2O overnight and stained in the same solution with 0.25% Coomassie Blue (R-250) for 4 h on the next day until the gel became a uniform blue colour. Finally, the gel was destained for 4 h in 5% MeOH, 7.5% HOAC, 87.5% H_2O until bands began to appear and the background became clear. In comparison, PVDF membranes were not prefixed and stained in the above Coomassie Blue solution for 30 sec. Destaining of PVDF membranes was undertaken using the same solutions and in the same way as that described for gels.

2.7.6 Generation of gel slices for mass spectrometry

Proteins of the *in vitro* isolated NET fractions from 5 donors were separated using SDS-PAGE as described above (section 2.7) and thin slices (2 x 4 mm) were dissected from the polyacrylamide gel at the molecular weight of 11 kD in a ventilation hood to avoid contamination with keratin. In-gel digestion of the gel slices followed by mass spectrometry analysis were performed by Jimmy Ytterberg at the Karolinska institutet in Sweden.

2.7.7 Generation of PVDF strips and incubation with patient sera or antibodies

Either precipitated proteins from *in vitro* NET fractions (from the supernatants of 36 wells) or 3.2 µg recombinant histone protein (New England Biolabs) were evenly distributed in one large well on the surface of an acrylamide gel,

separated using SDS-PAGE and blotted onto a PVDF membrane. After the blocking step, eight strips of PVDF membrane of the same size were dissected out of one membrane for the incubation with eight different patient sera or eight different antibodies.

2.8 Immunoprecipitation of PAD4 from the synovial fluid

Initially 100 µl of protein G microbeads (Miltenyi, 130-071-101) were pre-coupled with 3 µg of an anti PAD4 antibody (abcam, ab128086) in 0.4 ml ice-cold PBS and mixed for 3 h at 4°C on a rotating table. An isotype-, concentration- and species- matched antibody was used as negative control for the immunoprecipitation. In the subsequent step, SF samples were pre-cleared by addition of 40 µl A/G plus agarose beads (Santa-Cruz, sc-2003) per SF sample and incubated for 3 h at 4ºC on a rotating table. After centrifugation at 800 x g agarose beads were removed and 1.5 µg recombinant human PAD4 (rPAD4, Cayman, 10500) was added as a positive control in combination with the specific antibody. Pre-cleared SF samples were then combined with the pre-coupled Miltenyi beads and incubated overnight at 4°C with agitation to allow the binding of the PAD4 protein to the anti-PAD4 antibodies on the surface of the beads. Next day, the immune complexes were loaded on µMACS columns (Miltenyi) and allowed to filter through. After washing the columns according to the manufacturer's instructions, 20 µl 95°C pre-heated SDS loading buffer was added to the columns and the flow-through was discarded. Finally, another 20 µl 95°C-warm SDS loading buffer was added and the eluate with the protein-antibody complexes collected and loaded on SDS-PAGE gels (section 2.7).

2.9 Patient selection and sample collection

RA patients studied all fulfilled the 1987 ARA classification criteria (76). At initial assessment, the disease activity score in 28 joints (DAS28) was calculated, and blood samples were analysed for C-reactive protein (CRP), erythrocyte sedimentation rate (ESR), rheumatoid factor and anti-CCP antibody. Seropositivity for anti-ccp antibody was defined as a titre of ≥7 IU/ml and a maximum cut-off level of 340 IU/ml. Seropositivity for rheumatoid factor was defined as a titre of ≥11 IU/ml. Psoriatic arthritis was diagnosed according to established criteria (317). Samples were obtained from patients seen by consultant rheumatologists, Prof Karim Raza or Dr Andrew Filer. Synovial fluid was aspirated from joints under manual palpation or ultrasound guidance. Synovial tissue was obtained by ultrasound guided synovial biopsy (318). Ethical approval was obtained and participants gave informed, written consent. Clinical details of patients are provided in the appendix (section 8.1).

2.10 Measurement of PAD activity (ABAP-assay)

The Antibody Based Assay for PAD activity (ABAP) was purchased from ModiQuest Research, MQ-17.101-96. The assay utilises a solid Enzyme-linked immunosorbent assay (ELISA) for the determination of PAD enzyme activity (197). The wells of a 96-well plate were pre-coated with arginine containing peptides (Figure 2-5). After incubation with PAD enzyme-containing solutions, arginine residues can then be citrullinated and recognised by a monoclonal detection antibody specific for citrullinated arginine. In the final step wells are incubated with a HRP-labelled polyclonal anti-mouse immunoglobulin antibody which is then developed using the HRP substrate tetramethylbenzidine (TMB)

(Sigma) (Figure 2-5). The staining reaction is directly proportional to the amount of arginine residues that have been citrullinated. For quantification of the measured optical density at a wavelength of 450 nm a standard control PAD enzyme diluted in deimination buffer (40 mM Tris-HCl pH 7.5; 5 mM CaCl2; 1 mM DTT) was used. Synovial fluid samples from patients with RA and OA and supernatants from *in vitro* PMA stimulated neutrophils were diluted in deimination buffer according to the manufacturer's instructions.

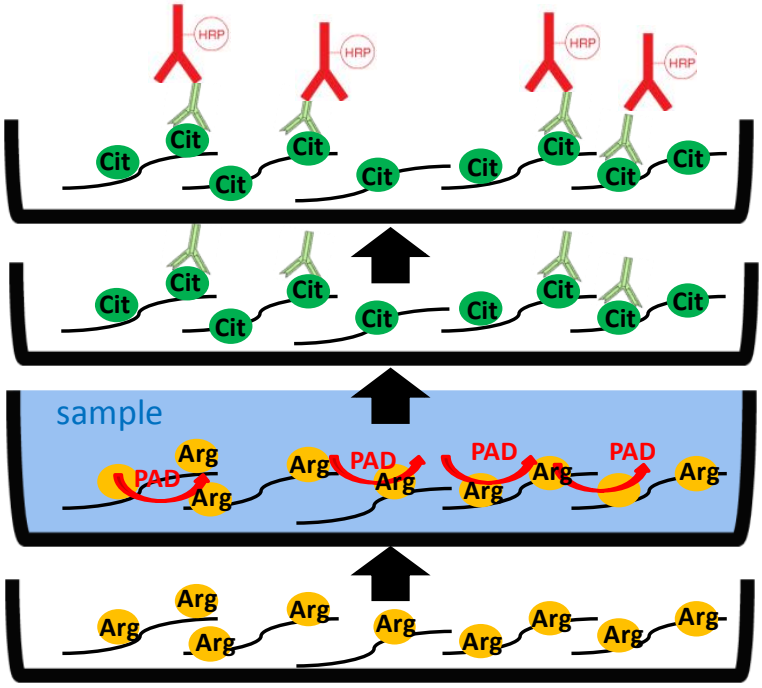

Figure 2-5 The Antibody Based Assay for PAD activity (ABAP)

Schematic diagram showing the sequential steps (bottom to top, as described in the text) involved in quantifying PAD activity in PAD enzyme-containing solutions using the ABAP-Assay (ModiQuest). Arginine-containing proteins (Arg), Citrulline-containing proteins (Cit).

2.10.1 PAD activity measurement in the supernatants of neutrophils (*in vitro*)

For analysis of PAD activity released by *in vitro* stimulated neutrophils, isolated cells were seeded at 1 x 10^6 ml^{-1} in individual wells of a 12-well plate and allowed to sediment for 1 h at 37 °C at 5% CO_2 in RPMI 1640 medium (Sigma-Aldrich). Following sedimentation, the supernatant was replaced either by 1 ml pre-warmed RPMI (unstimulated control) or with 1 ml 25 nM PMA in RPMI. Following stimulation the supernatants were collected and treated with 1:100 protease inhibitor cocktail (Sigma-Aldrich) with an additional 3.5 mM aminoethylbenzene-sulfonyl fluoride hydrochloride (AEBSF) on ice. Supernatants were centrifuged at 4 °C for 5 min at 300 x g to remove residual cells and diluted 1:2 with self-prepared deimination buffer (8.58 mM $CaCl_2$, 5 mM DTT and 40 mM Tris-HCl pH 7.5) which, together with the 0.42 mM calcium in RPMI 1640, resulting in a calcium concentration of 4.5 mM. Supernatants were transferred to the ABAP-Assay (ModiQuest), incubated for 1.5 h at 37 °C and further processed according to the manufacturer's instructions.

2.10.2 PAD activity assay in synovial fluid

Frozen, cell-free synovial fluid samples from patients with RA and OA were either used non-diluted (at physiological calcium concentration) or diluted 1:100 with deimination buffer (artifical calcium concentration of 5 mM) before transfer of 100 µl onto the ABAP assay plate.

2.11 *In vitro* citrullination

Human recombinant histones H3.3, H2A and H4 (New England Biolabs), His-tagged human recombinant vimentin (Sigma, SRP5150) and calf thymus histones (Worthington Biochemical Corporation) were used as a substrate for the human recombinant PAD4 enzyme (MQ-16.203-2.5, stock concentration 18.7 mU/µl). For the enzymatic reaction 1 µg of substrate was added to 5 mU of PAD4 enzyme and diluted in deimination buffer, which was provided with the ABAP assay kit (compare 2.10.1). After citrullination for 2 h at 37ºC proteins were diluted with 5 x SDS loading buffer and used for Western Blotting (section 2.7).

2.12 Peptide ELISAs

Citrullinated and non-citrullinated peptides from histone H3.3 were synthesised by Innovagen, Sweden. Nunc high-binding 96-well plates (Thermo Scientific, 442404) were coated overnight with the peptide, which was diluted in carbonate coating buffer (Na_2 CO_3 1,59g/l , $NaHCO_3$ 2,93g/l, pH 9.6) at a concentration of 5 µg/ml. Next day, plates were washed and blocked with 1% bovine serum albumin (BSA) in PBS for 1 h and then incubated for 2 h with control and test sera, which were previously diluted 1:50 in RIA-buffer (10 g/L BSA, 350 mM NaCl, 1% Triton-X-100, 5g/L Na-deoxycholate (0.5%), 0.1% SDS, 10 mM Tris-HCl pH 7.6). Positive control sera were pooled from four anti-ccp antibody positive RA patients and negative control sera were pooled from four healthy individuals.

After washing with PBS and 0.05%Tween, plates were incubated with a secondary goat anti-human IgG HRP-conjugated antibody (Jackson 109-036-

008) at a final concentration of 0.04 µg/ml for 1 h. The HRP substrate tetramethylbenzidine (TMB) (Sigma) was diluted in phosphate-citrate buffer with sodium perborate (P4922-100) and the reaction stopped by addition of 2 M H_2SO_4. The optical density was measured at a wavelength of 450 nm in a plate reader.

2.13 Immunofluorescence microscopy

All samples were visualised using a Zeiss UV confocal LSM 510 microscope (Zeiss, Germany) and captured and processed using Zeiss LSM Image Examiner software (Zeiss).

2.13.1 Immunofluorescence staining of synovial fluid preparations and synovial tissue sections

Synovial fluid slide preparations were generated by pipetting 30 µl synovial fluid from patients onto a glass slide and cells were allowed to sediment for 2 min at RT. Supernatant was subsequently carefully removed and slides were left to air dry and then frozen at -20°C prior to use. Immunofluorescence staining was also performed on 5 µm frozen synovial tissue sections from RA patients. When required, synovial fluid slide preparations and synovial tissue slides were defrosted and fixed in 4% paraformaldehyde (PFA) (P-6148, Sigma) for 10 min, hydrated in PBS and blocked for 30 minutes with 10% FCS/PBS. Primary antibody preparations (CD15, neutrophil elastase or CD68) were incubated for 1 h at room temperature in PBS supplemented with 10% FCS and then washed in PBS. Concentration-, species- and isotype-matched antibodies were used as controls. Secondary antibodies (donkey anti-mouse IgM-Dylight 488, donkey

anti-rabbit IgG-Alexa Fluor 647, goat anti-mouse IgG2a-Cy5, respectively) were incubated for 30 min at room temperature in the dark, and nuclei were counterstained using 10 µg/ml Hoechst S769121 (Life Technologies). Slides were mounted with mounting medium (DABCO, in-house).

2.13.2 Staining of *in vitro* isolated neutrophils on coverslips

For immunofluorescence staining of *in vitro* stimulated cells, neutrophils were seeded on coverslips and fixed with 4% PFA for 10 min after stimulation and incubated overnight at 4^{o}C. Coverslips were rinsed with PBS, blocked for 45 min with PBS in 2% BSA, 2% goat and/or donkey serum and 0.25% Triton-X-100 as described (21). Samples were then exposed to primary antibody in PBS with 2% BSA and 0.25% Triton-X-100, washed in PBS, revealed using Alexa Fluor conjugated secondary antibodies and counterstained with 10 µg/ml Hoechst S769121.

2.13.3 Staining of cytospins of isolated neutrophils and synovial fluid cells

Cytospins of neutrophils from the peripheral blood of six healthy individuals and of peripheral blood neutrophils or SF infiltrate cells of five RA patients were re-suspended in MACS buffer and 1 x 10^5 cells were transferred onto a clean glass slide using a cytocentrifuge. All cytospins were stained using the same protocol and the images were acquired with the same settings. Cytospins were initially fixed with 4% PFA for 10 min, rinsed with PBS and then blocked for 45 min with PBS in 2% BSA, 2% goat serum, 2% donkey serum and 0.25% Triton-X-100. They were then exposed to anti-PAD4 and anti-NE antibodies in PBS

with 2% BSA and 0.25% Triton-X-100, washed in PBS, revealed using Alexa Fluor conjugated secondary antibodies (Biotin- and Streptavidin-conjugated antibodies for anti-PAD4) and counterstained with 10 µg/ml Hoechst S769121.

2.13.4 Quantification of PAD4 signal in neutrophils

For the quantification of cytoplasmic PAD4 signal compared with the total PAD4 signal on the immunofluorescence stainings obtained from cytospins described in section 2.13.3, pixel counts per μm^2 area were analysed using the ZEN 2010 software (ZEISS). For this purpose all NE-positive and intact neutrophils (60-80 cells) from five different fields of vision were isolated using the overlay function within the ZEN software as shown in the example provided in Figure 2-6A. The Image calculator function was then applied to subtract all PAD4 pixels, which overlap with the nuclear DNA signal, from the total PAD4 signal. Importantly, when the pixels of the DNA signal were subtracted from the total PAD4 signal, only the overlapping pixels were subtracted and not the total DNA signal. The histogram function within the software was used to obtain the pixel counts for each channel. After the subtraction a separate pixel count was generated for the PAD4 channel. Pixel counts of all different intensities (Figure 2-6B) from all channels were then exported from the ZEN software into Excel software (Microsoft) excluding the first 30 intensities in order to avoid the inclusion of intensities, which are artificially high. In the Excel software, the sum of all pixel intensities per μm^2 area for individual cells was calculated and the average for each cytospin determined. The percent of cytoplasmic PAD4 signal was then calculated using the following equation:

%cytoplasmic PAD4=100×(total PAD4 positive pixels per μm^2 area - overlapping pixels per μm^2 area) /total PAD4 positive pixels per μm^2 area

These values were then plotted graphically to enable identification of differences between neutrophils from the synovial fluid and peripheral blood of patients and healthy controls.

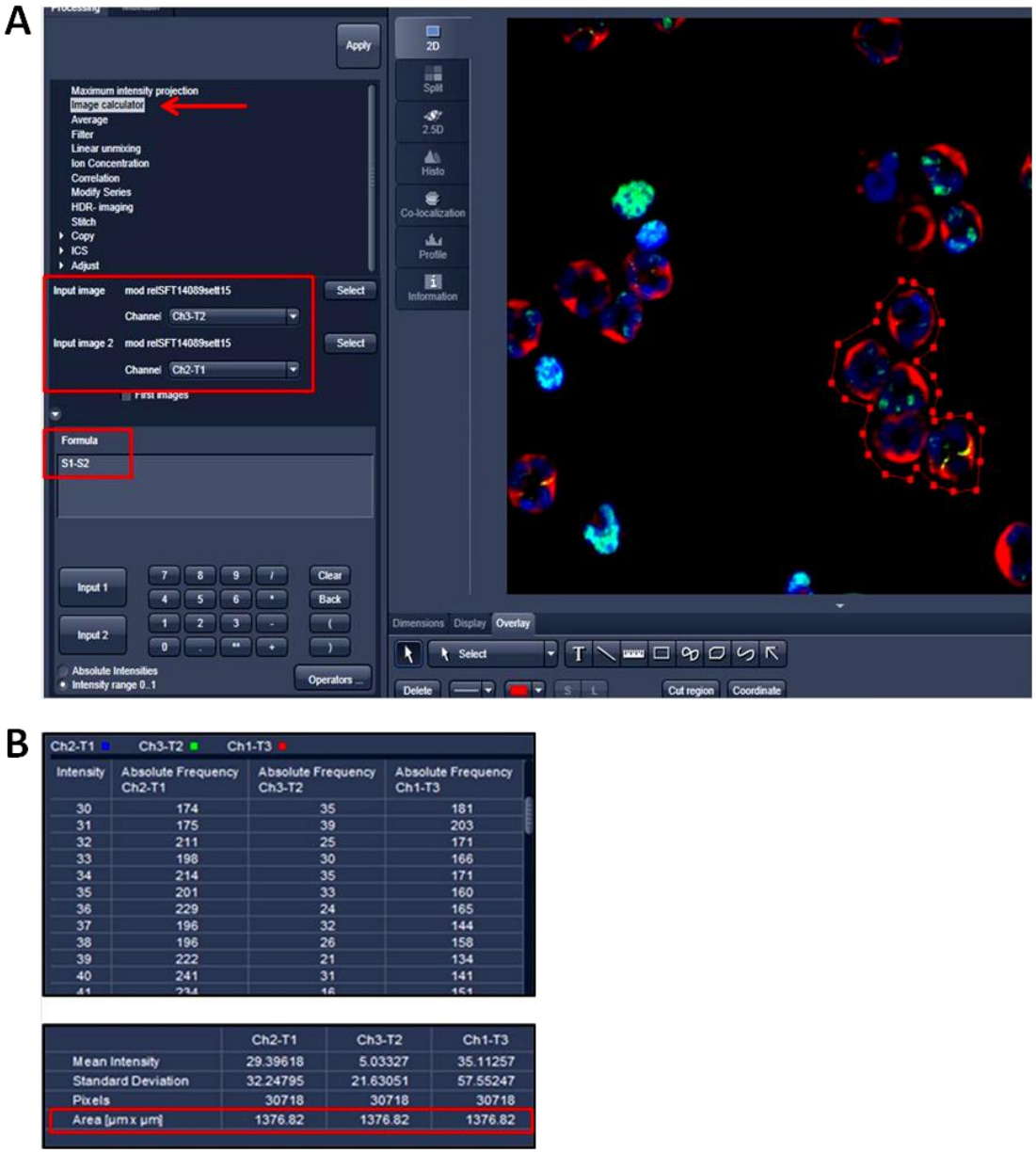

Figure 2-6 Image calculator function of the ZEN 2010 software

(A) To calculate the cytoplasmic pixel count of the PAD4 signal (green) in channel Ch3-T2 (Input S1), the Image calculator function in ZEN 2010 (indicated by the arrow) was used. With the subtraction of pixels in one channel (DNA signal, Input S2) from another channel (PAD4 signal, Input S1) only pixels overlapping in both channels are subtracted from the total PAD4 signal. For this purpose the formula Input S1 - Input S2 was typed into the formula display resulting in all pixels in Ch3-T2 without the one overlapping with the DNA signal. **(B)** Using the histogram function within the ZEN software all intensities excluding the first 30 strongest intensities (31-286) from each channel were exported into Excel software. Additionally, also the pixel intensities in Ch3-T2 (PAD4) excluding the one overlapping with Ch2-T1 (DNA) (not shown here) were added into the excel sheet. The sum of all intensities divided by the area [µm x µm] was then calculated for each channel separately and the ratio cytoplasmic PAD4/total PAD4 was determined.

2.14 Mass spectrometry

All mass spectrometry analyses were performed in collaboration with Jimmy Ytterberg at the Karolinska Institutet, Stockholm, Sweden.

2.14.1 Quantification of proteins in the supernatants and NET fractions of activated neutrophils

Quantitative comparison of protein levels in supernatant directly after PMA stimulation (SN) and DNase-I treated NETs (+DNase-I and/or D) were undertaken. Supernatant (SN) and DNase-I treated NETs (D) from stimulated neutrophils from 7 donors were digested with trypsin, analysed by mass spectrometry (4 donors by LTQ OrbitrapVelos ETD and 3 donors by Q Exactive), searched against the human complete proteome database and quantified by the Quanti software (319). Details are described in the appendix section 8.2. The list provided in the appendix (section 8.2.2) shows the 286 proteins that were quantified in both fractions of all patients. The data from the two instruments used for analysis is presented separately. The “PROTEIN ID” lists the UniProt accession numbers, the “PROTEIN IDs” lists all the accessions sharing peptides with the quantified accession, “log2 (D/SN)” lists the log2 of the ratio of medians of the two fractions, the “P (D vs SN)” lists the p-value using t-test, the “E” show the expectation value (n x p) together with the number of quantified proteins in the dataset. The Bonferroni corrected thresholds for significance are p = 1.70E-4 (Velos) and p = 9.01E-5 (Q Exactive) respectively.

2.14.2 Qualitative analysis of the presence of citrullinated proteins in the supernatants and NET fractions of activated neutrophils

The presence of citrullination in the total SN and DNase-I treated NET (alias "D") fractions was investigated by re-searching the data (generated as described in section 2.14.1) with the inclusion of citrullination (R) and deamidation (N/Q) as variable modifications. Spectra identifying citrullinated peptides were validated manually, by verifying that the precursor mass was correctly assigned and that the modified site was consistent with observed mass shifts in the fragment ions. All peptides identified as citrullinated with a Mascot score of at least 20 are shown. A score of 20 is a commonly used threshold (320) and is defined as $-10 \log(P)$, where P is the probability of a random match between the theoretical MS/MS spectra of a peptide and the measured MS/MS spectrum.

For the analysis of citrullinated peptides of 11 kD in the NET fractions, bands from five donors were excised from 1D-SDS-PAGE, reduced, alkylated and digested by trypsin using standard protocols (321). After zip tipping (Merck Millipore Ltd, Irland), the peptides were separated using on-line nLC-MS/MS (RP C18) and analysed on a LTQ Velos Orbitrap ETD MS (Thermo Fisher Scientific, Germany). The following gradient was used for the separation: 5-30% B in 35 min and 30-95% B in 5 min (A: 1% formic acid in water; B: 1% formic acid in acetonitrile), all at a flowrate of 300 nl/min.

2.15 Stimulation of neutrophils with enriched immune complexes from the SF of RA patients

Based on previous protocols published by Robinson et al. (322) and Mathson et al. (323) frozen and cell-free SF samples from RA patients were thawed and either pooled or used individually from each patient. Immune complexes (ICs) were enriched overnight at 4°C by combining the SF with an equal volume of ice-cold 5% polyethylene glycol (PEG) 6000 (Fluka, 03394) with a final concentration of 0.1 M EDTA. The following day, precipitates were centrifuged at 11600 x g at 4˚C for 10 min and washed twice with sterile PBS (Sigma). The precipitate, after centrifugation, was then diluted in the same volume of PBS as the original pool of synovial fluid samples. This solution of immune complexes (100%) was then further diluted to determine the percentage of 40% immune complexes sufficient to show an effect on freshly isolated neutrophils from the peripheral blood of healthy donors. For the blocking experiments antibodies against CD32a and CD16b (R&D) were used.

2.16 Statistical analyses

Each experiment was performed at least three times with a minimum number of two technical replicates unless otherwise stated. Non-parametric distribution was assumed for all assays. Individual tests used are indicated in the figure legends. p-values of less than 0.05 were considered statistically significant. Data were analysed using GraphPad Prism (version 5.0, GraphPad Software).

3 Detection of neutrophil extracellular traps in the joints of RA patients

3.1 Introduction

A considerable body of work suggests that neutrophils in patients with RA are functionally different from those isolated from healthy individuals (116). Neutrophils of RA patients, for example, are already primed for ROS production (109) and show an increased expression of several different cytokines (118). In the inflamed RA joints, these cells are rarely observed in synovial tissue, while they are the most abundant cell type in the SF (102). The abundance of neutrophils in early stages of disease (324–326) implicates a role in the pathogenesis of joint inflammation. This is also supported by several animal models of rheumatoid arthritis which depend on the presence of neutrophils (121,327,328).

SF neutrophils in RA patients have been shown to be activated and secrete cytokines which activate other immune cells such as B-cells (117,118) and promote further neutrophil recruitment from the circulation amplifying the inflammatory response (116). Additionally, exposure to immune complexes, cytokines and rheumatoid factor in the SF of RA patients can induce neutrophil activation and secretion of ROS and proteases (322,329) and may thus lead to damage of cartilage and surrounding tissue (330,331).

Autoantibodies against neutrophils have been described not only in systemic vasculitis and SLE but also in RA (332–334). Interestingly, anti-neutrophil cytoplasmic antibodies (ANCAs) were found to activate neutrophils causing degranulation and tissue damage and their presence was associated with higher joint scores in RA (335,336).

Recently, a novel cell death mechanism was described in neutrophils, the formation of neutrophil extracellular traps (NETs) or ‘NETosis’ (21). NETs are composed of chromatin associated with granular proteins and were found to primarily capture and immobilise microorganisms. Additionally, these structures were also demonstrated to be involved in the pathogenesis of several inflammatory conditions such as SLE, small vessel vasculitis, psoriasis or crystal arthritis (20–25).

Based on the above-described significance of neutrophils in RA and previous findings of extracellular DNA in the SF of RA patients (26,27) it was hypothesised here that neutrophils may contribute through NETosis to the pool of extracellular DNA detected in the synovial fluid of RA patients. In this chapter, the formation of NETs in the SF and ST in relation to evidence of neutrophil infiltration and extracellular DNA levels is investigated.

3.2 Extracellular DNA levels in the synovial fluid of patients with inflammatory arthritis correlate with neutrophil cell numbers

As described in detail by Fuchs et al. NETosis is characterised by the entire fragmentation of the nuclear envelope and the active release of free DNA into the extracellular space (24). In order to quantify extracellular DNA that may be released during NETosis into the SF the DNA dye SYTOX green was used, which has been previously described to be suitable for the staining of NETs due to its cell-impermeability (314). Subsequently SF samples were freshly obtained

and immediately processed without cryopreservation to exclude artificially induced necrosis of cells and thus release of DNA.

Quantification of extracellular DNA in untreated SF of patients with RA, OA and other types of inflammatory arthritis confirmed and extended previous findings that free extracellular DNA can be found in RA SF. Samples were compared to a known DNA standard solution in individual experiments and freshly isolated neutrophils from peripheral blood of healthy donors (PB PMNs) were used as negative control. Significantly higher DNA levels were found in SF of patients with RA compared to patients with osteoarthritis (OA) ($p<0.001$) and psoriatic arthritis (PsA) ($p<0.05$) (Figure 3-1A). A small number of patients with different types of inflammatory arthritis, including gout (n=2), pseudo gout (n=2), spondyloarthritis (SpA), reactive arthritis (n=1) or unclassified inflammatory arthritis (n=3), showed variable levels of extracellular DNA in the SF (Figure 3-1B). Validation experiments in which the DNA concentration in untreated SF samples was measured before and after centrifugation of cells showed that 78% (IQR 65-89, n=12) of the signal derived from cell-free SF samples suggesting that cells with permeable membranes such as necrotic or late-stage apoptotic cells contributed only a small proportion of the DNA signal (Figure 3-1C). In parallel experiments neutrophils from healthy donors were isolated and after inducing NETosis and necrosis the release of free extracellular DNA was compared. As shown in Figure 3-1D, a significantly higher amount of soluble extracellular DNA is released after NETosis compared with unstimulated and necrotic cells ($p<0.05$).

No statistically significant correlations were observed between DNA concentration and clinical parameters such as ESR, CRP, DAS28 (ESR), VAS, SJC and TJC (Figure 3-2 A-F). Interestingly, however, levels of free DNA in SF samples showed a weak, although significant positive correlation with disease duration ($r=0.4$; $p<0.01$), which could be increased when excluding patients receiving DMARDs (Figure 3-2G-H).

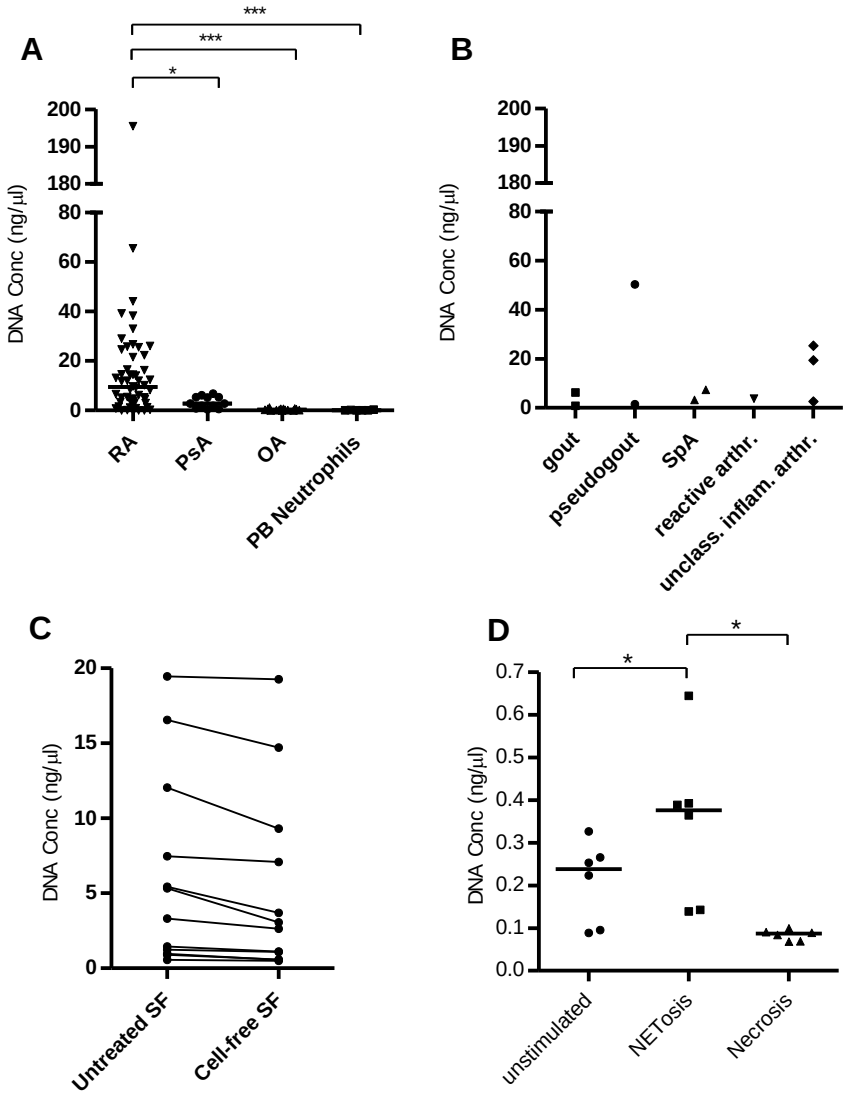

Figure 3-1 Detection of extracellular DNA in the synovial fluid of patients with inflammatory arthritis

(A) Extracellular DNA was quantified in the synovial fluid (SF) of patients with RA (n=54), osteoarthritis (OA) (n=15) and Psoriatic Arthritis (PsA) (n=12) using the cell-impermeable dye SYTOX Green. Freshly isolated neutrophils from peripheral blood of healthy donors (PB PMNs) (n=6) were used as negative control. **(B)** Quantification of extracellular DNA in the SF of patients with different types of inflammatory arthritis: gout (n=2), pseudo gout (n=2), spondyloarthropathy (SpA) (n=2), reactive arthritis (n=1), unclassified inflammatory arthritis (unclass. inflam. arthr.) (n=3). **(C)** Quantification of the DNA signal in 12 SF samples from patients with inflammatory arthritis revealed an approximate percentage of 78% (IQR 66-89) of the DNA signal derived from the cell-free fraction of SF samples. **(D)** Release of DNA into the supernatant of unstimulated, NETotic or necrotic neutrophils of healthy donors (n=6). To induce necrosis, neutrophils were frozen and then thawed and to induce NETosis the cells were stimulated with 25 nM PMA. Statistical analysis was performed using a Mann-Whitney test with horizontal bars representing median values (* indicates $p<0.05$, ** indicates $p<0.01$, *** indicates $p<0.001$).

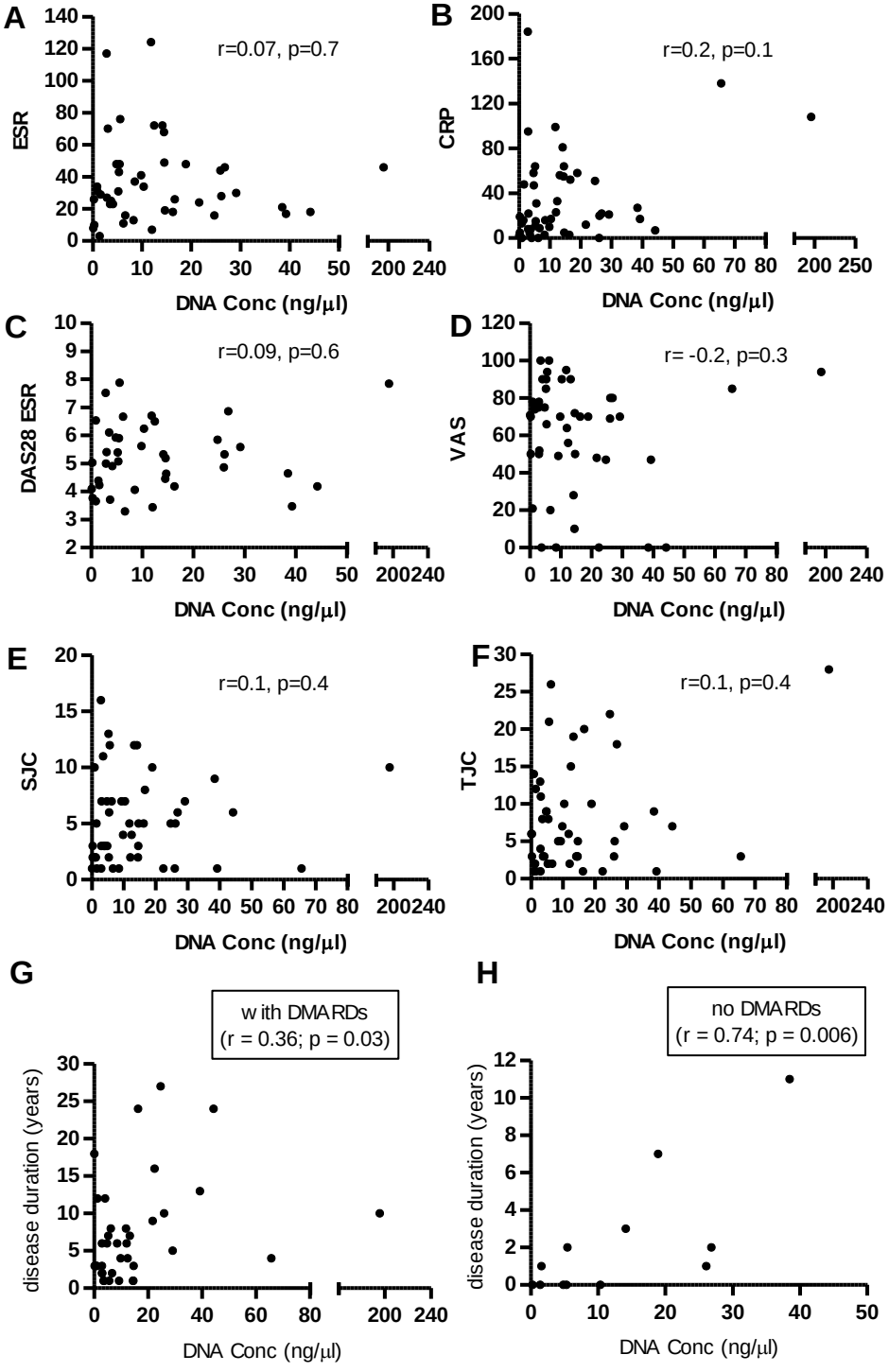

Figure 3-2 Relationship between DNA concentration and clinical parameters in RA patients

(A-F) Scatter plot showing relationship between DNA levels and erythrocyte sedimentation rate (ESR) (r=0.07; p=0.7), C-reactive protein (CRP) (r=0.2; p=0.1), DAS28(ESR) (r=0.09; p=0.6), visual analogue scale (VAS) (r= -0.2; p=0.3), swollen joint count (SJC) (r=0.1; p=0.4), and tender joint count (TJC) (r=0.1; p=0.4). **(G)** Scatter plot showing relationship between disease duration and DNA concentration in patients treated with DMARDs (n=37; r=0.36; p=0.03). **(H)** Scatter plot showing relationship between disease duration and DNA concentration in patients, which did not receive DMARDs (n=12; r=0.74; p=0.006). Data were analysed using Spearman's test for correlation. DMARDs= disease modifying anti-rheumatic drugs.

Concentrations of different cell populations including neutrophils in the SF infiltrate were determined using cytospins of cells, stained with a Romanowski stain (Diff Quick™). Using light microscopy cells were then quantified based on cell morphology. Occasionally, cells with decondensed nuclei within neutrophil aggregates could be detected suggesting the presence of neutrophils in the early stage NETosis (Figure 3-3A). Quantification of different cell populations revealed that neutrophils predominate in the synovial fluid infiltrate in most RA SF samples (Figure 3-3B).

Levels of free DNA in SF samples of RA patients showed a strong positive correlation both with total number of cells in the SF infiltrate (Figure 3-4A) and also neutrophil cell counts (Figure 3-4B). In contrast, no correlation between macrophage cell counts and DNA levels (Figure 3-4C) was observed. Instead, SF samples, in which neutrophil concentrations were higher than macrophage concentrations, displayed significantly higher DNA levels compared with SF samples, in which macrophages outnumbered neutrophils (Figure 3-4D). Additionally, a strong significant negative correlation between DNA levels and the proportion of macrophages from the total SF cell infiltrate could be observed (Figure 3-4E). Finally, a strong positive correlation between neutrophil numbers and disease duration was observed in RA patients when excluding those receiving methotrexate (MTX) treatment (Figure 3-4F).

In conclusion, these results support the notion that neutrophils may be a source of extracellular DNA in the SF while macrophages may be potentially

involved in the regulation of this DNA release from neutrophils, although additional investigations would be required to confirm this concept.

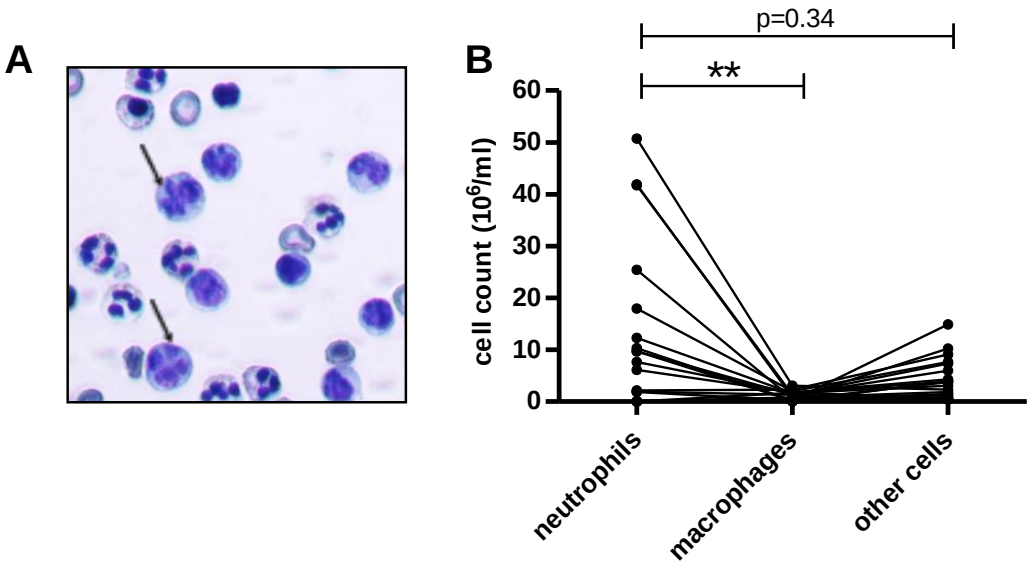

Figure 3-3 Determination of the cell composition in the RA synovial fluid

(A) Synovial fluid cells from RA patients were re-suspended in MACS buffer and 1 x 10^5 cells were transferred onto a clean glass slide using a cytocentrifuge, stained with Diff Quick™ and examined under light microscopy (40 x 10 original magnification). Representative synovial fluid sample with a predominantly neutrophilic infiltrate and cells with decondensed nuclei (indicated by arrows) are shown. **(B)** Comparison of the concentration of different cell populations in the SF infiltrate of RA patients. Other cells represent SF cells excluding macrophages and neutrophils, of which most were lymphocytes. Wilcoxon matched pairs test; n=20; **p<0.01.

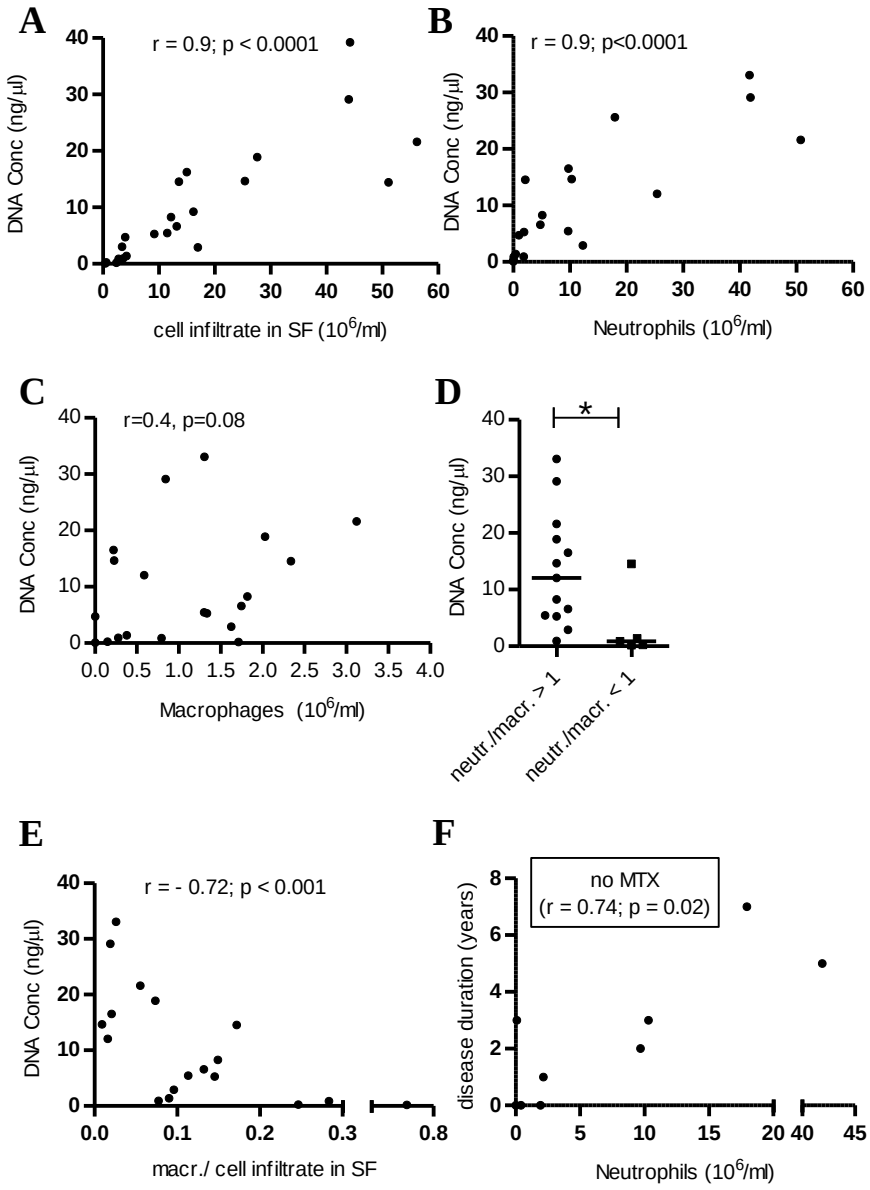

Figure 3-4 Neutrophil cell counts in RA patients correlate with DNA levels and disease duration

(A) Results are depicted as a scatter plot of DNA concentration (DNA Conc) against cell infiltrate and cell counts of different cell populations in SF from 22 patients with rheumatoid arthritis. **(B)** DNA concentration is shown in relation to neutrophil concentrations in SF from 20 patients with rheumatoid arthritis (n=20, r=0.88, p<0.0001). **(C)** DNA concentration is shown in relation to macrophage concentrations in SF from 20 patients with rheumatoid arthritis (n=20, r=0.4, p=0.88). **(D)** Significantly higher DNA levels are detected in RA SF samples with more neutrophils than macrophages (ratio Neutr./Macr. > 1) compared with SF samples, in which neutrophils are outnumbered by macrophages (ratio Neutr./Macr.< 1). Statistical analysis was performed using the Mann-Whitney test and horizontal bars represent median values (n=20; **indicates p<0.01). **(E)** Relationship between DNA concentration and the proportion of macrophages from the total number of cells in the SF infiltrate of RA patients (n=18, r=-0.7, p=0.001). **(F)** Neutrophil concentrations are shown in relation to disease duration in RA patients excluding those receiving methotrexate (MTX) treatment (n=9, r=0.74, p=0.2). Relationships between two variables were analysed using Spearman's test for correlation.

3.3 Visualisation of NETs in the synovial fluid and tissue of RA patients

Neutrophils are considered to be the most abundant cell type in the synovial fluid and show evidence of having initiated ROS generation *in vivo* (110), which is an absolute requisite for the induction of NETosis (24). Based on our findings of extracellular DNA in the SF and its strong correlation with neutrophil cell counts we hypothesised that the source of measured extracellular DNA may be NETs released from activated neutrophils in the joint. Therefore we sought to examine the neutrophil population in the joints of RA patients in more detail using confocal laser-scanning microscopy. To avoid NET disruption, synovial fluid was pipetted onto a glass slide and cells were allowed to sediment for 2 min. Subsequently the supernatant was carefully removed and slides were allowed to air dry. As shown in Figure 3-5, immunostaining of preparations of RA SF revealed a network of extracellular DNA strands similar to that reported for NETs in a range of studies. DNA co-localised with neutrophil elastase (Figure 3-5), a protein, which is tightly associated with NETs and currently widely accepted to represent a marker for NETosis (39,342). The majority of cells detected within this meshwork of DNA fibres were neutrophils, but also some macrophages were observed (Figure 3-6).

In frozen sections of synovial tissue, neutrophil aggregates were observed on the surface of the synovial lining, facing the joint cavity (Figure 3-7A). In agreement with the literature, relatively few neutrophils were detected within the

synovial tissue. As shown in Figure 3-7B, DNA staining revealed extracellular DNA associated within these aggregates.

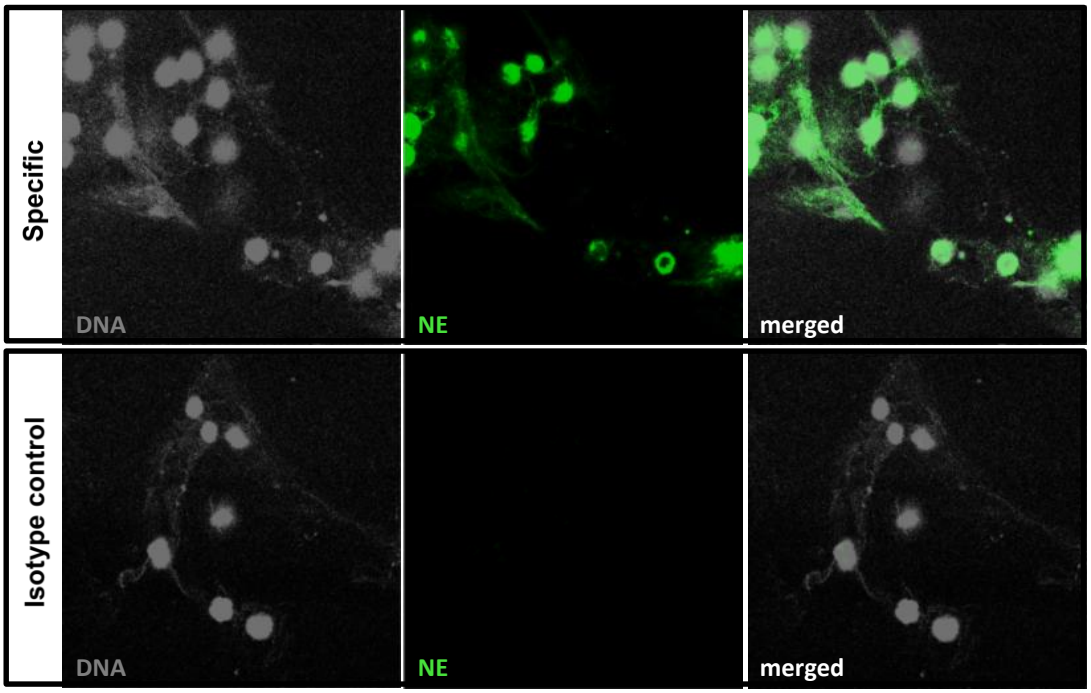

Figure 3-5 NETs can be detected in the synovial fluid of RA patients

Synovial fluid preparations from RA patients were stained for DNA (grey) and Neutrophil Elastase (green). Lower panel shows concentration and isotype matched control staining. Immunofluorescence staining was visualised using a confocal microscope and viewed at a final magnification of 63 x 10 original magnification. Images are representative of at least 10 SF samples.

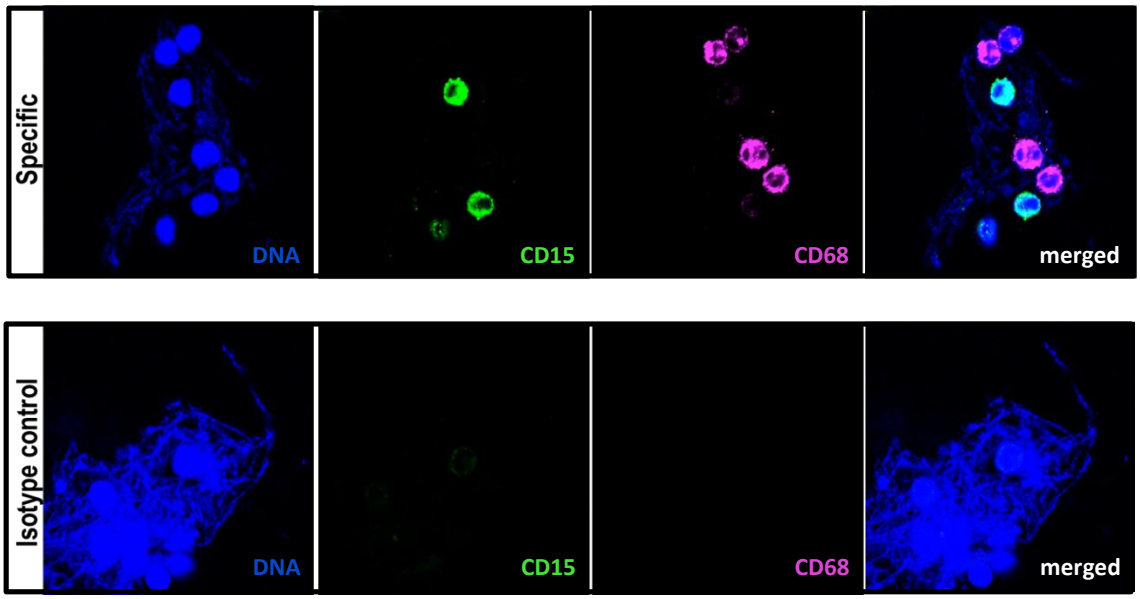

Figure 3-6 Neutrophil and macrophages staining in SF infiltrate

Confocal laser-scanning microscopy images of synovial fluid preparations (63 x 10 original magnification). Upper panel shows specific staining and lower panel concentration and isotype matched control staining. DNA is revealed with Hoechst dye (blue). CD15 is shown in green; CD68 is shown in violet. CD15-positive neutrophils and CD68-positive macrophages were found to be associated with NETs in the SF of RA patients.

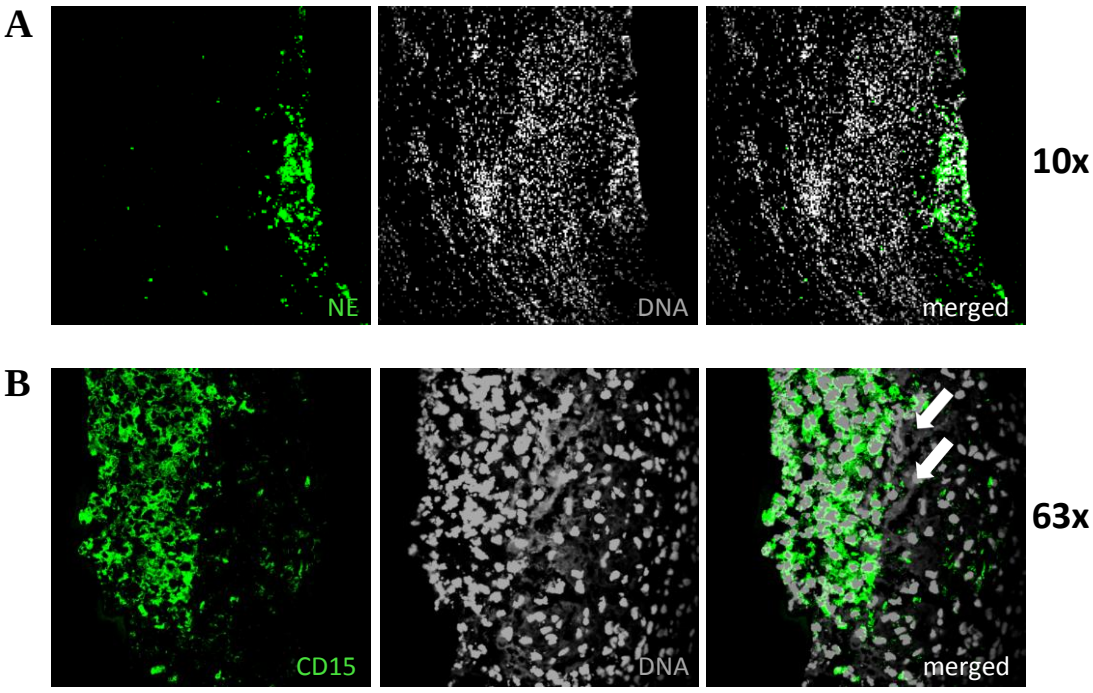

Figure 3-7 NETs within neutrophil infiltrate attached to synovial tissue of RA patients

(A) Confocal laser-scanning microscopy (10 x 10 original magnification) imaging revealed presence of neutrophil aggregates attached to synovial lining layer (n=3) (NE is shown in green and nuclear counterstain in grey). **(B)** 63 x 10 original magnification of neutrophils and extracellular DNA (indicated by arrows) attached to the surface of synovial tissue of RA patients (n=3). CD15 is shown in green; DNA is shown in grey.

3.4 Antibodies as potential triggers of NETosis in the synovial fluid of RA patients

The amount of extracellular DNA detected in the synovial fluid of RA patients suggests that the RA SF may represent an environment which promotes cell death. According to this scenario, studies were undertaken to determine whether NETosis of neutrophils could be induced after recognition of immune complexes by Fc receptors, especially as the induction of NETosis by autoantibodies such as ANCA or anti-ribonucleoprotein antibodies has been shown in SLE and small-vessel vasculitis (33,65). Although RF levels and ACPA levels above (7 units) and below (340 units) the threshold of detection in ACPA positive RA patients did not correlate with DNA levels in the SF (Figure 3-8A-B), a small but statistically significant difference in DNA levels of ACPA positive (n=34) compared with ACPA negative patients (n=12) could be observed (p=0.04) (Figure 3-8C), which could not be seen with RF levels (Figure 3-8D).

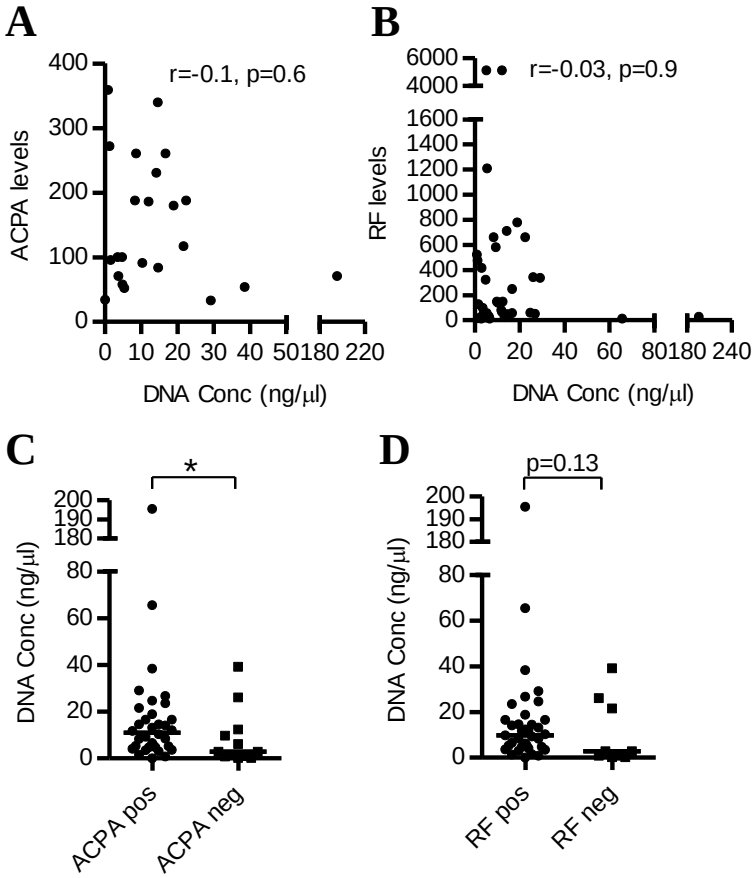

Figure 3-8 Influence of serum antibody levels on DNA levels in the SF

(A) DNA concentration is shown in relation to anti-citrullinated protein antibodies (ACPA) levels in the serum of 23 ACPA positive (ccp level >7 units) RA patients (r=0.1, p=0.6). Anti-ccp values above the detection limit of 340 units were excluded from the calculation. **(B)** DNA concentration is shown in relation to rheumatoid factor (RF) levels (r=-0.02, p=0.9) in 38 RA patients. **(C)** Statistically significant difference (p=0.04) of SF DNA levels between ACPA positive (anti-ccp value >7 units, including levels >340 units, n=34) and ACPA negative patients (anti-ccp vlaue <7 units, n=12). **(D)** Comparison of SF DNA levels between RF positive (n=37) and RF negative (n=9) RA patients (p=0.13). Statistical analysis was performed using Mann-Whitney test with horizontal bars representing median values.

To investigate the influence of antibodies in the synovial fluid of RA patients on neutrophils we enriched immune complexes (IC) based on previously reported protocols using precipitation with polyethylene glycol (PEG) (323,343). The synovial fluid of 8 ACPA positive and negative RA patients was pooled together and the immune complexes were enriched with PEG overnight. Subsequently the precipitate was centrifuged and diluted in the same volume of PBS as the original pool of synovial fluid samples. This solution of immune complexes (100%) was then further diluted to determine the percentage of immune complexes that is sufficient to show an effect on freshly isolated neutrophils from the peripheral blood of healthy donors. Validation experiments also excluded the possibility that PEG itself activates neutrophils (data not shown). As indicated by the co-staining of DNA and neutrophil elastase, a 40% IC solution was able to induce NETosis of neutrophils after only 30 min stimulation (Figure 3-9). In comparison, unstimulated neutrophils did not show any detectable signs of NETosis even at 240 min of culture (Figure 3-9). These findings were also confirmed using SYTOX green staining, which revealed significantly increased DNA levels in the supernatants of stimulated cells compared with unstimulated cells after only 30 min of stimulation, which could not be observed after 30 min of stimulation with 25 nM PMA, a well-described stimulant for NETosis (314) (Figure 3-10A). At 240 min, however, a comparable amount of DNA could be detected in immune complex-stimulated neutrophils compared with PMA-stimulated neutrophils (Figure 3-10A).

To investigate further whether the observed activation and NET release of neutrophils is influenced by the presence of ACPA within immune complexes,

neutrophils were separately stimulated with IC enriched from SF samples of ACPA negative (n=8) and ACPA positive (n=10) patients. Compared with neutrophils, which were stimulated with IC enriched from ACPA negative samples, a trend towards a higher DNA signal in the supernatant of cells, which were stimulated with IC enriched from ACPA positive SF samples could be observed (Figure 3-10B), although no statistically significant difference was detected (Figure 3-10C). Similarly, no statistically significant difference was observed when comparing RF positive and negative samples (data not shown). Additionally, to assess whether the induction of NETosis is mediated through Fc receptors, the two main Fc receptors, FcγRIIA (CD32a) and FcγRIIIb (CD16b), present on neutrophils were blocked. To exclude the possibility that the blocking antibodies themselves could activate neutrophils, unstimulated neutrophils were incubated with the same concentration of blocking antibodies as the stimulated cells, respectively. No reduction of NETosis, as induced by 40% IC, was observed after incubation with 20 µg/ml or 60 µg/ml blocking antibodies (Figure 3-10D).

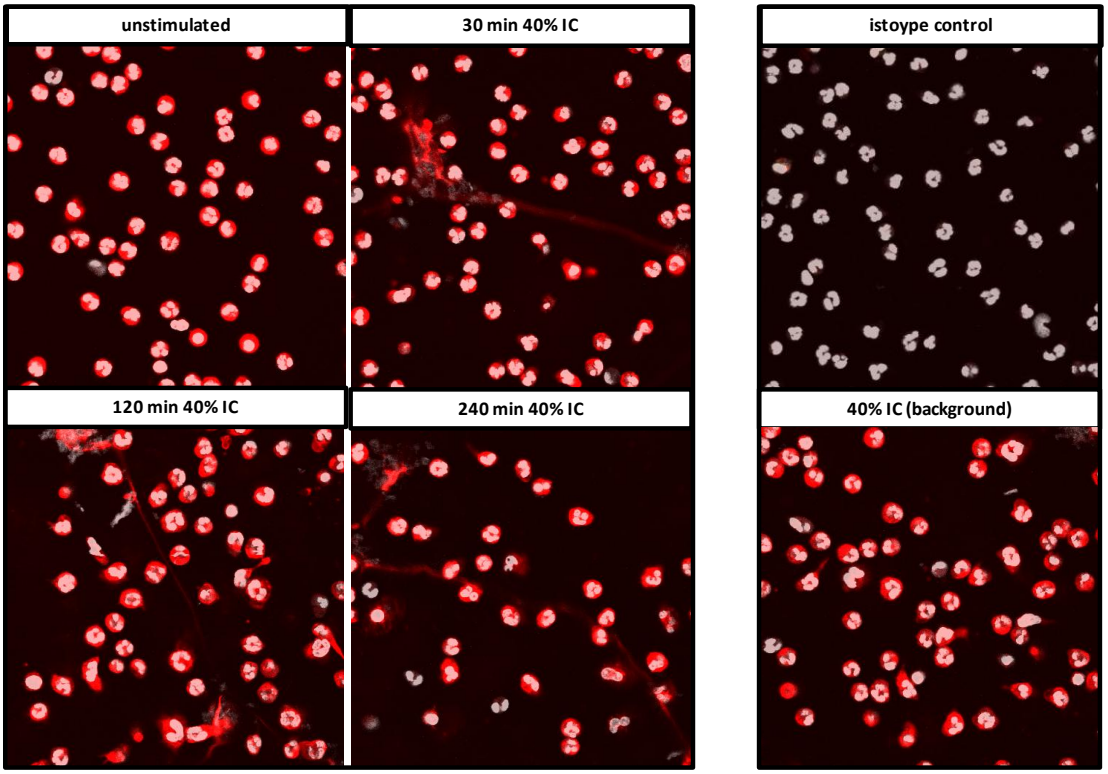

Figure 3-9 Immune complexes enriched from RA SF induce NETosis

Synovial fluid from 8 RA ACPA positive and ACPA negative patients were pooled; immune complexes (IC) were precipitated and used at a concentration corresponding to 40% of the original volume SF. Neutrophils were isolated from peripheral blood of healthy donors and left to adhere for 30 min before stimulation. Confocal laser-scanning microscopy analysis of neutrophils from healthy donors (63 x 10 original magnification). Cells were either left untreated for 240 min (unstimulated) or stimulated with 40% IC for 30 min, 120 min and 240 min. Upper panel on the right shows concentration and isotype matched control staining of unstimulated neutrophils at 0 min (isotype control). To exclude a possible enrichment of NETs within the added immune complexes, cells were fixed immediately after adding 40% IC (40% IC background) as a control (bottom panel on the right). Neutrophil elastase is shown in red and nuclear counterstain in grey. One representative experiment out of three independently performed experiments is shown.

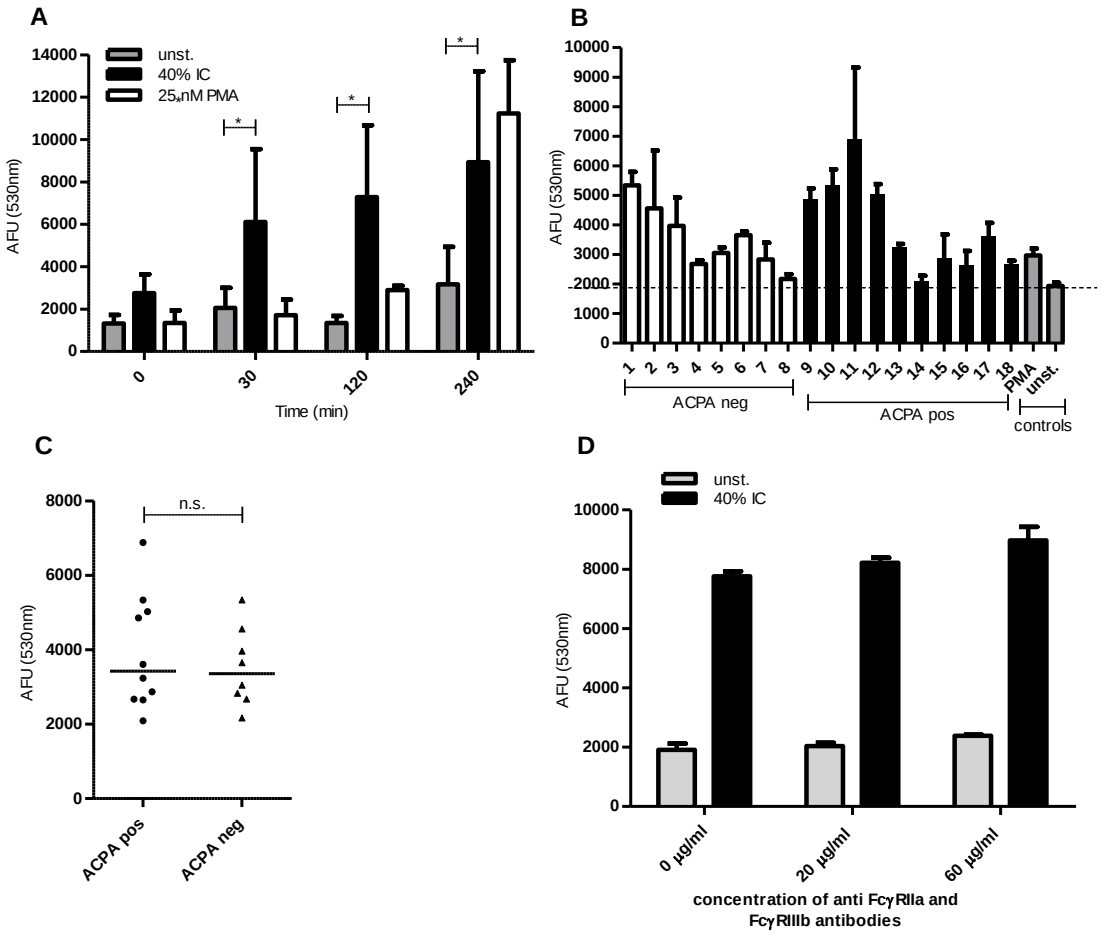

Figure 3-10 Influence of enriched immune complexes from RA synovial fluid on neutrophils

Release of extracellular DNA after stimulation with 40% IC is measured in arbitrary fluorescence units at 530 nm (AFU (530 nm)) using SYTOX green. **(A)** Time course study of release of extracellular DNA from neutrophils stimulated with 40% IC enriched from the pooled SF of 8 ACPA positive and negative patients in 5 independently performed experiments. 25 nM PMA was used as a positive control for the induction of NETosis and unstimulated neutrophils as a negative control. Statistical significance was determined by paired Student's t-test (*p<0.01). **(B)** Neutrophils were stimulated for 1 h separately with 40% IC isolated from the SF of 8 ACPA negative (1-8 ACPA neg) and 10 ACPA positive RA patients (9-18 ACPA pos). 25 nM PMA was used as positive control for the induction of NETosis (PMA). Horizontal broken line indicates background level of extracellular DNA in the supernatant adjusted to unstimulated neutrophils after 1 h in cell culture (unst.). One experiment out of 4 independently performed experiments is shown. **(C)** Statistical analysis of difference in DNA levels shown in (B) using Mann-Whitney test with horizontal bars representing median values (p=0.9). n.s.=non-significant. **(D)** Neutrophils were either stimulated with 40% ICs from pooled SF samples (40% IC) or left untreated (unst.) for 1 h in the presence of 20 µg/ml or 60 µg/ml receptor blocking antibodies against the Fc receptors FcγRIIA (CD32a) and FcγRIIIb (CD16b). One representative experiment out of two independently performed experiments is shown. All results are shown as mean ±S.D.

3.5 Discussion

This chapter addresses the question as to whether neutrophils could contribute through NETosis to the pool of extracellular DNA detected in the synovial fluid of RA patients. Previous findings of free DNA in the synovial fluid of RA patients were confirmed and found to be not only strongly correlated with neutrophil cell numbers in the RA SF but also with disease duration. Extensive NET formation in the joints of RA patients were visualised using confocal microscopy and NETosis of neutrophils from the peripheral blood of healthy donors could be induced with immune complexes enriched from the synovial fluid of RA patients.

The presence of free DNA in the synovial fluid and serum of patients with arthritis has already been described by Leon et al. in 1981 (340). In agreement with our findings, this study reported significantly increased levels of DNA in RA SF compared with DNA levels in the SF of OA patients. The same results were confirmed in a more recent study, which in addition also found a correlation between DNA levels in the synovial fluid and SF leukocytes (341). This is similar to our observations which demonstrate a strong correlation with the total population of synovial fluid cells and, more precisely, neutrophil cell counts.

Several previous studies have reported the presence of NETs at the site of inflammation. Although NETs were originally shown to be involved in the immobilisation and killing of microbes due to the concentrated presence of antimicrobial agents within NETs (24,36,315), their presence was recently also described in sterile inflammation (339,344). Confocal microscopy analysis used

in this study revealed the presence of a meshwork of DNA fibres co-localised with neutrophil elastase and associated with neutrophils and occasionally macrophages in the joints of RA patients, but also patients with other forms of inflammatory arthritis (data not shown). They were not only found in the SF but were also attached to the surface of the synovial lining facing the joint cavity and resembled the appearance of NETs reported in a range of studies. These results are therefore consistent with the concept that extracellular DNA is associated with the localisation and number of neutrophils present in the SF of patients with inflammatory arthritis and likely to be a result of extensive NET formation in the inflamed joint. These results are also in line with a recent study, in which NETs were generated upon activation of neutrophils by MSU or CPPD crystals in gout and pseudo gout patients, respectively (339,345), which indicate the different mechanisms for the induction of NETs in different types of inflammatory arthritis.

Whereas in chronically inflamed synovial tissue only relatively low numbers of neutrophils are observed, these cells are in general known to be the most abundant cell type present in the SF of patients with RA (103,116). In light of the high abundance of neutrophils, the strong correlation with DNA levels and the observed NET formation, these data suggest that NETosis may be a source of extracellular DNA in the synovial fluid. Interestingly, this notion is also reinforced by the finding of significantly lower DNA levels in psoriatic arthritis patients, in which a trend of decreased neutrophil cell counts was detected compared to RA SF samples. Nevertheless, this study cannot exclude the possibility that cells other than neutrophils contribute to the levels of DNA in RA

SF. As noted, macrophages can also account for a large proportion of the cellular infiltrate. Furthermore, cells such as eosinophils, mast cells or macrophages can release their chromatin in a process similar to NETosis (28,346,347). However, eosinophils and mast cells are present in only relatively low numbers in RA SF in a small proportion of RA patients (28). In addition, macrophage cell counts in this study showed no significant correlation with levels of extracellular DNA. Instead, SF samples, in which macrophages outnumbered neutrophils, showed significantly lower DNA levels compared with SF samples, in which neutrophils outnumbered macrophages in the SF infiltrate. As macrophages are one of the main professional phagocytes participating in the removal of dead cells (348,349), it is therefore conceivable that SF macrophages are involved in the removal of cellular debris derived from neutrophils. With regard to clearance mechanisms of dead cells it was also interesting to find that the only clinical parameter that DNA levels in the RA SF correlated with was disease duration. At the same time, a strong correlation between neutrophil but not macrophage numbers and disease duration could be found when excluding patients receiving treatment with methotrexate. There could be several possible explanations for this association between DNA levels in the SF with disease duration. One possibility is that the equilibrium between influx in, and removal of, neutrophils from the SF becomes disturbed over time due to changes in neutrophil recruitment or clearance defects. Another possibility, however, could also be that changes in the disease phenotype over time lead to an increased rate of cell death in the SF with disease duration. In support of this view and in the context of NETosis it was shown in SLE patients that complement protein C1q appears to protect NET DNA from DNase I

degradation, and that an increased binding of autoantibodies over time further increased C1q deposition which resulted in decreased NET degradation (64). Similar processes are also possible in RA, but would need to be proven experimentally in future studies. Additionally, it was interesting to observe that a much weaker correlation between DNA levels and/or neutrophils and disease duration was observed when patients receiving methotrexate or other DMARDs were included. This would indicate that neutrophil cell death could potentially be influenced by DMARDs and, more precisely, methotrexate. In this context it was reported that low doses of methotrexate can enhance adenosine release from connective tissue cells which inhibits neutrophil adherence to these cells (350,351). In view of these data, patients treated with methotrexate may therefore show decreased levels of neutrophil recruitment into the synovial fluid and neutrophil cell death, which could explain the observed weaker association of DNA levels and/or neutrophil concentrations with disease duration when including these patients in the statistical analysis.

In search of an answer to the question as to how neutrophils are possibly activated to enter into NETosis in the RA SF we hypothesised an influence of autoantibodies, as ANCA and anti-DNA antibodies in SLE and ANCA-associated vasculitides have been shown to induce NETosis (33,66). The exact molecular mechanism, as to how this may happen, still remains elusive. In addition, immune complexes in RA have long been proposed to play a role in neutrophil activation primarily based on data generated from murine arthritis models such as the K/BxN model (300,311). In humans, immune complexes (IC) have also been found in the SF and ACPA in the SF were shown to be

enriched compared to the peripheral blood (352). Recently, rheumatoid factor was reported to activate neutrophils via Fcγ receptors on neutrophils in arthritis-associated vasculitis (331). In view of these studies it was interesting to find that indeed PEG enriched immune complexes from SF of RA patients induced NETosis in neutrophils. PEG precipitation is a well-recognised technique for the isolation of high-molecular-weight ICs. However, earlier investigations showed PEG-precipitated sera to contain uncomplexed immunoglobulins, C3 (353) and a number of serum proteins including fibronectin and albumin (343). Therefore PEG precipitates are not only composed of ICs. This may explain why the rate of NETosis is not decreased by pre-incubating the cells with blocking antibodies against the Fc receptors FcγRIIA (CD32a) and FcγRIIIb (CD16b). This would suggest that other factors, which were co-enriched by PEG, are possibly also involved in the induction of NETosis.

In agreement with an ACPA-dependent induction of NETosis, a trend of increased release of extracellular DNA could be detected when stimulating neutrophils with IC enriched from the SF of ACPA positive patients compared with ACPA negative patients. Additionally, a small but statistically significant difference in DNA levels in the SF of ACPA-positive compared with ACPA-negative RA could be detected. However, it can be assumed that this study currently does not have sufficient statistical power to reveal the influence of ACPA on DNA levels in the SF. Additionally, due to the low number of available samples, in which the cell number could be determined, it could not be identified as to whether the difference in DNA levels arises because of a difference in neutrophil numbers between ACPA positive and negative RA patients or

whether other factors are involved. Interestingly, in the previously mentioned work of Leon et al., in which a larger sample number of 106 patients was studied, a statistically significant difference between seropositive and seronegative samples could be measured (340). Nevertheless, since no sufficient knowledge about ACPA was available at that time no further details can be drawn from this report. More recently, two publications reported on the association of NETosis with ACPA (120,354). In agreement with the IC experiments in this thesis, Khandpur et al. detected induction of NETosis in control and RA peripheral blood (PB) neutrophils upon exposure to sera and SF from RA patients. Interestingly, they also found a correlation between NET formation by peripheral blood (PB) neutrophils from RA patients and the titre of ACPA, but no correlation with disease duration. In this regard, our data therefore do not overlap with these results, however, due to missing information with regards to the number of experiments and samples included in their study it was difficult to make direct comparisons with the experiments presented here and ultimately draw definitive conclusions. With regard to additional stimuli that may induce NETosis in RA patients, Khandpur et al. also reported that the presence of TNF-α and IL-17 triggered NETosis in a ROS-dependent manner supporting our view of further antibody-independent ways of inducing NETosis in RA. Nevertheless, the exact explanation as to how this induction may occur remains elusive, as it is still unknown how neutrophils are activated by IL-17 since studies suggest that these cells do not express the IL-17 receptor C which forms a multimeric complex with IL-17 receptor A and is required for IL-17 receptor signal transduction (355,356). Others also report about the induction of NETosis by the alarmin HMGB1 (344) or GM-CSF in combination with the

complement factor 5a (C5a) (357). Taking into account that the concentrations of GM-CSF (358) and C5a (309) are much higher in the SF of RA patients, and considering the fact that we found macrophages which are known to produce GM-CSF in high amounts associated with neutrophils and NETs on SF preparations, these mediators could possibly be of great importance for NET formation. Moreover, findings in mouse models of inflammatory arthritis have revealed that C5a is critically involved in inflammatory joint damage and that anti-C5a antibodies have been proven effective in the prevention of the disease in these mice (359,360).

Although the *in vitro* experiments presented here demonstrate less DNA release from necrotic neutrophils compared with NETotic neutrophils and although attempts were made to exclude the measurement of DNA derived from SF cells with permeable membranes in our assays, it is still difficult to certain as to which type of cell death precisely contributed to the pool of extracellular DNA in the SF of patients with inflammatory arthritis. Indeed NETosis may well be not the only source of extracellular DNA in the joints of patients with inflammatory arthritis. Additionally, caution has to be taken with respect to the significance of NETosis for the RA pathogenesis compared with other cell death mechanisms in the RA joint since different types of cell death were reported to have either pro- or anti-inflammatory effects on macrophages (349,361).

Nevertheless, the discovery of NETosis in the joints of patients with inflammatory arthritis, no matter at what proportion, not only implies a possible pathogenic role due to cytotoxicity of NETs but also suggests an important role

for neutrophils in the supply of intracellular autoantigens. This concept associates with the widely-accepted hypotheses linking cell death to the initiation of systemic autoimmunity (361–363). This aspect will further be studied in the following chapters and its significance particularly for RA will be highlighted.

4 Peptidylarginine deiminase activity in the synovial fluid of RA patients

4.1 Introduction

Citrullination (or deimination) is a post-translational modification, in which arginine residues are converted into citrulline. This calcium-dependent enzymatic reaction is catalysed by peptidylarginine deiminases (PADs) and leads to a change in protein structure. The family of PADs consists of five highly homologous and functionally similar isoenzymes, but these enzymes differ in their expression pattern throughout organ systems and cell types (185,186). Activation of PAD isoforms is relevant to RA, as specific autoimmunity to citrullinated proteins can be observed in approximately 60% of RA patients (171,364) and their presence defines a group of patients with more aggressive disease and distinct genetic associations. Anti-citrullinated protein antibodies (ACPA) are enriched in the synovial fluid of RA patients compared with serum (352,365) and local B cell responses to citrullinated proteins have been observed in the rheumatoid joint (235). Although citrullination of intra- and extracellular proteins can be found in the synovial tissue and synovial fluid of RA patients (248,249,254), it is a general inflammation-dependent process and not specific for RA (251,252).

Neutrophils express PAD2, which is ubiquitously expressed, and PAD4 which is mainly expressed by myeloid cells. Recently, PAD3 expression in human primary neutrophils has also been described (203). PAD4 is the only PAD isoform with a nuclear localisation signal and its activity was described to be essential for NET formation (44,46).

Our observation of NETosis in arthritic joints raises the possibility that enzymatically active PADs are released into the SF during NET formation, and

thus implicates a central role for neutrophils in the generation of autoantigens for the local inflammatory response. In the work described in this chapter the development of an *in vitro* assay will initially be reported and the release of PADs from neutrophils entering into NETosis and the localisation of PADs in these cells is investigated. Furthermore levels of PAD activity in SF in relation to the observed neutrophil infiltration will be examined and lastly, possible additional PAD release mechanisms will be discussed.

4.2 Method development for the *in vitro* isolation of NETs

Since NETosis leads to the release of intracellular proteins, firstly it was sought to determine whether, and how, neutrophils undergoing NETosis release PADs into the extracellular space. If neutrophils in the SF contribute to the pool of available extracellular PADs it is important to know whether PAD isoforms during NETosis are released attached to the DNA/protein complex of the NETs or whether they diffuse freely. If PADs remain tethered to NETs, this would potentially limit the role of neutrophil-derived PADs to the SF. For this purpose, an *in vitro* assay of NET isolation and detection was developed based on a previously published method (315). Initially, to determine an optimal time point for the isolation of NETs, a time course after stimulation of neutrophils with 25 nM PMA was performed using SYTOX green in order to monitor DNA levels in the supernatants. As shown in Figure 4-1, a statistically significant difference between the release of extracellular DNA in stimulated and unstimulated

neutrophils could be observed 240 min after stimulation with 25 nM PMA. This time point was therefore selected for the isolation and purification of NETs in the following experiments.

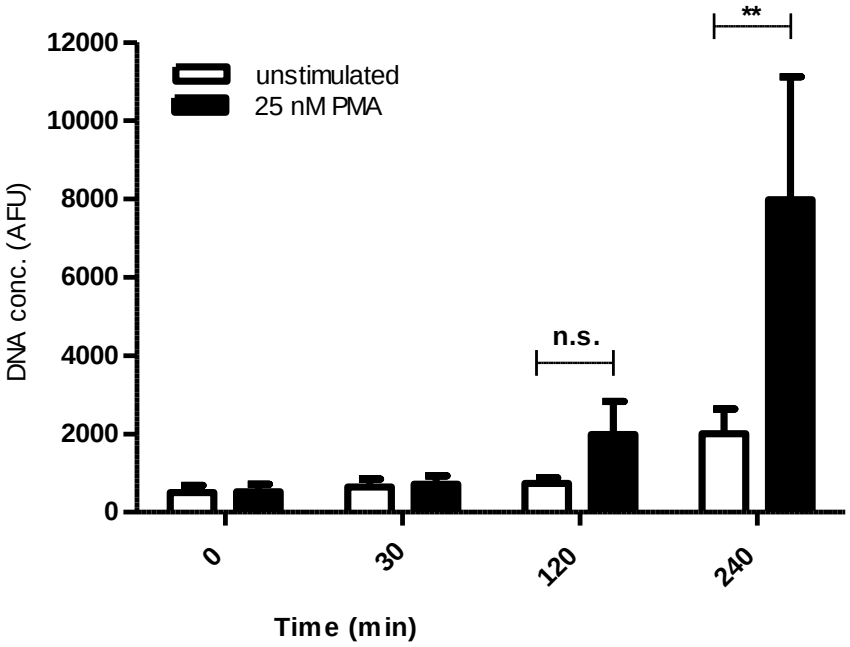

Figure 4-1 *In vitro* time course analysis of DNA release post-stimulation with PMA

Neutrophils were isolated from peripheral blood of healthy subjects and stimulated with 25 nM PMA. Significantly higher DNA levels were found in the supernatant after 4 h of stimulation with PMA compared with non-stimulated cells (Wilcoxon matched-pairs signed rank test, n=8; n.s.: non-significant; ** indicates $p<0.01$). Results are shown as mean ±S.D.

For the study of NET-associated proteins it is essential to avoid contamination with unbound proteins that are released freely into the extracellular space during NETosis. The method developed therefore took advantage of the capacity of activated neutrophils to attach firmly to the bottom of tissue culture plates. For this purpose, peripheral blood neutrophils were isolated from healthy donors and seeded in 12-well plates. After stimulation of 4 h with 25 nM PMA neutrophils were washed three times to remove unbound proteins. At this stage, the majority of the NETs remained associated with activated neutrophils at the bottom of the plate. In the final step DNase-I was used to release NETs from the cells into the supernatant. To verify the purification procedure, DNA levels in the supernatants generated during NET isolation were tracked using SYTOX green. As shown in Figure 4-2, only a small proportion of DNA was detectable in the supernatant of stimulated neutrophils (SN) indicating that NETs remain largely attached to the neutrophil-layer at this stage. After 3x washing (W1-W3) DNase-I treatment released a fraction containing significantly higher levels of DNA (+DNase-I) compared with fractions derived from stimulated neutrophils incubated without DNase-I (-DNase-I) or non-stimulated neutrophils treated with DNase-I (+DNase-I (unst.)) (Figure 4-2). Importantly, all supernatants were centrifuged once at 300 x g to remove cells and a second time for 16 000 x g to remove cell debris from the supernatants to ensure the specific measurement of NET-derived DNA.

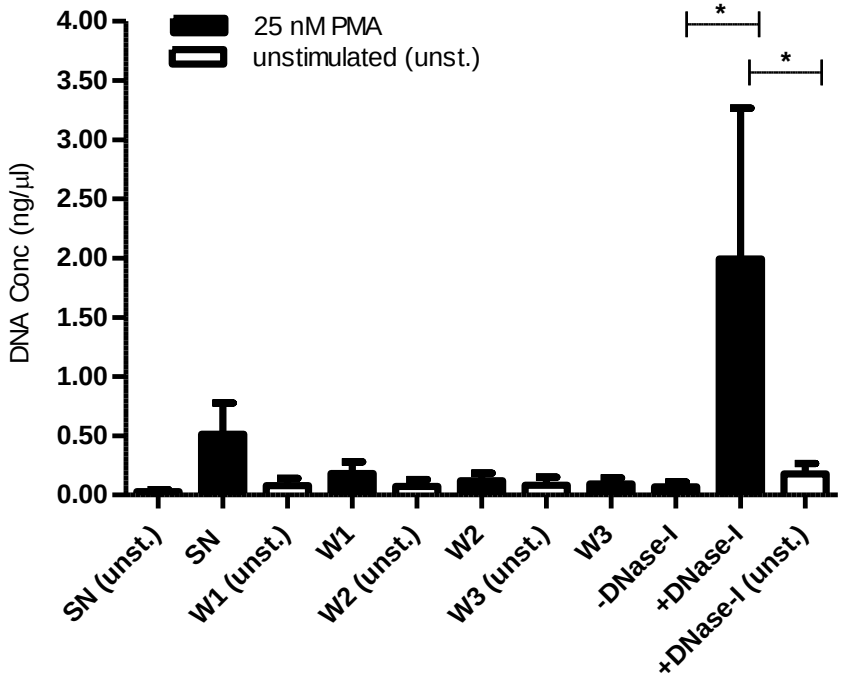

Figure 4-2 DNA levels in supernatants generated during *in vitro* NETosis

Supernatants of unstimulated (SN (unst.)) or stimulated neutrophils (SN) were collected. After stimulation, cells were washed 3 x with RPMI (W1-W3) and subsequently incubated with or without DNase-I (+DNase and –DNase). Non-stimulated cells were treated with DNase-I (+DNase (unst.)) as control. NETs could be specifically enriched in the supernatant of stimulated neutrophils treated with DNase-I (+DNase-I = NET fraction) compared with control fractions (Wilcoxon matched-pairs signed rank test, n=7; * indicates $p<0.05$). All fractions were centrifuged to remove cells and cell debris. Release of NETs was detected using SYTOX Green. Results are shown as mean ±S.D.

4.3 Analysis of PAD release during *in vitro* NETosis

Having established and validated a method for the isolation of NETs, the protein composition in the different fractions of the *in vitro* model were determined, as described in 4.2. The supernatants were precipitated using trichloroacetic acid (TCA) and western blotting was performed with each of the fractions. Importantly, anti-PAD2 and anti-PAD4 antibodies were assayed for cross-reactivity using human recombinant PAD4 and human skeletal muscle tissue, which is known to specifically express just the isoform PAD2, but not PAD4. As shown in Figure 4-3A, the antibodies did not show any cross-reactivity between different PAD isoforms. Using these antibodies it was then demonstrated that both PAD2 and PAD4 can be detected in the SN and in the NET fraction (+DNase-I), suggesting that PAD2 and PAD4 are both freely diffusible as well as released attached to NETs (Figure 4-3B). Neutrophil elastase, which was already shown to be one of the most abundant NET-associated proteins, was used as an additional control. As expected it was found to be associated with the NET fraction in this approach. Additionally, in accordance with the previously shown STYOX green assay (Figure 4-2) for DNA release, histone H3 could be detected both in the SN and the chromatin-rich NET fraction.

To validate these results quantitative proteomics after trypsin digestion was performed. In agreement with Urban et al. a small number of mainly granular and nuclear proteins were confirmed to be enriched in the NET fraction (315) (Table 4-1). In comparison, a wide range of proteins were found to be released into the supernatant during NETosis, which were either enhanced in the SN

fraction or present in both fractions (listed in Appendix, Table 8.5). In agreement with the western blotting data, PAD2 and PAD4 were detected both in the supernatant and in the DNase-I treated NET fraction from seven patients in two different analyses: while PAD2 was more abundant in the SN fraction, PAD4 was more abundant in the NET fraction (listed in Appendix, Table 8.5).

Furthermore, to test whether the PAD2 and PAD4 enzymes that are released into the supernatant during *in vitro* NETosis are enzymatically active, PAD activity was determined using a recently developed assay (19). Firstly, increased PAD activity with the addition of protease inhibitors was observed (Figure 4-4A). This is not potentially surprising, as enzymatically active PADs are known to be autocitrullinated (199,200) and citrullinated proteins have been reported to be more susceptible to proteolysis due to citrullination-induced protein unfolding (185,191,193). Additionally, enzymatic PAD activity in supernatants from neutrophils could be increased by diluting the supernatants 1:2 with calcium concentrations of up to 8.58 mM resulting in a final concentration of 4.5 mM calcium (Figure 4-4B). At final calcium concentrations at 10 mM and higher, however, no PAD activity could then be detected (Figure 4-4B). PAD activity in RPMI, which contains a physiological calcium concentration of 0.42 mM, was therefore minimally detectable but could be increased at non-physiological calcium concentrations in agreement with previous reports (48). Using a final calcium concentration of 4.5 mM together with protease inhibitors, the PAD activity assay could be optimised in a way that revealed significantly higher levels of PAD activity in the supernatants of *in vitro*

stimulated neutrophils compared with non-stimulated cells after 2.5 h of stimulation with 25 nM PMA (Figure 4-4C).

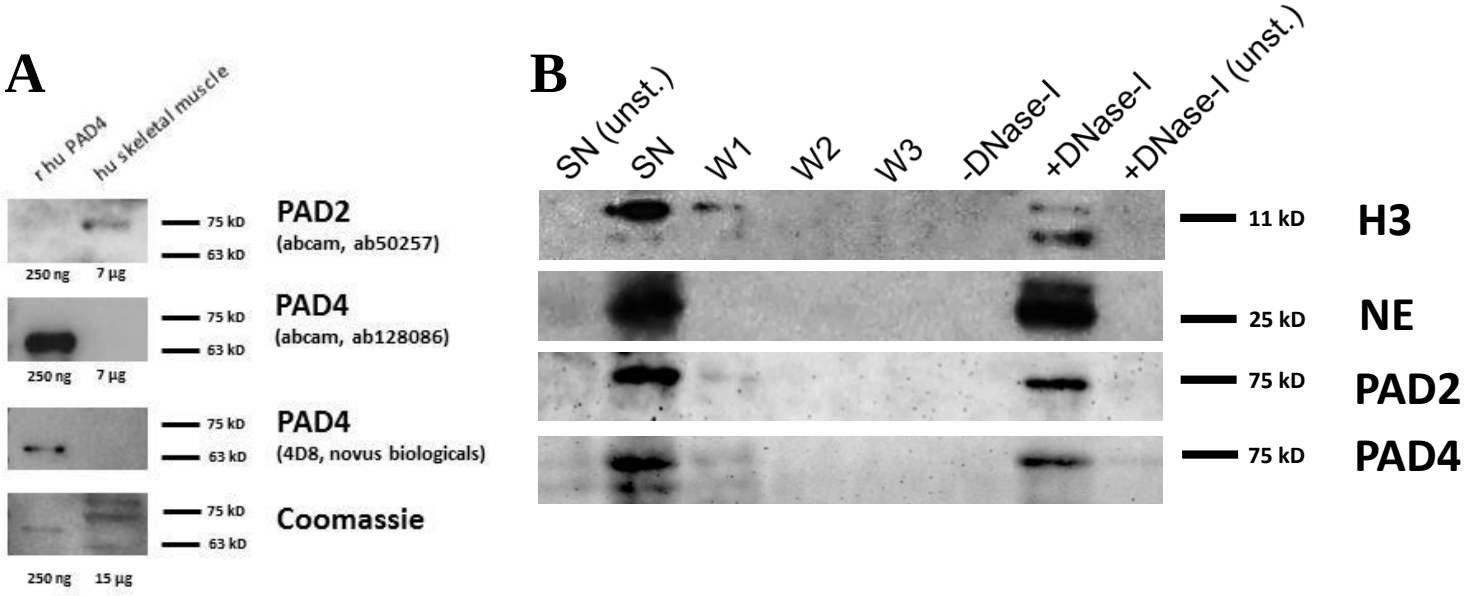

Figure 4-3 Identification of PADs released during NETosis *in vitro*

(A) Immunoblotting using human recombinant PAD4 (250 ng) and PAD2-expressing human skeletal muscle tissue lysate (7 or 15 µg). To demonstrate the absence of cross-reactivity, membranes were incubated with anti-PAD2 and two anti-PAD4 antibodies (Abcam and Novus Biologicals). **(B)** Proteins were precipitated from supernatants as described and their presence analysed by western blotting using antibodies against the proteins histone H3, neutrophil elastase, PAD4 and PAD2. One representative blot out of 4 independent experiments is shown.

Cellular localisation	Protein name
Granules	Neutrophil Elastase
	Azurocidin
	Myeloperoxidase
	Cathepsin G
	Non-secretory ribonuclease
Nucleus	Histone H4
	Histone H2B type 2-E
	Histone H2A (fragment)
	Histone H2A type 3
	Histone H2B
	MNDA
Cytoskeleton	Cytokeratin 10
other	Eosinophil cationic protein
	Complement C3

Table 4-1 Proteins enriched in the NET fraction

268 proteins from 3 matched SN and DNase-I treated NET fractions were quantified using 1% FDR and 2 peptides per protein. Abundance of proteins in D compared to SN was calculated using t-test (cut-off $p<0.05$). 14 proteins were found to be enhanced in the NET fraction of all 3 samples and are shown here.

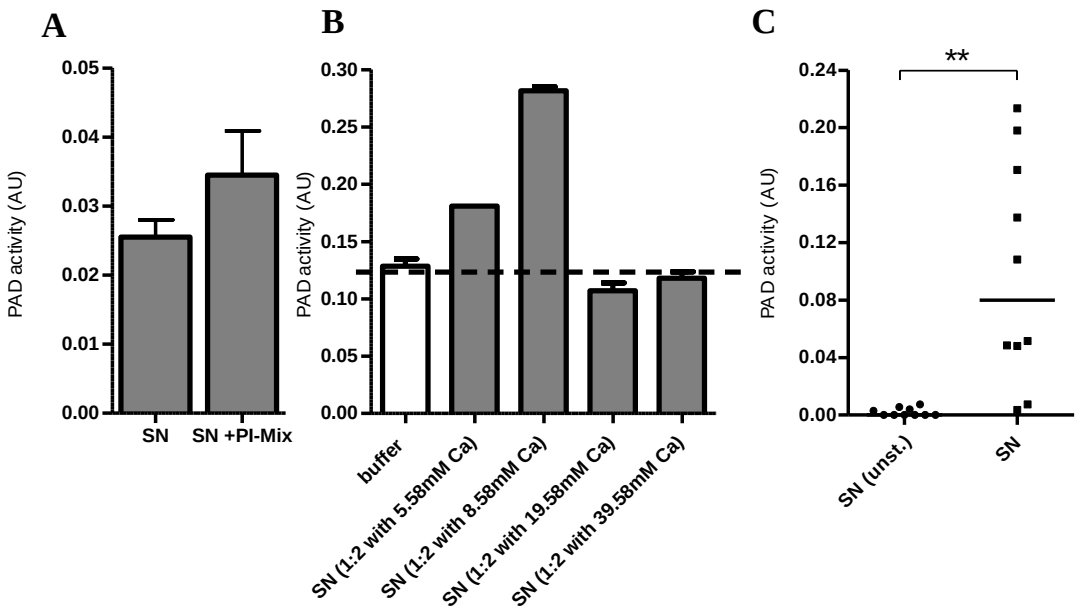

Figure 4-4 PAD activity in the supernatants of *in vitro* stimulated neutrophils entering into NETosis

PAD activity was determined in the supernatant of unstimulated neutrophils and neutrophils stimulated with 25 nM PMA. **(A)** PAD activity in the supernatant of neutrophils after 4 h stimulation was increased by adding protease inhibitor cocktail (PI-Mix). **(B)** PAD activity was increased when diluting the supernatant of neutrophils after 2 h stimulation 1:2 with a 5.58 or 8.58 mM calcium concentration, whereas activity was abolished over a 19.58 mM calcium concentration. **(C)** PAD activity in the supernatant of neutrophils after 2.5 h stimulation (SN) compared with unstimulated controls (SN (unst.)). Statistical significance was determined by Wilcoxon matched-pairs signed rank test (n=10; **p<0.01).

Furthermore, in order to visualise the time point of PAD2 and PAD4 release in relation to NETosis *in vitro,* immunofluorescence staining was performed. Since the localisation of PAD4 is still under debate, it was interesting to find that PAD4 localisation in unstimulated peripheral blood neutrophils from healthy donors was restricted to the nucleus (Figure 4-5) in agreement with Nakashima et al. (196) while PAD2 was largely restricted to the cytosol. Upon stimulation, at 120 and 240 min a proportion of the cells had changed their nuclear morphology. Nuclei appeared rounded and decondensed indicating a stage of NETosis directly preceding DNA release (Figure 4-5). PAD2 staining was reduced within 30 min of stimulation, while PAD4 staining was lost from the nuclei after DNA decondensation. Surprisingly, in contrast to our western blotting and mass spectrometry data, the association of PAD4 with NETs could not be confirmed. This could, however, be explained by the absence of protease inhibitors in the neutrophil cell culture. As previously mentioned, active autocitrullinated PAD4 could have been cleaved by proteases preventing the binding of anti-PAD4 antibodies.

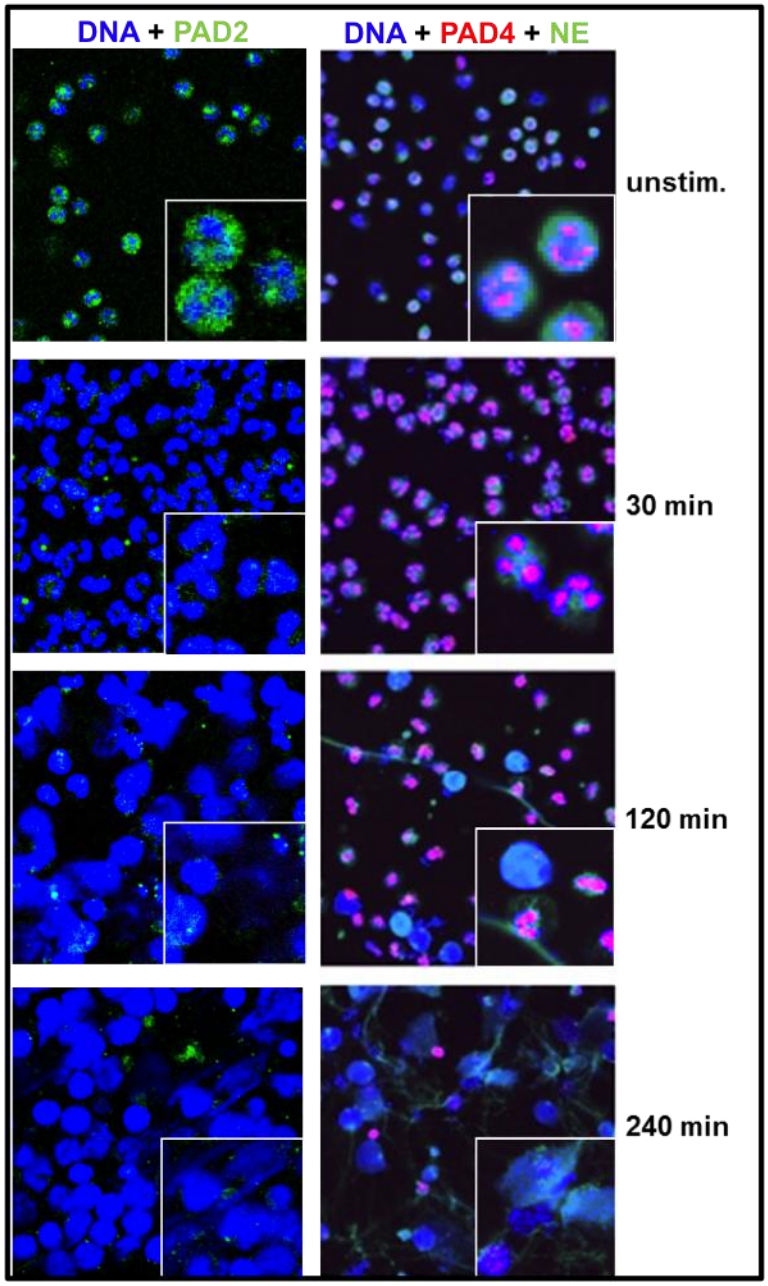

Figure 4-5 Time course of PAD2 and PAD4 release during *in vitro* NETosis

Confocal microscopy reveals that part of the cells begin entering NETosis after 120 min of stimulation. While PAD2 is only seen in the cytosol, in resting neutrophils PAD4 is localised in the nucleus. PAD2 levels decrease after 30 min and PAD4 is not detected in the nuclei of cells undergoing DNA decondensation (DNA is shown in blue, PAD2 in green, PAD4 in red and co-labelled with neutrophil elastase (NE) in green). No PAD4 signal was detected after 240 min of stimulation in cells that had reached a stage of NETosis at which nuclear morphology had changed.

4.4 Peptidylarginine deiminases in the SF of RA patients

After having demonstrated the release of extracellularly active PADs after NETosis *in vitro*, the presence and enzymatic activity of PADs in the synovial fluid of RA patients was assayed. In agreement with Kinloch et al. (249), PAD2, PAD4 and neutrophil elastase were detected in the cell-free SF of patients with RA (Figure 4-6A). Whereas PAD4 varied considerably in its expression level between patients, the amount of PAD2 was found to be more consistent. In preliminary experiments, attempts were made to immunoprecipitate endogenous PAD4 from the SF of RA patients using a purified mouse anti-human PAD4 antibody raised against the recombinant full length protein, corresponding to amino acids 1-663 of human PAD4. The same antibody was successfully used for immunofluorescence staining in the previously shown results (see Figure 4-5). In addition, the SF was spiked with recombinant human PAD4 to validate the method. Interestingly, similar to results of PAD4 in activated neutrophils in a publication by Andrade et al. (199), endogenous PAD4 from the SF could not be immunoprecipitated, whereas the spiked recombinant PAD4 was detected (Figure 4-6B). This would indicate that although this antibody recognises both denatured recombinant and denatured endogenous PAD4 in immunoblotting, it is unable to immunoprecipitate native endogenous PAD4 from the SF of RA patients in contrast to native recombinant PAD4 protein. Since it was previously reported that PAD4 can autocitrullinate itself during activation (199,200) and that citrullination leads to changes in protein structure (190), it is therefore likely that endogenous PAD4 in the SF is

in an autocitrullinated state, which alters its structure and recognition by antibodies generated against non-citrullinated PAD4 and suggests that the SF seems to provide high enough calcium concentration to enable enzymatic PAD4 activity. Indeed, PAD activity in the SF of RA patients could be detected using the previously described PAD activity assay. To assess, whether the variable citrullination efficiency in the samples can be related to the abundance of PAD2 and/or PAD4 in the RA SF samples and thus the signal strength on the immunoblot shown in Figure 4-6A, relative quantitation of the PAD2 and PAD4 signal was performed using the Image Lab 4.0 software by Bio-Rad. An exposure time below the saturation level of the signal was used. The band with the highest intensity was used as reference band and assigned a value of 1.0. The intensity of the remaining bands on the blot were then calculated by the software in relation to this reference band. Surprisingly, no correlation between citrullination efficiency and PAD2 or PAD4 signal strength on the immunoblot was deteted. This suggests that the efficiency by which the substrate in the assay was citrullinated by the PADs present in the SF of these patients cannot be exclusively explained by the quantity of PAD2 and/or PAD4 protein present in the samples (Figure 4-6C-D).

As shown in Figure 4-7A, PAD enzymatic activity was significantly higher in the SF of RA patients than in that of OA patients at the supraphysiological calcium concentrations used in the assay ($p<0.05$). Variable amounts of PAD activity at supraphysiological calcium levels could also be detected in the SF of patients with different forms of inflammatory arthritis (Figure 4-7B). Interestingly, the difference between RA and OA could also be observed with non-diluted SF samples at their native calcium concentration, however this was at ~140-fold

lower median value of PAD activity in the RA SF samples when accounting for the dilution factor (Figure 4-7C).

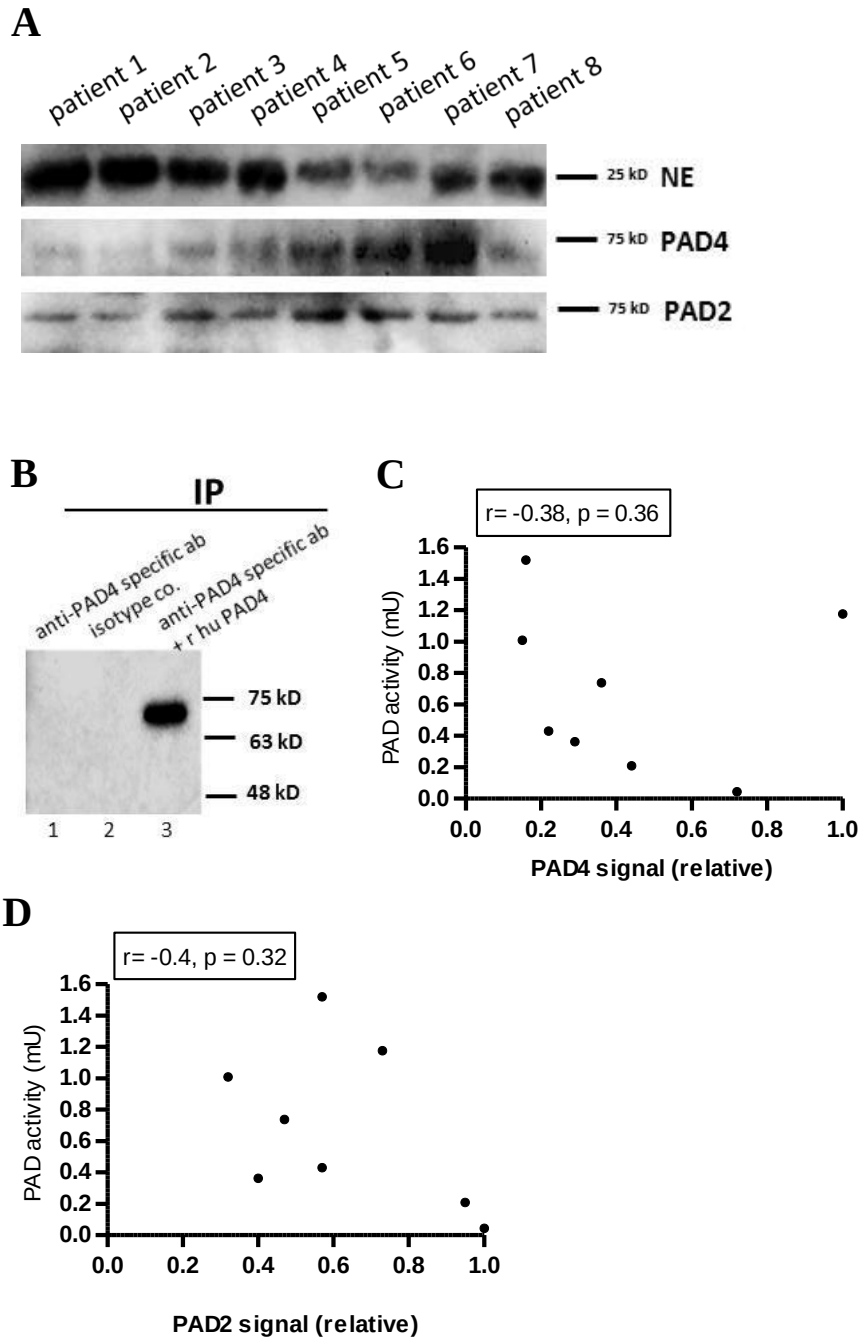

Figure 4-6 Presence of PAD2 and PAD4 in the synovial fluid of RA patients

(A) Immunoblotting of albumin depleted SF samples from 8 RA patients incubated with antibodies against neutrophil elastase (NE), PAD4 and PAD2. **(B)** Immunoprecipitation (IP) of PAD4 from SF of an RA patient using mouse anti-human PAD4 antibody (ab128086) (lane 1) and mouse anti-human IgG2a isotype control (lane 2). In lane 3, SF was spiked with recombinant human PAD4 protein (r hu PAD4) and the same amount of specific mouse anti-human PAD4 antibody was added as in lane 1. All lanes are probed with mouse anti-human PAD4 antibody (ab128086). As secondary antibody an anti-mouse IgG, HRP-linked antibody was used. **(C,D)** Relationship between citrullination efficiency (expressed as PAD activity measured with the PAD activity assay) and PAD2 or PAD4 signal strength (relative quantification) calculated from blot shown in (A). Relative quantification was performed using the Image Lab 4.0 software by Bio-Rad and the reference band with the highest intensity was assigned the value 1.0. The intensity of all other bands was then calculated by the software in relation to this reference band. Data were analysed using Spearman's test for correlation.

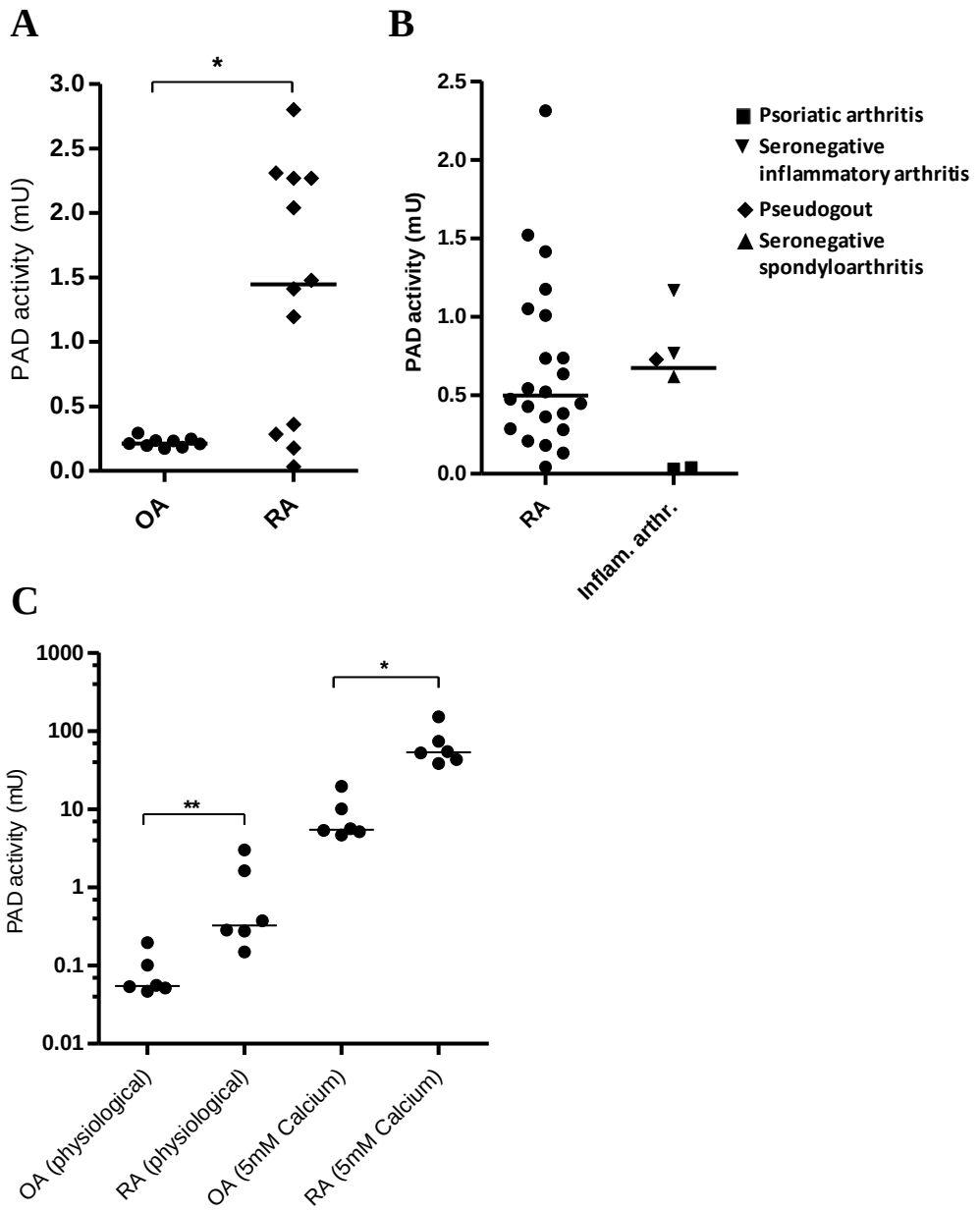

Figure 4-7 PAD activity at physiological and supraphysiological calcium levels

(A) Comparison of PAD activity in RA patients and OA patients. SF samples were diluted 1:100 with deimination buffer. Data were analysed using Mann-Whitney test. **(B)** Comparison of PAD activity in RA patients and patients with different forms of inflammatory arthritis. **(C)** PAD activity in SF samples, which were either diluted 1:100 in deimination buffer with 5 mM calcium concentration (supra-physiological) or were used undiluted (physiological). Significantly higher PAD activity could be observed in RA patients (n=6) compared to osteoarthritis (OA) patients (n=9) (Mann-Whitney test; * indicates $p<0.05$; ** indicates $p<0.01$). Horizontal bars represent median values.

Furthermore, PAD activity strongly correlated not only with the level of extracellular DNA in the SF ($r = 0.8$; $p < 0.001$) (Figure 4-8A) but also with total cell counts (Figure 4-8B) and neutrophil cell counts ($r = 0.8$; $p = 0.002$) (Figure 4-8C) in untreated, fresh SF samples. Interestingly, whereas a statistically significant difference in DNA levels between ACPA positive and ACPA negative RA patients could be detected (chapter 3.4), no statistically significant difference in PAD activity between ACPA positive and ACPA negative RA patients could be observed (Figure 4-8D). However, PAD activity was found to correlate with disease duration similar to the DNA levels in SF samples shown in chapter 3.2 (Figure 4-8E).

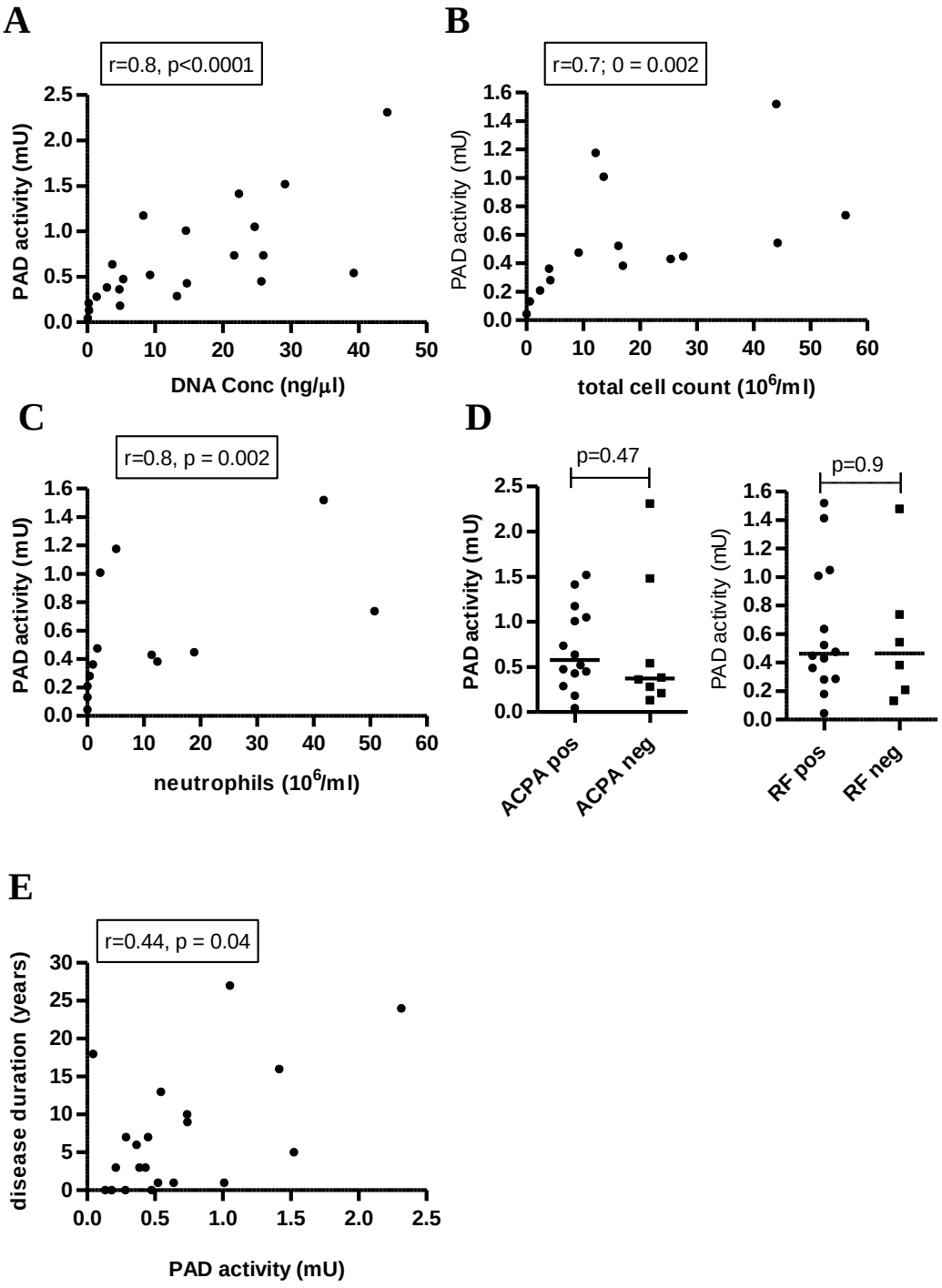

Figure 4-8 Correlation of PAD activity with DNA levels, neutrophil numbers and disease duration

(A) PAD activity correlates significantly with DNA levels in the SF of RA patients (n=22; r=0.8, p<0.0001). Data were analysed using Spearman's test for correlation. **(B)** PAD activity correlates significantly with the total cell count in untreated synovial fluid of RA patients (n=15; r=0.72, p=0.002). Data were analysed using Spearman's test for correlation. **(C)** PAD activity correlated significantly with neutrophil cell counts in the synovial fluid of RA patients (n=13; r=0.8, p=0.002). Data were analysed using Spearman's test for correlation. **(D)** Comparison of PAD activity in ACPA positive and ACPA negative (p=0.47) and/or rheumatoid factor (RF) positive and negative patients (p=0.9), respectively. Data were analysed using Mann-Whitney test. **(E)** Relationship between PAD activity and disease duration. Data were analysed using Spearman's test for correlation (n=21; r=0.44, p=0.04).

4.5 Localisation of PAD4 in neutrophils from RA patients

After having studied localisation and PAD release mechanisms in *in vitro* stimulated neutrophils and having detected PAD activity in the SF of RA patients, we were also interested in visualising the localisation of PAD4 in neutrophils from RA patients. Similar to unstimulated neutrophils, PAD4 localisation was found to be restricted to the nucleus. Unexpectedly, however, a proportion of neutrophils within the synovial fluid infiltrate of RA patients displayed an additional cytoplasmic localisation, whereas at the same time a reduced co-localisation between PAD4 and the DNA signal was detected in these cells (Figure 4-9) suggesting a potential translocation of the protein from the cell nucleus to the cytoplasm. The amount of cells displaying a cytoplasmic PAD4 localisation varied between the analysed 5 RA patients; this needs to be further confirmed and studied in more detail due to the low number of available samples. Interestingly, the cytoplasmic PAD4 staining displayed a granular pattern and would suggest a possible release mechanism via degranulation. Which of the four types of granules are involved, however, needs to be a target of further investigation.

To determine whether the increased cytoplasmic PAD4 staining can be explained by the translocation of the enzyme from the cell nucleus to the cytoplasm, the percentage of cytoplasmic PAD4 signal compared with the total PAD4 signal in each cell was calculated based on pixel count per μm^2 area

using the histogram function and the image calculator function of the ZEN2010 software (details are provided in the Materials and Methods Chapter 2). Importantly, all intact neutrophil elastase positive neutrophils on a cytospin from a patient sample were included into the calculation (Figure 4-10A). Each data point in Figure 4-10B therefore represents the average percentage of cytoplasmic PAD4 pixel count of the total PAD4 pixel count in neutrophils in one RA patient sample. As shown in Figure 4-10B, a significantly increased percentage of cytoplasmic PAD4 in neutrophils within the SF infiltrate of RA patients (RA SF) was found compared to the signal in peripheral blood neutrophils of RA patients (RA PB) and peripheral blood neutrophils of healthy controls (HC PB) (Figure 4-10B). These data therefore indicate that there may be a role for cytoplasmic PAD4 expression in the SF of RA patients.

At this stage, no correlation of cytoplasmic PAD4 expression with DNA levels, PAD4 activity or any clinical parameters could be assessed due to the small number of analysed samples, however, cytoplasmic PAD4 expression was present in both ACPA positive and ACPA negative RA patients. No information can also be provided with regard to the presence of cytoplasmic PAD4 in patients with different types of inflammatory arthritis. In light of the importance of anti-citrulline immunity in RA, however, these preliminary observations are intriguing and would warrant further investigation.

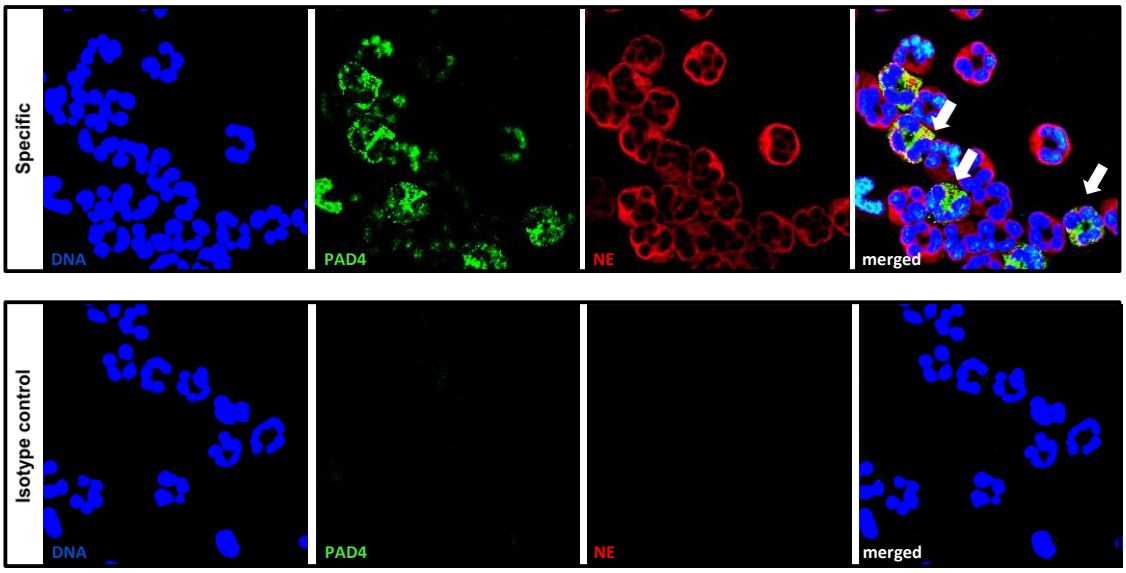

Figure 4-9 Cytoplasmic localisation of PAD4 in a population of SF neutrophils from RA patients

Immunofluorescence of cytospins from cells of the SF of RA patients. Cells were stained for DNA (grey), PAD4 (green) and neutrophil elastase (NE) (red). Lower panel shows concentration and isotype matched control staining. Immunofluorescence staining was visualised using a confocal microscope and viewed at a final magnification of 63 x 10 original magnification. Images are representative of 5 SF samples from RA patients.

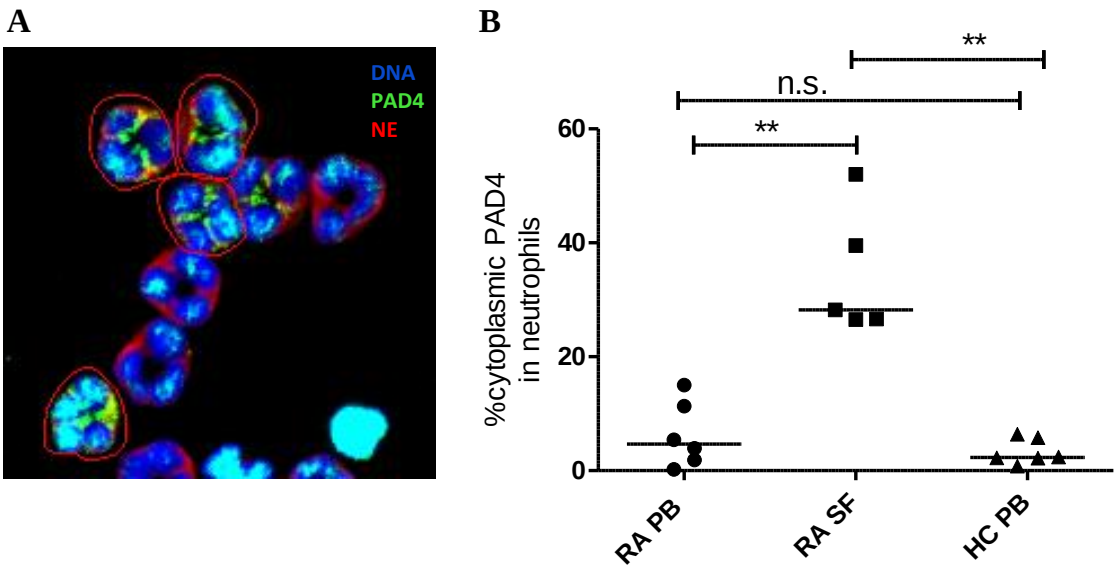

Figure 4-10 Quantification of percentage of cytoplasmic PAD4 signal of total PAD4 signal in neutrophils using the ZEN 2010 software

(A) Immunofluorescence staining of a cytospin from SF cells taken from an RA patient. The cytospins were stained with antibodies specific for PAD4 (green) and neutrophil elastase (NE) (red). Nuclei were counterstained using Hoechst 33258 (blue). Cytospins were stained alongside isotype- and concentration-matched controls, which were negative. Images were taken at x 630 total magnification using a Zeiss confocal LSM 510 microscope. To perform the analysis, neutrophil elastase positive neutrophils were selected (drawn around) using the overlay function within the ZEN software. **(B)** Percentage of cytoplasmic PAD4 of total PAD4 pixel count was determined using the method described in (A). Significantly increased percentage of cytoplasmic PAD4 in relation to the total PAD4 signal in neutrophils within the SF infiltrate of RA patients (RA SF) was compared with the signal in peripheral blood neutrophils of RA patients (RA PB) and peripheral blood neutrophils of healthy control subjects (HC PB). Mann-Whitney test was used to determine statistical significance with ** indicating $p<0.01$.

4.6 Discussion

The mechanisms behind the activation of PADs in RA patients, as well as the sites and circumstances of citrullination of autoantigens in RA remain unknown. In this chapter an *in vitro* assay for NETosis was established which demonstrates that NETosis provides a source of freely diffusible enzymatically active PADs. Importantly, significantly increased PAD activity in the SF of RA patients compared with OA patients was shown and found to strongly correlate with neutrophil numbers. Together with these findings regarding NETosis in arthritic joints these results therefore indicate NET formation as one possible source of PAD activity and thus a prerequisite for the generation of citrullinated autoantigens in ACPA positive RA.

In line with the *in vitro* findings demonstrating the presence and activity of PADs in the supernatants of neutrophils stimulated to go into NETosis, the presence and activity of PADs could also be demonstrated in the SF of RA patients. These findings are in agreement with previous reports demonstrating the presence of PAD2, PAD4 and citrullinated proteins in the joints of RA patients (249,250). Kinloch and colleagues showed that PAD4 protein is present in SF samples of OA patients, although at lower levels than in SF samples of RA and SpA patients. Presence of PAD2 and citrullinated proteins, however, could only be detected in RA and SpA SF samples but not in OA SF samples, subsequently the hypothesis was proposed that it may be mainly the PAD2 enzyme that is responsible for the extracellular citrullination of synovial fluid proteins in patients with inflammatory arthritis (249). The assay for the detection of PAD activity used in the experiments presented here however cannot

distinguish between different isoforms of PADs. This hypothesis can therefore not be tested here, although indeed significantly higher PAD activity in RA patients and in patients with other forms of inflammatory arthritis was found compared with OA patients. Interestingly, however, it has to be noted that even though no presence of PAD2 protein in OA SF samples was found by Kinloch et al., the PAD activity assay in our experiments revealed a low, but still existing activity of up to 0.3 mU in some OA patients, suggesting that the enzymatic activity of PAD isoforms other than PAD2 should not be discounted. Furthermore, it should be considered that the measured PAD activity in cell lysates or SF only reflects the efficiency with which moles of substrate are converted in a given time. Not only the PAD isoform but also the quantity of enzyme as well as the state of activity of the enzymes within the samples are, however, unknown factors. PAD activity in the SF of RA patients may therefore not only be based on the quantity of enzymes alone but could also be influenced by additional factors such as endogenous PAD activators or inhibitors. In support of this idea data presented here indeed revealed no significant correlation between the intensity of PAD2 and/or PAD4 protein signal on immunoblots and measured PAD activity. Although this would suggest that the general citrullination efficiency in the SF does probably not increase with higher abundance of the enzymes, these data have to be interpreted with caution due to the small number of analysed samples. In this context, Darrah and colleagues suggested in a recent study that PAD4 activity can be regulated by PAD3/PAD4-cross-reacting autoantibodies binding to and changing the protein structure of PAD4 (366), which is itself known to be an autoantigen in ACPA positive RA (199,367,368). This change in protein structure strikingly

increased the catalytic efficiency of PAD4 by decreasing the enzyme's requirement for calcium *in vitro*. Patients with these antibodies displayed a higher likelihood of radiographic progression compared with individuals who responded negatively for these antibodies (369). Interestingly, these cross-reacting autoantibodies are only present in a subpopulation of anti-PAD4 antibody positive individuals, which themselves are known to be strongly associated with anti-ccp antibodies (368). This may also explain why no statistically significant difference in PAD activity levels was detected here when comparing ACPA positive with ACPA negative RA SF samples. A comparison between patients positive and negative for PAD3/PAD4-cross-reactive antibodies in this study would have been potentially interesting in order to determine whether the *in vitro* observations by Darrah et al. could be confirmed *in vivo*.

The above mentioned study by Darrah et al. is also interesting in another aspect as it provides a potential mechanism for the well-known mismatch between the *in vitro* and *in vivo* calcium requirements for PAD4 activity (47,48,369). PAD enzymatic activity depends on the presence of calcium and intracellular calcium levels are reportedly below the level needed for *in vitro* PAD activity. Whereas most *in vitro* citrullination assays including the ABAP assay used in this study utilise calcium concentrations of 5-10 mM calcium to achieve maximal PAD activation (47,48,197), cytosolic levels of free Ca^{2+} are known to increase in activated cells only up to 10 µM. Under pathological conditions these levels can further rise up to 100 µM for a short time, but need to return to original levels to ensure cell survival (370). In comparison, calcium levels in the extracellular

space are estimated to range between 1.1-1.3mM in plasma and 0.49-0.98mM in SF (369,371). In line with these observations it was interesting to see that PAD activity in RA SF samples measured at 5 mM calcium concentration decreased ~140-fold when measuring PAD activity at physiological calcium levels and accounting for the dilution factor. This indicates that PAD enzymes in the SF appear to possess a “general fitness” of increased activity towards the substrate used in the assay when they come into contact with higher calcium concentrations. Although it is in general possible that a PAD activity below the theoretical potential activity is still sufficient for citrullination of synovial fluid proteins at the heightened calcium levels in the extracellular space, it is, nevertheless, imaginable that additional factors such as cross-reactive antibodies or other modulators regulate PAD activity *in vivo*.

Other possible factors suggested to modulate PAD activity are proteolysis and citrullination itself. Although Andrade et al. described in 2010 that autocitrullination of PAD4 at several sites of the enzyme inactivates its function (199), this finding could not be confirmed in a more recent study by Slack and colleagues (200). Interestingly, the main difference in Andrade’s data was that citrullinated and native PAD4 was incubated with lysates from HL-60 cells whereas highly purified substrates were used by Slack et al. It is therefore possible that factors present in the lysate could have inactivated specifically the citrullinated form of the enzyme. Although enzyme degradation was excluded by Andrade et al., it is surprising that in the studies presented here PAD activity in the supernatant of activated neutrophils was only detectable in the presence of a protease inhibitor cocktail containing components such as AEBSF, E-64 and

Pepstatin A. Indeed, citrullination of proteins is known to lead to their degradation by proteases. For example, Hsu et al. reported that citrullination of human fillaggrin-2 by PAD1, PAD2 and PAD3 promotes its proteolytic degradation by calpain-1 (191). Since citrullination induces a decrease in positive charge of the protein, the conformation is changed and makes the protein more susceptible to proteolysis (185).

As the assay used for measuring PAD activity does not distinguish between different PAD isoforms, it has to be considered that a contribution to the total PAD activity by PAD2, PAD3 and PAD4 is possible. Interestingly, mass spectrometry data did not identify any unique peptides matching PAD3 as being present in neutrophils. Identification of PAD isoforms that are responsible for the observed PAD activity is of interest as it was recently reported that different PAD enzymes display distinct substrate specificities (203) and could therefore lead to the citrullination of different autoantigens. Interestingly, Darrah et al. also showed that the citrullination activity of each PAD isoform appears to be specific and directed preferentially against distinct substrates, independent of their cellular localisation. Indeed this substrate preference becomes even more evident when the enzymes are exposed to a larger number of substrates. For example, in cell lysates, actin and histone H3 are only citrullinated by PAD2 and PAD4, respectively, which means that although actin and histone H3 can be citrullinated by all PAD isotypes, each enzyme has a clear, intrinsic substrate preference. These results are also in agreement with data from Nakayama-Hamada et al. who demonstrated that human rPAD2 citrullinates purified fibrinogen and filaggrin more efficiently than human rPAD4 (372). In this context

different PAD isoforms may have different citrullination efficiency towards the substrate used in the PAD activity assay presented here.

In relation to the presence of extensive NET formation in the joints of RA patients it was interesting to observe that the PAD activity in the SF of RA patients showed, in general, very similar properties compared with DNA levels described in Chapter 3: PAD activity was significantly increased in RA patients compared with OA patients, it was present in the SF of patients with different forms of inflammatory arthritis and also correlated strongly with neutrophil numbers. Intriguingly, PAD activity also increased with disease duration. A decrease of regulatory factors over time may lead to increases of both DNA levels and PAD activity with disease duration and/or degradation and removal of the products of NETosis may be affected. Interestingly, Makrygiannakis et al. published in a recent study that intra-articular injection of glucocorticoids, and not oral methotrexate, resulted in a reduction in synovial inflammation, intracellular citrullination, and PAD expression (373). In this study, we could not see a significant difference between PAD activity levels in the SF of patients taking methotrexate compared with patients taking other medication (data not shown). Additionally, no difference between patients taking oral prednisolone was found, although the number of analysed samples was relatively small. In the future it would be interesting to determine whether the results published by Makrygiannakis could be confirmed when examining PAD activity levels in the SF of patients after intra-articular injection of glucocorticoids.

Citrullination of histones H2A, H3 and H4 is catalysed by PAD4 and was shown to be an important step in the decondensation of DNA and NET formation (34,44), however, the exact mechanism through which PAD4 is involved in the unwinding of chromatin is still unclear. Additionally, PAD4 was reported to have a crucial role in gene regulation by citrullinating arginine residues on histones and thus counteracting arginine methylation that coincides with the transcriptionally active state (194). It was therefore not unexpected to find PAD4 localised in the cell nucleus of unstimulated neutrophils and in the NET fraction of *in vitro* stimulated neutrophils. In contrast, the significantly increased percentage of cytoplasmic staining in neutrophils from RA patients compared with healthy controls was a novel and unexpected finding. Few studies have so far attempted to visualise PAD4 in cells using confocal microscopy due the lack of specific and non-cross-reactive antibodies. In a study by Asaga et al. in 2001 it was initially reported that PAD4 could be localised in myeloperoxidase-negative neutrophil granules (45), however, the same group published a year later results which questioned their previous observations (196). The cytoplasmic staining in the previous study was explained by overfixation which masked nuclear antigens within the nucleus. Interestingly, in a third study, after examining synovial tissue from RA patients it became apparent that whereas PAD2 localisation was restricted to the cytosol, PAD4 appeared to be present in both cytosol and nucleus (372). Since then no other studies have examined PAD4 localisation using immunofluorescence, however, Lominadze et al. detected PAD4 in gelatinase as well as specific granules of unstimulated human neutrophils using mass spectrometry (374). Interestingly, the cytosolic localisation of PAD4 in granules was confirmed by the group of Niels

Borregaard in 2013 using proteomics, however, PAD4 was this time found to be enriched in secretory granules (13) of unstimulated human neutrophils. Similar to previous publications in mouse and human oligodendroglial cell lines stimulated with TNF-α (240), translocation of PAD4 from the cytoplasm to the nucleus upon stimulation was also speculated to be present in neutrophils from RA patients (354). However, no experimental data were provided in this study to confirm the theory of PAD4 redistribution, and therefore, in summary, it can be concluded that there does not seem to be agreement in the literature with regard to cytoplasmic PAD4 localisation. Since cytoplasmic PAD4 expression could not be induced with PEG-enriched immune complexes from the SF of RA patients (data not shown), it is concluded here that the stimulus inducing cytoplasmic PAD4 expression can either not be enriched with PEG and therefore present in the discarded SF fraction or it is based on cell-cell contact with cells present in the SF.

As previously discussed in Chapter 3, the study presented here cannot exclude the possibility of cells other than neutrophils contributing to the extracellular DNA concentration and PAD activity in the SF of RA patients. In addition, NETosis may also not be the only source of citrullinated proteins in the joints of patients with inflammatory arthritis. Intracellular citrullination was reported in several cell populations in the synovium (250,251) and in SF cells (53) and further studies are required to examine mechanisms underlying the initial intracellular activation of PADs in relation to different cell death pathways.

Nevertheless, in agreement with our findings on PAD activity in the SF, several studies have already described the presence of citrullinated proteins in the SF of patients with inflammatory arthritis (249,375). The view that NETosis contributes to citrullination is also supported by data from De Rycke et al. who observed localisation of citrullinated proteins within extra-synovial deposits of polymorphonuclear cells on the surface of the lining layer in RA patients (248). Understanding the mechanisms that generate citrullinated antigens in ACPA positive RA may identify unique pathways that regulate antigen drive in this disease, which might be relevant to the development of novel therapies. In the following chapter, the generation of citrullinated antigens during NETosis will be examined and its relevance for the autoimmunity in RA will be discussed.

5 Investigation into the antigenicity of NETs in RA patients

5.1 Introduction

Rheumatoid arthritis is characterised by the presence of a range of autoantibodies of which rheumatoid factor (RF) and anti-citrullinated protein antibodies (ACPA) are best characterised and used clinically for patient disease classification (158,233,376,377). Whereas RF and other autoantibodies can also occur in healthy individuals or patients with other inflammatory conditions, ACPA represent the most specific autoantibodies in RA discovered to date and can be detected in 60-70% of RA patients (69,377,378). ACPA can be detected several years before the onset of clinical symptoms (81,151) and their presence is associated with more erosive disease (205). Additionally, several environmental (214) and genetic (210,379,380) risk factors are associated specifically with the ACPA positive subtype of RA patients. For the above-mentioned reasons it was therefore proposed that ACPA positive and negative RA are regarded as two different disease entities (168) and a test for ACPA, the anti-ccp antibody test, was included into the ACR criteria in 2010 (77). ACPA target a wide range of citrullinated proteins with the best characterised autoantigens being fibrinogen, vimentin, α-enolase, and type II collagen (CII) (70,178) with others awaiting further characterisation.

Key questions regarding the observed autoimmunity against citrullinated proteins that have still remained unanswered are whether ACPA are causally related to the disease or whether they are just a consequence of the condition. Furthermore, it is not known where autoimmunity to citrullinated proteins is initiated and whether there is a single or restricted group of antigens responsible for the breakdown of tolerance. Since several studies suggest the absence of synovial inflammation in individuals who have pre-existing ACPA

and joint pain but no clinically apparent joint swelling (85,87,88), the concept was proposed that the initiating event leading to ACPA production is more likely to be located outside the joint. Examples for such extra-articular locations that are currently being discussed are the periodontal tissues (276,278), the lungs (381) and the gut (80). In view of this concept it was therefore proposed that an unrelated “second-hit” could represent an episode of otherwise self-limiting synovial inflammation resulting in an exacerbation and perpetuation of the synovitis in ACPA positive individuals (168).

In the previous chapters the presence of NETs and enzymatically active PADs in the SF of RA patients has been demonstrated. The following chapter reports on the identification of citrullinated proteins that are potentially generated during NETosis. Since NETs provide an explanation for how otherwise intracellular proteins could be released into the extracellular space and exposed to the immune system, it was of interest to determine whether NETs contain already known intracellular candidate autoantigens such as vimentin or α-enolase. Additionally, the analysis of further citrullinated targets was planned using mass spectrometry. Finally, it was aimed to determine whether citrullinated proteins in NETs isolated from *in vitro* stimulated neutrophils, but also isolated *ex vivo* from the SF, are targeted by autoantibodies in RA patients.

5.2 Citrullinated proteins are released during NETosis *in vitro*

In the work presented in Chapter 4, a method for the isolation of NETs from *in vitro* activated neutrophils was established in order to study the release of enzymatically active peptidylarginine deiminases. In this chapter the same assay was applied to assay whether the process of NETosis would result in the generation of citrullinated proteins. Briefly, peripheral blood neutrophils from healthy volunteers were stimulated for 4 h with 25 nM PMA, washed and finally incubated with DNase-I to release NETs from the cells and into the supernatant. All generated culture supernatants were centrifuged to remove intact cells and cell debris and the proteins precipitated and modified according to the Senshu protocol (316) (see Chapter 2 for details). Modified citrullinated proteins could then be detected using an anti-modified citrulline antibody (AMC) on western blots. As shown in Figure 5-1A, a large number of citrullinated proteins were released from stimulated neutrophils into the supernatant after 4 h of stimulation (SN) compared to only a relatively small number of citrullinated proteins being present in the DNase-I treated NET fraction (+DNase-I). One prominent band was detected at 11 kD and, interestingly, a band of the same size was also detected using an antibody, which was raised against a synthetic peptide corresponding to human histone H3, aa 1-100 and citrullinated at the arginine residues 2, 8 and 17 (Figure 5-1A). The presence of this 11 kD band was further confirmed in the NET fraction of several donors (Figure 5-1B). Additionally, some other citrullinated proteins of a size ranging between 48 and 75 kD was detected in some of the donors.

The detection of an 11 kD band with the anti-citrullinated histone antibody was unexpected as the predicted molecular mass for histone H3 is 15.2 kD. It was therefore subsequently decided to test for potential cross-reactivity of this antibody. For this purpose recombinant histones were first *in vitro* citrullinated with PAD4 enzyme. Histones H2A, H3 and H4 were selected, as these are well-known targets of PAD4 (50,194,196,382) in contrast to histone H2B, which has not been reported to be citrullinated by PAD4 yet. As shown in Figure 5-1C, indeed only citrullinated histone H3 was recognised by the anti-citrullinated histone H3 antibody confirming its specificity. Interestingly, Urban et al. have reported a specific reduction in the molecular weight of histones, but not of other proteins, in NETs compared with proteins found in unstimulated neutrophils following SDS-PAGE analysis (315). The authors proposed that post-translational modifications may be responsible for this phenomenon. Indeed, the same mass shift when comparing citrullinated with native forms of recombinant histones H2A, H3 and H4 using coomassie blue staining was observed (Figure 5-1C). Importantly, the staining did not appear equal as each histone type is known to have a different affinity for Coomassie blue (383). To conclude, these data indicate that the citrullination of histones results in an increased mobility of these proteins during reducing SDS-PAGE, which could explain their apparent decreased molecular weight of citrullinated histone H3.

Mass spectrometry data presented here potentially indicated a significant enrichment of histones H2A, H2B and H4 but not H3 in the NET fraction compared with the supernatant fraction (SN) (refer to Table 4-1 in Chapter 4 and Figure 8.1 in the Appendix). Indeed, total histone H3 protein was also found

to be present in both fractions on immunoblot (Chapter 4, Figure 4.3). These findings therefore suggest that the enrichment of citrullinated histone H3 cannot be explained by its overall increased abundance within NETs. Instead the citrullinated form of histone H3 appears to be specifically associated with NETs as reported in several previous publications (34,44).

Importantly, to validate the method of detection of citrullinated proteins, the specificity of the anti-modified citrulline antibody for citrullinated proteins after Senshu modification was demonstrated using concentration and isotype-matched control antibody (Figure 5-2A). Additionally, it was aimed to establish whether the citrullinated proteins that are released during *in vitro* NETosis are generated *de novo* during activation or whether they are already present in unstimulated neutrophils. For this purpose, lysed unstimulated neutrophils were assessed for the presence of citrullinated proteins. As shown in Figure 5-2B, even with double the amount of protein loaded from lysed unstimulated neutrophils compared with supernatants of stimulated neutrophils from matched donors along with an increased exposure time, no citrullinated proteins were detected in unstimulated neutrophils (Figure 5-2B). These data therefore suggest the specific generation of citrullinated proteins during NETosis and the absence of detectable levels of citrullination in unstimulated neutrophils.

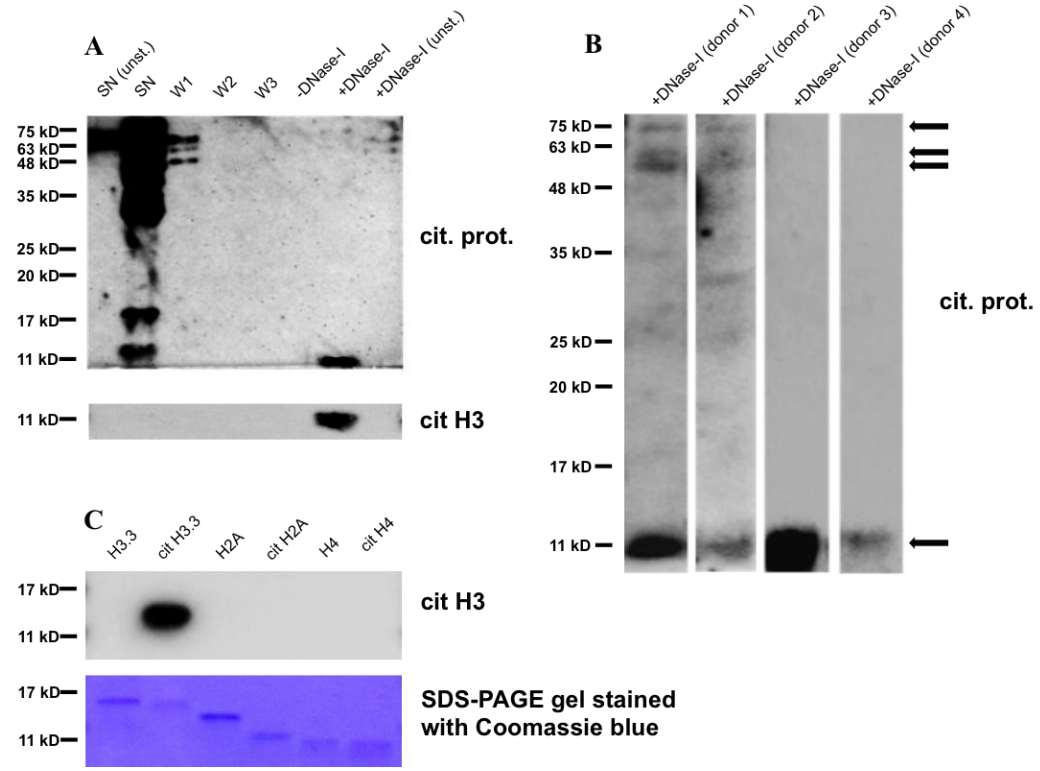

Figure 5-1 Release of citrullinated proteins from neutrophils undergoing NETosis

The supernatants of unstimulated (SN (unst.)) or PMA stimulated neutrophils (SN) were collected. After stimulation cells were washed 3 x with RPMI (W1-W3) and subsequently incubated with or without DNase-I (+DNase and –DNase). Non-stimulated cells were treated with DNase-I (+DNase (unst.)) as control. Proteins were precipitated from supernatants and analysed by western blotting. Citrullinated proteins (cit.prot.) on western blots are detected using the previously described Senshu method (316) and a monoclonal human anti-modified citrulline antibody from ModiQuest. **(A)** Western blots from all supernatants were probed with a monoclonal human anti-modified citrulline antibody after Senshu-modification and an anti-citrullinated histone H3 antibody. One representative blot out of at least 3 independent experiments is shown. **(B)** Detection of citrullinated proteins in +DNase-I treated NET fractions from four different donors out of six independent experiments are shown. **(C)** To demonstrate specificity of the human anti-citrullinated histone H3 antibody, western blots from non-citrullinated and citrullinated recombinant histones H3.3, H2A and H4 (expected size of 15.2 kD, 14 kD and 11.2 kD, respectively) were incubated with anti-citrullinated histone H3 antibody. Coomassie blue staining of the SDS-PAGE gel is also shown in the bottom panel. One representative blot out of 3 independent experiments is shown

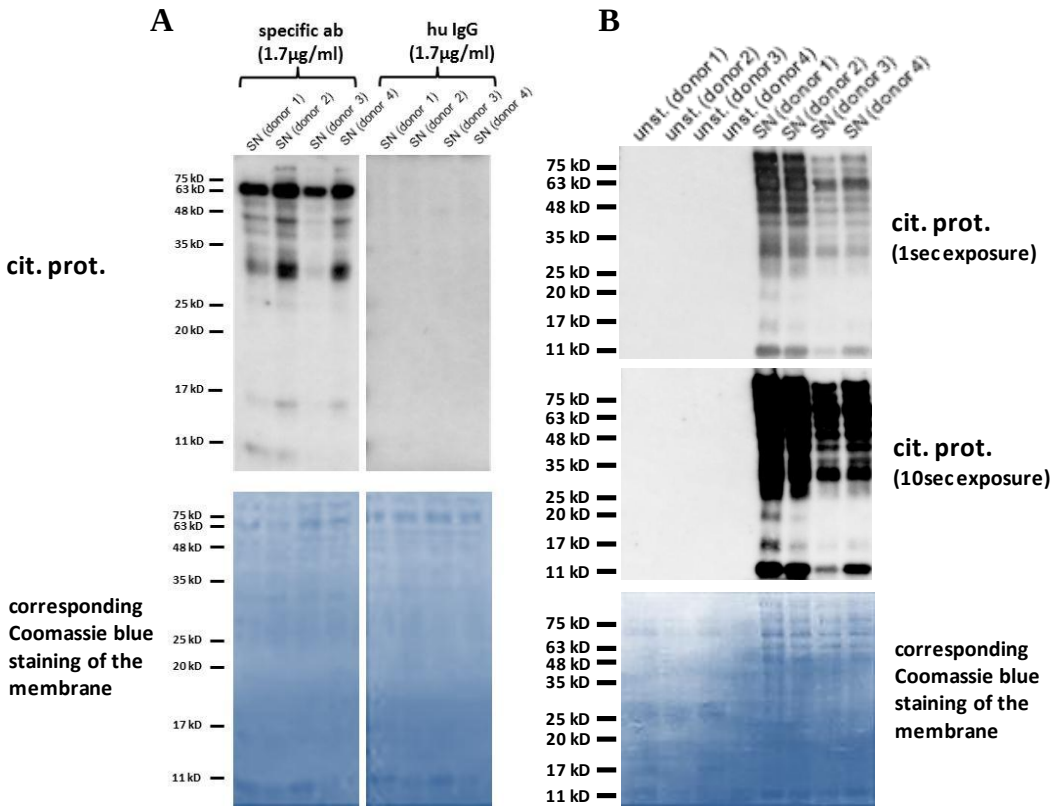

Figure 5-2 Demonstration of specific detection of citrullinated proteins

Neutrophils from 4 donors were purified and immediately lysed in RIPA buffer after purification (unst.). In parallel, neutrophils from the same 4 donors were stimulated for 4 h with PMA and the supernatants were collected (SN). Both supernatants and lysed neutrophils were centrifuged at 300 x g and a second time at 16 000 x g to remove intact cells and cell debris. Proteins were precipitated from the supernatants of stimulated neutrophils and the protein amount was determined for both fractions (SN and unst.). Citrullinated proteins (cit.prot.) are detected using the modified Senshu method. **(A)** To demonstrate specificity of the human anti-modified citrulline antibody (specific ab), the same blot was incubated after chemical modification with a concentration- and isotype-matched control antibody, human IgG (hu IgG). Coomassie blue staining of the PVDF membrane is shown in blue below to test equal protein loading (20 µg per lane). **(B)** Comparison of the amount of citrullinated proteins in lysed, unstimulated neutrophils from 4 donors (unst. donor 1-4) and the SN fractions of the same donors (SN donors 1-4) using immunoblotting after Senshu modification. Blots were developed with a short exposure time of 1 sec and a longer exposure time of 10 sec. Twenty µg of supernatant proteins and 40 µg of lysed neutrophils were loaded per lane. Coomassie blue staining of the membrane is shown below.

5.3 Qualitative analysis of protein composition of NETs using mass spectrometry

To determine the origin of the citrullinated 11 kD band in PMA-generated NETs, mass spectrometry was kindly performed by Jimmy Ytterberg from the Karolinska Institutet in Stockholm, Sweden. In an initial approach, the total DNase-I treated NET fraction (NET) and the supernatant fraction after 4 h of PMA stimulation (SN) from two different data sets were analysed and data is presented in tables 5-1 and 5-2: Two different donor groups (different patients on two different days) were analysed on two different instruments (Q Exactive MS and LTQ Velos Orbitrap ETD MS) but with otherwise same search parameters (for details refer to Chapter 2.14.2). In light of the immunoblotting data, it was not unexpected to find a wide range of citrullinated peptides in the SN fraction, although the variability between donors was very high and many citrullinated peptides, which were present in one donor group, were not detected in the other. Nevertheless, two different peptides from coronin-1A were identified using both approaches and were present in both the SN as well as the NET fraction (compare Table 5-1 and 5-2). Interestingly, one of these peptides, which was present in NETs, has also been reported to be present in the SF of RA patients (375). Additionally, two previously published citrullinated peptide sequences derived from vimentin (375,384,385) and myeloid cell nuclear differentiation antigen (MNDA) (375) were detected in the NET fraction of one donor, respectively. Furthermore, a peptide sequence which is shared by histone H3.1 and H3.2 was detected in the NET fraction of one donor using the Q Exactive MS instrument (Table 5-1). It is interesting to note that the citrullinated arginine in this peptide was immediately next to a dimethyl-

modification of a lysine and that the same peptide was also detected after in-gel digestion of an 11 kD gel slice in two out of five donors from a separate analysis (Table 5-3). The data generated from the in-gel digestion of the 11 kD gel slices not only demonstrated the presence of this peptide but also of an additional peptide from histone H3 in one of the donors (Table 5-3). This peptide was shared between all histone H3 subtypes and was derived from the N-terminus of histone H3 (Figure 5-3). In contrast, neither peptide was detected in the SN fraction. This finding was unexpected with regard to the previously used anti-citrullinated histone H3 antibody purchased from Abcam, which reacted strongly with the *in vitro* generated NET fractions. Since this antibody was raised against a synthetic peptide containing citrullinated arginines at the positions 2, 8 and 17 in histone H3, it should theoretically also react with a peptide sequence corresponding to the immunogen peptide sequence. Such a sequence, however, was neither detected in the total NET fraction nor in the 11 kD gel slices. It is therefore possible that the antibody also cross-reacts with additional epitopes in histone H3 such as the two sequences that have been detected using mass spectrometry analysis. To conclude, these data suggest that the citrullinated protein detected at the molecular weight of 11 kD on immunoblots from NET fractions of *in vitro* stimulated neutrophils is likely to be citrullinated histone H3, especially as no other citrullinated peptides from histones in the gel slices of the five analysed donors could be detected using the mass spectrometry approach. As mentioned previously, the difference between the expected molecular weight of 15 kD for histone H3 and the actual presence of citrullinated H3 peptides at 11 kD in SDS-PAGE analysis may be explained by

the presence of post-translational modifications such as citrullination or methylation.

Protein	Peptide Sequence	SN 1	SN 2	SN 3	NET 1	NET 2	NET 3
Actin	AGFAGDDAP(Cit)AVFPSIVGRPR				28.58		
Vimentin	TVET(Cit)DGQVINETSQHHDDLE				21		
Coronin-1A	VN(Cit)GLDTGR	28.48	22.96		23.83		
Unconventional myosin-Ie	KENWGPWSAGGS(Cit)	31.51					
Protein LAP2	EQVL(Cit)HIEAK	35.11					
Histone H3.1/ H3.2	AA(Cit)(dimethyllysine)SAPATGGK				27.19		

Table 5-1 Citrullinated proteins released from neutrophils undergoing NETosis – Q Exactive MS

Neutrophils from 3 different donors were stimulated to enter into NETosis and after 4 h supernatants were collected (SN1-3). After stimulation cells were washed 3 x with RPMI and subsequently incubated with DNase-I to generate the NET fraction (NET1-3). All fractions were centrifuged and subsequently precipitated with TCA. After trypsinisation samples were processed and analysed by mass spectrometry (**Q Exactive from Thermo Scientific**). The data were searched against Swiss Prot (human protein database) using Mascot. All spectra identified as citrullinated with a score of at least 20 were analysed. Values in the table represent Mascot scores. Empty cells signify that either no peptides or peptides with a Mascot score below 20 were identified.

Protein	Peptide Sequence	SN 1	SN 2	SN 3	SN 4	NET 1	NET 2	NET 3	NET 4
Coronin-1A	VN(Cit)GLDTGR								30.63
	(Cit)AAPEASGTPSSDAVSR		81.75		58.75				
SH2B adapter protein 1	C(Cit)LLLR			30.12					
ATPase family AAA domain-containing protein 3A	EQI(Cit)LKAAEHR								22.12
Actin-related protein 2	FEAPEALFQPHLINVEGVGVAE LLFNTIQAADIDT(Cit)SEFYK	30.84							
Alpha-(1,3)-fucosyltransferase 11	GACVASRN(Cit)R							36.58	
Bcl2 antagonist of cell death	KGLP(Cit)PK					23.29			
Fanconi anemia group F protein	LHNQW(Cit)QEGGFGR				31.94				
Caspase recruitment domain-containing protein 11	MNLKGIQLQ(Cit)AK	28.76							
Actin-related protein 2/3 complex subunit 1B	QSSQ(Cit)GLTAR				22.69				
Myeloid cell nuclear differentiation antigen	(Cit)NVPQNDPVTVVVLK					65.82			

Table 5-2 Citrullinated proteins released from neutrophils undergoing NETosis – LTQ Velos Orbitrap ETD MS

Neutrophils from 4 different donors were stimulated and after 4 h supernatants were collected (SN1-4). After stimulation cells were washed 3 x with RPMI and subsequently incubated with DNase-I to generate the NET fraction (NET1-4). All fractions were centrifuged and subsequently precipitated with TCA. After trypsinisation samples were processed and analysed by mass spectrometry (**LTQ Velos Orbitrap ETD MS**). The data were searched against Swiss Prot (human) using Mascot. All spectra identified as citrullinated with a score of at least 20 were analysed. Values in the table represent Mascot scores. Empty cells signify that either no peptides or peptides with a Mascot score below 20 were identified.

Protein	Peptide Sequence	slice 1	slice 2	slice 3	slice 4	slice 5
Histone H3.1/ H3.2	AA(Cit)(dimethyllysine)SAPATGGK	16.55			8	
Histone H3.1/ H3.2/H3.3/H3.1t	YRPGTVAL(Cit)EIR	35.27				

Table 5-3 Citrullinated proteins detected in the 11 kD band of the NET fraction

NET fractions from 5 different donors were loaded and analysed by SDS-PAGE and the 11 kD bands, which were shown to be citrullinated, were excised from gels, digested with trypsin and subjected to LTQ Velos Orbitrap ETD MS analysis. Values in the table represent Mascot scores. Empty cells signify that no peptides were identified.

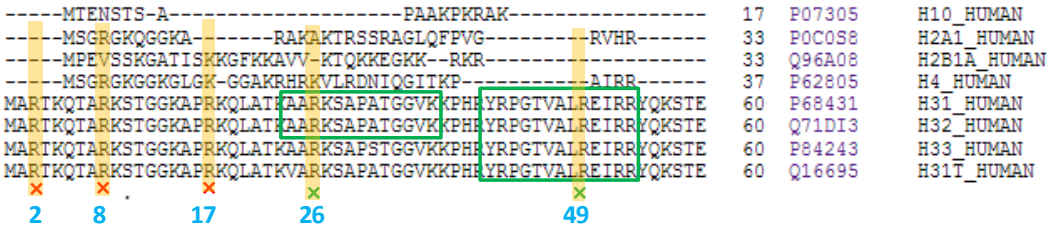

Figure 5-3 Alignment of protein sequences from histone subtypes

Protein sequence alignment of the N-terminus of histones H1, H2A, H2B, H3.1, H3.2, H3.3 and H3.1t using UniProt. Residues 26 and 49 were found to be citrullinated within 2 peptides in NETs (indicated with green boxes) using mass spectrometry by this approach (compare with Table 5-3) . Arginine residues at position 2, 8 and 17 are previously described targets of citrullination by PAD4 in histone H3 (386,387).

5.4 Purified ACPA specifically recognise an 11 kD band within *in vitro* and *ex vivo* NETs

After the identification of citrullinated proteins in NETs generated by *in vitro* stimulated neutrophils, it was of interest to determine whether these structures were antigenic in RA and, in particular, whether the citrullinated 11 kD protein is specifically recognised. For this purpose, Prof Karin Lundberg at the Karolinska Institutet in Stockholm kindly provided us with ACPA, which were purified from serum and plasma of RA patients using affinity chromatography on columns with covalently bound CCP2 peptides (388). The anti-CCP IgG that bound to the columns were finally eluted and pooled. The corresponding flow through (FT) IgG pool therefore contained all antibodies except for the one reacting with CCP2 peptides. Both the ACPA and FT IgG pool were validated for their binding specificity for citrullinated proteins. First of all, it was demonstrated that citrullinated recombinant vimentin and calf thymus histones (CTH) can be specifically detected using Senshu modification and human anti-modified citrulline antibody (Figure 5-4A). Finally, the native and citrullinated form of the proteins were probed with the same concentration of ACPA and FT IgG to confirm and validate the specificity of the eluted antibodies for known autoantigens such as vimentin. As shown in Figure 5-4B, the specific binding of these purified anti-CCP IgG (purified ACPA) and not FT IgG with the citrullinated form but not the native form of vimentin was confirmed. Interestingly, this specific binding with the citrullinated form of the protein could also be observed for calf thymus histones, which were not previously studied by Lundberg and colleagues (personal communication). Furthermore, both the first supernatant after 4 h of PMA stimulation of neutrophils (SN) and the DNase-I

treated NET-fraction were probed with purified ACPA and human IgG but not FT IgG as negative control. This decision was based on the fact that many antibodies present in FT IgG may still bind to neutrophil proteins and thus mask a specific binding of anti-CCP IgG when compared with this antibody pool. In addition, the detection system using the Senshu modification and anti-modified citrulline antibodies does not discriminate between citrulline and homocitrulline residues (389) so that non-CCP2-cross-reactive anti-carbamylated antibodies present in the FT IgG pool could bind to carbamylated neutrophil proteins and thus prevent a specific recognition of protein targets. As shown in Figure 5-5, purified ACPA could not specifically bind to neutrophil proteins present in the SN fraction. In contrast, a strong reactivity of purified ACPA compared with human IgG could be observed with an 11 kD band present in the NET fraction, although the signal strength exhibited variability between donors (Figure 5-6). Additionally, several bands in the molecular weight range 48-75 kD were observed, which resembled the pattern of citrullinated proteins in NET fractions detected on immunoblots, which were modified with the Senshu method and developed with a monoclonal human anti-modified citrulline antibody (compare Figure 5-1B). These proteins were, however, not consistently present in the NET fraction from all donors. For this reason, analysis concentrated on the citrullinated proteins present at the molecular weight of 11 kD.

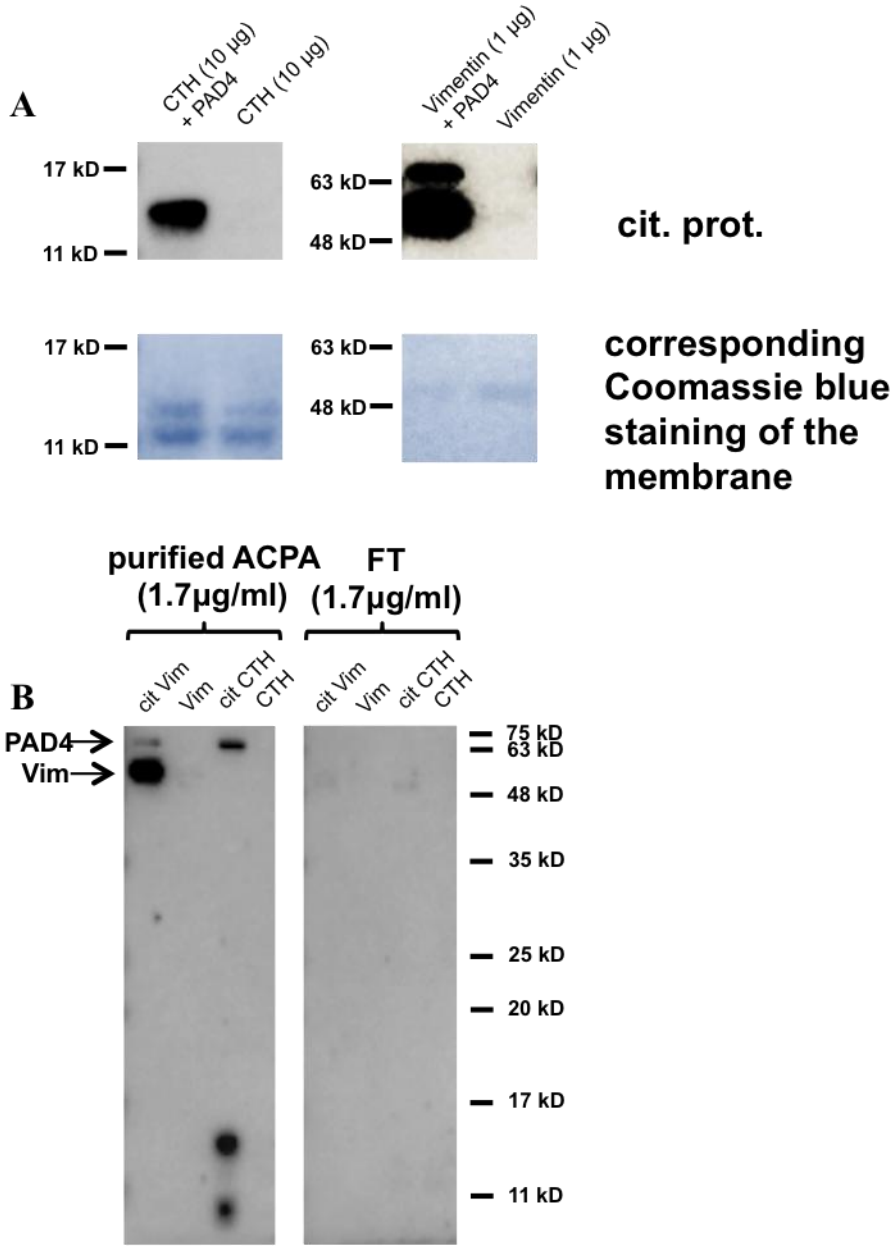

Figure 5-4 Specific recognition of the citrullinated form of Vimentin and calf thymus histones by purified ACPA from RA patient sera

Recombinant vimentin (Vim) and calf thymus histones (CTH) were *in vitro* citrullinated with enzymatically active PAD4 for 2h. **(A)** Specificity of citrullination was first demonstrated using Senshu modification and human anti-modified citrulline antibody. **(B)** Citrullinated and non-citrullinated forms of vimentin and calf thymus histones were probed in parallel with purified ACPA and the corresponding flow through fraction (FT) following affinity chromatography on columns with covalently bound CCP2 peptide. PAD4, which was added for the citrullination, was also detected.

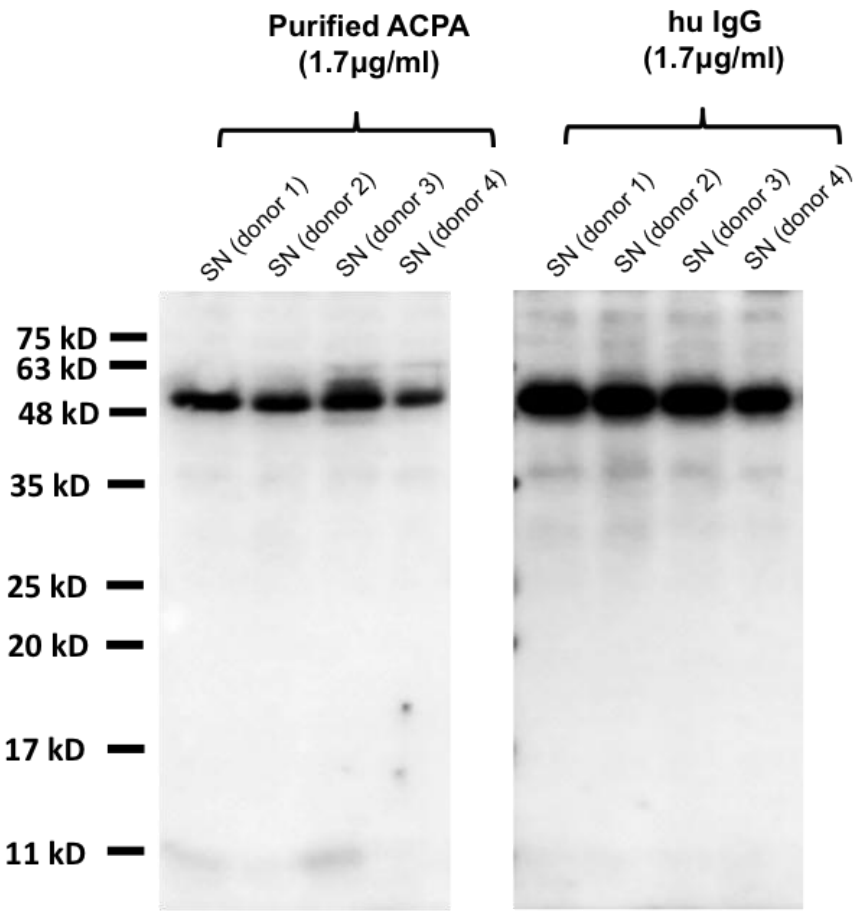

Figure 5-5 No specific recognition of antigens in the SN fraction of activated neutrophils by purified ACPA

Supernatants from 4 donors after 4 h of stimulation with PMA (SN) were collected, centrifuged and precipitated with TCA. Western blots were probed with purified ACPA and human immunoglobulin (hu IgG), which was used as a concentration-matched control.

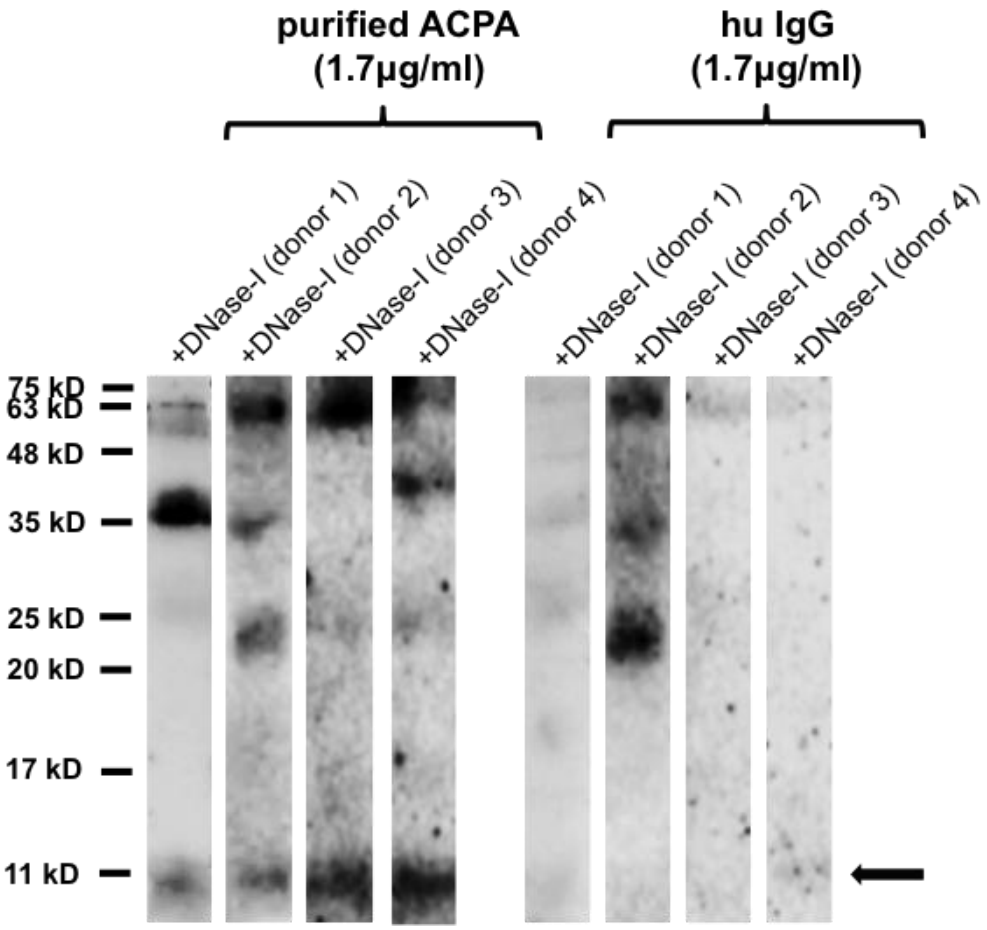

Figure 5-6 ACPA specifically and consistently recognise a 11 kD antigen in NETs

After stimulation with PMA neutrophils were washed and subsequently incubated with DNase-I. All fractions were centrifuged to remove cell debris. Proteins in the DNase-I treated NET fraction were precipitated from supernatants and analysed by western blotting. Purified ACPA and human immunoglobulin (hu IgG), which was used as concentration-matched control, were used at the same concentration. Four representative blots from four different donors out of eight independent experiments with eight different donors are shown.

As antigens could specifically be detected in the NET fraction of *in vitro* stimulated neutrophils, it was of interest to determine whether the same antigen of 11 kD size could also be identified within NETs from the SF of RA patients. For this purpose, NETs were initially isolated *ex vivo* from the SF using a method modified from the protocol used for the isolation of *in vitro* generated NETs (see Chapter 4.2). As shown in Figure 5-7A, a significantly higher DNA concentration could be detected in the DNase-I treated NET fraction (+DNase-I) suggesting that NETs can specifically be enriched after eight washing steps from the SF. Additionally, similar to the previously shown *in vitro* NET isolation, the presence of neutrophil elastase (NE) and PAD4 could be demonstrated specifically in the DNase-I treated NET fraction (+DNase-I), whereas no PAD4 and NE were detected in the final washing fraction (W8) and in the fraction of SF cells, which were solely incubated with RPMI under the same conditions (-DNase-I) (Figure 5-7B). Finally, the same fractions were incubated with purified ACPA to assay whether the same reactivity that was observed with *in vitro* isolated NETs (Figure 5-6) could also be found with *ex vivo* isolated NETs from the SF. As shown in Figure 5-7C, indeed, a specific reactivity of ACPA was detected against an 11 kD protein in the NET fraction compared with the W8 and –DNase-I-control fractions. Although these data suggest that the same antigen of an approximate molecular weight of 11 kD was detected as the antigen in *in vitro* NETs, the presence of citrullinated proteins using mass spectrometry analysis in these *ex vivo* NETs could not be studied further in more detail and therefore would need to be assessed in future studies.

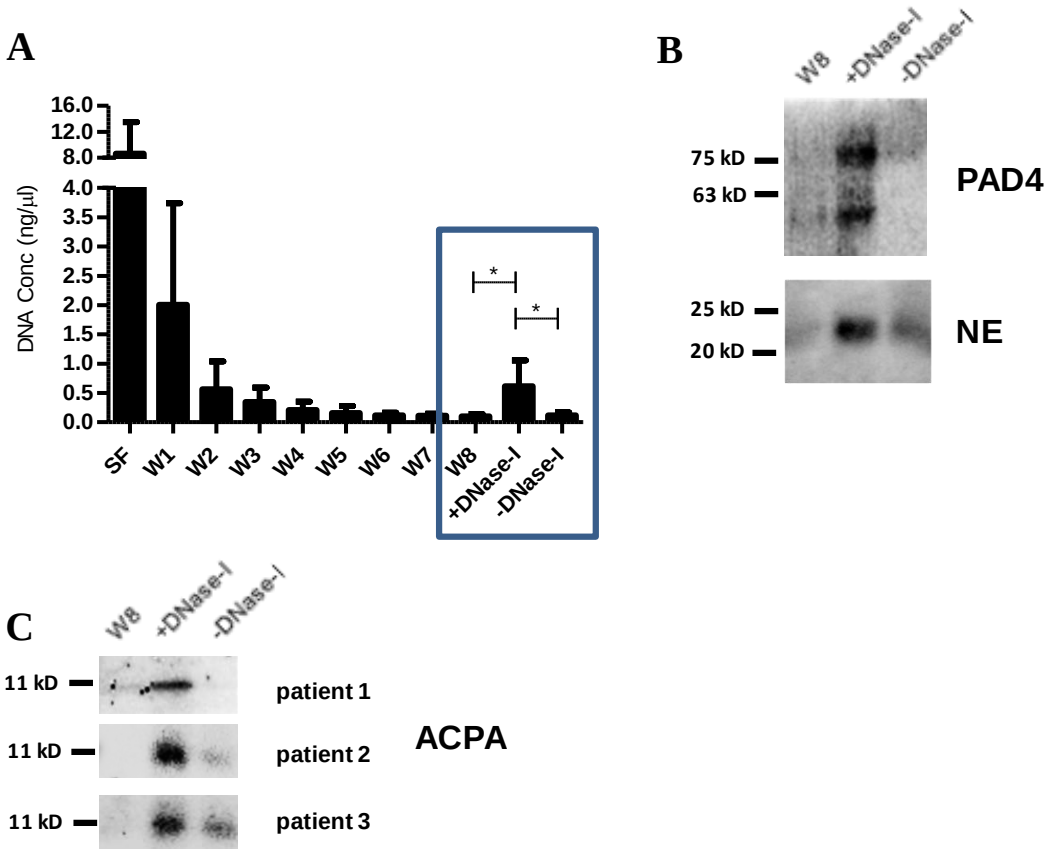

Figure 5-7 ACPA recognise an 11kD band within *ex vivo* NETs

(A) SF cells were seeded on 12-well plates. The supernatant was then removed and the cells attached to the bottom of the well were washed 8 x with RPMI (washing steps W1-W8). After the final washing step, cells were incubated with or without DNase-I (+DNase-I and –DNase-I). Extracellular DNA was quantified using SYTOX Green. Extracellular DNA could be specifically enriched in the supernatant of SF cells treated with DNase-I (Wilcoxon matched-pairs signed rank test, n = 7, *p<0.05). Results are shown as mean ±S.D. **(B)** Western blot of the final washing step W8, the DNase-I treated NET fraction (+DNase-I) and the mock-digested NET fraction (-DNase-I) probed for the presence of neutrophil elastase (NE) and PAD4; representative of at least 3 independent experiments per protein. **(C)** *Ex vivo* isolated NETs (+DNase-I) from the SF of 3 RA patients were probed with 1.7 µg/ml purified ACPA. The final washing step (W8) and the supernatant of the mock-digested cells (-DNase) are shown as controls.

5.5 Citrullinated Histone H3 is an autoantigen in RA patients

Core histones were previously reported to account for 70% of all NET-associated proteins (315). Using immunoblotting we revealed the presence of a protein with an approximate molecular weight of 11 kD, which is recognised by purified ACPA. In the same samples the presence of two citrullinated histone H3 peptides using mass spectrometry were also demonstrated. In the following section, characterisation of the immune response towards histones in RA patients in more detail is reported using the citrullinated and native form of recombinant histone H3 and compared with the reactivity for histones H2A and H4. For this purpose all three types of histones *in vitro* were citrullinated using the PAD4 enzyme. As shown in Figure 5-8A, 5 mU enzyme per 1 µg protein for the enzyme-to-substrate-ratio was sufficient to detect maximum citrullination on immunoblots. Interestingly, it could be detected that despite using the same enzyme- and substrate- concentrations under exactly the same reaction conditions, the efficiency of citrullination of different histone types differed. Indeed this efficiency was highest for citrullinated H3.3, but decreased for citrullinated H2A and was the lowest for histone H4 (Figure 5-8B). Similarly, a strong reactivity of ACPA was found for citrullinated H3.3, however, despite the low citrullination efficiency, a faint signal was detected for citrullinated H4 whereas no reactivity was found with H2A, which was citrullinated more efficiently than histone H4 (Figure 5-8B). Since the purified ACPA that were used for the previous experiments reflect a global reactivity of all antibodies present in pooled sera from at least 10 different ACPA positive RA patients, it is conceivable that the observed reactivity in our experiments derives from

antibodies present in relatively few patient sera. For this reason, it was decided to examine the reactivity with recombinant histones in individual patient sera. In agreement with results using purified ACPA, practically no reactivity with histone H2A was observed in the 8 tested sera, which derived from treatment-naïve RA patients (Figure 5-9). The strongest response, similarly to the purified ACPA, was however detected with citrullinated histone H3.3 in 2 out of the 4 tested ACPA positive RA sera. The same sera also reacted to a lesser degree with citrullinated histone H4. Interestingly, serum 8 also reacted additionally with the native form of histone H4 but not the native form of histone H3.3. In conclusion, both purified ACPA as well as RA patient sera seem to most strongly recognise the citrullinated form of recombinant histone H3 compared with the native form and other histone types. These data support our findings of strong reactivity of anti-citrullinated histone H3 antibodies and purified ACPA with citrullinated histone H3 in *in vitro* and possibly also *ex vivo* NETs.

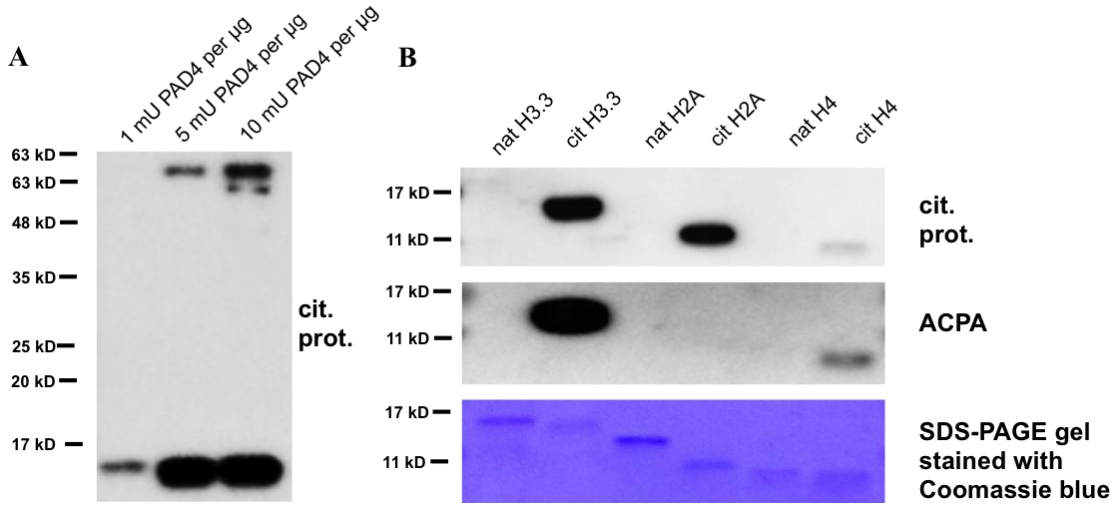

Figure 5-8 Purified ACPA strongly react with *in vitro* citrullinated histone H3.3

In vitro citrullination of recombinant human histone H3.3, H2A and H4 for 2 h. **(A)** Different enzyme-substrate ratios for PAD4 and its substrate H3.3 were used to test for maximum signal on immunoblot after Senshu modification and incubation with anti-modified citrulline antibody. **(B)** Immunoblot revealing different efficiency of *in vitro* citrullination of 400 ng histone H3.3, H2A and H4 by PAD4 (5 mU) under the same reaction conditions. One representative blot out of three independent experiments is shown. The same blot is shown below after re-probing with purified ACPA. Equal protein loading is demonstrated by Coomassie blue staining of the gel.

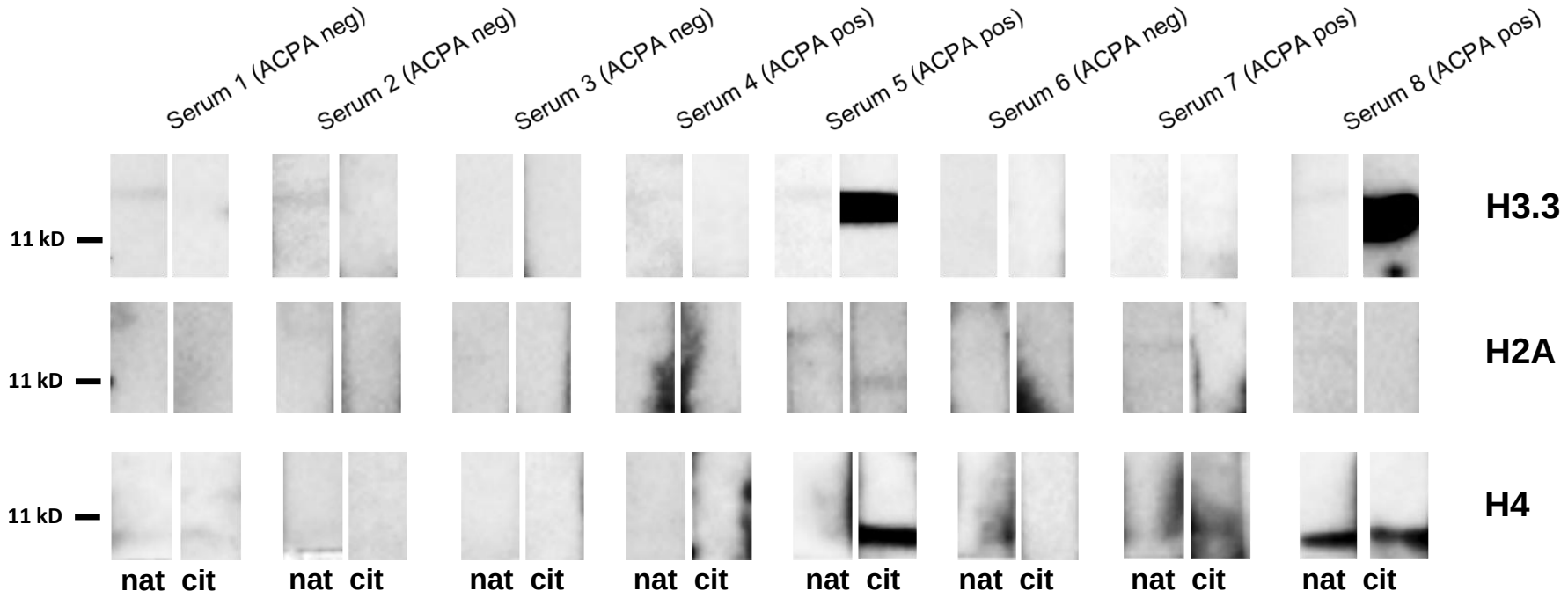

Figure 5-9 ACPA positive RA patient sera recognise histones

Native and citrullinated form of histone H3.3, H2A and H4 (400 ng) probed with RA sera from 4 ACPA positive and 4 ACPA negative RA patients diluted 1:100 in 5% milk/TBS-Tween.

5.6 Antibodies derived from SF B cells recognise histones

Anti-citrullinated protein antibodies, especially a high abundance of ACPA from the IgM isotype, were previously reported to be enriched in the SF compared with serum (365) suggesting a continuous autoimmune response in the joints. In light of data that demonstrated the presence of NETs in the SF of RA patients, we wished to investigate whether histones in NETs could be recognised by local B cells in the joints of RA patients and thus represent a potential local driver for the immune response. In collaboration with Prof Vivianne Malmström from the Karolinska Institutet, single B cells were sorted from the SF of patients with active RA and their Ig variable region genes were sequenced and subsequently expressed to generate recombinant monoclonal antibodies as has been previously described (235). This part of the project was undertaken by Dr Khaled Amara from the Karolinska Institutet, Stockholm, and Lorraine Yeo from the University of Birmingham. Equal amounts of non-citrullinated native recombinant histones (nat) alongside *in vitro* citrullinated histones (cit) were probed with an equal concentration of these recombinant antibodies from RA patients on immunoblots. The antibodies used were all derived from ACPA postivie RA patients. Initially 14 different antibodies were tested at a concentration of 5 µg/ml. From these 14 antibodies, 4 derived from 3 different patients and showed reactivity with histones H3.3 and H4 whereas no reactivity with histone H2A could be detected (data not shown). As shown in Figure 5-10, the reactivity of these antibodies from 3 ACPA positive RA patients are analysed at a higher concentration of 10 µg/ml. Purified ACPA and human IgG

were used as positive and negative controls, respectively. Whereas antibodies from B cells from patient 1 and 2 showed only a weak or comparable reactivity with the native and citrullinated form of H3.3 and/or H4, the three recombinant antibodies from patient 3 (clone 4-6) reacted more strongly with the citrullinated form of histone H3.3 and H4 compared to the native form (Figure 5-10). In conclusion, although these data are preliminary and a wider range of different antibodies would need to be screened for reactivity with histones, they suggest that joints of RA patients contain B cell clones with a stronger reactivity with the citrullinated form of histone H3 and H4 compared with the non-citrullinated form. Additionally, similar to purified ACPA and RA patient sera, no reactivity could be detected with histone H2A (data not shown). Histones released into the extracellular space during NETosis in the SF may therefore well be recognised by SF B cells.

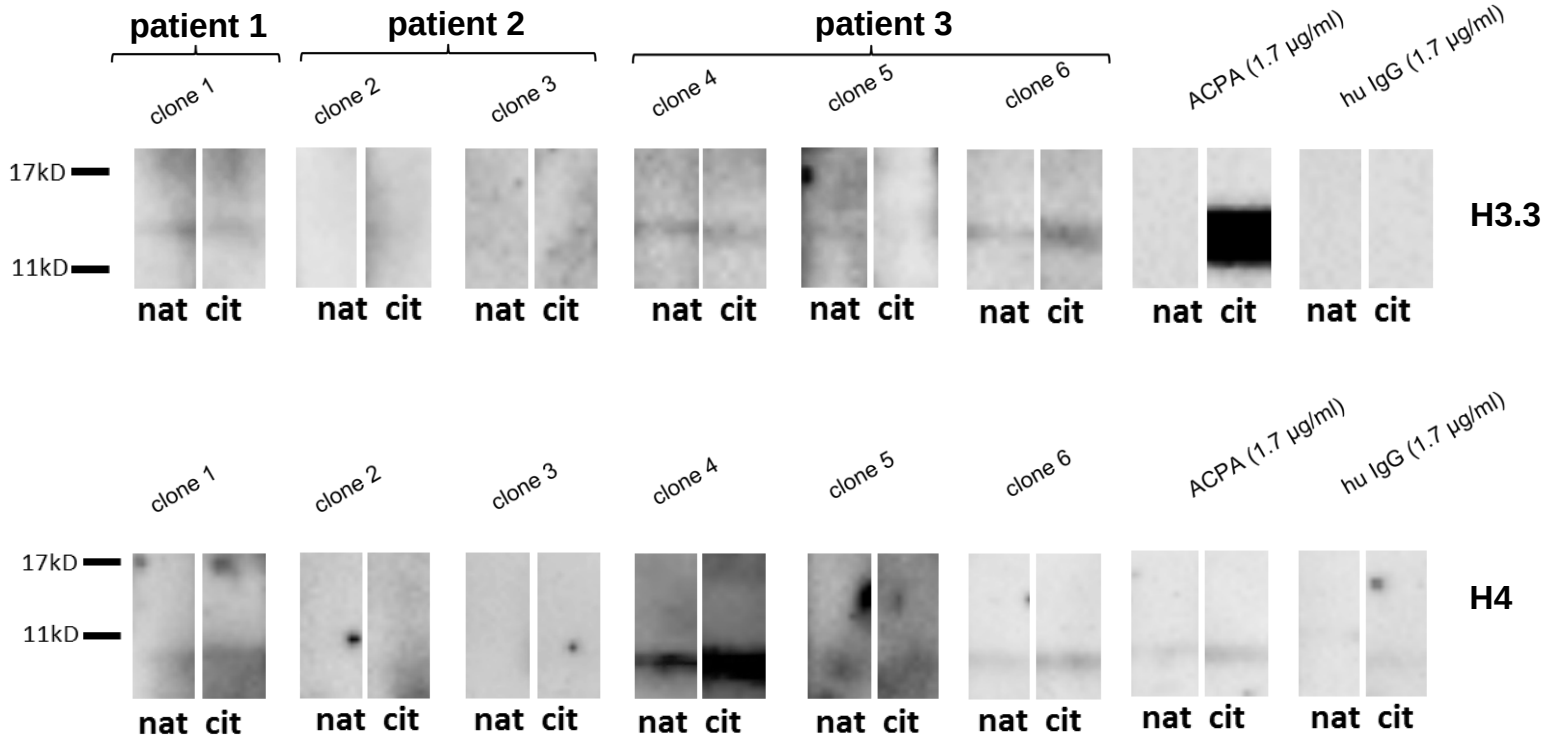

Figure 5-10 Antibodies from SF B cells react with both the native and citrullinated form of histone H3 and H4

Single B cells were sorted from the SF of patients with active RA. Their Ig variable region genes were sequenced and subsequently expressed to generate recombinant monoclonal antibodies. Equal amounts of non-citrullinated recombinant histones H3.3 and H4 (nat) alongside *in vitro* citrullinated histones (cit) were probed with an equal concentration of recombinant antibodies (10 µg/ml) derived from 6 B cell clones from 3 ACPA positive RA patients (patient 1: clone 1; patient 2: clone 2 & 3; patient 3: clone 4-6) using immunoblotting. Purified ACPA and human IgG were used as positive and negative controls, respectively.

5.7 RA patient sera recognise citrullinated epitopes in histone H3

Several different experimental approaches presented in this chapter have supported the notion of the presence and antigenicity of citrullinated histone H3 in NETs. To further characterise the reactivity of RA patient sera with this protein it was decided to investigate different epitopes of this protein in more detail. Based on mass spectrometry analysis (see chapter 5.3), two native and two citrullinated peptide sequences from the N-terminus of histone H3 were designed, and termed peptide 2 and 3 (Figure 5-11A). The citrullinated form of peptide 2 also contained a dimethylated lysine at position 27, which was present in *in vitro* generated NETs (see chapter 5.3). In addition, another citrullinated peptide sequence, cit peptide 1, was generated, which contained citrullinated residues at three positions (2, 8 and 17). This epitope was chosen due to the fact that it is an important target of PAD4 during decondensation of chromatin in NETosis (34,43). Furthermore, some reactivity of sera from SLE patients has recently been demonstrated against this post-translationally modified epitope (390) making it therefore an interesting antigenic target. All three peptides were coated on ELISA binding plates and tested for antigenicity with sera from 14 treatment-naïve RA patients. Pooled sera from 4 healthy individuals was used to determine the background level and was set to the value 0.0 as shown in Figure 5-11B. In total 10 out of 14 sera reacted with the citrullinated form of peptide 1 while only 3 sera reacted with the native form. Although the number of sera in these preliminary experiments was very low, a significantly higher reactivity could be found with the citrullinated form of peptide

1 compared with the native form, while the other 2 peptides showed a similar trend.

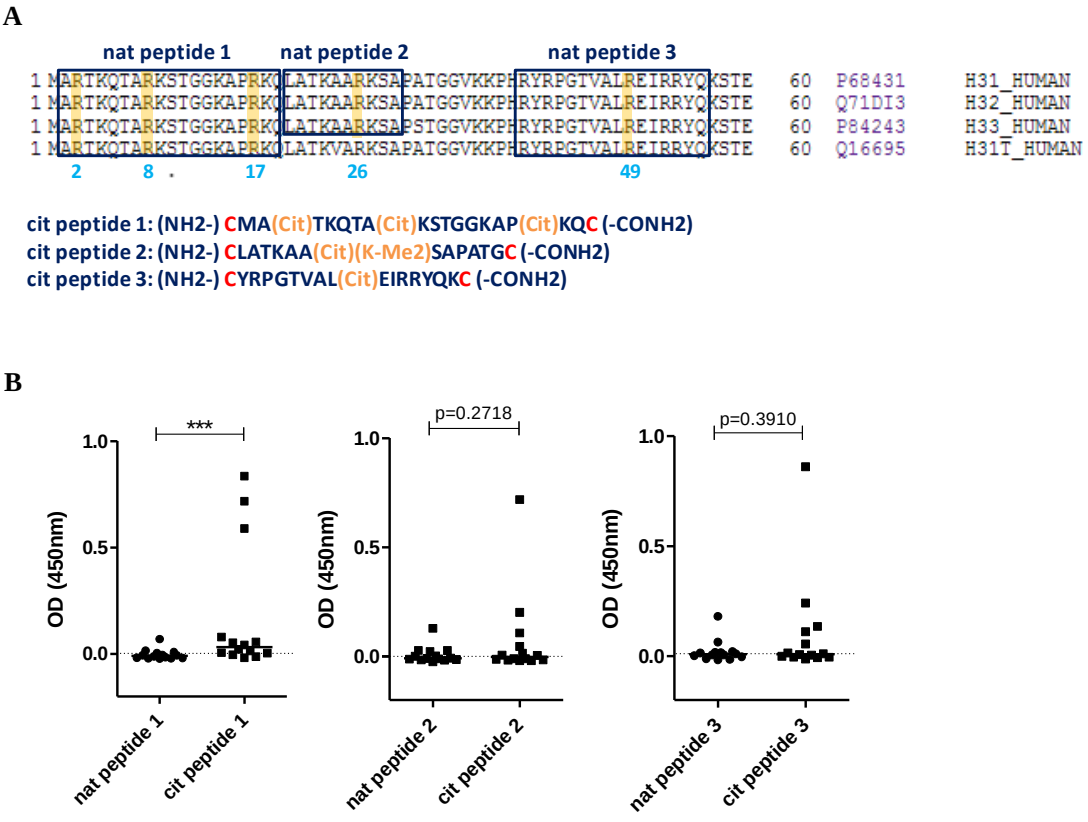

Figure 5-11 Reactivity of RA patient sera with three synthetic citrullinated cyclic peptides from histone H3

(A) Three different peptides from the N-terminus of histone H3 (peptide 1-3) with native arginine-residues (nat) (shown in the sequence alignment) and the corresponding 3 peptide sequences, in which the arginine residues were replaced by citrulline (cit) or the lysine residues by dimethylene residues (K-Me2), were synthesised by the company Innovagen. In total, six different protein sequences were synthesised. For the use of these peptides in ELISA assays, one cysteine residue at the N- and C-terminus was added (highlighted in red). **(B)** ELISA with the synthesised peptides were generated and their antigenicity was tested using sera from 14 RA patients. The background level was determined using pooled sera from healthy individuals (n=4) and set to 0.0 (dashed line). A significantly higher reactivity of RA sera against the citrullinated form of peptide 1 compared to the native form could be detected (Wilcoxon matched-pairs signed rank test, n=14, ***p<0.001).

5.8 Discussion

The overarching aim of the work presented in this chapter was to address the question as to whether citrullinated proteins are released during NETosis and whether they could serve as autoantigens in ACPA positive RA patients. Firstly, the release of free and NET-bound citrullinated proteins was demonstrated. Purified ACPA from RA sera were then found to specifically react with a citrullinated antigen of 11 kD in NETs from activated neutrophils. A band running at the same apparent molecular weight was recognised by anti-citrullinated histone H3 antibodies. Mass spectrometric analysis detected only two citrullinated peptides in gel slices from this molecular weight. These were identified as citrullinated histone H3. In further confirmatory studies, antibodies from RA patients were shown to strongly and specifically react with citrullinated recombinant histone H3 and with citrullinated epitopes from histone H3. Therefore results from a range of different experimental strategies point towards a strong immune response to citrullinated histone H3 in RA patients.

Post-translational modifications (PTMs) are known to lead to the generation of neo-epitopes and are proposed to initiate autoimmune responses in a range of autoimmune diseases (391–393). These modifications have also been described to occur in different forms of cell death, such as in apoptosis (394–396). With regard to rheumatoid arthritis the PTM citrullination is of utmost interest as anticitrulline autoimmunity is highly specific for this disease (70). In this study it was therefore interesting to observe that a large number of citrullinated proteins can be generated during PMA-induced NETosis. However, in agreement with previous work using HL-60 cells and human primary

neutrophils (34,44,390) no citrullinated proteins could be observed in unstimulated neutrophils using immunoblotting, although some degree of citrullination in unstimulated cells would be conceivable due to its role in gene transcription (50). It is possible that the levels of citrullination in the context of gene regulation are too low to be detected with the methods used here. Indeed global *de novo* generation of a wide range of citrullinated proteins after neutrophil activation observed in this study, which in some publications is referred to as hypercitrullination (43,44,53), could therefore be regarded as a consequence of activation and NETosis.

Citrullination of a range of proteins such as fibrinogen, filaggrin, collagen and histones has previously been described to induce a shift in the mobility of the citrullinated form of the proteins during reducing SDS-PAGE analysis. Whereas citrullination of filaggrin and fibrinogen by PAD2 and PAD4, was shown to induce a decrease in the mobility compared with the native form of the proteins (175,372,397), an increased mobility in reducing SDS-PAGE analysis has been demonstrated for citrullinated histones (50,315,398) and was indeed confirmed in data presented here. Interestingly, although a mobility shift for fibrinogen chains under reducing conditions was confirmed by Okumura and colleagues in another study, the authors did not observe this mobility shift when using non-reducing conditions (397). For this reason, this phenomenon cannot simply be explained by a loss of protein charge after citrullination alone. It is conceivable that the number and position of citrullinated arginine residues within the protein alters intermolecular interactions in a way that affects its susceptibility to reducing conditions, which can ultimately result in decreased or increased

mobility through the SDS-PAGE-gel. Citrullination could therefore be one explanation for the detection of histone H3 in *in vitro* NETs at the size of 11 instead of 15 kD. Since the citrullination of recombinant histone H3.3 expressed in *E.coli*, which is devoid of eukaryotic posttranslational modifications, could not induce a mobility shift to 11 kD in these experiments, additional post-translational modifications other than citrullination may also add to the observed shift in the mobility of histones generated during NETosis.

Currently, there are several lines of evidence indicating the occurrence of histone citrullination as a result of PAD4 activity. PAD4 was shown to citrullinate arginine residues at the positions 2, 8, 17 and 26 in histone H3 (194) and at position 3 on the N-terminal sequence shared by histone H2A and H4 (382), whereas the citrullination of histone H2B, to our knowledge, has yet to be described in the literature. These results are consistent with our observation of recombinant histone H3, H2A and H4 *in vitro* citrullination by PAD4. In NETs citrullinated histone H3 has been detected in several reports using confocal microscopy (34,354,399) with the same antibody that was used in the approach presented here using immunoblots, thus supporting the presence of this histone subtype in NETs. Furthermore, histone citrullination in NETs from *in vitro* stimulated neutrophils in our study could also be demonstrated using mass spectrometry. In excised 11 kD gel slices from NET fractions separated on SDS-PAGE gels two citrullinated peptides derived from histone H3 were detected and among these one was found to be citrullinated at the arginine residue 26. The second H3 peptide was shown to be citrullinated at position 49. This finding is intriguing as this same peptide was the only citrullinated peptide

detected in the SF of RA patients by van Beers and colleagues (375) and thus supports our notion that histone H3 citrullination occurs during NETosis in the SF. Furthermore, similar to our approach, Pratesi et al. recently reported the reactivity of RA patient sera with an 11 kD band using NET fractions generated with PMA (400), which is also in agreement with findings presented here. At variance with this data, however, Pratesi et al. only identified one citrullinated peptide from histone H4, which was citrullinated at arginine residue 3 and no citrullinated peptides from histone H3 were detected (400). Although Arg3 in histone H4 is a well-described target of PAD4 (390) and a weak reactivity of citrullinated recombinant histone H4 with purified ACPA could also be demonstrated in experiments presented here, this peptide was not found in the SF by van Beers and colleagues (375). The discrepancy in the data may be explained by the different protocols used for processing of protein samples for mass spectrometry, the use of different analytical instruments and also the search parameters used in the downstream analysis in the study.

It is interesting to note in this context that Neeli et al. recently proposed that although PMA is able to induce NETosis it would neither cause PAD4 activation nor histone citrullination (52). However citrullination of histones induced by PMA has been shown not only in data presented here but also previously by others (399–401). Furthermore, the finding described by Neeli and colleagues also challenge the current view that citrullination is a requirement for chromatin decondensation during NETosis (44,46). One possible explanation, however, could be that a shorter PMA stimulation time of 2 h compared with 4 h as undertaken here, did not allow sufficient histone citrullination. Additionally, differences in the concentration of the PMA stimulus may be responsible for

these strikingly different results. Since it is not known how PAD4 is activated during NET formation and how it exactly leads to the citrullination of histones (402), further investigations are required to elucidate the role of PAD4 in NET formation.

PAD4 is the only PAD isoenzyme with a nuclear localisation signal, which allows the translocation of the enzyme into the nucleus enabling the citrullination of histones (196). However, recent studies have also reported on the presence and activity of PAD2 in the cell nucleus (403,404). Indeed Zhang et al. have described that the arginine at position 26 in recombinant histone H3 is citrullinated more efficiently by PAD2 than by PAD4 (403) suggesting that more than one PAD isoform may be involved in the citrullination of different arginine residues and/or histone types during NET formation. In this context, data presented here indeed showed a difference in the efficiency between citrullination of histones H3, H2A and H4 by PAD4 enzyme. This observation is in agreement with a report from Darrah et al. which demonstrated that although PAD2 and PAD4 are in principle both capable of citrullinating histones, only PAD4 would target histone H3 in cell lysates whereas PAD2 would show an instrinsic substrate preference for other targets such as beta actins (203). It is therefore necessary to consider that both detected citrullinated peptides from histone H3 are likely to be citrullinated by PAD4 during NET formation.

In addition to citrullinated peptides derived from histone H3 we detected three additional citrullinated peptides derived from vimentin, myeloid cell nuclear differentiation antigen (MNDA) and coronin-1A released from *in vitro* activated neutrophils. Coronin-1A was identified in both the SN as well as the NET

fraction whereas vimentin and MNDA were exclusively present in NETs. Interestingly, citrullinated peptides from all three proteins were among 53 citrullinated proteins detected in albumin depleted SF samples from RA patients in the previously mentioned study by van Beers and colleagues (375). Together with the evidence that vimentin and MNDA are both known ACPA targets it can thus be assumed that NETosis might be a source for the generation of not only citrullinated histone H3 but also of further known autoantigens in the SF of RA patients. Since synthetic citrullinated peptides, which were used for the purification of ACPA, however, do not represent physiologic peptides, it can be assumed that potentially not all anti-citrulline reactive ACPA could be purified using this method. Future experiments with *in vitro* NETs and ACPA positive RA patient sera may therefore reveal whether the additionally identified citrullinated proteins such as coronin-1A could be specifically targeted by autoantibodies in RA patients. Additionally, it should be considered that the mass spectrometry data revealed a large variability between donors and different instruments and therefore not all citrullinated peptides were consistently present in all samples analysed. Methods are therefore under development to control for this issue and thereby reduce the risk of obtaining false-positive or false-negative hits.

As demonstrated in this chapter the isolation of *ex vivo* NETs was not as efficient as in the *in vitro* experiments leading to mean DNA concentrations in the NET fractions being four times lower than *in vitro* (compare Chapter 4, Figure 4-2). The low abundance of NETs released after DNase-I treatment could, however, be explained by the fact that cell associated NETs are less frequently present in the SF due to the fragile nature of these structures.

Mechanical stress during the assay procedure could lead to the dissociation of NETs from neutrophils over time, which may decrease the efficiency of the *ex vivo* NET isolation approach. Nevertheless, although the stimulus of PMA used in the experiments here is not physiological and therefore unlikely represents a stimulus for NET formation in the joints, it was interesting to find that purified ACPA showed not only a specific reactivity with a protein at 11 kD in PMA induced *in vitro* NETs, but also with a protein of the same size in NETs isolated *ex vivo* from the SF of RA patients. Although the identity of this protein could so far not be determined in this thesis it is tempting to speculate at this point that this protein at 11 kD may be citrullinated histone H3. Indeed, a preliminary proteomic analysis of the total protein composition in an 11 kD gel slice from the *ex vivo* NET fraction of one RA patient sample showed the presence of histone H3.1 (data not shown). An analysis of citrullinated proteins, however, has not been performed yet.

Following the identification of citrullinated peptides from histone H3 in *in vitro* NETs, several validation experiments have been performed with recombinant histones to demonstrate antibody reactivity with citrullinated histone H3 in RA patients. The antigenicity of citrullinated and native histones was not only assessed using purified ACPA from pooled patient sera, but also using single RA patient sera and with antibodies derived from single SF B cells. Both purified ACPA and two out of four analysed ACPA positive RA patient sera showed similar results with the strongest reactivity indeed detected against citrullinated recombinant histone H3. In addition, despite lower citrullination efficiency by

PAD4, some reactivity against citrullinated recombinant histone H4 was present.

In comparison, the reactivity pattern of antibodies derived from SF B cells showed a high degree of variability and thus slightly differed from the results obtained with antibodies present in RA patient sera. With a low number of only 14 antibodies from SF B cells analysed on western blots so far, the strongest reactivity of one antibody was noted with citrullinated histone H4. The same reactivity pattern could also be seen with two other clones from the same patient, although not all analysed B cell clones from the same patient showed reactivity with histones (data not shown). Concomitantly, the same antibody also displayed some cross-reactivity with citrullinated histone H3. Interestingly, Amara et al. reported in this context that a high proportion of these IgG-expressing memory B cells and early plasmablasts from the joints of ACPA positive RA patients are biased toward reactivity with known citrullinated autoantigens and subsequently suggested that the generation of citrulline-specific antibodies may result from T cell-dependent B cell immune responses (235). Based on these studies it is therefore tempting to speculate that synovial IgG-expressing B cells specific for citrullinated autoantigens such as citrullinated histones could represent APCs important for T cell reactivation.

Overall, the work detailed in this chapter demonstrates that citrullinated histone H3 and citrullinated histone H4 can be recognised not only by antibodies in RA patient sera but also by antibodies derived from SF B cells. Two recent studies indeed reported about the reactivity of RA patient sera with citrullinated histones present in NETs. Whereas Pratesi et al. identified a strong reactivity of RA

patient sera with citrullinated histone H4 (400), Dwivedi and colleagues, however, found the strongest reactivity of patient sera with Felty's syndrome and RA directed against citrullinated histone H3 (398). These different results may be explained by different experimental protocols of the ELISA or a different degree of the purity of histones. Additionally, due to the different type of linear or conformational epitopes detected in western blotting or ELISA, discrepancies may be found in the results depending on the technique. Finally, core histones are known to be heavily post-translationally modified and anti-histone antibodies can be found in healthy individuals, RA, SLE, drug-induced SLE and different other conditions (390,405,406). The use of total histones in combination with patient sera from different cohorts may thus also lead to differences in the background and impede the detection of antibodies that target citrullinated histones. Future studies with a higher number of patient sera and antibodies from SF B cells would be needed to investigate the disease specificity and citrulline specificity of the anti-citrullinated histone H3 response in RA patients with peptide ELISAs as a potential method of choice.

Currently, it is still not known whether ACPA are directly pathogenic or whether they contribute to local perpetuation of synovial inflammation. Assuming that ACPA indeed just enhance synovial inflammation, the continuous supply of citrullinated ACPA targets from newly recruited neutrophils would potentially provide an explanation for the persistence of B cell clones specific for citrullinated proteins in the inflamed synovium and the enrichment of ACPA in the SF compared to serum.

6 General Discussion

The main purpose of the immune system is to rapidly detect and destroy pathogens. Only when the pathogen is removed from the body can the immune response return to its homeostatic state which is essential to prevent development of chronic inflammation and subsequent tissue damage. In autoimmune diseases the immune system is directed against self-molecules and can ultimately fail to remove these autoantigens from the body so that subsequently the inflammation finally evolves into a chronic state. While autoantibody responses in some autoimmune diseases are well-characterised, the initiating triggers and source of autoantigens still remain largely unknown. In ACPA positive RA patients the generation of citrullinated autoantigens after protein deimination by PADs is a key stage in the autoimmune response (168). Nevertheless, the mechanisms behind the activation of PADs, as well as the sites and circumstances of citrullination of autoantigens in RA have remained unclear. In this thesis I have investigated whether neutrophils undergoing NETosis can contribute to the production of citrullinated autoantigens in RA patients. Using different experimental approaches NETosis was identified as a source of freely diffusible enzymatically active PADs as well as of citrullinated proteins. Moreover, I have provided evidence that isolated NETs are antigenic and have demonstrated a reactivity of RA patient sera with citrullinated histones, particularly with citrullinated histone H3. Altogether, these data suggest a central role for neutrophils in the generation of autoantigens in RA.

Neutrophils are the most abundant cell type present in the SF of patients with RA (102,105), where they are found in an activated state producing ROS and releasing cytokines and proteases with cytotoxic potential (109,117,407,408).

Similar to what has been previously reported regarding the presence of NETs in infections (409), autoinflammatory conditions (339) and autoimmune diseases such as SLE (410) or ANCA vasculitis (33), the data presented here show that neutrophils undergo NETosis in the joints of patients with inflammatory arthritis and thereby release decondensed DNA. In agreement with a previous study by Khandpur and colleagues (120) extracellular DNA in RA joints was observed within neutrophil infiltrates attached to the surface of the synovial lining layer. In addition to these findings the presence of NETs on synovial fluid preparations was demonstrated.

The data presented here indicate that extracellular DNA levels and neutrophil concentrations in the SF correlate with PAD activity in agreement with the proposition that PADs are released and activated as a result of NETosis in the joints of patients with RA while in SF from patients with OA minimal PAD activity was demonstrated. PAD enzymatic activity is regulated by calcium ions (47), indeed intracellular Ca^{2+} levels are below the level required for *in vitro* PAD activity, indicating further yet undefined regulatory mechanisms (411). Hence, *in vitro* PAD activity was initially measured at supraphysiological calcium concentrations. However, while the PAD activity measured in RA SF at physiological calcium concentrations was lower, it was still detectable with the ABAP assay used in this study and was significantly higher than in OA SF. This observation was also confirmed by others in a recent relatively small study using human fibrinogen as the substrate for PAD activity (412). In agreement with the data presented in this thesis, calcium concentrations in RA SF samples in that publication were found to be sufficient to support PAD activity. It can

therefore be concluded that the conditions for optimal activity *in vitro* differ from the conditions *in vivo*. In this regard, a recent study by Darrah et al. reported a mismatch between the *in vitro* and *in vivo* calcium requirements for PAD4 activity and explained this by the presence of PAD3/PAD4 cross-reactive antibodies that may play a major role in decreasing the enzyme's requirement for calcium into the physiologic range *in vivo* (369). Future studies are needed to identify the contribution of different isoenzymes to the overall PAD activity observed during NETosis and to investigate regulatory factors that might modulate enzymatic activity.

As the assay used for measuring PAD activity does not distinguish between different PAD isoforms, a contribution to the total PAD activity by PAD2, PAD3 and PAD4 is possible (411). Interestingly, mass spectrometry data did not identify any unique peptides matching PAD3 as being present in neutrophils. Identification of PAD isoforms that are responsible for the observed PAD activity is of interest as it was recently reported that different PAD enzymes display distinct substrate specificities (203) and could therefore lead to the citrullination of different autoantigens.

Additionally, the mass spectrometry data shown here could demonstrate that PAD2 and PAD4 both diffuse freely into the supernatant during NETosis and also remain attached to the DNA/protein complex of the NETs. This finding is important since PADs that remained exclusively tethered to NETs, would potentially limit the role of neutrophil-derived PADs to the SF. The lack of a basement membrane and tight junctions in the synovial lining together with these results regarding freely diffusible PADs therefore suggest that freely diffusible PADs released from neutrophils within the SF could enter synovial

tissue and potentially contribute to the local production of autoantigens throughout the inflamed synovium (250).

Though currently topical, the discovery of extracellular DNA in autoimmune diseases is not novel. Circulating nucleosomal DNA has been observed in patients with SLE (413), scleroderma, Sjögren syndrome and ANCA-associated vasculitis (414). DNA has also been found in the SF of RA patients (340,341). For many years, the presence of extracellular DNA in these diseases has been explained with clearance defects and secondary necrosis of apoptotic cells and linked to the pathogenesis of autoimmune diseases, particularly SLE (415). When studying cell death mechanisms, however, we must be aware that different cell death mechanisms are difficult to distinguish due to the lack of understanding of their complexity. In many publications at present, for example, the most widely accepted way to define necrosis has been to demonstrate the absence of apoptosis (416). Furthermore, since NETosis shares many features initially ascribed to apoptosis and necrosis in systemic autoimmunity, and since the exact signalling pathways inducing NETosis are not fully investigated yet (compare section 1.1.4.1), the discovery of NETs has added layers of more complexity. The data presented in this thesis cannot exclude the possibility of cells other than neutrophils contributing to the extracellular DNA levels, PAD activity and/or citrullination detected in the SF of RA patients. In addition, activation of other cell death mechanisms in neutrophils other than NETosis cannot entirely be ruled out. Intracellular citrullination was reported in several cell populations in the synovium (250,251) and in SF cells (53), and cell lysis induced by immune-mediated membranolytic pathways, for example, could

represent another source of PADs and citrullinated proteins (53). Furthermore, monocytes and macrophages can also be a source of PADs (195), and cells such as eosinophils, mast cells or macrophages can reportedly release their chromatin in a process related to NETosis (346). However, eosinophils and mast cells are present in relatively very low numbers in RA SF (417). Moreover, extracellular DNA levels in the SF showed no significant correlation with macrophage counts while there was a highly significant association between DNA levels and neutrophil numbers. In addition, comparison of neutrophils undergoing necrosis and NETosis showed that there is significantly less release of soluble extracellular DNA from necrotic neutrophils (411). This difference may be explained by the high level of nuclear decondensation during the process of NETosis. However, these results should be interpreted with caution as they may not reflect the true situation in the joints *in vivo*.

While the role of NETs during infections was identified primarily as a process for the immobilisation of microbes (24,36,315), the reason for their release in autoimmune diseases remains less clear. NETs could theoretically be involved in the initiation of autoimmunity based on the concept of cryptic antigens originally proposed by Sercarz and colleagues (418). According to this hypothesis cryptic antigens that are otherwise located intracellularly and are not visible to the immune system could become exposed during NETosis and activate autoreactive lymphocytes. A further possibility is that NETs could contribute to the propagation of inflammation at a later stage of the inflammatory process after the breakdown of tolerance and thereby fuel the chronic inflammatory cycle by releasing cytotoxic proteins and autoantigens

(419,420). Interestingly, a large amount of NET-associated proteins are known autoantigens in systemic autoimmune diseases (21,66,315,361,419) (compare section 1.1.4.3) suggesting that autoantigens present in NETs may be targeted across the broad spectrum of different autoimmune diseases (361). Importantly, these autoantigens clearly differ from the ones exposed during apoptosis with a different range of post-translational modifications (PTMs). Nuclear autoantigens such as Ro, La and Sm have not been detected in NETs previously (419,421) and were also not identified in the experiments performed here. Additionally, PTMs of autoantigens that have been described in apoptotic cells, for example, phosphorylation or transglutamination (361,422) have also not been detected in NETs thus far. One exception with regard to PTMs appears, however, to exist with regard to methylation and acetylation. Similar to data previously reported in apoptotic cells (395,396) both PTMs were detected in a recent study in NETs (390) and a dimethlyated lysine residue in histone H3 was observed in the study presented here. Nevertheless, the induction of PTMs in NETs seems to be much more limited than in apoptosis. A further PTM in addition to methylation and acetylation has been described in NETosis: citrullination. While apoptotic cells have yet not been reported to generate citrullinated proteins (34), PAD4 induced citrullination is known to be essential for NETosis (43,44,46). Indeed, the mass spectrometry data presented in this thesis has revealed a number of citrullinated proteins in NETs and among these were vimentin and MNDA which are already known autoantigens in RA (304,352,375). Furthermore, certain proteins including several peptides were identified which are already published as being present in the SF of patients with inflammatory arthritis (249,375,423) supporting the supposition that NETs are a possible source for these

citrullinated proteins. The view that NETosis contributes to citrullination in the joints of RA patients is also supported by data from De Rycke et al. who observed localisation of citrullinated proteins within extra-synovial deposits of polymorphonuclear cells on the surface of the lining layer in RA patients (248).

To determine whether the citrullinated proteins released during NETosis could represent antigenic targets in RA patients, experimental approaches in this thesis, including immunoblotting and ELISAs using total proteins or cyclic peptides, were undertaken to narrow the broad range of possible candidates. In concordance with recently published work (398,400) a particularly prominent and consistent reactivity against citrullinated histones within NETs could be observed. Whereas Pratesi et al. identified a strong reactivity of RA patient sera with citrullinated histone H4 using peptide ELISA (400), Dwivedi and colleagues used ELISA with total histone proteins and found the strongest reactivity against citrullinated histone H3 with sera from patients with Felty's syndrome and some reactivity with RA patient sera (398). In agreement with Pratesi and co-workers a strong reactivity of ACPA and RA patient sera with a citrullinated protein of the size of 11 kD in *in vitro* NETs was observed in this study. Notably, ACPA were also found to react with *ex vivo* NETs isolated from the SF of RA patients. In addition, similar to the data reported by Pratesi et al., some reactivity of RA patient sera with citrullinated histone H4 (400) on immunoblots was detected, however, a much stronger reactivity was observed with citrullinated H3. Moreover, no peptides from citrullinated H4 could be detected after in-gel digestion of 11 kD gel slices from NET fractions in the work presented here. Instead, peptides from citrullinated H3 were identified in the gel slices and a

reactivity of RA patient sera could be observed against these peptides. The number of citrullinated proteins identified with mass spectrometry is relatively small and the very rigorous validation process used to minimise false positives (as described in the Materials and Methods Chapter 2 and the Appendix Chapter 8) may have contributed to this. Further work therefore remains to be undertaken to ensure more consistency in the detection of citrullinated proteins using mass spectrometry analysis. Additional citrullinated antigens, such as, for example, autocitrullinated PAD4 have been identified by others and could (199,200) well be also generated during NETosis.

One of the major questions in autoimmunity is why many autoantibodies are already generated before the onset of clinical symptoms and which role these autoantibodies play in the pathogenesis. ACPA can be found several years before onset of clinical symptoms (81) and ACPA positive RA patients generally develop a more severe disease (204,205). In addition, genetic susceptibility and environmental factors in RA are associated with autoimmunity to citrullinated proteins (210,211). Taken together, these observations suggest that ACPA are likely to be involved in the pathogenesis of RA (23) but that they on their own are not sufficient to cause disease. For this reason, we need to determine the answer to the question as to how exactly the pathogenesis in ACPA positive individuals differs from ACPA negative individuals as this would provide a major step forward in our understanding of the disease process. One possible mechanism as to how ACPA could contribute to an aggravation of disease was demonstrated in a recent study in which anti-citrullinated vimentin antibodies were able to directly interact with osteoclasts and induce osteoclastogenesis

and bone loss (312). Interesting in this context is also the finding that other autoantibodies such as ANCA in ANCA-associated vasculitides were shown to activate neutrophils *in vitro* (55), and are able to induce vasculitis in animal models (56,57). The exact mechanisms responsible for this activation, however, still remain to be characterised. A further possibility as to how ACPA may be involved in disease pathogenesis may depend on the formation of ICs and activation of the complement system. While neither the injection of NETs (390), nor of apoptotic or necrotic debris on their own have been shown to be able to induce inflammation in animal models (424–426), autoantibodies were found to convert cell debris into immunostimulatory ICs, which bind to Fc receptors on macrophages, neutrophils and B cells, leading to their activation (112,305,427). This effect may also be enhanced by the presence of RF, which was suggested to participate in forming ICs by crosslinking IgG (161,428). Indeed, data presented in this thesis suggest that PEG enriched ICs from SF of RA patients appear to have the potential to induce NETosis. Since the preliminary results in this study, however, were not able to show that this phenomenon is mediated through Fc receptors, additional molecules within NETs, such as damage-associated molecular patterns (DAMPs) may contribute to the activation of immune cells through their binding to PRRs (429,430). To follow up on the findings reported here, it would therefore be interesting to investigate which mechanisms may contribute to the induction of NETosis in the SF of RA patients to potentially develop therapeutic compounds, which may inhibit the deleterious aspects triggered by NET released locally within the joints.

Several studies indicate that the absence of synovial inflammation (as determined histologically and by imaging) in individuals who have RA-specific autoantibodies and joint pain but no clinically apparent joint swelling (85,87,88), and therefore propose the concept that the initiating event leading to ACPA production is more likely to occur outside the joint. Recent findings of increased protein citrullination and ACPA enrichment in the lungs (431) or the periodontium (432) early after disease onset support this notion. Based on findings of NETs in inflamed gingiva (433) and lungs (342) it is possible that PAD release during NETosis contributes to generation of citrullinated proteins initiating the ACPA response at these sites. In addition, other mechanisms such as the generation of citrullinated peptide-MHC complexes in autophagosomes of APCs followed by the induction of autoimmunity are possible (434). The production of citrullinated proteins during NETosis in the joint is therefore unlikely to represent the original breakdown of immune tolerance to citrullinated proteins.

Based on the work presented in this thesis and as illustrated in Figure 6-1, release of PADs from neutrophils in the joints of RA patients is more likely to represent a later event in the disease process where citrullinated proteins and pre-existing ACPA form pro-inflammatory immune complexes drive a continuous inflammatory response in the joints. This notion is also supported by the finding of significantly higher DNA levels in ACPA positive RA patients compared with ACPA negative RA patients. In this context a recent publication reporting that PAD4 is not essential for disease in the K/BxN murine autoantibody-mediated model of arthritis does not conflict with these observations, as this model does not depend upon autoimmunity to citrullinated

proteins (435). According to our proposed model (Figure 6-1), NETosis and the release of enzymatically active PADs in the SF of patients with inflammatory arthritis may, as has been described by Vossenaar et al., represent 'sparks that may ignite the fire of RA' (247). The continuous supply of citrullinated ACPA targets from newly recruited neutrophils could potentially provide an explanation for the persistence of B cell clones specific for citrullinated proteins in the inflamed synovium of RA patients (235) and the enrichment of ACPA in the SF compared to serum (352).

Since the data presented in this thesis cannot prove a causal relationship between the observed neutrophil concentration and DNA levels and PAD activity in the SF, future investigations into different cell death mechanisms of neutrophils and other cells in RA patients is warranted. Furthermore studies in patients with other forms of autoimmune diseases, where cell death of neutrophils appears to play an essential role, may provide important insights into the role of these cells in autoimmunity. Assuming that neutrophils are cells that are particularly prone to die at the site of inflammation and expose autoantigens, the mechanisms of recruitment and activation in sterile inflammation requires further research with the aim of development of novel therapeutic interventions which antagonise their recruitment to the site of inflammation and modulate their death and clearance.

Although NETs can be distinguished morphologically from other cell death mechanisms *in vitro*, further studies of signalling pathways and specific markers of NETosis would be useful to avoid difficulties in distinguishing NETosis from other modes of cell death *in vivo*. This may enable a much better understanding

of the *in vivo* pathogenic mechanisms relating to this process which occur within the joints of RA patients.

Another aspect that would be interesting to address in future studies concerns the possibility that the composition of NETs may also change depending on the stimulus that is used for their induction. This has already been demonstrated for the total amount of NET proteins (12) and would be also interesting to explore with regard to citrullinated proteins. Currently, there are experiments under way in house which utilise a larger cohort of RA patients, disease and healthy control subjects to validate the preliminary ELISA results presented here, and to address the question as to which degree RA patient sera react with different citrulline-containing epitopes of histone H3.

Although each serum sample from an RA patient has its own pattern of reactivity, many sera are known to react with more than just one citrullinated antigen (70,436). Recent studies have started to characterise the fine specificity and epitope spreading in RA patients with the aim to define ACPA reactivities predictive of a particular clinical phenotype and disease development (215,216,267,437,438). Likewise, it would be interesting to extend these studies by investigating a broader spectrum of reactivities and/or targets such as, for example, citrullinated histones. In this context it is interesting to highlight the fact that patients with the previously mentioned Felty's syndrome (FS), which is characterised by a severe arthritis and neutropenia, also seem to produce antibodies against citrullinated histones (398). FS has been reported to occur in 1-3% of RA patients after an average of 10-15 years of arthritis (439,440) and it has been proposed to be a more aggressive form of RA (441). While preferential binding to citrullinated histones over non-citrullinated histones by

ELISA was found in the majority of sera from FS patients in the previously mentioned study by Dwivedi and colleagues (398), RA sera generally bound less avidly to histones and a smaller proportion of RA sera showed preference for citrullinated histones (398). It is tempting to speculate in this context that the existence of APCA fine specificities that are reactive against citrullinated histones before the onset of disease may predispose ACPA positive individuals to develop a more aggressive arthritis or certain clinical symptoms that are typically associated with FS patients.

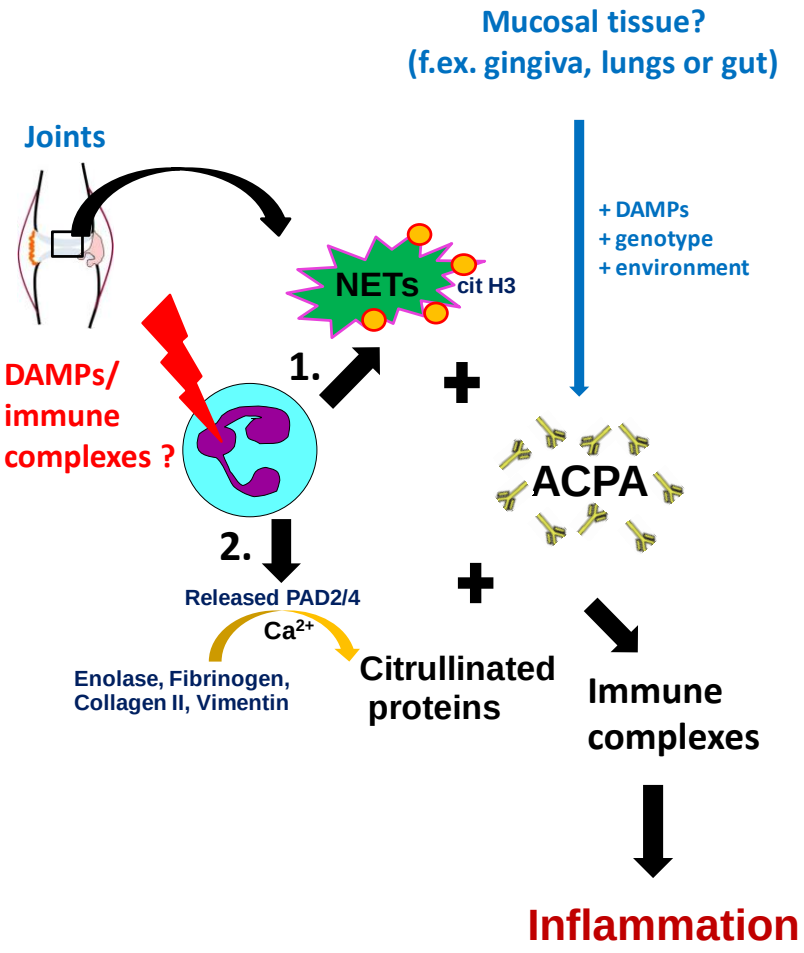

Figure 6-1 Model of NETs as a source of PADs and citrullinated proteins in RA pathogenesis

Upon activation of neutrophils by as yet unknown mechanisms, for example, DAMPs in combination with immune complexes, these cells undergo NETosis and release NETs decorated with citrullinated proteins such as citrullinated histone H3 (cit H3) (**1.**). In addition, NETosis may lead to the release of PAD enzymes, which are activated by the increased calcium levels in the extracellular space and generate citrullinated proteins (**2.**). In ACPA positive RA patients citrullinated proteins within NETs and/or citrullinated proteins that are generated in the extracellular space can be recognised by pre-existing ACPA that have entered the joints. These processes result in the formation of immune complexes and chronic inflammation. ACPA are believed to be generated at mucosal surfaces (f.ex. gingiva, the lungs or the gut) in individuals with a certain genetic background and upon exposure of certain environmental risk factors under inflammatory conditions and/or tissue damage.

7 References

1. Athens JW, Haab OP, Raab SO, Mauer AM, Ashenbrucker H, Cartwright GE, et al. Leukokinetic studies. IV. The total blood, circulating and marginal granulocyte pools and the granulocyte turnover rate in normal subjects. J Clin Invest. 1961 Jun;40:989–95.

2. Kruger P, Saffarzadeh M, Weber ANR, Rieber N, Radsak M, von Bernuth H, et al. Neutrophils: Between Host Defence, Immune Modulation, and Tissue Injury. Dehio C, editor. PLOS Pathog. 2015 Mar 12;11(3):e1004651.

3. Akgul C, Moulding DA, Edwards SW. Molecular control of neutrophil apoptosis. FEBS Lett. 2001 Jan 5;487(3):318–22.

4. Sweeney SE, Firestein GS. Rheumatoid arthritis: regulation of synovial inflammation. Int J Biochem Cell Biol. 2004 Mar;36(3):372–8.

5. Nauseef WM, Borregaard N. Neutrophils at work. Nat Immunol. 2014;15(7):602–11.

6. Wang J, Arase H. Regulation of immune responses by neutrophils. Ann N Y Acad Sci. 2014;1319(1):66–81.

7. Christopher MJ, Liu F, Hilton MJ, Long F, Link DC. Suppression of CXCL12 production by bone marrow osteoblasts is a common and critical pathway for cytokine-induced mobilization. Blood. 2009 Aug 13;114(7):1331–9.

8. Borregaard N. Neutrophils, from marrow to microbes. Immunity. Elsevier Inc.; 2010 Nov 24;33(5):657–70.

9. Segal AW. How neutrophils kill microbes. Annu Rev Immunol. 2005 Jan;23:197–223.

10. Häger M, Cowland JB, Borregaard N. Neutrophil granules in health and disease. J Intern Med. 2010;268:25–34.

11. Amulic B, Cazalet C, Hayes GL, Metzler KD, Zychlinsky A. Neutrophil Function: From Mechanisms to Disease. Annu Rev Immunol. 2011 Mar 24;(December 2011).

12. Borregaard N, Cowland JB. Granules of the human neutrophilic polymorphonuclear leukocyte. Blood. 1997 May 15;89(10):3503–21.

13. Rørvig S, Østergaard O, Heegaard NHH, Borregaard N. Proteome profiling of human neutrophil granule subsets, secretory vesicles, and cell membrane: correlation with transcriptome profiling of neutrophil precursors. J Leukoc Biol. 2013 Oct 1;94(4):711–21.

14. Kolaczkowska E, Kubes P. Neutrophil recruitment and function in health and inflammation. Nat Rev Immunol. Nature Publishing Group, a division

of Macmillan Publishers Limited. All Rights Reserved.; 2013 Mar;13(3):159–75.

15. Constantin G, Majeed M, Giagulli C, Piccio L, Kim JY, Butcher EC, et al. Chemokines trigger immediate beta2 integrin affinity and mobility changes: differential regulation and roles in lymphocyte arrest under flow. Immunity. 2000 Dec;13(6):759–69.

16. McDonald B, McAvoy EF, Lam F, Gill V, de la Motte C, Savani RC, et al. Interaction of CD44 and hyaluronan is the dominant mechanism for neutrophil sequestration in inflamed liver sinusoids. J Exp Med. 2008 Apr 14;205(4):915–27.

17. Lämmermann T, Afonso P V, Angermann BR, Wang JM, Kastenmüller W, Parent C a, et al. Neutrophil swarms require LTB4 and integrins at sites of cell death in vivo. Nature. 2013 Jun 20;498(7454):371–5.

18. Wright HL, Moots RJ, Bucknall RC, Edwards SW. Neutrophil function in inflammation and inflammatory diseases. Rheumatology (Oxford). 2010 Sep;49(9):1618–31.

19. Lee WL, Harrison RE, Grinstein S. Phagocytosis by neutrophils. Microbes Infect. 2003 Nov;5(14):1299–306.

20. Bedard K, Krause K-H. The NOX family of ROS-generating NADPH oxidases: physiology and pathophysiology. Physiol Rev. 2007 Jan;87(1):245–313.

21. Brinkmann V, Reichard U, Goosmann C, Fauler B, Uhlemann Y, Weiss DS, et al. Neutrophil extracellular traps kill bacteria. Science. 2004 Mar 5;303(5663):1532–5.

22. Menegazzi R, Decleva E, Dri P. Killing by neutrophil extracellular traps: fact or folklore? Blood. 2012 Feb 2;119(5):1214–6.

23. Spengler J, Scheel-Toellner D. Neutrophils and their contribution to autoimmunity in Rheumatoid Arthritis. In: Bhattacharya S, Nicholas AP, editors. Protein Deimination in Human Health and Disease. Springer; 2013. p. 97–112.

24. Fuchs TA, Abed U, Goosmann C, Hurwitz R, Schulze I, Wahn V, et al. Novel cell death program leads to neutrophil extracellular traps. J Cell Biol. 2007 Jan 15;176(2):231–41.

25. Brinkmann V, Zychlinsky A. Neutrophil extracellular traps: is immunity the second function of chromatin? J Cell Biol. 2012 Sep 3;198(5):773–83.

26. Yousefi S, Mihalache C, Kozlowski E, Schmid I, Simon HU. Viable neutrophils release mitochondrial DNA to form neutrophil extracellular

traps. Cell Death Differ. Nature Publishing Group; 2009 Nov;16(11):1438–44.

27. Yipp BG, Petri B, Salina D, Jenne CN, Scott BN V, Zbytnuik LD, et al. Infection-induced NETosis is a dynamic process involving neutrophil multitasking in vivo. Nat Med. 2012 Sep;18(9):1386–93.

28. Von Köckritz-Blickwede M, Goldmann O, Thulin P, Heinemann K, Norrby-Teglund A, Rohde M, et al. Phagocytosis-independent antimicrobial activity of mast cells by means of extracellular trap formation. Blood. 2008 Mar 15;111(6):3070–80.

29. Brinkmann V, Zychlinsky A. Beneficial suicide: why neutrophils die to make NETs. Nat Rev Microbiol. 2007 Aug;5(8):577–82.

30. Guimarães-Costa AB, Nascimento MTC, Wardini AB, Pinto-da-Silva LH, Saraiva EM. ETosis: A Microbicidal Mechanism beyond Cell Death. J Parasitol Res. 2012 Jan;2012:929743.

31. Yipp BG, Kubes P. NETosis: how vital is it? Blood. American Society of Hematology; 2013 Oct 17;122(16):2784–94.

32. Von Köckritz-Blickwede M, Nizet V. Innate immunity turned inside-out: antimicrobial defense by phagocyte extracellular traps. J Mol Med (Berl). 2009 Aug;87(8):775–83.

33. Kessenbrock K, Krumbholz M, Schönermarck U, Back W, Gross WL, Werb Z, et al. Netting neutrophils in autoimmune small-vessel vasculitis. Nat Med. 2009 Jun;15(6):623–5.

34. Neeli I, Khan SN, Radic M. Histone deimination as a response to inflammatory stimuli in neutrophils. J Immunol. 2008 Feb 1;180(3):1895–902.

35. Geering B, Simon H-U. Peculiarities of cell death mechanisms in neutrophils. Cell Death Differ. Macmillan Publishers Limited; 2011 Sep;18(9):1457–69.

36. Bianchi M, Hakkim A, Brinkmann V, Siler U, Seger RA, Zychlinsky A, et al. Restoration of NET formation by gene therapy in CGD controls aspergillosis. Blood. 2009 Sep 24;114(13):2619–22.

37. Metzler KD, Fuchs T a, Nauseef WM, Reumaux D, Roesler J, Schulze I, et al. Myeloperoxidase is required for neutrophil extracellular trap formation: implications for innate immunity. Blood. 2011 Jan 20;117(3):953–9.

38. Palmer LJ, Cooper PR, Ling MR, Wright HJ, Huissoon A, Chapple ILC. Hypochlorous acid regulates neutrophil extracellular trap release in humans. Clin Exp Immunol. 2012 Feb 11;167(2):261–8.

39. Papayannopoulos V, Metzler KD, Hakkim A, Zychlinsky A. Neutrophil elastase and myeloperoxidase regulate the formation of neutrophil extracellular traps. J Cell Biol. 2010 Nov 1;191(3):677–91.

40. Remijsen Q, Vanden Berghe T, Wirawan E, Asselbergh B, Parthoens E, De Rycke R, et al. Neutrophil extracellular trap cell death requires both autophagy and superoxide generation. Cell Res. Nature Publishing Group; 2011 Feb;21(2):290–304.

41. Hakkim A, Fuchs TA, Martinez NE, Hess S, Prinz H, Zychlinsky A, et al. Activation of the Raf-MEK-ERK pathway is required for neutrophil extracellular trap formation. Nat Chem Biol. 2011 Feb;7(2):75–7.

42. Lim MBH, Kuiper JWP, Katchky A, Goldberg H, Glogauer M. Rac2 is required for the formation of neutrophil extracellular traps. J Leukoc Biol. 2011 Oct;90(4):771–6.

43. Leshner M, Wang S, Lewis C, Zheng H, Chen XA, Santy L, et al. PAD4 mediated histone hypercitrullination induces heterochromatin decondensation and chromatin unfolding to form neutrophil extracellular trap-like structures. Front Immunol. 2012 Jan;3:307.

44. Wang Y, Li M, Stadler S, Correll S, Li P, Wang D, et al. Histone hypercitrullination mediates chromatin decondensation and neutrophil extracellular trap formation. J Cell Biol. 2009 Jan 26;184(2):205–13.

45. Asaga H, Nakashima K, Senshu T, Ishigami A, Yamada M. Immunocytochemical localization of peptidylarginine deiminase in human eosinophils and neutrophils. J Leukoc Biol. 2001 Jul;70(1):46–51.

46. Li P, Li M, Lindberg MR, Kennett MJ, Xiong N, Wang Y. PAD4 is essential for antibacterial innate immunity mediated by neutrophil extracellular traps. J Exp Med. 2010 Aug 30;207(9):1853–62.

47. Arita K, Hashimoto H, Shimizu T, Nakashima K, Yamada M, Sato M. Structural basis for Ca(2+)-induced activation of human PAD4. Nat Struct Mol Biol. 2004 Aug;11(8):777–83.

48. Kearney PL, Bhatia M, Jones NG, Yuan L, Glascock MC, Catchings KL, et al. Kinetic characterization of protein arginine deiminase 4: A transcriptional corepressor implicated in the onset and progression of rheumatoid arthritis. Biochemistry. 2005;44:10570–82.

49. Knuckley B, Causey CP, Jones JE, Bhatia M, Dreyton CJ, Osborne TC, et al. Substrate specificity and kinetic studies of PADs 1, 3, and 4 identify potent and selective inhibitors of protein arginine deiminase 3. Biochemistry. 2010 Jun 15;49(23):4852–63.

50. Wang Y, Wysocka J, Sayegh J, Lee Y-H, Perlin JR, Leonelli L, et al. Human PAD4 regulates histone arginine methylation levels via demethylimination. Science. 2004 Oct 8;306(5694):279–83.

51. Neeli I, Dwivedi N, Khan S, Radic M. Regulation of extracellular chromatin release from neutrophils. J Innate Immun. 2009 Jan;1(3):194–201.

52. Neeli I, Radic M. Opposition between PKC isoforms regulates histone deimination and neutrophil extracellular chromatin release. Front Immunol. 2013 Jan;4:38.

53. Romero V, Fert-Bober J, Nigrovic PA, Darrah E, Haque UJ, Lee DM, et al. Immune-mediated pore-forming pathways induce cellular hypercitrullination and generate citrullinated autoantigens in rheumatoid arthritis. Sci Transl Med. 2013 Oct 30;5(209):209ra150.

54. Lüdemann J, Utecht B, Gross WL. Anti-neutrophil cytoplasm antibodies in Wegener's granulomatosis recognize an elastinolytic enzyme. J Exp Med. 1990 Jan 1;171(1):357–62.

55. Chen M, Kallenberg CGM. New advances in the pathogenesis of ANCA-associated vasculitides. Clin Exp Rheumatol. 2009;27(1 Suppl 52):S108–14.

56. Xiao H, Heeringa P, Hu P, Liu Z, Zhao M, Aratani Y, et al. Antineutrophil cytoplasmic autoantibodies specific for myeloperoxidase cause glomerulonephritis and vasculitis in mice. J Clin Invest. 2002 Oct;110(7):955–63.

57. Pfister H, Ollert M, Fröhlich LF, Quintanilla-Martinez L, Colby T V, Specks U, et al. Antineutrophil cytoplasmic autoantibodies against the murine homolog of proteinase 3 (Wegener autoantigen) are pathogenic in vivo. Blood. 2004 Sep 1;104(5):1411–8.

58. Tsokos GC. Systemic lupus erythematosus. N Engl J Med. 2011 Dec 1;365(22):2110–21.

59. Kaplan MJ. Neutrophils in the pathogenesis and manifestations of SLE. Nat Rev Rheumatol. Nature Publishing Group; 2011 Dec;7(12):691–9.

60. Vordenbäumen S, Fischer-Betz R, Timm D, Sander O, Chehab G, Richter J, et al. Elevated levels of human beta-defensin 2 and human neutrophil peptides in systemic lupus erythematosus. Lupus. 2010 Dec;19(14):1648–53.

61. Ma C, Jiao Y, Zhang J, Yang Q, Zhang Z, Shen Y, et al. Elevated plasma level of HMGB1 is associated with disease activity and combined alterations with IFN-alpha and TNF-alpha in systemic lupus erythematosus. Rheumatol Int. 2010 Dec 1;32(2):395–402.

62. Villanueva E, Yalavarthi S, Berthier CC, Hodgin JB, Khandpur R, Lin AM, et al. Netting neutrophils induce endothelial damage, infiltrate tissues, and expose immunostimulatory molecules in systemic lupus erythematosus. J Immunol. 2011 Jul 1;187(1):538–52.

63. Hakkim A, Fürnrohr BG, Amann K, Laube B, Abed UA, Brinkmann V, et al. Impairment of neutrophil extracellular trap degradation is associated with lupus nephritis. Proc Natl Acad Sci U S A. 2010 May 25;107(21):9813–8.

64. Leffler J, Martin M, Gullstrand B, Tydén H, Lood C, Truedsson L, et al. Neutrophil Extracellular Traps That Are Not Degraded in Systemic Lupus Erythematosus Activate Complement Exacerbating the Disease. J Immunol. 2012 Feb 17;

65. Garcia-Romo GS, Caielli S, Vega B, Connolly J, Allantaz F, Xu Z, et al. Netting neutrophils are major inducers of type I IFN production in pediatric systemic lupus erythematosus. Sci Transl Med. 2011 Mar 9;3(73):73ra20.

66. Lande R, Ganguly D, Facchinetti V, Frasca L, Conrad C, Gregorio J, et al. Neutrophils activate plasmacytoid dendritic cells by releasing self-DNA-peptide complexes in systemic lupus erythematosus. Sci Transl Med. 2011 Mar 9;3(73):73ra19.

67. Banchereau J, Pascual V. Type I interferon in systemic lupus erythematosus and other autoimmune diseases. Immunity. 2006 Sep;25(3):383–92.

68. Elkon KB, Stone V V. Type I interferon and systemic lupus erythematosus. J Interferon Cytokine Res. 2011 Nov;31(11):803–12.

69. Klareskog L, Catrina AI, Paget S. Rheumatoid arthritis. Lancet. Elsevier Ltd; 2009 Feb 21;373(9664):659–72.

70. Wegner N, Lundberg K, Kinloch A, Fisher B, Malmström V, Feldmann M, et al. Autoimmunity to specific citrullinated proteins gives the first clues to the etiology of rheumatoid arthritis. Immunol Rev. 2010 Jan;233(1):34–54.

71. Lee DM, Weinblatt ME. Rheumatoid arthritis. Lancet. 2001;358(9285):903–11.

72. Firestein GS. Rheumatoid Arthritis. Kelley’s textbook of Rheumatology. 9th editio. 2013.

73. McInnes IB, Schett G. The pathogenesis of rheumatoid arthritis. N Engl J Med. 2011 Dec 8;365(23):2205–19.

74. Van Vollenhoven RF. Unresolved issues in biologic therapy for rheumatoid arthritis. Nat Rev Rheumatol. Nature Publishing Group; 2011;7(4):205–15.

75. Smith JB, Haynes MK. Rheumatoid Arthritis - A Molecular Understanding. Ann Intern Med. 2002;

76. Arnett FC, Edworthy SM, Bloch DA, McShane DJ, Fries JF, Cooper NS, et al. The American Rheumatism Association 1987 revised criteria for the classification of rheumatoid arthritis. Arthritis Rheum. 1988 Mar;31(3):315–24.

77. Aletaha D, Neogi T, Silman AJ, Funovits J, Felson DT, Bingham CO, et al. 2010 rheumatoid arthritis classification criteria: an American College of Rheumatology/European League Against Rheumatism collaborative initiative. Ann Rheum Dis. 2010 Sep;69(9):1580–8.

78. Arend WP, Firestein GS. Pre-rheumatoid arthritis: predisposition and transition to clinical synovitis. Nat Rev Rheumatol. 2012 Oct;8(10):573–86.

79. Deane KD. Learning about the natural history of rheumatoid arthritis development through prospective study of subjects at high risk of rheumatoid arthritis-related autoimmunity. Arthritis Rheum. 2012;64(6):1708–12.

80. Demoruelle MK, Deane KD, Holers VM. When and where does inflammation begin in rheumatoid arthritis? Curr Opin Rheumatol. 2014 Jan;26(1):64–71.

81. Nielen MMJ, Van Schaardenburg D, Reesink HW, Van De Stadt RJ, Van Der Horst-Bruinsma IE, De Koning MHMT, et al. Specific Autoantibodies Precede the Symptoms of Rheumatoid Arthritis: A Study of Serial Measurements in Blood Donors. Arthritis Rheum. 2004;50(2):380–6.

82. Nielen MMJ, van Schaardenburg D, Reesink HW, Twisk JWR, van de Stadt RJ, van der Horst-Bruinsma IE, et al. Increased levels of C-reactive protein in serum from blood donors before the onset of rheumatoid arthritis. Arthritis Rheum. 2004 Aug;50(8):2423–7.

83. Kokkonen H, Söderström I, Rocklöv J, Hallmans G, Lejon K, Rantapää Dahlqvist S. Up-regulation of cytokines and chemokines predates the onset of rheumatoid arthritis. Arthritis Rheum. 2010 Feb;62(2):383–91.

84. Krabben A, Stomp W, van der Heijde DMFM, van Nies JAB, Bloem JL, Huizinga TWJ, et al. MRI of hand and foot joints of patients with anticitrullinated peptide antibody positive arthralgia without clinical arthritis. Ann Rheum Dis. 2013 Sep 1;72(9):1540–4.

85. Van de Stadt LA, Bos WH, Meursinge Reynders M, Wieringa H, Turkstra F, van der Laken CJ, et al. The value of ultrasonography in predicting arthritis in auto-antibody positive arthralgia patients: a prospective cohort study. Arthritis Res Ther. 2010 Jan;12(3):R98.

86. Gent YYJ, Voskuyl AE, Kloet RW, van Schaardenburg D, Hoekstra OS, Dijkmans BAC, et al. Macrophage positron emission tomography imaging as a biomarker for preclinical rheumatoid arthritis: findings of a prospective pilot study. Arthritis Rheum. 2012 Jan;64(1):62–6.

87. Van de Sande MGH, de Hair MJH, van der Leij C, Klarenbeek PL, Bos WH, Smith MD, et al. Different stages of rheumatoid arthritis: features of the synovium in the preclinical phase. Ann Rheum Dis. 2011 May;70(5):772–7.

88. De Hair MJH, van de Sande MGH, Ramwadhdoebe TH, Hansson M, Landewé R, van der Leij C, et al. Features of the synovium of individuals at risk of developing rheumatoid arthritis: implications for understanding preclinical rheumatoid arthritis. Arthritis Rheumatol (Hoboken, NJ). 2014 Mar;66(3):513–22.

89. Gerlag DM, Raza K, van Baarsen LGM, Brouwer E, Buckley CD, Burmester GR, et al. EULAR recommendations for terminology and research in individuals at risk of rheumatoid arthritis: report from the Study Group for Risk Factors for Rheumatoid Arthritis. Ann Rheum Dis. 2012 May;71(5):638–41.

90. McInnes IB, Schett G. Cytokines in the pathogenesis of rheumatoid arthritis. Nat Rev Immunol. 2007 Jun;7(6):429–42.

91. Lee DM, Kiener HP, Agarwal SK, Noss EH, Watts GFM, Chisaka O, et al. Cadherin-11 in synovial lining formation and pathology in arthritis. Science. 2007 Feb 16;315(5814):1006–10.

92. Randen I, Mellbye OJ, Førre O, Natvig JB. The identification of germinal centres and follicular dendritic cell networks in rheumatoid synovial tissue. Scand J Immunol. 1995 May;41(5):481–6.

93. Thurlings RM, Wijbrandts C a, Mebius RE, Cantaert T, Dinant HJ, van der Pouw-Kraan TCTM, et al. Synovial lymphoid neogenesis does not define a specific clinical rheumatoid arthritis phenotype. Arthritis Rheum. 2008 Jun;58(6):1582–9.

94. Cantaert T, Kolln J, Timmer T, van der Pouw Kraan TC, Vandooren B, Thurlings RM, et al. B lymphocyte autoimmunity in rheumatoid synovitis is independent of ectopic lymphoid neogenesis. J Immunol. 2008 Jul 1;181(1):785–94.

95. Pitzalis C, Kelly S, Humby F. New learnings on the pathophysiology of RA from synovial biopsies. Curr Opin Rheumatol. 2013;25(3):334–44.

96. Humby F, Bombardieri M, Manzo A, Kelly S, Blades MC, Kirkham B, et al. Ectopic lymphoid structures support ongoing production of class-switched autoantibodies in rheumatoid synovium. PLoS Med. 2009;6(1):0059–75.

97. Hitchon CA, El-Gabalawy HS. The synovium in rheumatoid arthritis. Open Rheumatol J. 2011 Jan;5:107–14.

98. Reece RJ, Canete JD, Parsons WJ, Emery P, Veale DJ. Distinct vascular patterns of early synovitis in psoriatic, reactive, and rheumatoid arthritis. Arthritis Rheum. 1999 Jul;42(7):1481–4.

99. Joseph A, Brasington R, Kahl L, Ranganathan P, Cheng TP, Atkinson J. Immunologic rheumatic disorders. J Allergy Clin Immunol. 2010 Feb;125(2 Suppl 2):S204–15.

100. Schumacher HR, Kitridou RC. Synovitis of recent onset. A clinicopathologic study during the first month of disease. Arthritis Rheum. 1972;15(5):465–85.

101. Pillinger MH, Burg ND, Abramson SB. Neutrophils and small molecule mediators. In: St.Clair EW, Pisetsky DS, Haynes BF, editors. Rheumatoid Arthritis. Lippincott Williams & Wilkins; 2004. p. 174.

102. Bjelle A, Norberg B, Sjögren G. The cytology of joint exudates in rheumatoid arthritis. Morphology and preparation techniques. Scand J Rheumatol. 1982 Jan;11(2):124–8.

103. Mohr W, Westerhellweg H, Wessinghage D. Polymorphonuclear granulocytes in rheumatic tissue destruction. III. an electron microscopic study of PMNs at the pannus-cartilage junction in rheumatoid arthritis. Ann Rheum Dis. 1981 Aug;40(4):396–9.

104. Cascão R, Moura RA, Perpétuo I, Canhão H, Vieira-Sousa E, Mourão AF, et al. Identification of a cytokine network sustaining neutrophil and Th17 activation in untreated early rheumatoid arthritis. Arthritis Res Ther. 2010 Jan;12(5):R196.

105. Raza K, Scheel-Toellner D, Lee C-Y, Pilling D, Curnow SJ, Falciani F, et al. Synovial fluid leukocyte apoptosis is inhibited in patients with very early rheumatoid arthritis. Arthritis Res Ther. BioMed Central; 2006 Jan;8(4):R120.

106. Buckley CD, Ross EA, McGettrick HM, Osborne CE, Haworth O, Schmutz C, et al. Identification of a phenotypically and functionally distinct population of long-lived neutrophils in a model of reverse endothelial migration. J Leukoc Biol. 2006 Feb;79(2):303–11.

107. Woodfin A, Voisin M-B, Beyrau M, Colom B, Caille D, Diapouli F-M, et al. The junctional adhesion molecule JAM-C regulates polarized transendothelial migration of neutrophils in vivo. Nat Immunol. 2011 Aug;12(8):761–9.

108. Shelef MA, Tauzin S, Huttenlocher A. Neutrophil migration: moving from zebrafish models to human autoimmunity. Immunol Rev. 2013 Nov;256(1):269–81.

109. Eggleton P, Wang L, Penhallow J, Crawford N, Brown KA. Differences in oxidative response of subpopulations of neutrophils from healthy subjects and patients with rheumatoid arthritis. Ann Rheum Dis. 1995 Nov;54(11):916–23.

110. Cedergren J, Forslund T, Sundqvist T, Skogh T. Intracellular oxidative activation in synovial fluid neutrophils from patients with rheumatoid arthritis but not from other arthritis patients. J Rheumatol. 2007 Nov 1;34(11):2162–70.

111. Fossati G, Moots RJ, Bucknall RC, Edwards SW. Differential role of neutrophil Fcgamma receptor IIIB (CD16) in phagocytosis, bacterial killing, and responses to immune complexes. Arthritis Rheum. 2002 May;46(5):1351–61.

112. Fossati G, Bucknall RC, Edwards SW. Insoluble and soluble immune complexes activate neutrophils by distinct activation mechanisms: changes in functional responses induced by priming with cytokines. Ann Rheum Dis. 2002 Jan;61(1):13–9.

113. Sopata I, Wize J, Filipowicz-Sosnowska A, Stanisławska-Biernat E, Brzezińska B, Maśliński S. Neutrophil gelatinase levels in plasma and synovial fluid of patients with rheumatic diseases. Rheumatol Int. 1995 Jan;15(1):9–14.

114. Van den Steen PE, Proost P, Grillet B, Brand DD, Kang AH, Van Damme J, et al. Cleavage of denatured natural collagen type II by neutrophil gelatinase B reveals enzyme specificity, post-translational modifications in the substrate, and the formation of remnant epitopes in rheumatoid arthritis. FASEB J. 2002 Mar;16(3):379–89.

115. Hilbert N, Schiller J, Arnhold J, Arnold K. Cartilage degradation by stimulated human neutrophils: elastase is mainly responsible for cartilage damage. Bioorg Chem. 2002 May;30(2):119–32.

116. Wright HL, Moots RJ, Edwards SW. The multifactorial role of neutrophils in rheumatoid arthritis. Nat Rev Rheumatol. 2014 Oct;10(10):593–601.

117. Assi LK, Wong SH, Ludwig A, Raza K, Gordon C, Salmon M, et al. Tumor necrosis factor alpha activates release of B lymphocyte stimulator by neutrophils infiltrating the rheumatoid joint. Arthritis Rheum. 2007 Jun;56(6):1776–86.

118. Yeo L, Toellner K-M, Salmon M, Filer A, Buckley CD, Raza K, et al. Cytokine mRNA profiling identifies B cells as a major source of RANKL in rheumatoid arthritis. Ann Rheum Dis. 2011 Nov;70(11):2022–8.

119. Iking-Konert C, Ostendorf B, Sander O, Jost M, Wagner C, Joosten L, et al. Transdifferentiation of polymorphonuclear neutrophils to dendritic-like cells at the site of inflammation in rheumatoid arthritis: evidence for activation by T cells. Ann Rheum Dis. BMJ Group; 2005 Oct 1;64(10):1436–42.

120. Khandpur R, Carmona-Rivera C, Vivekanandan-Giri a., Gizinski a., Yalavarthi S, Knight JS, et al. NETs Are a Source of Citrullinated Autoantigens and Stimulate Inflammatory Responses in Rheumatoid Arthritis. Sci Transl Med. 2013 Mar 27;5(178):178ra40–178ra40.

121. Wipke BT, Allen PM. Essential Role of Neutrophils in the Initiation and Progression of a Murine Model of Rheumatoid Arthritis. J Immunol. American Association of Immunologists; 2001 Aug 1;167(3):1601–8.

122. Nandakumar KS, Svensson L, Holmdahl R. Collagen type II-specific monoclonal antibody-induced arthritis in mice: description of the disease and the influence of age, sex, and genes. Am J Pathol. 2003 Nov;163(5):1827–37.

123. Tsuboi N, Ernandez T, Li X, Nishi H, Cullere X, Mekala D, et al. Regulation of human neutrophil Fcγ receptor IIa by C5a receptor promotes inflammatory arthritis in mice. Arthritis Rheum. 2011 Mar;63(2):467–78.

124. Sadik CD, Kim ND, Iwakura Y, Luster AD. Neutrophils orchestrate their own recruitment in murine arthritis through C5aR and FcγR signaling. Proc Natl Acad Sci U S A. 2012 Dec 13;109(46):E3177–85.

125. Kim ND, Chou RC, Seung E, Tager AM, Luster AD. A unique requirement for the leukotriene B4 receptor BLT1 for neutrophil recruitment in inflammatory arthritis. J Exp Med. 2006 May 17;203(4):829–35.

126. Silverstein a M. Autoimmunity versus horror autotoxicus: the struggle for recognition. Nat Immunol. 2001;2(4):279–81.

127. Roitt IM, Doniach D, Campbell PN, Hudson R V. Auto-antibodies in Hashimoto's disease (lymphadenoid goitre). Lancet. 1956 Oct 20;271(6947):820–1.

128. Rose NR, Witebsky E. Studies on organ specificity. V. Changes in the thyroid glands of rabbits following active immunization with rabbit thyroid extracts. J Immunol. 1956 Jun;76(6):417–27.

129. Burnett FM, Fenner F. The Production of Antibodies. 2nd ed. Macmillan; 1949.

130. Davidson A, Diamond B. General features of autoimmune disease. The Autoimmune Diseases. 5th ed. Elsevier Inc.; 2014. p. 19–37.

131. Kono DH, Theofilopoulos AN. Autoimmunity. In: Firestein GS, Budd RC, Gabriel SE, McInnes IB, O'Dell JR, editors. Kelley's textbook of Rheumatology. 9th ed. 2013. p. 281–98.

132. Silverstein AM. Autoimmunity: A History of the Early Struggle for Recognition. The Autoimmune Diseases. Elsevier Inc.; 1986. p. 1367–8.

133. Cooper GS, Stroehla BC. The epidemiology of autoimmune diseases. Autoimmun Rev. 2003 May;2(3):119–25.

134. Patterson CC, Dahlquist GG, Gyürüs E, Green A, Soltész G. Incidence trends for childhood type 1 diabetes in Europe during 1989-2003 and predicted new cases 2005-20: a multicentre prospective registration study. Lancet. 2009 Jun 13;373(9680):2027–33.

135. Uramoto KM, Michet CJ, Thumboo J, Sunku J, O'Fallon WM, Gabriel SE. Trends in the incidence and mortality of systemic lupus erythematosus, 1950-1992. Arthritis Rheum. 1999 Jan;42(1):46–50.

136. McLeod DSA, Cooper DS. The incidence and prevalence of thyroid autoimmunity. Endocrine. 2012 Oct;42(2):252–65.

137. Bach J-F. The effect of infections on susceptibility to autoimmune and allergic diseases. N Engl J Med. 2002 Sep 19;347(12):911–20.

138. Nossal GJ. A purgative mastery. Nature. 2001 Aug 16;412(6848):685–6.

139. McGonagle D, McDermott MF. A proposed classification of the immunological diseases. PLoS Med. 2006 Aug;3(8):e297.

140. Stoffels M, Simon A. The concept of autoinflammatory diseases. The Autoimmune Diseases. Elsevier Inc.; 1986. p. 1367–8.

141. Liao L, Sindhwani R, Rojkind M, Factor S, Leinwand L, Diamond B. Antibody-mediated autoimmune myocarditis depends on genetically determined target organ sensitivity. J Exp Med. 1995 Mar 1;181(3):1123–31.

142. Liu K, Li Q-Z, Delgado-Vega AM, Abelson A-K, Sánchez E, Kelly JA, et al. Kallikrein genes are associated with lupus and glomerular basement membrane-specific antibody-induced nephritis in mice and humans. J Clin Invest. 2009 Apr;119(4):911–23.

143. Cho JH, Gregersen PK. Genomics and the multifactorial nature of human autoimmune disease. N Engl J Med. 2011 Oct 27;365(17):1612–23.

144. Liu X, Wu Y, Yang Y, Wang J, Tao Y, Fu P, et al. Identical twins:one with anti-glomerular basement membrane glomerulonephritis,the other with systemic lupus erythematosus. BMC Nephrol. 2013 Jan;14:277.

145. Arason GJ, Jorgensen GH, Ludviksson BR. Primary immunodeficiency and autoimmunity: lessons from human diseases. Scand J Immunol. 2010 May;71(5):317–28.

146. Anderson MS, Su MA. Aire and T cell development. Curr Opin Immunol. 2011 Apr;23(2):198–206.

147. Gupta S, Louis AG. Tolerance and autoimmunity in primary immunodeficiency disease: a comprehensive review. Clin Rev Allergy Immunol. 2013 Oct;45(2):162–9.

148. Waaler E. On the occurrence of a factor in human serum activating the specific agglutintion of sheep blood corpuscles. Acta path microbiol scand. 1940;17:178–88.

149. Gualtierotti R, Ciavarella T, Meroni PL. Chapter 89 – Rheumatoid Factors. Autoantibodies. Third Edit. Elsevier; 2014. p. 751–60.

150. Vallbracht I, Rieber J, Oppermann M, Förger F, Siebert U, Helmke K. Diagnostic and clinical value of anti-cyclic citrullinated peptide antibodies compared with rheumatoid factor isotypes in rheumatoid arthritis. Ann Rheum Dis. BMJ Group; 2004 Sep;63(9):1079–84.

151. Rantapää-Dahlqvist S, De Jong BAW, Berglin E, Hallmans G, Wadell G, Stenlund H, et al. Antibodies Against Cyclic Citrullinated Peptide and IgA Rheumatoid Factor Predict the Development of Rheumatoid Arthritis. Arthritis Rheum. 2003 Oct;48(10):2741–9.

152. Bax M, Huizinga TWJ, Toes REM. The pathogenic potential of autoreactive antibodies in rheumatoid arthritis. Semin Immunopathol. 2014 May;36(3):313–25.

153. Stewart JJ, Agosto H, Litwin S, Welsh JD, Shlomchik M, Weigert M, et al. A Solution to the Rheumatoid Factor. J Immunol. 1997;(25):19–24.

154. Mewar D, Wilson AG. Autoantibodies in rheumatoid arthritis: a review. Biomed Pharmacother. 2006 Dec;60(10):648–55.

155. Van Schaardenburg D, Lagaay AM, Otten HG, Breedveld FC. The relation between class-specific serum rheumatoid factors and age in the general population. Br J Rheumatol. 1993 Jul;32(7):546–9.

156. Børretzen M, Chapman C, Natvig JB, Thompson KM. Differences in mutational patterns between rheumatoid factors in health and disease are related to variable heavy chain family and germ-line gene usage. Eur J Immunol. 1997 Mar;27(3):735–41.

157. Van Snick JL, Van Roost E, Markowetz B, Cambiaso CL, Masson PL. Enhancement by IgM rheumatoid factor of in vitro ingestion by

macrophages and in vivo clearance of aggregated IgG or antigen-antibody complexes. Eur J Immunol. 1978;8:279–85.

158. Newkirk MM. Rheumatoid factors: host resistance or autoimmunity? Clin Immunol. 2002 Jul;104(1):1–13.

159. Nielsen SF, Bojesen SE, Schnohr P, Nordestgaard BG. Elevated rheumatoid factor and long term risk of rheumatoid arthritis: a prospective cohort study. BMJ. 2012 Jan;345:e5244.

160. Williams DG, Moyes SP, Mageed RA. Rheumatoid factor isotype switch and somatic mutation variants within rheumatoid arthritis synovium. Immunology. 1999 Sep;98(1):123–36.

161. Dörner T, Egerer K, Feist E, Burmester GR. Rheumatoid factor revisited. Curr Opin Rheumatol. 2004;16(Table 1):246–53.

162. Yoshida T, Mei H, Dörner T, Hiepe F, Radbruch A, Fillatreau S, et al. Memory B and memory plasma cells. Immunol Rev. 2010 Sep;237(1):117–39.

163. Aletaha D, Alasti F, Smolen JS. Rheumatoid factor determines structural progression of rheumatoid arthritis dependent and independent of disease activity. Ann Rheum Dis. 2013 Jun;72(6):875–80.

164. Böhler C, Radner H, Smolen JS, Aletaha D. Serological changes in the course of traditional and biological disease modifying therapy of rheumatoid arthritis. Ann Rheum Dis. 2013 Feb;72(2):241–4.

165. Smolen JS, Redlich K. Rheumatoid Arthritis. The Autoimmune Diseases. Elsevier Inc.; 2014. p. 511–23.

166. Van Boekel M a M, Vossenaar ER, van den Hoogen FHJ, van Venrooij WJ. Autoantibody systems in rheumatoid arthritis: specificity, sensitivity and diagnostic value. Arthritis Res. 2002;4:87–93.

167. Nell VPK, Machold KP, Stamm TA, Eberl G, Heinzl H, Uffmann M, et al. Autoantibody profiling as early diagnostic and prognostic tool for rheumatoid arthritis. Ann Rheum Dis. 2005 Dec;64(12):1731–6.

168. Klareskog L, Rönnelid J, Lundberg K, Padyukov L, Alfredsson L. Immunity to citrullinated proteins in rheumatoid arthritis. Annu Rev Immunol. 2008 Jan;26(c):651–75.

169. Schellekens GA, de Jong BA, van den Hoogen FH, van de Putte LB, van Venrooij WJ. Citrulline is an essential constituent of antigenic determinants recognized by rheumatoid arthritis-specific autoantibodies. J Clin Invest. 1998 Jan 1;101(1):273–81.

170. Sebbag M, Simon M, Vincent C, Masson-Bessière C, Girbal E, Durieux JJ, et al. The antiperinuclear factor and the so-called antikeratin antibodies are the same rheumatoid arthritis-specific autoantibodies. J Clin Invest. 1995 Jun;95(6):2672–9.

171. Schellekens GA, Visser H, de Jong BA, van den Hoogen FH, Hazes JM, Breedveld FC, et al. The diagnostic properties of rheumatoid arthritis antibodies recognizing a cyclic citrullinated peptide. Arthritis Rheum. 2000 Jan;43(1):155–63.

172. Simon M, Girbal E, Sebbag M, Gomès-Daudrix V, Vincent C, Salama G, et al. The cytokeratin filament-aggregating protein filaggrin is the target of the so-called “antikeratin antibodies,” autoantibodies specific for rheumatoid arthritis. J Clin Invest. 1993 Sep;92(3):1387–93.

173. Vossenaar ER, Després N, Lapointe E, van der Heijden A, Lora M, Senshu T, et al. Rheumatoid arthritis specific anti-Sa antibodies target citrullinated vimentin. Arthritis Res Ther. 2004 Jan;6(2):R142–50.

174. Kinloch A, Tatzer V, Wait R, Peston D, Lundberg K, Donatien P, et al. Identification of citrullinated alpha-enolase as a candidate autoantigen in rheumatoid arthritis. Arthritis Res Ther. 2005 Jan;7(6):R1421–9.

175. Masson-Bessière C, Sebbag M, Girbal-Neuhauser E, Nogueira L, Vincent C, Senshu T, et al. The major synovial targets of the rheumatoid arthritis-specific antifilaggrin autoantibodies are deiminated forms of the alpha- and beta-chains of fibrin. J Immunol. 2001 Mar 15;166(6):4177–84.

176. Takizawa Y, Suzuki A, Sawada T, Ohsaka M, Inoue T, Yamada R, et al. Citrullinated fibrinogen detected as a soluble citrullinated autoantigen in rheumatoid arthritis synovial fluids. Ann Rheum Dis. 2006 Aug;65(8):1013–20.

177. Burkhardt H, Sehnert B, Bockermann R, Engström A, Kalden JR, Holmdahl R. Humoral immune response to citrullinated collagen type II determinants in early rheumatoid arthritis. Eur J Immunol. 2005;35:1643–52.

178. Fisher B a. ACPA. Autoantibodies. Third Edit. Elsevier; 2014. p. 761–9.

179. Willemze A, Trouw LA, Toes REM, Huizinga TWJ. The influence of ACPA status and characteristics on the course of RA. Nat Rev Rheumatol. Nature Publishing Group, a division of Macmillan Publishers Limited. All Rights Reserved.; 2012 Mar;8(3):144–52.

180. Shi J, Knevel R, Suwannalai P, van der Linden MP, Janssen GMC, van Veelen PA, et al. Autoantibodies recognizing carbamylated proteins are present in sera of patients with rheumatoid arthritis and predict joint damage. Proc Natl Acad Sci U S A. 2011 Oct 18;108(42):17372–7.

181. Trouw LA, Huizinga TWJ, Toes REM. Autoimmunity in rheumatoid arthritis: different antigens--common principles. Ann Rheum Dis. 2013 Apr;72 Suppl 2:ii132–6.

182. Kroese FGM, Baeten D, Huizinga TWJ. Autoimmunity: break-through in the diagnosis and treatment of immune-mediated inflammatory diseases. Immunol Lett. 2014 Dec;162(2 Pt B):150–62.

183. Muller S, Radic M. Citrullinated Autoantigens: From Diagnostic Markers to Pathogenetic Mechanisms. Clin Rev Allergy Immunol. 2014 Oct 30;

184. György B, Tóth E, Tarcsa E, Falus A, Buzás EI. Citrullination: a posttranslational modification in health and disease. Int J Biochem Cell Biol. 2006 Jan;38(10):1662–77.

185. Vossenaar ER, Zendman AJW, van Venrooij WJ, Pruijn GJM. PAD, a growing family of citrullinating enzymes: genes, features and involvement in disease. Bioessays. 2003 Nov;25(11):1106–18.

186. Bhattacharya S, Nicholas AP. Protein Deimination in Human Health and Disease. Springer; Bhattacharya S, Nicholas AP, editors. Springer; 2014 edition; 2013. 448 p.

187. Wang S, Wang Y. Peptidylarginine deiminases in citrullination, gene regulation, health and pathogenesis. Biochim Biophys Acta. 2013 Oct;1829(10):1126–35.

188. Chang X, Zhao Y, Sun S, Zhang Y, Zhu Y. The expression of PADI4 in synovium of rheumatoid arthritis. Rheumatol Int. 2009 Oct;29(12):1411–6.

189. Esposito G, Vitale AM, Leijten FPJ, Strik AM, Koonen-Reemst AMCB, Yurttas P, et al. Peptidylarginine deiminase (PAD) 6 is essential for oocyte cytoskeletal sheet formation and female fertility. Mol Cell Endocrinol. 2007 Jul 15;273(1-2):25–31.

190. Tarcsa E, Marekov LN, Mei G, Melino G, Lee SC, Steinert PM. Protein unfolding by peptidylarginine deiminase. Substrate specificity and structural relationships of the natural substrates trichohyalin and filaggrin. J Biol Chem. 1996 Nov 29;271(48):30709–16.

191. Hsu C-Y, Henry J, Raymond A-A, Méchin M-C, Pendaries V, Nassar D, et al. Deimination of human filaggrin-2 promotes its proteolysis by calpain 1. J Biol Chem. 2011 Jul 1;286(26):23222–33.

192. Chavanas S, Méchin MC, Nachat R, Adoue V, Coudane F, Serre G, et al. Peptidylarginine deiminases and deimination in biology and pathology: Relevance to skin homeostasis. J Dermatol Sci. 2006;44:63–72.

193. Pritzker LB, Joshi S, Gowan JJ, Harauz G, Moscarello MA. Deimination of myelin basic protein. 1. Effect of deimination of arginyl residues of myelin

basic protein on its structure and susceptibility to digestion by cathepsin D. Biochemistry. 2000 May 9;39(18):5374–81.

194. Cuthbert GL, Daujat S, Snowden AW, Erdjument-Bromage H, Hagiwara T, Yamada M, et al. Histone deimination antagonizes arginine methylation. Cell. 2004 Sep 3;118(5):545–53.

195. Vossenaar ER, Radstake TRD, van der Heijden A, van Mansum MAM, Dieteren C, de Rooij D-J, et al. Expression and activity of citrullinating peptidylarginine deiminase enzymes in monocytes and macrophages. Ann Rheum Dis. 2004 Apr;63(4):373–81.

196. Nakashima K, Hagiwara T, Yamada M. Nuclear localization of peptidylarginine deiminase V and histone deimination in granulocytes. J Biol Chem. 2002 Dec 20;277(51):49562–8.

197. Zendman AJW, Raijmakers R, Nijenhuis S, Vossenaar ER, Tillaart M van den, Chirivi RGS, et al. ABAP: antibody-based assay for peptidylarginine deiminase activity. Anal Biochem. 2007 Oct 15;369(2):232–40.

198. Watanabe K, Senshu T. Isolation and characterization of cDNA clones encoding rat skeletal muscle peptidylarginine deiminase. J Biol Chem. 1989 Sep 15;264(26):15255–60.

199. Andrade F, Darrah E, Gucek M, Cole RN, Rosen A, Zhu X. Autocitrullination of human peptidyl arginine deiminase type 4 regulates protein citrullination during cell activation. Arthritis Rheum. 2010 Jun;62(6):1630–40.

200. Slack JL, Jones LE, Bhatia MM, Thompson PR. Autodeimination of Protein Arginine Deiminase 4 Alters Protein-Protein interactions but not activity. Digestion. 2011;3997–4010.

201. Knuckley B, Bhatia M, Thompson PR. Protein arginine deiminase 4: evidence for a reverse protonation mechanism. Biochemistry. 2007 Jun 5;46(22):6578–87.

202. Willis VC, Gizinski AM, Banda NK, Causey CP, Knuckley B, Cordova KN, et al. N-α-benzoyl-N5-(2-chloro-1-iminoethyl)-L-ornithine amide, a protein arginine deiminase inhibitor, reduces the severity of murine collagen-induced arthritis. J Immunol. 2011 Apr 1;186(7):4396–404.

203. Darrah E, Rosen A, Giles JT, Andrade F. Peptidylarginine deiminase 2, 3 and 4 have distinct specificities against cellular substrates: novel insights into autoantigen selection in rheumatoid arthritis. Ann Rheum Dis. 2012 Jan;71(1):92–8.

204. Kastbom A. Anti-CCP antibody test predicts the disease course during 3 years in early rheumatoid arthritis (the Swedish TIRA project). Ann Rheum Dis. BMJ Group; 2004 Sep 1;63(9):1085–9.

205. Forslind K, Ahlmén M, Eberhardt K, Hafström I, Svensson B. Prediction of radiological outcome in early rheumatoid arthritis in clinical practice: role of antibodies to citrullinated peptides (anti-CCP). Ann Rheum Dis. 2004 Sep;63(9):1090–5.

206. Gregersen PK, Silver J, Winchester RJ. The shared epitope hypothesis. An approach to understanding the molecular genetics of susceptibility to rheumatoid arthritis. Arthritis Rheum. 1987 Nov;30(11):1205–13.

207. Begovich AB, Carlton VEH, Honigberg LA, Schrodi SJ, Chokkalingam AP, Alexander HC, et al. A missense single-nucleotide polymorphism in a gene encoding a protein tyrosine phosphatase (PTPN22) is associated with rheumatoid arthritis. Am J Hum Genet. 2004 Aug;75(2):330–7.

208. Rawlings DJ, Dai X, Buckner JH. The Role of PTPN22 Risk Variant in the Development of Autoimmunity: Finding Common Ground between Mouse and Human. J Immunol. 2015 Apr 1;194(7):2977–84.

209. Kallberg H, Padyukov L, Plenge RM, Ronnelid J, Gregersen PK, van der Helm-van Mil AHM, et al. Gene-gene and gene-environment interactions involving HLA-DRB1, PTPN22, and smoking in two subsets of rheumatoid arthritis. Am J Hum Genet. 2007 May;80(5):867–75.

210. Van der Helm-van Mil AHM, Verpoort KN, Breedveld FC, Huizinga TWJ, Toes REM, de Vries RRP. The HLA-DRB1 shared epitope alleles are primarily a risk factor for anti-cyclic citrullinated peptide antibodies and are not an independent risk factor for development of rheumatoid arthritis. Arthritis Rheum. 2006 Apr;54(4):1117–21.

211. Huizinga TWJ, Amos CI, van der Helm-van Mil AHM, Chen W, van Gaalen FA, Jawaheer D, et al. Refining the complex rheumatoid arthritis phenotype based on specificity of the HLA-DRB1 shared epitope for antibodies to citrullinated proteins. Arthritis Rheum. 2005 Nov;52(11):3433–8.

212. Padyukov L, Seielstad M, Ong RTH, Ding B, Rönnelid J, Seddighzadeh M, et al. A genome-wide association study suggests contrasting associations in ACPA-positive versus ACPA-negative rheumatoid arthritis. Ann Rheum Dis. 2011 Feb;70(2):259–65.

213. Verpoort KN, Jol-van der Zijde CM, Papendrecht-van der Voort E a M, Ioan-Facsinay a, Drijfhout JW, van Tol MJD, et al. Isotype distribution of anti-cyclic citrullinated peptide antibodies in undifferentiated arthritis and rheumatoid arthritis reflects an ongoing immune response. Arthritis Rheum. 2006 Dec;54(12):3799–808.

214. Klareskog L, Stolt P, Lundberg K, Källberg H, Bengtsson C, Grunewald J, et al. A new model for an etiology of rheumatoid arthritis: smoking may trigger HLA-DR (shared epitope)-restricted immune reactions to

autoantigens modified by citrullination. Arthritis Rheum. 2006 Jan;54(1):38–46.

215. Willemze A, van der Woude D, Ghidey W, Levarht EWN, Stoeken-Rijsbergen G, Verduyn W, et al. The interaction between HLA shared epitope alleles and smoking and its contribution to autoimmunity against several citrullinated antigens. Arthritis Rheum. 2011 Jul;63(7):1823–32.

216. Lundberg K, Bengtsson C, Kharlamova N, Reed E, Jiang X, Kallberg H, et al. Genetic and environmental determinants for disease risk in subsets of rheumatoid arthritis defined by the anticitrullinated protein/peptide antibody fine specificity profile. Ann Rheum Dis. 2012;(May 2006):652–8.

217. Holers VM. Autoimmunity to citrullinated proteins and the initiation of rheumatoid arthritis. Curr Opin Immunol. 2013 Dec;25(6):728–35.

218. Koch AE, Robinson PG, Radosevich JA, Pope RM. Distribution of CD45RA and CD45RO T-lymphocyte subsets in rheumatoid arthritis synovial tissue. J Clin Immunol. 1990 Jul;10(4):192–9.

219. Kurosaka M, Ziff M. Immunoelectron microscopic study of the distribution of T cell subsets in rheumatoid synovium. J Exp Med. 1983 Oct 1;158(4):1191–210.

220. Firestein GS, Zvaifler NJ. How important are T cells in chronic rheumatoid synovitis? II. T cell-independent mechanisms from beginning to end. Arthritis Rheum. 2002;46(2):298–308.

221. Brennan FM, Hayes AL, Ciesielski CJ, Green P, Foxwell BMJ, Feldmann M. Evidence that rheumatoid arthritis synovial T cells are similar to cytokine-activated T cells: involvement of phosphatidylinositol 3-kinase and nuclear factor kappaB pathways in tumor necrosis factor alpha production in rheumatoid arthritis. Arthritis Rheum. 2002 Jan;46(1):31–41.

222. Cantaert T, Brouard S, Thurlings RM, Pallier A, Salinas GF, Braud C, et al. Alterations of the synovial T cell repertoire in anti-citrullinated protein antibody-positive rheumatoid arthritis. Arthritis Rheum. 2009;60(7):1944–56.

223. Snir O, Rieck M, Gebe JA, Yue BB, Rawlings CA, Nepom G, et al. Identification and functional characterization of T cells reactive to citrullinated vimentin in HLA-DRB1*0401-positive humanized mice and rheumatoid arthritis patients. Arthritis Rheum. 2011 Oct;63(10):2873–83.

224. Scally SW, Petersen J, Law SC, Dudek NL, Nel HJ, Loh KL, et al. A molecular basis for the association of the HLA-DRB1 locus, citrullination, and rheumatoid arthritis. J Exp Med. 2013 Nov 18;210(12):2569–82.

225. Wagner UG, Koetz K, Weyand CM, Goronzy JJ. Perturbation of the T cell repertoire in rheumatoid arthritis. Proc Natl Acad Sci U S A. 1998 Nov 24;95(24):14447–52.

226. Goronzy JJ, Zettl A, Weyand CM. T cell receptor repertoire in rheumatoid arthritis. Int Rev Immunol. 1998 Jan;17(5-6):339–63.

227. Panayi GS. Even though T-cell-directed trials have been of limited success, is there reason for optimism? Nat Clin Pract Rheumatol. 2006 Feb;2(2):58–9.

228. Kraan MC, Haringman JJ, Post WJ, Versendaal J, Breedveld FC, Tak PP. Immunohistological analysis of synovial tissue for differential diagnosis in early arthritis. Rheumatology (Oxford). 1999 Nov;38(11):1074–80.

229. Van de Sande MGH, Thurlings RM, Boumans MJH, Wijbrandts CA, Modesti MG, Gerlag DM, et al. Presence of lymphocyte aggregates in the synovium of patients with early arthritis in relationship to diagnosis and outcome: is it a constant feature over time? Ann Rheum Dis. 2011 Apr;70(4):700–3.

230. Herlands RA, Christensen SR, Sweet RA, Hershberg U, Shlomchik MJ. T cell-independent and toll-like receptor-dependent antigen-driven activation of autoreactive B cells. Immunity. 2008 Aug 15;29(2):249–60.

231. Daridon C, Loddenkemper C, Spieckermann S, Kühl AA, Salama A, Burmester GR, et al. Splenic proliferative lymphoid nodules distinct from germinal centers are sites of autoantigen stimulation in immune thrombocytopenia. Blood. 2012 Dec 13;120(25):5021–31.

232. Dörner T, Lipsky PE. B cells. Curr Opin Rheumatol. 2014;26(2):228–36.

233. Klareskog L, Lundberg K, Malmström V. Autoimmunity in Rheumatoid Arthritis: Citrulline Immunity and Beyond. Adv Immunol. 2013;118:129–58.

234. Van Oosterhout M, Bajema I, Levarht EWN, Toes REM, Huizinga TWJ, van Laar JM. Differences in synovial tissue infiltrates between anti-cyclic citrullinated peptide-positive rheumatoid arthritis and anti-cyclic citrullinated peptide-negative rheumatoid arthritis. Arthritis Rheum. 2008 Jan;58(1):53–60.

235. Amara K, Steen J, Murray F, Morbach H, Fernandez-Rodriguez BM, Joshua V, et al. Monoclonal IgG antibodies generated from joint-derived B cells of RA patients have a strong bias toward citrullinated autoantigen recognition. J Exp Med. 2013 Mar 11;210(3):445–55.

236. Suwannalai P, Scherer HU, van der Woude D, Ioan-Facsinay a, Jol-van der Zijde CM, van Tol MJD, et al. Anti-citrullinated protein antibodies have

a low avidity compared with antibodies against recall antigens. Ann Rheum Dis. 2011 Feb;70(2):373–9.

237. Flores-Borja F, Bosma A, Ng D, Reddy V, Ehrenstein MR, Isenberg DA, et al. CD19+CD24hiCD38hi B cells maintain regulatory T cells while limiting TH1 and TH17 differentiation. Sci Transl Med. 2013 Feb 20;5(173):173ra23.

238. Yeo L, Lom H, Juarez M, Snow M, Buckley CD, Filer A, et al. Expression of FcRL4 defines a pro-inflammatory, RANKL-producing B cell subset in rheumatoid arthritis. Ann Rheum Dis. 2014 Jan 15;annrheumdis – 2013–204116 – .

239. Moscarello MA, Pritzker L, Mastronardi FG, Wood DD. Peptidylarginine deiminase: a candidate factor in demyelinating disease. J Neurochem. 2002 Apr;81(2):335–43.

240. Mastronardi FG, Wood DD, Mei J, Raijmakers R, Tseveleki V, Dosch H-M, et al. Increased citrullination of histone H3 in multiple sclerosis brain and animal models of demyelination: a role for tumor necrosis factor-induced peptidylarginine deiminase 4 translocation. J Neurosci. 2006 Nov 1;26(44):11387–96.

241. Ishigami A, Ohsawa T, Hiratsuka M, Taguchi H, Kobayashi S, Saito Y, et al. Abnormal accumulation of citrullinated proteins catalyzed by peptidylarginine deiminase in hippocampal extracts from patients with Alzheimer's disease. J Neurosci Res. 2005 Apr 1;80(1):120–8.

242. Ishida-Yamamoto A, Senshu T, Eady RAJ, Takahashi H, Shimizu H, Akiyama M, et al. Sequential reorganization of cornified cell keratin filaments involving filaggrin-mediated compaction and keratin 1 deimination. J Invest Dermatol. 2002 Feb;118(2):282–7.

243. Jiang Z, Cui Y, Wang L, Zhao Y, Yan S, Chang X. Investigating citrullinated proteins in tumour cell lines. World J Surg Oncol. 2013 Jan;11:260.

244. Chang X, Han J. Expression of peptidylarginine deiminase type 4 (PAD4) in various tumors. Mol Carcinog. 2006 Mar;45(3):183–96.

245. Baeten D, Peene I, Union A, Meheus L, Sebbag M, Serre G, et al. Specific presence of intracellular citrullinated proteins in rheumatoid arthritis synovium: relevance to antifilaggrin autoantibodies. Arthritis Rheum. 2001 Oct;44(10):2255–62.

246. Suzuki A, Yamada R, Chang X, Tokuhiro S, Sawada T, Suzuki M, et al. Functional haplotypes of PADI4, encoding citrullinating enzyme peptidylarginine deiminase 4, are associated with rheumatoid arthritis. Nat Genet. 2003 Aug;34(4):395–402.

247. Vossenaar ER, van Venrooij WJ. Citrullinated proteins: sparks that may ignite the fire in rheumatoid arthritis. Arthritis Res Ther. 2004 Jan;6(3):107–11.

248. De Rycke L, Nicholas AP, Cantaert T, Kruithof E, Echols JD, Vandekerckhove B, et al. Synovial intracellular citrullinated proteins colocalizing with peptidyl arginine deiminase as pathophysiologically relevant antigenic determinants of rheumatoid arthritis-specific humoral autoimmunity. Arthritis Rheum. 2005 Aug;52(8):2323–30.

249. Kinloch A, Lundberg K, Wait R, Wegner N, Lim NH, Zendman AJW, et al. Synovial fluid is a site of citrullination of autoantigens in inflammatory arthritis. Arthritis Rheum. 2008 Aug;58(8):2287–95.

250. Foulquier C, Sebbag M, Clavel C, Chapuy-Regaud S, Al Badine R, Méchin M-C, et al. Peptidyl arginine deiminase type 2 (PAD-2) and PAD-4 but not PAD-1, PAD-3, and PAD-6 are expressed in rheumatoid arthritis synovium in close association with tissue inflammation. Arthritis Rheum. 2007 Nov;56(11):3541–53.

251. Vossenaar ER, Smeets TJM, Kraan MC, Raats JM, van Venrooij WJ, Tak PP. The presence of citrullinated proteins is not specific for rheumatoid synovial tissue. Arthritis Rheum. 2004 Nov;50(11):3485–94.

252. Makrygiannakis D, af Klint E, Lundberg IE, Löfberg R, Ulfgren a-K, Klareskog L, et al. Citrullination is an inflammation-dependent process. Ann Rheum Dis. 2006 Sep;65(9):1219–22.

253. Van Gaalen FA, Linn-Rasker SP, van Venrooij WJ, de Jong BA, Breedveld FC, Verweij CL, et al. Autoantibodies to cyclic citrullinated peptides predict progression to rheumatoid arthritis in patients with undifferentiated arthritis: a prospective cohort study. Arthritis Rheum. 2004 Mar;50(3):709–15.

254. Masson-Bessiere C, Sebbag M, Durieux J-J, Nogueira L, Vincent C, Girbal-Neuhauser E, et al. In the rheumatoid pannus, anti-filaggrin autoantibodies are produced by local plasma cells and constitute a higher proportion of IgG than in synovial fluid and serum. Clin Exp Immunol. Blackwell Publishing; 2000 Mar 1;119(3):544–52.

255. Rönnelid J, Wick MC, Lampa J, Lindblad S, Nordmark B, Klareskog L, et al. Longitudinal analysis of citrullinated protein/peptide antibodies (anti-CP) during 5 year follow up in early rheumatoid arthritis: anti-CP status predicts worse disease activity and greater radiological progression. Ann Rheum Dis. 2005 Dec;64(12):1744–9.

256. Catrina a. I, Deane KD, Scher JU. Gene, environment, microbiome and mucosal immune tolerance in rheumatoid arthritis. Rheumatology. 2014;1–12.

257. Källberg H, Ding B, Padyukov L, Bengtsson C, Rönnelid J, Klareskog L, et al. Smoking is a major preventable risk factor for rheumatoid arthritis: estimations of risks after various exposures to cigarette smoke. Ann Rheum Dis. 2011 Mar;70(3):508–11.

258. CAPLAN A. Rheumatoid disease and pneumoconiosis (Caplan's syndrome). Proc R Soc Med. 1959 Dec;52:1111–3.

259. Stolt P, Yahya A, Bengtsson C, Källberg H, Rönnelid J, Lundberg I, et al. Silica exposure among male current smokers is associated with a high risk of developing ACPA-positive rheumatoid arthritis. Ann Rheum Dis. 2010 Jun;69(6):1072–6.

260. Hart JE, Laden F, Puett RC, Costenbader KH, Karlson EW. Exposure to traffic pollution and increased risk of rheumatoid arthritis. Environ Health Perspect. 2009 Jul;117(7):1065–9.

261. Willis VC, Demoruelle MK, Derber LA, Chartier-Logan CJ, Parish MC, Pedraza IF, et al. Sputum autoantibodies in patients with established rheumatoid arthritis and subjects at risk of future clinically apparent disease. Arthritis Rheum. 2013 Oct;65(10):2545–54.

262. Scher JU, Sczesnak A, Longman RS, Segata N, Ubeda C, Bielski C, et al. Expansion of intestinal Prevotella copri correlates with enhanced susceptibility to arthritis. Elife. 2013 Jan;2:e01202.

263. Sant AJ, Chaves FA, Leddon SA, Tung J. The control of the specificity of CD4 T cell responses: thresholds, breakpoints, and ceilings. Front Immunol. 2013 Jan;4:340.

264. Shlomchik MJ, Craft JE, Mamula MJ. From T to B cell and back again: positive feedback in systemic autoimmune disease. Immunology. 2001;1(November).

265. Monneaux F, Muller S. Review: Epitope spreading in systemic lupus erythematosus: Identification of triggering peptide sequences. Arthritis Rheum. 2002;46(6):1430–8.

266. Cornaby C, Gibbons L, Mayhew V, Sloan CS, Welling A, Poole BD. B cell epitope spreading: Mechanisms and contribution to autoimmune diseases. Immunol Lett. 2015 Jan;163(1):56–68.

267. Sokolove J, Bromberg R, Deane KD, Lahey LJ, Derber LA, Chandra PE, et al. Autoantibody epitope spreading in the pre-clinical phase predicts progression to rheumatoid arthritis. PLoS One. 2012 Jan;7(5):e35296.

268. Suwannalai P, van de Stadt LA, Radner H, Steiner G, El-Gabalawy HS, Zijde CMJ der, et al. Avidity maturation of anti-citrullinated protein antibodies in rheumatoid arthritis. Arthritis Rheum. 2012 May;64(5):1323–8.

269. Van der Woude D, Rantapää-Dahlqvist S, Ioan-Facsinay A, Onnekink C, Schwarte CM, Verpoort KN, et al. Epitope spreading of the anti-citrullinated protein antibody response occurs before disease onset and is associated with the disease course of early arthritis. Ann Rheum Dis. 2010 Aug;69(8):1554–61.

270. Kokkonen H, Mullazehi M, Berglin E, Hallmans G, Wadell G, Rönnelid J, et al. Antibodies of IgG, IgA and IgM isotypes against cyclic citrullinated peptide precede the development of rheumatoid arthritis. Arthritis Res Ther. 2011 Jan;13(1):R13.

271. Brink M, Hansson M, Mathsson L, Jakobsson P-J, Holmdahl R, Hallmans G, et al. Multiplex analyses of antibodies against citrullinated peptides in individuals prior to development of rheumatoid arthritis. Arthritis Rheum. 2013 Apr;65(4):899–910.

272. Rock B, Martins CR, Theofilopoulos AN, Balderas RS, Anhalt GJ, Labib RS, et al. The pathogenic effect of IgG4 autoantibodies in endemic pemphigus foliaceus (fogo selvagem). N Engl J Med. 1989 Jun 1;320(22):1463–9.

273. Arbuckle MR, McClain MT, Rubertone M V, Scofield RH, Dennis GJ, James JA, et al. Development of autoantibodies before the clinical onset of systemic lupus erythematosus. N Engl J Med. 2003 Oct 16;349(16):1526–33.

274. Damian RT. Molecular mimicry revisited. Parasitol Today. 1987 Sep;3(9):263–6.

275. Delves PJ, Martin SJ, Dennis R. Burton et al. Roitt's Essential Immunology. 12th editi. Wiley-Blackwell; 2011.

276. De Pablo P, Chapple ILC, Buckley CD, Dietrich T. Periodontitis in systemic rheumatic diseases. Nat Rev Rheumatol. 2009 Apr;5(4):218–24.

277. Lundberg K, Wegner N, Yucel-Lindberg T, Venables PJ. Periodontitis in RA-the citrullinated enolase connection. Nat Rev Rheumatol. Nature Publishing Group; 2010 Dec;6(12):727–30.

278. Rosenstein ED, Greenwald R a, Kushner LJ, Weissmann G. Hypothesis: the humoral immune response to oral bacteria provides a stimulus for the development of rheumatoid arthritis. Inflammation. 2004 Dec;28(6):311–8.

279. Wegner N, Wait R, Sroka A, Eick S, Nguyen K-A, Lundberg K, et al. Peptidylarginine deiminase from Porphyromonas gingivalis citrullinates human fibrinogen and α-enolase: implications for autoimmunity in rheumatoid arthritis. Arthritis Rheum. 2010 Sep;62(9):2662–72.

280. Mercado FB, Marshall RI, Bartold PM. Inter-relationships between rheumatoid arthritis and periodontal disease. A review. J Clin Periodontol. 2003 Sep;30(9):761–72.

281. White DA, Tsakos G, Pitts NB, Fuller E, Douglas GVA, Murray JJ, et al. Adult Dental Health Survey 2009: common oral health conditions and their impact on the population. Br Dent J. 2012 Dec;213(11):567–72.

282. Kebschull M, Demmer RT, Papapanou PN. “Gum bug, leave my heart alone!”--epidemiologic and mechanistic evidence linking periodontal infections and atherosclerosis. J Dent Res. 2010 Sep;89(9):879–902.

283. Hajishengallis G. Periodontitis: from microbial immune subversion to systemic inflammation. Nat Rev Immunol. Nature Publishing Group, a division of Macmillan Publishers Limited. All Rights Reserved.; 2014 Dec 23;15(1):30–44.

284. Han YW, Wang X. Mobile microbiome: oral bacteria in extra-oral infections and inflammation. J Dent Res. 2013 Jun;92(6):485–91.

285. Hajishengallis G, Liang S, Payne MA, Hashim A, Jotwani R, Eskan MA, et al. Low-abundance biofilm species orchestrates inflammatory periodontal disease through the commensal microbiota and complement. Cell Host Microbe. 2011 Nov 17;10(5):497–506.

286. Polak D, Wilensky A, Shapira L, Halabi A, Goldstein D, Weiss EI, et al. Mouse model of experimental periodontitis induced by Porphyromonas gingivalis/Fusobacterium nucleatum infection: bone loss and host response. J Clin Periodontol. 2009 May;36(5):406–10.

287. Calsina G, Ramón J-M, Echeverría J-J. Effects of smoking on periodontal tissues. J Clin Periodontol. 2002 Aug;29(8):771–6.

288. McGraw WT, Potempa J, Farley D, Travis J. Purification, characterization, and sequence analysis of a potential virulence factor from Porphyromonas gingivalis, peptidylarginine deiminase. Infect Immun. 1999 Jul;67(7):3248–56.

289. Wegner N, Wait R, Venables PJ. Evolutionarily conserved antigens in autoimmune disease: implications for an infective aetiology. Int J Biochem Cell Biol. 2009 Feb;41(2):390–7.

290. Lundberg K, Kinloch A, Fisher B a, Wegner N, Wait R, Charles P, et al. Antibodies to citrullinated alpha-enolase peptide 1 are specific for rheumatoid arthritis and cross-react with bacterial enolase. Arthritis Rheum. 2008 Oct;58(10):3009–19.

291. Maresz KJ, Hellvard A, Sroka A, Adamowicz K, Bielecka E, Koziel J, et al. Porphyromonas gingivalis facilitates the development and progression of

destructive arthritis through its unique bacterial peptidylarginine deiminase (PAD). PLoS Pathog. 2013 Sep;9(9):e1003627.

292. Gully N, Bright R, Marino V, Marchant C, Cantley M, Haynes D, et al. Porphyromonas gingivalis peptidylarginine deiminase, a key contributor in the pathogenesis of experimental periodontal disease and experimental arthritis. PLoS One. 2014 Jan;9(6):e100838.

293. Quirke A-M, Lugli EB, Wegner N, Hamilton BC, Charles P, Chowdhury M, et al. Heightened immune response to autocitrullinated Porphyromonas gingivalis peptidylarginine deiminase: a potential mechanism for breaching immunologic tolerance in rheumatoid arthritis. Ann Rheum Dis. 2014 Jan;73(1):263–9.

294. Konig MF, Bingham CO, Andrade F. PPAD is not targeted as a citrullinated protein in rheumatoid arthritis, but remains a candidate for inducing autoimmunity. Ann Rheum Dis. 2015 Jan 1;74(1):e8.

295. Konig MF, Paracha AS, Moni M, Bingham CO, Andrade F. Defining the role of Porphyromonas gingivalis peptidylarginine deiminase (PPAD) in rheumatoid arthritis through the study of PPAD biology. Ann Rheum Dis. 2014;1–8.

296. Quirke a.-M, Lundberg K, Potempa J, Mikuls TR, Venables PJ. PPAD remains a credible candidate for inducing autoimmunity in rheumatoid arthritis: comment on the article by Konig et al. Ann Rheum Dis. 2014;74(1):e7–e7.

297. Shah A. The pathologic and clinical intersection of atopic and autoimmune disease. Curr Allergy Asthma Rep. 2012 Dec;12(6):520–9.

298. Rajan TV. The Gell–Coombs classification of hypersensitivity reactions: a re-interpretation. Trends Immunol. 2003 Jul;24(7):376–9.

299. Kouskoff V, Korganow AS, Duchatelle V, Degott C, Benoist C, Mathis D. Organ-specific disease provoked by systemic autoimmunity. Cell. 1996 Nov 29;87(5):811–22.

300. Matsumoto I, Maccioni M, Lee DM, Maurice M, Simmons B, Brenner M, et al. How antibodies to a ubiquitous cytoplasmic enzyme may provoke joint-specific autoimmune disease. Nat Immunol. 2002 Apr;3(4):360–5.

301. Binstadt B a, Patel PR, Alencar H, Nigrovic P a, Lee DM, Mahmood U, et al. Particularities of the vasculature can promote the organ specificity of autoimmune attack. Nat Immunol. 2006;7(3):284–92.

302. Ishikawa H, Smiley JD, Ziff M. Electron microscopic demonstration of immunoglobulin deposition in rheumatoid cartilage. Arthritis Rheum. Jan;18(6):563–76.

303. Zhao X, Okeke NL, Sharpe O, Batliwalla FM, Lee AT, Ho PP, et al. Circulating immune complexes contain citrullinated fibrinogen in rheumatoid arthritis. Arthritis Res Ther. 2008 Jan;10(4):R94.

304. Van Steendam K, Tilleman K, De Ceuleneer M, De Keyser F, Elewaut D, Deforce D. Citrullinated vimentin as an important antigen in immune complexes from synovial fluid of rheumatoid arthritis patients with antibodies against citrullinated proteins. Arthritis Res Ther. BioMed Central; 2010;12(4):R132.

305. Sokolove J, Zhao X, Chandra PE, Robinson WH. Immune complexes containing citrullinated fibrinogen costimulate macrophages via toll-like receptor 4 and Fcg receptor. Arthritis Rheum. 2011;63(1):53–62.

306. Laurent L, Anquetil F, Clavel C, Ndongo-Thiam N, Offer G, Miossec P, et al. IgM rheumatoid factor amplifies the inflammatory response of macrophages induced by the rheumatoid arthritis-specific immune complexes containing anticitrullinated protein antibodies. Ann Rheum Dis. 2014;1–7.

307. Mihai S, Nimmerjahn F. The role of Fc receptors and complement in autoimmunity. Autoimmun Rev. 2012 Nov 29;

308. Brunkhorst BA, Strohmeier G, Lazzari K, Weil G, Melnick D, Fleit HB, et al. Differential roles of Fc gamma RII and Fc gamma RIII in immune complex stimulation of human neutrophils. J Biol Chem. 1992 Oct 15;267(29):20659–66.

309. Sturfelt G, Truedsson L. Complement in the immunopathogenesis of rheumatic disease. Nat Rev Rheumatol. Nature Publishing Group; 2012;8(8):458–68.

310. Chou RC, Kim ND, Sadik CD, Seung E, Lan Y, Byrne MH, et al. Lipid-cytokine-chemokine cascade drives neutrophil recruitment in a murine model of inflammatory arthritis. Immunity. 2010 Aug 27;33(2):266–78.

311. Elliott ER, Van Ziffle JA, Scapini P, Sullivan BM, Locksley RM, Lowell CA. Deletion of Syk in neutrophils prevents immune complex arthritis. J Immunol. 2011 Oct 15;187(8):4319–30.

312. Harre U, Georgess D, Bang H, Bozec A, Axmann R, Ossipova E, et al. Induction of osteoclastogenesis and bone loss by human autoantibodies against citrullinated vimentin. J Clin Invest. 2012 May 1;122(5):1791–802.

313. Miles K, Clarke DJ, Lu W, Sibinska Z, Beaumont PE, Davidson DJ, et al. Dying and necrotic neutrophils are anti-inflammatory secondary to the release of alpha-defensins. J Immunol. 2009 Aug 1;183(3):2122–32.

314. Brinkmann V, Laube B, Abu Abed U, Goosmann C, Zychlinsky A. Neutrophil extracellular traps: how to generate and visualize them. J Vis Exp. 2010 Jan;(36):3–5.

315. Urban CF, Ermert D, Schmid M, Abu-Abed U, Goosmann C, Nacken W, et al. Neutrophil extracellular traps contain calprotectin, a cytosolic protein complex involved in host defense against Candida albicans. PLoS Pathog. 2009 Oct;5(10):e1000639.

316. Senshu T, Sato T, Inoue T, Akiyama K, Asaga H. Detection of citrulline residues in deiminated proteins on polyvinylidene difluoride membrane. Anal Biochem. 1992 May 15;203(1):94–100.

317. Gladman DD, Shuckett R, Russell ML, Thorne JC, Schachter RK. Psoriatic arthritis (PSA)--an analysis of 220 patients. Q J Med. 1987 Feb;62(238):127–41.

318. Kelly S, Humby F, Filer A, Ng N, Di Cicco M, Hands RE, et al. Ultrasound-guided synovial biopsy: a safe, well-tolerated and reliable technique for obtaining high-quality synovial tissue from both large and small joints in early arthritis patients. Ann Rheum Dis. 2013 Dec 13;

319. Lyutvinskiy Y, Yang H, Rutishauser D, Zubarev RA. In silico instrumental response correction improves precision of label-free proteomics and accuracy of proteomics-based predictive models. Mol Cell Proteomics. 2013 Aug;12(8):2324–31.

320. Boersema PJ, Foong LY, Ding VMY, Lemeer S, van Breukelen B, Philp R, et al. In-depth qualitative and quantitative profiling of tyrosine phosphorylation using a combination of phosphopeptide immunoaffinity purification and stable isotope dimethyl labeling. Mol Cell Proteomics. 2010 Jan 1;9(1):84–99.

321. Shevchenko A, Wilm M, Vorm O, Mann M. Mass spectrometric sequencing of proteins silver-stained polyacrylamide gels. Anal Chem. 1996 Mar 1;68(5):850–8.

322. Robinson JJ, Watson F, Phelan M, Bucknall RC, Edwards SW. Activation of neutrophils by soluble and insoluble immunoglobulin aggregates from synovial fluid of patients with rheumatoid arthritis. Ann Rheum Dis. 1993;52:347–53.

323. Mathsson L, Lampa J, Mullazehi M, Rönnelid J. Immune complexes from rheumatoid arthritis synovial fluid induce FcgammaRIIa dependent and rheumatoid factor correlated production of tumour necrosis factor-alpha by peripheral blood mononuclear cells. Arthritis Res Ther. 2006 Jan;8(3):R64.

324. Matsubara S, Yamamoto T, Tsuruta T, Takagi K, Kambara T. Complement C4-derived monocyte-directed chemotaxis-inhibitory factor.

A molecular mechanism to cause polymorphonuclear leukocyte-predominant infiltration in rheumatoid arthritis synovial cavities. Am J Pathol. 1991 May;138(5):1279–91.

325. Pillinger MH, Abramson SB. The neutrophil in rheumatoid arthritis. Rheum Dis Clin North Am. 1995 Aug;21(3):691–714.

326. Kaplan MJ. Role of neutrophils in systemic autoimmune diseases. Arthritis Res Ther. 2013 Jan;15(5):219.

327. Griffiths RJ, Pettipher ER, Koch K, Farrell CA, Breslow R, Conklyn MJ, et al. Leukotriene B4 plays a critical role in the progression of collagen-induced arthritis. Proc Natl Acad Sci U S A. 1995 Jan 17;92(2):517–21.

328. Schrier D, Gilbertsen RB, Lesch M, Fantone J. The role of neutrophils in type II collagen-induced arthritis in rats. Am J Pathol. 1984 Oct;117(1):26–9.

329. Mohr W, Wessinghage D. The relationship between polymorphonuclear granulocytes and cartilage destruction in rheumatoid arthritis. Z Rheumatol. 1978;37(3-4):81–6.

330. Baici A, Salgam P, Cohen G, Fehr K, Böni A. Action of collagenase and elastase from human polymorphonuclear leukocytes on human articular cartilage. Rheumatol Int. 1982 Jan;2(1):11–6.

331. Rollet-Labelle E, Vaillancourt M, Marois L, Newkirk MM, Poubelle PE, Naccache PH. Cross-linking of IgGs bound on circulating neutrophils leads to an activation of endothelial cells: possible role of rheumatoid factors in rheumatoid arthritis-associated vascular dysfunction. J Inflamm (Lond). 2013 Jan;10(1):27.

332. Brimnes J, Halberg P, Jacobsen S, Wiik A, Heegaard NH. Specificities of anti-neutrophil autoantibodies in patients with rheumatoid arthritis (RA). Clin Exp Immunol. 1997 Nov;110(2):250–6.

333. Locht H, Skogh T, Wiik A. Characterisation of autoantibodies to neutrophil granule constituents among patients with reactive arthritis, rheumatoid arthritis, and ulcerative colitis. Ann Rheum Dis. 2000 Nov;59(11):898–903.

334. Cambridge G, Williams M, Leaker B, Corbett M, Smith CR. Anti-myeloperoxidase antibodies in patients with rheumatoid arthritis: prevalence, clinical correlates, and IgG subclass. Ann Rheum Dis. 1994 Jan;53(1):24–9.

335. Falk RJ, Terrell RS, Charles LA, Jennette JC. Anti-neutrophil cytoplasmic autoantibodies induce neutrophils to degranulate and produce oxygen radicals in vitro. Proc Natl Acad Sci U S A. 1990 Jun;87(11):4115–9.

336. Kida I, Kobayashi S, Takeuchi K, Tsuda H, Hashimoto H, Takasaki Y. Antineutrophil cytoplasmic antibodies against myeloperoxidase, proteinase 3, elastase, cathepsin G and lactoferrin in Japanese patients with rheumatoid arthritis. Mod Rheumatol. 2011 Feb;21(1):43–50.

337. Kelley JM, Monach PA, Ji C, Zhou Y, Wu J, Tanaka S, et al. IgA and IgG antineutrophil cytoplasmic antibody engagement of Fc receptor genetic variants influences granulomatosis with polyangiitis. Proc Natl Acad Sci U S A. 2011 Dec 20;108(51):20736–41.

338. Lin AM, Rubin CJ, Khandpur R, Wang JY, Riblett M, Yalavarthi S, et al. Mast cells and neutrophils release IL-17 through extracellular trap formation in psoriasis. J Immunol. 2011 Jul 1;187(1):490–500.

339. Mitroulis I, Kambas K, Chrysanthopoulou A, Skendros P, Apostolidou E, Kourtzelis I, et al. Neutrophil extracellular trap formation is associated with IL-1β and autophagy-related signaling in gout. PLoS One. 2011 Jan;6(12):e29318.

340. Leon SA, Revach M, Ehrlich GE, Adler R, Petersen V, Shapiro B. DNA in synovial fluid and the circulation of patients with arthritis. Arthritis Rheum. 1981 Sep;24(9):1142–50.

341. Yu D, Rumore PM, Liu Q, Steinman CR. Soluble oligonucleosomal complexes in synovial fluid from inflamed joints. Arthritis Rheum. 1997 Apr;40(4):648–54.

342. Papayannopoulos V, Staab D, Zychlinsky A. Neutrophil elastase enhances sputum solubilization in cystic fibrosis patients receiving DNase therapy. PLoS One. 2011 Jan;6(12):e28526.

343. Robinson MW, Scott DG, Bacon PA, Walton KW, Coppock JS, Scott DL. What proteins are present in polyethylene glycol precipitates from rheumatic sera? Ann Rheum Dis. 1989 Jun;48(6):496–501.

344. Tadie J-M, Bae H-B, Jiang S, Park DW, Bell CP, Yang H, et al. HMGB1 promotes neutrophil extracellular trap formation through interactions with Toll-like receptor 4. Am J Physiol Lung Cell Mol Physiol. 2013 Mar 1;304(5):L342–9.

345. Pang L, Hayes CP, Buac K, Yoo D, Rada B. Pseudogout-associated inflammatory calcium pyrophosphate dihydrate microcrystals induce formation of neutrophil extracellular traps. J Immunol. 2013 Jun 15;190(12):6488–500.

346. Goldmann O, Medina E. The expanding world of extracellular traps: not only neutrophils but much more. Front Immunol. 2012 Jan;3:420.

347. Yousefi S, Gold JA, Andina N, Lee JJ, Kelly AM, Kozlowski E, et al. Catapult-like release of mitochondrial DNA by eosinophils contributes to antibacterial defense. Nat Med. 2008 Sep;14(9):949–53.

348. Brouckaert G, Kalai M, Krysko D V, Saelens X, Vercammen D, Ndlovu MN, et al. Phagocytosis of necrotic cells by macrophages is phosphatidylserine dependent and does not induce inflammatory cytokine production. Mol Biol Cell. 2004 Mar;15(3):1089–100.

349. Bratton DL, Henson PM. Neutrophil clearance: when the party is over, clean-up begins. Trends Immunol. 2011 Aug;32(8):350–7.

350. Cronstein BN, Eberle MA, Gruber HE, Levin RI. Methotrexate inhibits neutrophil function by stimulating adenosine release from connective tissue cells. Proc Natl Acad Sci U S A. 1991 Mar 15;88(6):2441–5.

351. Haskó G, Cronstein B. Regulation of inflammation by adenosine. Front Immunol. 2013 Jan;4:85.

352. Snir O, Widhe M, Hermansson M, von Spee C, Lindberg J, Hensen S, et al. Antibodies to several citrullinated antigens are enriched in the joints of rheumatoid arthritis patients. Arthritis Rheum. 2010 Jan;62(1):44–52.

353. Crowley-Nowick PA, Campbell E, Schrohenloher RE, Mestecky J, Jackson S. Polyethylene glycol precipitates of serum contain a large proportion of uncomplexed immunoglobulins and C3. Immunol Invest. 25(1-2):91–101.

354. Sur Chowdhury C, Giaglis S, Walker UA, Buser A, Hahn S, Hasler P. Enhanced neutrophil extracellular trap generation in rheumatoid arthritis: analysis of underlying signal transduction pathways and potential diagnostic utility. Arthritis Res Ther. 2014 Jan;16(3):R122.

355. Pelletier M, Maggi L, Micheletti A, Lazzeri E, Tamassia N, Costantini C, et al. Evidence for a cross-talk between human neutrophils and Th17 cells. Blood. 2010 Jan 14;115(2):335–43.

356. Branzk N, Papayannopoulos V. Molecular mechanisms regulating NETosis in infection and disease. Semin Immunopathol. 2013 Jul;35(4):513–30.

357. Martinelli S, Urosevic M, Daryadel A, Oberholzer PA, Baumann C, Fey MF, et al. Induction of genes mediating interferon-dependent extracellular trap formation during neutrophil differentiation. J Biol Chem. 2004 Oct 15;279(42):44123–32.

358. Wright HL, Bucknall RC, Moots RJ, Edwards SW. Analysis of SF and plasma cytokines provides insights into the mechanisms of inflammatory arthritis and may predict response to therapy. Rheumatology (Oxford). 2012 Mar;51(3):451–9.

359. Okroj M, Heinegård D, Holmdahl R, Blom AM. Rheumatoid arthritis and the complement system. Ann Med. 2007 Jan;39(7):517–30.

360. Nandakumar KS, Jansson A, Xu B, Rydell N, Ahooghalandari P, Hellman L, et al. A recombinant vaccine effectively induces c5a-specific neutralizing antibodies and prevents arthritis. PLoS One. 2010 Jan;5(10):e13511.

361. Darrah E, Andrade F. NETs: the missing link between cell death and systemic autoimmune diseases? Front Immunol. 2012 Jan;3:428.

362. Plotz PH. The autoantibody repertoire: searching for order. Nat Rev Immunol. 2003 Jan;3(1):73–8.

363. Muñoz LE, Lauber K, Schiller M, Manfredi AA, Herrmann M. The role of defective clearance of apoptotic cells in systemic autoimmunity. Nat Rev Rheumatol. 2010 May;6(5):280–9.

364. Klareskog L, Amara K, Malmström V. Adaptive immunity in rheumatoid arthritis: anticitrulline and other antibodies in the pathogenesis of rheumatoid arthritis. Curr Opin Rheumatol. 2014 Jan;26(1):72–9.

365. Willemze A, Shi J, Mulder M, Stoeken-Rijsbergen G, Drijfhout JW, Huizinga TWJ, et al. The concentration of anticitrullinated protein antibodies in serum and synovial fluid in relation to total immunoglobulin concentrations. Ann Rheum Dis. 2013 Mar 13;

366. Kolfenbach JR, Deane KD, Derber LA, O'Donnell CI, Gilliland WR, Edison JD, et al. Autoimmunity to peptidyl arginine deiminase type 4 precedes clinical onset of rheumatoid arthritis. Arthritis Rheum. 2010 Sep;62(9):2633–9.

367. Zhao J, Zhao YI, He J, Jia R, Li Z. Prevalence and Significance of Anti-Peptidylarginine Deiminase 4 Antibodies in Rheumatoid Arthritis Prevalence and Significance of Anti-Peptidylarginine Deiminase 4 Antibodies in Rheumatoid Arthritis. J Rheumatol. 2008;35(6).

368. Halvorsen EH, Pollmann S, Gilboe I-M, van der Heijde D, Landewé R, Ødegård S, et al. Serum IgG antibodies to peptidylarginine deiminase 4 in rheumatoid arthritis and associations with disease severity. Ann Rheum Dis. 2008 Mar 1;67(3):414–7.

369. Darrah E, Giles JT, Ols ML, Bull HG, Andrade F, Rosen A. Erosive rheumatoid arthritis is associated with antibodies that activate PAD4 by increasing calcium sensitivity. Sci Transl Med. 2013 May 22;5(186):186ra65.

370. Campbell AK. Intracellular Calcium, 2 Volume Set. Wiley; 2014. 848 p.

371. Robertson WG, Marshall RW. Ionized calcium in body fluids. Crit Rev Clin Lab Sci. 1981 Jan;15(2):85–125.

372. Nakayama-Hamada M, Suzuki A, Kubota K, Takazawa T, Ohsaka M, Kawaida R, et al. Comparison of enzymatic properties between hPADI2 and hPADI4. Biochem Biophys Res Commun. 2005 Mar 4;327(1):192–200.

373. Makrygiannakis D, Revu S, Engstrom M, Af Klint E, Nicholas AP, Pruijn GJ, et al. Local administration of glucocorticoids decrease synovial citrullination in rheumatoid arthritis. Arthritis Res Ther. 2012 Jan 27;14(1):R20.

374. Lominadze G, Powell DW, Luerman GC, Link AJ, Ward RA, McLeish KR. Proteomic analysis of human neutrophil granules. Mol Cell Proteomics. 2005 Oct;4(10):1503–21.

375. Van Beers JJBC, Schwarte CM, Stammen-Vogelzangs J, Oosterink E, Božič B, Pruijn GJM. The rheumatoid arthritis synovial fluid citrullinome reveals novel citrullinated epitopes in apolipoprotein E, myeloid nuclear differentiation antigen, and β-actin. Arthritis Rheum. 2013 Jan;65(1):69–80.

376. Auger I, Martin M, Balandraud N, Roudier J. Rheumatoid arthritis-specific autoantibodies to peptidyl arginine deiminase type 4 inhibit citrullination of fibrinogen. Arthritis Rheum. 2010 Jan;62(1):126–31.

377. Van Venrooij WJ, van Beers JJBC, Pruijn GJM. Anti-CCP antibodies: the past, the present and the future. Nat Rev Rheumatol. Nature Publishing Group; 2011 Jul;7(7):391–8.

378. Van Venrooij WJ, Pruijn GJM. How citrullination invaded rheumatoid arthritis research. Arthritis Res Ther. 2014 Jan;16(1):103.

379. Johansson M, Arlestig L, Hallmans G, Rantapää-Dahlqvist S. PTPN22 polymorphism and anti-cyclic citrullinated peptide antibodies in combination strongly predicts future onset of rheumatoid arthritis and has a specificity of 100% for the disease. Arthritis Res Ther. 2006 Jan;8(1):R19.

380. Szodoray P, Szabó Z, Kapitány A, Gyetvai A, Lakos G, Szántó S, et al. Anti-citrullinated protein/peptide autoantibodies in association with genetic and environmental factors as indicators of disease outcome in rheumatoid arthritis. Autoimmun Rev. 2010 Jan;9(3):140–3.

381. Catrina AI, Ytterberg AJ, Reynisdottir G, Malmström V, Klareskog L. Lungs, joints and immunity against citrullinated proteins in rheumatoid arthritis. Nat Rev Rheumatol. Nature Publishing Group, a division of Macmillan Publishers Limited. All Rights Reserved.; 2014 Nov;10(11):645–53.

382. Hagiwara T, Hidaka Y, Yamada M. Deimination of histone H2A and H4 at arginine 3 in HL-60 granulocytes. Biochemistry. 2005 Apr 19;44(15):5827–34.

383. Muller S. Histone Autoantibodies. Autoantibodies. Third Edit. Elsevier; 2014. p. 195–201.

384. Ytterberg AJ, Joshua V, Reynisdottir G, Tarasova NK, Rutishauser D, Ossipova E, et al. Shared immunological targets in the lungs and joints of patients with rheumatoid arthritis: identification and validation. Ann Rheum Dis. 2014 May 9;annrheumdis – 2013–204912 – .

385. Kamphorst JJ, van der Heijden R, DeGroot J, Lafeber FPJG, Reijmers TH, van El B, et al. Profiling of endogenous peptides in human synovial fluid by NanoLC-MS: method validation and peptide identification. J Proteome Res. 2007 Nov;6(11):4388–96.

386. Arita K, Shimizu T, Hashimoto H, Hidaka Y, Yamada M, Sato M. Structural basis for histone N-terminal recognition by human peptidylarginine deiminase 4. Proc Natl Acad Sci U S A. 2006 Apr 4;103(14):5291–6.

387. Saiki M, Watase M, Matsubayashi H, Hidaka Y. Recognition of the N-terminal histone H2A and H3 peptides by peptidylarginine deiminase IV. Protein Pept Lett. 2009 Jan;16(9):1012–6.

388. Ossipova E, Cerqueira CF, Reed E, Kharlamova N, Israelsson L, Holmdahl R, et al. Affinity purified anti-citrullinated protein/peptide antibodies target antigens expressed in the rheumatoid joint. Arthritis Res Ther. 2014 Aug 12;16(4):R167.

389. Shi J, Willemze A, Janssen GMC, van Veelen PA, Drijfhout JW, Cerami A, et al. Recognition of citrullinated and carbamylated proteins by human antibodies: specificity, cross-reactivity and the “AMC-Senshu” method. Ann Rheum Dis. 2013 Jan;72(1):148–50.

390. Liu CL, Tangsombatvisit S, Rosenberg JM, Mandelbaum G, Gillespie EC, Gozani OP, et al. Specific post-translational histone modifications of neutrophil extracellular traps as immunogens and potential targets of lupus autoantibodies. Arthritis Res Ther. 2012 Jan;14(1):R25.

391. Molberg O, Mcadam SN, Körner R, Quarsten H, Kristiansen C, Madsen L, et al. Tissue transglutaminase selectively modifies gliadin peptides that are recognized by gut-derived T cells in celiac disease. Nat Med. 1998 Jun;4(6):713–7.

392. Mor-Vaknin N, Kappes F, Dick AE, Legendre M, Damoc C, Teitz-Tennenbaum S, et al. DEK in the synovium of patients with juvenile idiopathic arthritis: characterization of DEK antibodies and

posttranslational modification of the DEK autoantigen. Arthritis Rheum. 2011 Feb;63(2):556–67.

393. Doyle H a., Mamula MJ. Autoantigenesis: The evolution of protein modifications in autoimmune disease. Curr Opin Immunol. 2012;24:112–8.

394. Rosen A, Casciola-Rosen L. Autoantigens as substrates for apoptotic proteases: implications for the pathogenesis of systemic autoimmune disease. Cell Death Differ. 1999 Jan;6(1):6–12.

395. Dieker JW, Fransen JH, van Bavel CC, Briand J-P, Jacobs CW, Muller S, et al. Apoptosis-induced acetylation of histones is pathogenic in systemic lupus erythematosus. Arthritis Rheum. 2007 Jun;56(6):1921–33.

396. Van Bavel CC, Dieker JW, Kroeze Y, Tamboer WP, Voll R, Muller S, et al. Apoptosis-induced histone H3 methylation is targeted by autoantibodies in systemic lupus erythematosus. Ann Rheum Dis. 2011 Jan;70(1):201–7.

397. Okumura N, Haneishi A, Terasawa F. Citrullinated fibrinogen shows defects in FPA and FPB release and fibrin polymerization catalyzed by thrombin. Clin Chim Acta. 2009 Mar;401(1-2):119–23.

398. Dwivedi N, Upadhyay J, Neeli I, Khan S, Pattanaik D, Myers L, et al. Felty's syndrome autoantibodies bind to deiminated histones and neutrophil extracellular chromatin traps. Arthritis Rheum. 2012 Apr 27;64(4):982–92.

399. Gupta AK, Giaglis S, Hasler P, Hahn S. Efficient neutrophil extracellular trap induction requires mobilization of both intracellular and extracellular calcium pools and is modulated by cyclosporine a. Palaniyar N, editor. PLoS One. Public Library of Science; 2014 Jan;9(5):e97088.

400. Pratesi F, Dioni I, Tommasi C, Alcaro MC, Paolini I, Barbetti F, et al. Antibodies from patients with rheumatoid arthritis target citrullinated histone 4 contained in neutrophils extracellular traps. Ann Rheum Dis. 2013 Jun 1;1–9.

401. Anzilotti C, Pratesi F, Tommasi C, Migliorini P. Peptidylarginine deiminase 4 and citrullination in health and disease. Autoimmun Rev. Elsevier B.V.; 2010 Jan;9(3):158–60.

402. Rohrbach AS, Slade DJ, Thompson PR, Mowen KA. Activation of PAD4 in NET formation. Front Immunol. 2012 Jan;3:360.

403. Zhang X, Bolt M, Guertin MJ, Chen W, Zhang S, Cherrington BD, et al. Peptidylarginine deiminase 2-catalyzed histone H3 arginine 26 citrullination facilitates estrogen receptor α target gene activation. Proc Natl Acad Sci U S A. 2012 Aug 14;109(33):13331–6.

404. Cherrington BD, Zhang X, McElwee JL, Morency E, Anguish LJ, Coonrod SA. Potential role for PAD2 in gene regulation in breast cancer cells. PLoS One. 2012 Jan;7(7):e41242.

405. Hobbs RN, Lea DJ, Ward DJ. A fluorimetric assay for human antibodies to all the histones. J Immunol Methods. 1983 Dec 16;65(1-2):235–43.

406. Costa O, Monier JC. Antihistone antibodies detected by ELISA and immunoblotting in systemic lupus erythematosus and rheumatoid arthritis. J Rheumatol. 1986 Aug;13(4):722–5.

407. S W Edwards VH, Edwards SW, Hughes V, Barlow J, Bucknall R. Immunological detection of myeloperoxidase in synovial fluid from patients with rheumatoid arthritis. Biochem J. Portland Press Ltd; 1988 Feb 15;250(1):81–5.

408. Wong SH, Francis N, Chahal H, Raza K, Salmon M, Scheel-Toellner D, et al. Lactoferrin is a survival factor for neutrophils in rheumatoid synovial fluid. Rheumatology. Oxford University Press; 2008 Nov 23;48(1):39–44.

409. Papayannopoulos V, Zychlinsky A. NETs: a new strategy for using old weapons. Trends Immunol. 2009 Nov;30(11):513–21.

410. Dörner T. SLE in 2011: Deciphering the role of NETs and networks in SLE. Nat Rev Rheumatol. Nature Publishing Group; 2012 Feb;8(2):68–70.

411. Spengler J, Lugonja B, Ytterberg AJ, Zubarev RA, Creese AJ, Pearson MJ, et al. Release of active peptidyl arginine deiminases by neutrophils can explain production of extracellular citrullinated autoantigens in RA synovial fluid. Arthritis Rheumatol (Hoboken, NJ). 2015 Aug 5;

412. Damgaard D, Senolt L, Nielsen MF, Pruijn GJ, Nielsen CH. Demonstration of extracellular peptidylarginine deiminase (PAD) activity in synovial fluid of patients with rheumatoid arthritis using a novel assay for citrullination of fibrinogen. Arthritis Res Ther. 2014 Jan;16(6):498.

413. Rumore PM, Steinman CR. Endogenous circulating DNA in systemic lupus erythematosus. Occurrence as multimeric complexes bound to histone. J Clin Invest. 1990 Jul;86(1):69–74.

414. Holdenrieder S, Eichhorn P, Beuers U, Samtleben W, Schoenermarck U, Zachoval R, et al. Nucleosomal DNA fragments in autoimmune diseases. Ann N Y Acad Sci. 2006 Sep;1075:318–27.

415. Emlen W, Niebur J, Kadera R. Accelerated in vitro apoptosis of lymphocytes from patients with systemic lupus erythematosus. J Immunol. 1994 Apr 1;152(7):3685–92.

416. Zong W-X, Thompson CB. Necrotic death as a cell fate. Genes Dev. 2006 Jan 1;20(1):1–15.

417. Freemont AJ, Denton J. Disease distribution of synovial fluid mast cells and cytophagocytic mononuclear cells in inflammatory arthritis. Ann Rheum Dis. 1985 May;44(5):312–5.

418. Sercarz EE, Lehmann P V, Ametani A, Benichou G, Miller A, Moudgil K. Dominance and crypticity of T cell antigenic determinants. Annu Rev Immunol. 1993 Jan;11:729–66.

419. Saffarzadeh M, Juenemann C, Queisser M a, Lochnit G, Barreto G, Galuska SP, et al. Neutrophil extracellular traps directly induce epithelial and endothelial cell death: a predominant role of histones. PLoS One. 2012 Jan;7(2):e32366.

420. Clark SR, Ma AC, Tavener SA, McDonald B, Goodarzi Z, Kelly MM, et al. Platelet TLR4 activates neutrophil extracellular traps to ensnare bacteria in septic blood. Nat Med. 2007 Apr;13(4):463–9.

421. Urban C, Zychlinsky A. Netting bacteria in sepsis Providing AID to p53 mutagenesis. Nat Med. 2007;13(4):403–4.

422. Hall JC, Casciola-Rosen L, Rosen A. Altered structure of autoantigens during apoptosis. Rheum Dis Clin North Am. 2004 Aug;30(3):455–71, vii.

423. Tutturen AE V, Fleckenstein B, De Souza G a. Assessing the citrullinome in rheumatoid arthritis synovial fluid with and without enrichment of citrullinated peptides. J Proteome Res. 2014;13(6):2867–73.

424. Fransen JH, Berden JH, Koeter CM, Adema GJ, Van Der Vlag J, Hilbrands LB. Effect of administration of apoptotic blebs on disease development in lupus mice. Autoimmunity. 2012 Jun;45(4):290–7.

425. Radic M. Clearance of Apoptotic Bodies, NETs, and Biofilm DNA: Implications for Autoimmunity. Front Immunol. 2014;5(July):1–5.

426. Lövgren T, Eloranta M-L, Böve U, Alm G V., Rönnblom L. Induction of interferon-? production in plasmacytoid dendritic cells by immune complexes containing nucleic acid released by necrotic or late apoptotic cells and lupus IgG. Arthritis Rheum. 2004 Jun;50(6):1861–72.

427. Leadbetter E a, Rifkin IR, Hohlbaum AM, Beaudette BC, Shlomchik MJ, Marshak-Rothstein A. Chromatin-IgG complexes activate B cells by dual engagement of IgM and Toll-like receptors. Nature. 2002;416:603–7.

428. Williams RC. Rheumatoid factors: historical perspective, origins and possible role in disease. J Rheumatol Suppl. 1992 Jan;32:42–5.

429. Goh FG, Midwood KS. Intrinsic danger: Activation of Toll-like receptors in rheumatoid arthritis. Rheumatology. 2012;51(October 2011):7–23.

430. Nathan C. Neutrophils and immunity: challenges and opportunities. Nat Rev Immunol. 2006 Mar;6(3):173–82.

431. Reynisdottir G, Karimi R, Joshua V, Olsen H, Hensvold AH, Harju A, et al. Structural changes and antibody enrichment in the lungs are early features of anti-citrullinated protein antibody-positive rheumatoid arthritis. Arthritis Rheumatol (Hoboken, NJ). 2014 Jan;66(1):31–9.

432. Nesse W, Westra J, van der Wal JE, Abbas F, Nicholas AP, Vissink A, et al. The periodontium of periodontitis patients contains citrullinated proteins which may play a role in ACPA (anti-citrullinated protein antibody) formation. J Clin Periodontol. 2012 Mar 30;

433. Vitkov L, Klappacher M, Hannig M, Krautgartner WD. Neutrophil fate in gingival crevicular fluid. Ultrastruct Pathol. 2010 Feb;34(1):25–30.

434. Ireland JM, Unanue ER. Autophagy in antigen-presenting cells results in presentation of citrullinated peptides to CD4 T cells. J Exp Med. 2011 Dec 19;208(13):2625–32.

435. Rohrbach AS, Hemmers S, Arandjelovic S, Corr M, Mowen KA. PAD4 is not essential for disease in the K/BxN murine autoantibody-mediated model of arthritis. Arthritis Res Ther. 2012 May 2;14(3):R104.

436. Ioan-Facsinay A, el-Bannoudi H, Scherer HU, van der Woude D, Ménard H a, Lora M, et al. Anti-cyclic citrullinated peptide antibodies are a collection of anti-citrullinated protein antibodies and contain overlapping and non-overlapping reactivities. Ann Rheum Dis. 2011 Jan;70(1):188–93.

437. Ioan-Facsinay A, Willemze A, Robinson DB, Peschken C a., Markland J, Van Der Woude D, et al. Marked differences in fine specificity and isotype usage of the anti-citrullinated protein antibody in health and disease. Arthritis Rheum. 2008 Oct;58(10):3000–8.

438. Scherer HU, van der Woude D, Willemze A, Trouw L a, Knevel R, Syversen SW, et al. Distinct ACPA fine specificities, formed under the influence of HLA shared epitope alleles, have no effect on radiographic joint damage in rheumatoid arthritis. Ann Rheum Dis. 2011;70:1461–4.

439. Campion G, Maddison PJ, Goulding N, James I, Ahern MJ, Watt I, et al. The Felty syndrome: a case-matched study of clinical manifestations and outcome, serologic features, and immunogenetic associations. Medicine (Baltimore). 1990 Mar;69(2):69–80.

440. Owlia MB, Newman K, Akhtari M. Felty's Syndrome, Insights and Updates. Open Rheumatol J. 2014 Jan;8:129–36.

441. Sienknecht CW, Urowitz MB, Pruzanski W, Stein HB. Felty's syndrome. Clinical and serological analysis of 34 cases. Ann Rheum Dis. 1977 Dec;36(6):500–7.

442. Ytterberg AJ, Peltier J-B, van Wijk KJ. Protein profiling of plastoglobules in chloroplasts and chromoplasts. A surprising site for differential accumulation of metabolic enzymes. Plant Physiol. 2006 Mar;140(3):984–97.

8 Appendix

8.1 Patient clinical data

	Gender	Age (yrs)	Disease duration (yrs)	Rheumatoid factor (value)	ACPA (value)	TJC (28)	SJC (28)	ESR	CRP	DAS 28 ESR	Medication
1	f	52	NA	58.1	261	20	8	26	52	NA	NSAID
2	m	67	1	128	96	1	1	29	48	4.23	nil
3	f	65	4	148	6.8	7	4	41	10	5.62	MTX, SSZ, HCQ, RTX
4	m	85	4	13.4	>340	3	1	na	138	NA	SSZ, prednisolone
5	m	65	3	713	231	3	12	72	81	5.33	nil
6	m	42	6	<11	NA	4	3	27	95	5.00	SSZ, MTX, prednisolone, TCZ
7	m	58	2	50.8	>340	18	6	46	22	6.86	nil
8	m	42	6	5120	NA	2	2	7	23	3.45	MTX, prednisolone, RTX
9	f	65	4	148	6.8	15	4	72	33	6.51	SSZ, HCQ, MTX, RTX
10	m	43	7	5120	NA	2	13	31	64	5.40	MTX, prednisolone, RTX
11	f	72	3	NA	0.7	1	2	31	0	3.65	MTX, HCQ, etanercept
12	m	82	1	NA	>340	21	12	76	31	7.88	prednisolone, adalimumab
13	m	50	2	12.3	5	13	16	117	184	7.52	MTX, SSZ, etanercept
14	f	35	1	100	100	8	11	23	4	6.11	MTX
15	f	26	1	47	71	3	3	25	8	3.71	MTX
16	f	43	10	343	NA	3	1	44	0	4.86	leflunomide, HCQ
17	m	72	27	61.4	>340	22	5	16	51	5.85	MTX
18	f	44	6	1in128	261	5	1	37	16	4.06	etanercept, MTX, prednisolone
19	f	57	1	0	1	5	5	28	20	5.33	nil
20	f	61	11	NA	54	9	9	21	27	4.65	diclofenac
21	f	56	12	61.7	>340	3	3	23	0	4.91	cimzia, HCQ
22	f	58	8	80	>340	6	5	124	99	6.70	MTX
23	f	47	0	140	91	10	7	34	17	6.24	ibuprofen
24	f	82	8	31.2	<7	26	7	11	0	6.67	HCQ, prednisolone TCZ
25	f	76	12	476	272	2	2	NA	NA	NA	leflunomide
26	f	70	7	24.7	>340	19	12	NA	56	NA	MTX
27	f	62	10	27.2	71	28	10	46	108	7.84	MTX, prednisolone, nabumetone
28	f	75	24	NA	NA	7	6	18	7	4.19	MTX
29	m	71	16	661	188	1	1	NA	NA	NA	MTX, HCQ, etanercept
30	f	56	0	22	58	9	3	48	47	5.92	naproxen
31	f	57	1	37.7	NA	3	2	68	55	4.46	HCQ, MTX, prednisolone
32	m	54	1	583	>340	5	7	NA	<5	NA	MTX, prednisolone
33	f	48	2	417	>340	11	7	70	22	5.41	MTX, HCQ,
34	f	59	24	NA	NA	1	5	18	3	4.19	etanercept
35	f	32	13	<11	2.1	1	1	17	17	3.48	MTX, HCQ, prednisolone, RTX
36	m	61	5	338	33	7	7	30	21	5.58	prednisolone, leflunomide
37	f	50	1	48	340	3	3	49	64	5.19	HCQ
38	f	58	0	57	52	2	2	43	11	5.08	ibuprofen
39	f	77	3	NA	84	5	5	19	5	4.64	SSZ, HCQ
40	f	23	0	15	1	12	5	3	16	4.39	nil
41	f	56	6	324	100	9	7	NA	58	NA	MTX, SSZ
42	f	51	3	0	1.8	6	2	26	19	5.03	MTX, SSZ, HCQ
43	m	60	0	0	1	3	3	10	5	3.77	ibuprofen
44	f	58	3	0	1	1	1	NA	8	NA	MTX, HCQ
45	f	64	18	NA	34	6	1	8	2	4.10	MTX
46	m	71	2	14.7	>340	2	1	16	9	3.29	MTX HCQ
47	m	72	NA	661	188	NA	NA	13	3	NA	MTX, HLQ, etanercept
48	f	49	7	780	180	10	10	48	58	NA	prednisolone
49	f	40	9	<11	117	NA	NA	24	12	NA	MTX
50	f	52	3	524	359	14	10	34	13	6.54	NA
51	f	33	2	1211	>340	8	6	48	15	5.90	ibuprofen, loratidine
52	f	42	11	<11	1.3	5	2	52	77	5.62	MTX, etanercept
53	m	62	NA	66	186	NA	NA	NA	NA	NA	etanercept, alendronic acid, prednisolone

Table 8-1 Clinical data for RA patients

Synovial fluid samples from these patients were used for experiments described in Chapter 3, Chapter 4 and Chapter 5. Erythrocyte Sedimentation Rate (ESR), C Reactive Protein (CRP), Rheumatoid Factor (RF), Cyclic Citrullinated Peptide Antibody (CCP), Tender Joint Count 28 (TJC), Swollen Joint Count 28 (SJC), Disease Activity Score 28 (DAS28), data not available (NA).

	Gender	Age (yrs)	Disease duration (yrs)	Rheumatoid factor (value)	ACPA (value)	TJC (28)	SJC (28)	ESR	CRP	DAS 28 ESR	Medication
1	f	44	NA	NA	NA	1	1	NA	NA	NA	nil
2	f	26	1	<11	1.3	4	2	100	25	5.90	SSZ, ibuprofen
3	m	51	21	NA	NA	1	1	8	3	3.00	etanercept
4	m	46	NA	<11	1	4	1	5	<5	2.85	NA
5	m	43	NA	<11	1.5	2	2	2	10	2	etanercept, prednisolone
6	f	43	19	NA	NA	1	1	6	9	2.09	MTX, infliximab
7	m	31	10	NA	NA	2	4	2	0	2.26	adalimumab
8	m	58	NA	NA	NA	NA	NA	NA	NA	NA	MTX
9	m	39	5	NA	NA	NA	NA	6	NA	NA	MTX
10	m	58	9	NA	3	3	NA	NA	NA	NA	MTX
11	f	41	7	NA	NA	NA	NA	3	NA	NA	topical steroids
12	m	44	NA	<11	1.5	2	2	10	10	2.9	etanercept

Table 8-2 Clinical data for PsA patients

Synovial fluid samples from these patients were used for experiments described in Chapter 3, Chapter 4 and Chapter 5. Erythrocyte Sedimentation Rate (ESR), C Reactive Protein (CRP), Rheumatoid Factor (RF), Cyclic Citrullinated Peptide Antibody (CCP), Tender Joint Count 28 (TJC), Swollen Joint Count 28 (SJC), Disease Activity Score 28 (DAS28), data not available (NA).

	Gender	Age (yrs)	BMI (Scales)	Hip:Waist	Height (cm)	Weight (kg)	Waist (cm)	Hip (cm)	Fat %	systolic BP	diastolic BP
1	m	50	31.3	1.06	179	100.4	116	109	30.1	131	87
2	f	65	22.6	0.83	161.5	58.7	81	98	33.6	120	62
3	f	64	20.3	0.70	172	60.1	66	94	30.1	177	99
4	m	68	21.2	0.90	186	73.4	94	104	18.7	159	102
5	f	44	33.1	0.88	174	100.1	105	119	46.3	123	75
6	m	70	34.4	1.05	176.5	107.3	118	112	34.4	171	88
7	m	71	27	0.88	173	80.7	95	108	28	139	88
8	f	53	43.7	0.74	150	105.1	102	137	45.8	130	73
9	m	65	21.4	0.87	182.5	71.800	86	99	18.6	119	66
10	f	53	29.3	0.82	164	78.8	93	114	41.5	146	94
11	f	52	25.7	0.80	160	65.75	80	100	35.7	110	59
12	f	54	29.9	0.89	169	85.5	104	117	42.8	122	68
13	m	66	23.4	0.90	175	72.1	94	104	21.4	136	76
14	f	67	32.5	0.96	164	87.5	110	114	45.6	152	83
15	m	64	24.9	0.97	170	72.1	96	99	25.6	129	85

Table 8-3 Clinical data for OA patients

Synovial fluid samples from these patients were used for experiments described in Chapter 3.

	Gender	Age	BMI (Scales)	Hip:Waist	Height (cm)	Weight (kg)	Waist (cm)	Hip (cm)	Fat %	systolic BP	diastolic BP
1	f	53	28.9	0.79	167	80.5	88	111	44.2	120	76
2	f	63	29.2	0.83	155	70.2	95	115	45.2	153	81
3	f	71	30.7	0.88	163	81.6	101	115	44.5	140	75
4	f	50	43.1	0.92	161	111.8	47	51	49.2	137	80
5	f	44	33.1	0.88	174	100.1	105	119	46.3	123	75

Table 8-4 Clinical data for OA patients

Synovial fluid samples from these patients were used for experiments described in Chapter 4.

8.2 Quantitative proteomics data on the protein composition in the supernatant of cells going into NETosis

Pellets from the D (+DNase-I, alias "NET fractions") and SN supernatant fractions isolated from 7 patients were cleaned using acetone precipitation and resuspended in 2 % SDS. The protein concentrations were determined by the Pierce BCA protein assay kit (Thermo Fisher, USA). 10 µg of each sample were reduced, alkylated and digested in-solution according to Ytterberg et al. 2006 (442). After zip tipping (Merck Millipore Ltd, Irland), 1 µg of each sample

was separated using C18 RP columns coupled on-line to an LC-MS/MS. The chromatographic separation was achieved using an ACN/water solvent system containing 0.1 % formic acid. The gradient was set up as following: 3−35 % ACN in 89 min, 35−95 % ACN in 5 min and 95 % ACN for 8 min all at a flow rate of 300 nl/min. The samples from 4 patients were analyzed by LTQ Orbitrap Velos ETD and 3 by Q Exactive MS (Thermo Fisher Scientific, Germany). The spectra were acquired on the Velos with a resolution of 60,000 in MS mode, and the top 5 precursors were selected for fragmentation using CID. The spectra on the Q Exactive were acquired with a resolution of 70,000 in MS mode, and the top 10 precursors were selected for HCD fragmentation with a resolution of 17,000.

The data acquired using the Velos and the Q Exactive were quantified in separate analyses. Mass lists were extracted from the raw data using Raw2MGF v2.1.3 and combined into one file using Cluster MGF v2.1.1, programs part of the Quanti work flow (319). The data was searched against a concatenated version of the human complete proteome database (2013/4) using the Mascot search engine v2.4.1 (Matrix Science Ltd., London, UK). The following parameters were used: tryptic digestion (max 2 miscleavages); carbamethylation (C) as fixed modification; oxidation (M), pyroglutamate (Q) as variable modifications; 5 ppm as precursor tolerance; 0.25 Da (Velos) or 0.01 Da (Q Exactive) as fragment tolerance. The threshold for 2% FDR was calculated to a peptide score of 22.80 (Velos) and 13.97 (Q Exactive). The quantification was done using the Quanti work flow, which is a quantification software based on extracted ion chromatograms.(319) In short, after searching the combined mgf against the human complete proteome, the resulting dat file and the 6 respectively 8 raw files (representing D and SN fractions from 3 respectively 4 patients) were uploaded into Quanti v2.5.4.3. The following parameters were used: score threshold 20.8 (Velos) or 13.97 (Q Exactive); mass tolerance 10 ppm; minimum peptides/protein 2; maximum allowed deviation in retention time 3% or 5 min; rt order 50 (Velos) or 70 (Q Exactive); only “charge deconvolution” and “use best mascot peptide” were used. The quantitative values were further processed by multiplying the values with the reference abundance and normalizing each sample to the median of the summed intensities for all the samples. The values were finally log 10

transformed. p-values were calculated using Student’s t-test and expectation values were calculated by multiplying the p-values with the number of observations. Prior normalisation, the serum albumin and keratins were removed.

8.2.1 Proteins enriched in the NET (D) fraction

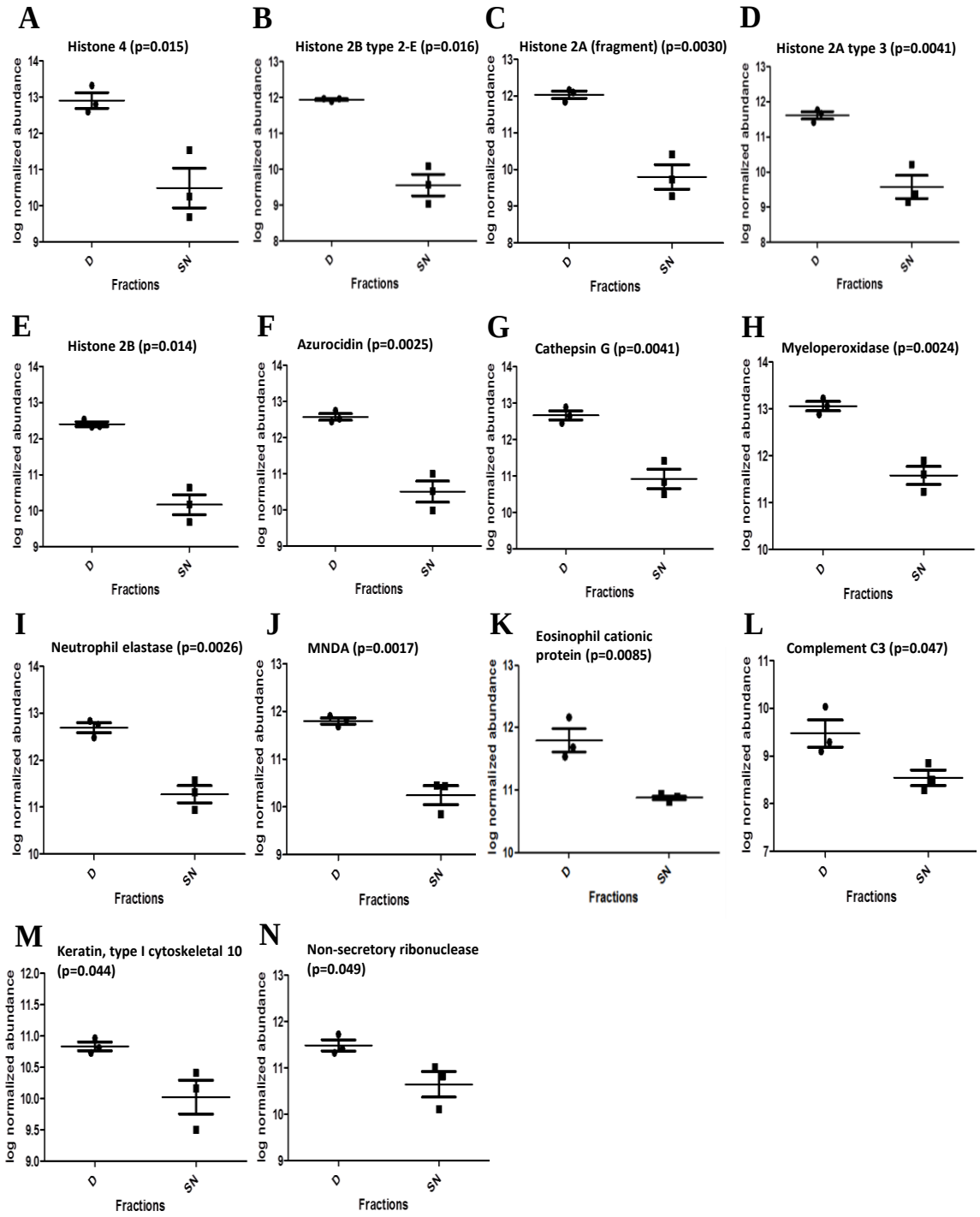

Figure 8-1 Enriched proteins in D (DNase-I treated NET fraction) fraction

268 proteins from 3 matched D/SN samples were quantified using 1%FDR and 2 peptides per protein. Abundance of proteins in D compared to SN was calculated using t-test (cut-off $p<0.05$). 14 proteins were found to be enriched in all 3 matched samples.

8.2.2 Total list of proteins quantified in SN and NET fraction

Patient 1-4 (LTQ Velos Orbitrap ETD MS)						Patient 5-7 (Q Exactive MS)					
PROTEIN ID	DESCRIPTION	PROTEIN IDs	log2(D/SN)	P (D vs SN)	E (n = 294)	PROTEIN ID	DESCRIPTION	PROTEIN IDs	log2(D/SN)	P (D vs SN)	E (n =555)
PADI2_HUMAN	Protein-arginine deiminase type-2	PADI2_HUMAN;B4DIU3_HUMAN;Q96DA7_HUMAN	-2.26	7.50E-03	2.44E+00	PADI2_HUMAN	Protein-arginine deiminase type-2	PADI2_HUMAN;B4DIU3_HUMAN;Q96DA7_HUMAN	-4.94	1.58E-02	8.77E+00
PADI4_HUMAN	Protein-arginine deiminase type-4	PADI4_HUMAN;KI26B_HUMAN;B7WPD9_HUMAN	2.60	5.38E-03	1.75E+00	PADI4_HUMAN	Protein-arginine deiminase type-4	PADI3_HUMAN;PADI4_HUMAN;KI26B_HUMAN;B7WPD9_HUMAN	3.91	2.59E-01	1.44E+02
1433B_HUMAN	14-3-3 protein beta/alpha	1433B_HUMAN;Q4VY19_HUMAN;Q4VY20_HUMAN	-2.74	4.78E-03	1.56E+00	1433B_HUMAN	14-3-3 protein beta/alpha	1433B_HUMAN;Q4VY19_HUMAN;Q4VY20_HUMAN	-1.11	6.98E-01	3.87E+02
1433E_HUMAN	14-3-3 protein epsilon	1433E_HUMAN;K7EM20_HUMAN;K7EIT4_HUMAN	-3.91	1.54E-03	5.02E-01	1433E_HUMAN	14-3-3 protein epsilon	1433E_HUMAN;K7EM20_HUMAN;B4DJF2_HUMAN;J3L3T1_HUMAN;K7EIT4_HUMAN	-2.74	1.78E-01	9.90E+01
1433G_HUMAN	14-3-3 protein gamma	1433G_HUMAN	13.05	2.16E-03	7.05E-01	1433G_HUMAN	14-3-3 protein gamma	1433G_HUMAN	-2.06	5.64E-01	3.13E+02
1433T_HUMAN	14-3-3 protein theta	1433T_HUMAN;E9PG15_HUMAN	-4.70	1.76E-04	5.73E-02	1433T_HUMAN	14-3-3 protein theta	1433T_HUMAN;E9PG15_HUMAN	-0.04	6.09E-01	3.38E+02
1433Z_HUMAN	14-3-3 protein zeta/delta	1433Z_HUMAN;E5RGE1_HUMAN;E7EVZ2_HUMAN;E7ESK7_HUMAN;E7EX29_HUMAN;E5RIR4_HUMAN;E9PD24_HUMAN;B7Z2E6_HUMAN;B0AZS6_HUMAN;E7EX24_HUMAN;H0YB80_HUMAN	-3.40	6.25E-04	2.04E-01	1433Z_HUMAN	14-3-3 protein zeta/delta	1433Z_HUMAN;B0AZS6_HUMAN;E7EVZ2_HUMAN;E7ESK7_HUMAN;E7EX29_HUMAN;E9PD24_HUMAN;B7Z2E6_HUMAN;E7EX24_HUMAN;H0YB80_HUMAN;E5RGE1_HUMAN;E5RIR4_HUMAN	-3.86	1.68E-01	9.32E+01
6PGL_HUMAN	6-phosphogluconolactonase	6PGL_HUMAN;M0R1L2_HUMAN;M0R261_HUMAN;M0R0U3_HUMAN	-5.87	9.08E-03	2.96E+00	6PGL_HUMAN	6-phosphogluconolactonase	6PGL_HUMAN;M0R261_HUMAN;M0R0U3_HUMAN;M0R1L2_HUMAN	-5.07	1.01E-02	5.58E+00
A1AG1_HUMAN	Alpha-1-acid glycoprotein 1	A1AG1_HUMAN;A1AG2_HUMAN	-0.53	8.41E-01	2.74E+02	A1AG1_HUMAN	Alpha-1-acid glycoprotein 1	A1AG1_HUMAN	-0.82	2.29E-01	1.27E+02
A1AT_HUMAN	Alpha-1-antitrypsin	A1AT_HUMAN;G3V5R8_HUMAN;G3V544_HUMAN;G3V387_HUMAN;G3V2B9_HUMAN	-3.30	3.68E-03	1.20E+00	A1AT_HUMAN	Alpha-1-antitrypsin	A1AT_HUMAN;G3V2B9_HUMAN;G3V544_HUMAN;G3V5R8_HUMAN;G3V387_HUMAN;REVERSED_DYH10_HUMAN	-4.37	1.42E-02	7.86E+00
A6NGS1_HUMAN	Spectrin alpha chain, non-erythrocytic 1	SPTN1_HUMAN;A6NGS1_HUMAN	-3.12	9.55E-07	3.11E-04	A6NGS1_HUMAN	Spectrin alpha chain, non-erythrocytic 1	SPTN1_HUMAN;A6NGS1_HUMAN	-3.63	2.21E-02	1.23E+01
A6NKB8_HUMAN	Aminopeptidase B	AMPB_HUMAN;A6NKB8_HUMAN;C9JMZ3_HUMAN;H7C2T3_HUMAN	-3.19	1.42E-02	4.63E+00	A6NKB8_HUMAN	Aminopeptidase B	AMPB_HUMAN;A6NKB8_HUMAN;C9JMZ3_HUMAN;H7C2T3_HUMAN	-2.25	5.38E-03	2.99E+00
A6PW80_HUMAN	Elongation factor 1-alpha 1 (Fragment)	EF1A1_HUMAN;EF1A3_HUMAN;Q5JR01_HUMAN;A6PW80_HUMAN;EF1A2_HUMAN	-2.97	1.66E-02	5.42E+00	EF1A3_HUMAN	Putative elongation factor 1-alpha-like 3	EF1A1_HUMAN;EF1A2_HUMAN;EF1A3_HUMAN;Q5JR01_HUMAN;A6PW80_HUMAN	-1.82	7.98E-02	4.43E+01
A8MU27_HUMAN	Small ubiquitin-related modifier 3	SUMO2_HUMAN;SUMO3_HUMAN;A8MUA9_HUMAN;J3KRH1_HUMAN;A8MU27_HUMAN;SUMO4_HUMAN;B4DUW4_HUMAN;H7BZT4_HUMAN	-4.88	8.98E-03	2.93E+00	A8MU27_HUMAN	Small ubiquitin-related modifier 3	SUMO2_HUMAN;SUMO3_HUMAN;SUMO4_HUMAN;A8MUA9_HUMAN;B4DUW4_HUMAN;A8MU27_HUMAN;H7BZT4_HUMAN;J3KRH1_HUMAN	-0.96	6.90E-02	3.83E+01
A8MYE6_HUMAN	Integrin beta	ITB2_HUMAN;A8MYE6_HUMAN	-2.98	1.39E-02	4.53E+00	ITB2_HUMAN	Integrin beta-2	ITB2_HUMAN;J3KNI6_HUMAN;E7EVZ9_HUMAN;ITB7_HUMAN;F5H6T4_HUMAN;A8MYE6_HUMAN;E5RK25_HUMAN;E5RIG7_HUMAN	-2.11	1.33E-01	7.39E+01
ACTC_HUMAN	Actin, alpha cardiac muscle 1	ACTA_HUMAN;ACTC_HUMAN;ACTH_HUMAN;ACTS_HUMAN;C9JFL5_HUMAN;F6UVQ4_HUMAN;A6NL76_HUMAN;F6QUT6_HUMAN;Q5T8M8_HUMAN;Q5T8M7_HUMAN	-2.05	9.99E-02	3.26E+01	ACTS_HUMAN	Actin, alpha skeletal muscle	ACTC_HUMAN;ACTS_HUMAN;A6NL76_HUMAN;Q5T8M8_HUMAN;ACTA_HUMAN;ACTH_HUMAN;C9JFL5_HUMAN;F6UVQ4_HUMAN;F6QUT6_HUMAN	-3.66	1.07E-01	5.92E+01
ACTG_HUMAN	Actin, cytoplasmic 2	ACTB_HUMAN;ACTG_HUMAN;J3L3I4_HUMAN;POTEE_HUMAN;J3L4N8_HUMAN;ACTBM_HUMAN;POTEF_HUMAN;POTEI_HUMAN;POTEJ_HUMAN;J3L1U9_HUMAN;J3L3I0_HUMAN;G5E9R0_HUMAN;K7EM38_HUMAN;J3KT65_HUMAN;J3L3R2_HUMAN;E7EVS6_HUMAN;ACTBL_HUMAN	-1.57	9.74E-03	3.18E+00	ACTG_HUMAN	Actin, cytoplasmic 2	ACTB_HUMAN;ACTG_HUMAN;J3L3I4_HUMAN;J3L1U9_HUMAN;J3L4N8_HUMAN;J3L3I0_HUMAN;ACTBM_HUMAN;POTEE_HUMAN;POTEF_HUMAN;POTEI_HUMAN;POTEJ_HUMAN;G5E9R0_HUMAN;K7EM38_HUMAN;J3KT65_HUMAN;J3L3R2_HUMAN;E7EVS6_HUMAN;ACTBL_HUMAN	-1.04	1.53E-01	8.50E+01
ACTN1_HUMAN	Alpha-actinin-1	ACTN1_HUMAN;B7TY16_HUMAN;H9KV75_HUMAN;H0YJW3_HUMAN;G3V2N5_HUMAN;G3V2W4_HUMAN;H7C5W8_HUMAN;G3V380_HUMAN;G3V5M4_HUMAN;G3V2X9_HUMAN;H0YJ11_HUMAN	-4.89	2.28E-03	7.43E-01	ACTN1_HUMAN	Alpha-actinin-1	ACTN1_HUMAN;B7TY16_HUMAN;H7C5W8_HUMAN;H9KV75_HUMAN;G3V2N5_HUMAN;G3V2W4_HUMAN;G3V2X9_HUMAN;H0YJW3_HUMAN;H0YJ11_HUMAN;G3V380_HUMAN;G3V5M4_HUMAN;REVERSED_RHDF1_HUMAN;REVERSED_Q4TT58_HUMAN;REVERSED_B8ZZ07_HUMAN;REVERSED_A2IDA2_HUMAN;REVERSED_F8WCF7_HUMAN;REVERSED_F5GWL4_HUMAN;REVERSED_F8WBS4_HUMAN	-4.41	2.05E-02	1.14E+01
ACTN4_HUMAN	Alpha-actinin-4	ACTN4_HUMAN;D6PXK4_HUMAN;H7C144_HUMAN;F5GXS2_HUMAN;K7EP19_HUMAN;K7EJH8_HUMAN	-4.72	3.62E-03	1.18E+00	ACTN4_HUMAN	Alpha-actinin-4	ACTN4_HUMAN;D6PXK4_HUMAN;F5GXS2_HUMAN;H7C144_HUMAN;K7EJH8_HUMAN;K7EP19_HUMAN	-3.21	2.00E-02	1.11E+01
ALDOA_HUMAN	Fructose-bisphosphate aldolase A	ALDOA_HUMAN;J3KPS3_HUMAN;H3BQN4_HUMAN;H3BPS8_HUMAN;H3BUH7_HUMAN;H3BR04_HUMAN;H3BMQ8_HUMAN;H3BU78_HUMAN;H3BR68_HUMAN	-4.22	1.18E-04	3.83E-02	ALDOA_HUMAN	Fructose-bisphosphate aldolase A	ALDOA_HUMAN;J3KPS3_HUMAN;H3BQN4_HUMAN;H3BPS8_HUMAN;H3BUH7_HUMAN;H3BR68_HUMAN;H3BU78_HUMAN;H3BR04_HUMAN;H3BMQ8_HUMAN	-2.16	1.36E-02	7.56E+00
ALDOC_HUMAN	Fructose-bisphosphate aldolase C	ALDOC_HUMAN;J3KSV6_HUMAN;J3QKP5_HUMAN;K7EKH5_HUMAN;A8MVZ9_HUMAN;C9J8F3_HUMAN;J3QKK1_HUMAN	-3.36	2.44E-03	7.96E-01	ALDOC_HUMAN	Fructose-bisphosphate aldolase C	ALDOC_HUMAN;J3KSV6_HUMAN;C9J8F3_HUMAN;J3QKK1_HUMAN;J3QKP5_HUMAN;K7EKH5_HUMAN;A8MVZ9_HUMAN	-2.61	5.32E-02	2.95E+01
ANXA1_HUMAN	Annexin A1	ANXA1_HUMAN;Q5T3N1_HUMAN;Q5T3N0_HUMAN	-0.08	5.49E-01	1.79E+02	ANXA1_HUMAN	Annexin A1	ANXA1_HUMAN;Q5T3N1_HUMAN;Q5T3N0_HUMAN	1.32	3.96E-01	2.20E+02
ANXA3_HUMAN	Annexin A3	ANXA3_HUMAN;D6RA82_HUMAN;D6RFG5_HUMAN;D6RCA8_HUMAN;D6RAZ8_HUMAN;D6RFJ9_HUMAN	-1.98	2.03E-02	6.62E+00	ANXA3_HUMAN	Annexin A3	ANXA3_HUMAN;D6RA82_HUMAN;D6RFG5_HUMAN;D6RAZ8_HUMAN;D6RCA8_HUMAN;D6RFJ9_HUMAN	-1.76	6.74E-01	3.74E+02
APEX1_HUMAN	DNA-(apurinic or apyrimidinic site) lyase	APEX1_HUMAN;G3V3M6_HUMAN;G3V5Q1_HUMAN;G3V574_HUMAN;G3V5M0_HUMAN;G3V3C7_HUMAN;G3V5D9_HUMAN;G3V359_HUMAN;H7C4A8_HUMAN	-2.30	2.21E-02	7.20E+00	APEX1_HUMAN	DNA-(apurinic or apyrimidinic site) lyase	APEX1_HUMAN;G3V3M6_HUMAN;G3V5Q1_HUMAN;G3V574_HUMAN;H7C4A8_HUMAN;G3V5M0_HUMAN;G3V3Y6_HUMAN;G3V3C7_HUMAN;G3V5D9_HUMAN;G3V359_HUMAN	-3.35	2.33E-02	1.29E+01
APT_HUMAN	Adenine phosphoribosyltransferase	APT_HUMAN;H3BQZ9_HUMAN;H3BQB1_HUMAN;H3BQF1_HUMAN;H3BSW3_HUMAN	-0.21	9.49E-01	3.09E+02	H3BQF1_HUMAN	Adenine phosphoribosyltransferase (Fragment)	APT_HUMAN;H3BSW3_HUMAN;H3BQB1_HUMAN;H3BQZ9_HUMAN;H3BQF1_HUMAN	-1.71	3.30E-01	1.83E+02
ARC1B_HUMAN	Actin-related protein 2/3 complex subunit 1B	ARC1B_HUMAN;F8WCG3_HUMAN;ARC1A_HUMAN;B4DLQ7_HUMAN;E9PF58_HUMAN;C9JQM8_HUMAN;C9J4Z7_HUMAN;C9JIT6_HUMAN;C9J6C8_HUMAN;C9JFG9_HUMAN;C9K057_HUMAN;C9JBJ7_HUMAN;C9JEY1_HUMAN	-4.48	7.16E-03	2.33E+00	ARC1B_HUMAN	Actin-related protein 2/3 complex subunit 1B	ARC1B_HUMAN;F8WCG3_HUMAN;C9JQM8_HUMAN;C9J4Z7_HUMAN;C9JIT6_HUMAN;C9J6C8_HUMAN;C9JFG9_HUMAN;C9K057_HUMAN;C9JBJ7_HUMAN;C9JEY1_HUMAN;ARC1A_HUMAN;B4DLQ7_HUMAN;E9PF58_HUMAN	-3.74	1.46E-02	8.10E+00
ARGI1_HUMAN	Arginase-1	ARGI1_HUMAN	-4.66	1.14E-03	3.71E-01	ARGI1_HUMAN	Arginase-1	ARGI1_HUMAN	-4.12	1.33E-02	7.41E+00
ARP2_HUMAN	Actin-related protein 2	ARP2_HUMAN;F5H6T1_HUMAN	-4.49	1.32E-03	4.32E-01	ARP2_HUMAN	Actin-related protein 2	ARP2_HUMAN;F5H6T1_HUMAN	-3.90	2.32E-02	1.29E+01
ARP3_HUMAN	Actin-related protein 3	ARP3_HUMAN;B4DXW1_HUMAN;F5H3P5_HUMAN;ARP3B_HUMAN;F8WEW2_HUMAN;F8WE84_HUMAN;ARP3C_HUMAN;C9IZN3_HUMAN;H7C4J1_HUMAN	-4.92	1.71E-05	5.57E-03	ARP3_HUMAN	Actin-related protein 3	ARP3_HUMAN;B4DXW1_HUMAN;F5H3P5_HUMAN;ARP3B_HUMAN;F8WEW2_HUMAN;F8WE84_HUMAN;ARP3C_HUMAN;C9IZN3_HUMAN;H7C4J1_HUMAN	-3.97	1.26E-02	6.97E+00
ARPC2_HUMAN	Actin-related protein 2/3 complex subunit 2	ARPC2_HUMAN;H7C3F9_HUMAN;G5E9J0_HUMAN;C9JTV5_HUMAN;G5E9S7_HUMAN	-4.81	2.22E-04	7.23E-02	ARPC2_HUMAN	Actin-related protein 2/3 complex subunit 2	ARPC2_HUMAN;H7C3F9_HUMAN;G5E9J0_HUMAN;G5E9S7_HUMAN;C9JTV5_HUMAN	-4.49	3.79E-02	2.10E+01
ARPC3_HUMAN	Actin-related protein 2/3 complex subunit 3	ARPC3_HUMAN;C9JZD1_HUMAN;F8VRS0_HUMAN	-5.37	7.91E-05	2.58E-02	ARPC3_HUMAN	Actin-related protein 2/3 complex subunit 3	ARPC3_HUMAN;C9JZD1_HUMAN;F8VRS0_HUMAN	-5.30	1.38E-01	7.64E+01

ARPC5_HUMAN	Actin-related protein 2/3 complex subunit 5	ARPC5_HUMAN;B1ALC0_HUMAN	-3.80	6.04E-04	1.97E-01	ARPC5_HUMAN	Actin-related protein 2/3 complex subunit 5	ARPC5_HUMAN;B1ALC0_HUMAN; ARP5L_HUMAN	-3.73	1.22E-01	6.75E+01
ASC_HUMAN	Apoptosis-associated speck-like protein containing a CARD	ASC_HUMAN;H3BP42_HUMAN	-5.13	1.94E-05	6.34E-03	ASC_HUMAN	Apoptosis-associated speck-like protein containing a CARD	ASC_HUMAN;H3BP42_HUMAN	-0.27	5.80E-01	3.22E+02
B0V0T3_HUMAN	Proteasome subunit beta type	PSB9_HUMAN;A2ACR1_HUMAN;B0V0T3_HUMAN;A2ACR0_HUMAN;B0V0T2_HUMAN	-3.52	1.44E-04	4.71E-02	A2ACR1_HUMAN	Proteasome subunit beta type	PSB9_HUMAN;A2ACR1_HUMAN;B0V0T3_HUMAN;A2ACR0_HUMAN; B0V0T2_HUMAN	-0.70	2.59E-01	1.44E+02
B0YJC4_HUMAN	Vimentin	VIME_HUMAN;B0YJC4_HUMAN;B0YJC5_HUMAN;Q5JVS8_HUMAN;PERI_HUMAN;H7C5W5_HUMAN;DESM_HUMAN;GFAP_HUMAN;K7EKH6_HUMAN;E9PAX3_HUMAN	-4.19	6.97E-04	2.27E-01	B0YJC4_HUMAN	Vimentin	PERI_HUMAN;VIME_HUMAN;B0YJC4_HUMAN;B0YJC5_HUMAN;Q5JVS8_HUMAN;H7C5W5_HUMAN;GFAP_HUMAN;K7EKH6_HUMAN;E9PAX3_HUMAN	-5.40	1.75E-01	9.71E+01
B1AHC9_HUMAN	X-ray repair cross-complementing protein 6	XRCC6_HUMAN;B1AHC9_HUMAN; B1AHC8_HUMAN;F5H1I8_HUMAN	0.56	3.14E-01	1.02E+02	B1AHC9_HUMAN	X-ray repair cross-complementing protein 6	XRCC6_HUMAN;B1AHC8_HUMAN; B1AHC9_HUMAN;F5H1I8_HUMAN	-2.75	5.75E-02	3.19E+01
B1AK88_HUMAN	Capping protein (Actin filament) muscle Z-line, beta, isoform CRA_d	CAPZB_HUMAN;B1AK87_HUMAN;B1AK88_HUMAN;B1AK85_HUMAN;F6USW4_HUMAN;F6Q0E3_HUMAN	-5.20	2.60E-03	8.46E-01	B1AK88_HUMAN	Capping protein (Actin filament) muscle Z-line, beta, isoform CRA_d	CAPZB_HUMAN;B1AK87_HUMAN; B1AK85_HUMAN;B1AK88_HUMAN;F6USW4_HUMAN;F6Q0E3_HUMAN	-5.03	2.90E-03	1.61E+00
B3AT_HUMAN	Band 3 anion transport protein	B3AT_HUMAN	1.94	1.20E-02	3.90E+00	B3AT_HUMAN	Band 3 anion transport protein	B3AT_HUMAN	3.93	1.38E-01	7.66E+01
B4DJP7_HUMAN	Small nuclear ribonucleoprotein Sm D3	SMD3_HUMAN;B4DJP7_HUMAN;H3BT13_HUMAN	-3.26	2.59E-06	8.44E-04	B4DJP7_HUMAN	Small nuclear ribonucleoprotein Sm D3	SMD3_HUMAN;B4DJP7_HUMAN; H3BT13_HUMAN	-0.98	2.23E-01	1.24E+02
B4DQJ8_HUMAN	6-phosphogluconate dehydrogenase, decarboxylating	6PGD_HUMAN;B4DQJ8_HUMAN;F5H7U0_HUMAN;K7EPF6_HUMAN;K7EMN2_HUMAN;K7EM49_HUMAN; K7ELN9_HUMAN	-3.98	1.18E-04	3.84E-02	B4DQJ8_HUMAN	6-phosphogluconate dehydrogenase, decarboxylating	6PGD_HUMAN;B4DQJ8_HUMAN;F5H7U0_HUMAN;K7EPF6_HUMAN; K7EMN2_HUMAN;K7EM49_HUMAN;K7ELN9_HUMAN	-2.99	1.29E-02	7.16E+00
B4DTG2_HUMAN	Elongation factor 1-gamma	EF1G_HUMAN;B4DTG2_HUMAN;E7EMT2_HUMAN	-4.25	5.40E-04	1.76E-01	B4DTG2_HUMAN	Elongation factor 1-gamma	EF1G_HUMAN;B4DTG2_HUMAN;E7EMT2_HUMAN	-2.61	1.43E-02	7.94E+00
B4DU58_HUMAN	Macrophage-capping protein	CAPG_HUMAN;E7ENU9_HUMAN;B4DU58_HUMAN;B8ZZL6_HUMAN;H7C0X8_HUMAN	-4.47	5.64E-04	1.84E-01	CAPG_HUMAN	Macrophage-capping protein	CAPG_HUMAN;B4DU58_HUMAN; H7C0X8_HUMAN;E7ENU9_HUMAN;B8ZZL6_HUMAN	-2.93	1.12E-02	6.22E+00
B4DVE7_HUMAN	Annexin	ANX11_HUMAN;B4DVE7_HUMAN; H0Y6E1_HUMAN	-4.18	2.14E-03	6.99E-01	B4DVE7_HUMAN	Annexin	ANX11_HUMAN;B4DVE7_HUMAN; H0Y6E1_HUMAN	-1.43	4.02E-01	2.23E+02
B4E0K5_HUMAN	Mitogen-activated protein kinase 14	MK14_HUMAN;B4E0K5_HUMAN;B5TY33_HUMAN;E7EX54_HUMAN;H7C4E2_HUMAN	-3.15	6.45E-02	2.10E+01	B4E0K5_HUMAN	Mitogen-activated protein kinase 14	MK14_HUMAN;B4E0K5_HUMAN;E7EX54_HUMAN;B5TY33_HUMAN	-4.69	2.56E-01	1.42E+02
B4E2V5_HUMAN	Erythrocyte band 7 integral membrane protein	STOM_HUMAN;B4E2V5_HUMAN	0.11	5.30E-01	1.73E+02	B4E2V5_HUMAN	Erythrocyte band 7 integral membrane protein	STOM_HUMAN;B4E2V5_HUMAN	2.91	1.61E-01	8.92E+01
B4E3K9_HUMAN	Superoxide dismutase	SODM_HUMAN;B3KUK2_HUMAN;B4E3K9_HUMAN;G5E9P6_HUMAN;F5GXZ9_HUMAN;G8JLJ2_HUMAN;F5GYZ5_HUMAN;F5H4R2_HUMAN;F5H3C5_HUMAN	-1.74	1.71E-02	5.56E+00	B4E3K9_HUMAN	Superoxide dismutase	SODM_HUMAN;B3KUK2_HUMAN;B4E3K9_HUMAN;F5GYZ5_HUMAN;F5H4R2_HUMAN;F5H3C5_HUMAN;G5E9P6_HUMAN;F5GXZ9_HUMAN;G8JLJ2_HUMAN	-1.54	3.02E-01	1.68E+02
B4E3P0_HUMAN	ATP-citrate synthase	ACLY_HUMAN;B4E3P0_HUMAN	-0.04	9.86E-01	3.21E+02	ACLY_HUMAN	ATP-citrate synthase	ACLY_HUMAN;B4E3P0_HUMAN;K7ESG8_HUMAN;K7EIE7_HUMAN	-2.05	9.04E-02	5.01E+01
B7Z3I9_HUMAN	Delta-aminolevulinic acid dehydratase	HEM2_HUMAN;B7Z3I9_HUMAN;B7ZBK6_HUMAN	-2.36	6.75E-04	2.20E-01	B7Z3I9_HUMAN	Delta-aminolevulinic acid dehydratase	HEM2_HUMAN;B7Z3I9_HUMAN;B7ZBK6_HUMAN	-2.46	1.59E-01	8.82E+01
B7Z7E9_HUMAN	Aspartate aminotransferase	AATC_HUMAN;B7Z7E9_HUMAN	-5.06	9.24E-04	3.01E-01	AATC_HUMAN	Aspartate aminotransferase, cytoplasmic	AATC_HUMAN;B7Z7E9_HUMAN	-3.84	9.76E-04	5.42E-01
B7Z9G5_HUMAN	BRO1 domain-containing protein BROX	BROX_HUMAN;B7Z9G5_HUMAN;Q5VW33_HUMAN;F5GXQ0_HUMAN	-0.67	6.99E-01	2.28E+02	B7Z9G5_HUMAN	BRO1 domain-containing protein BROX	BROX_HUMAN;B7Z9G5_HUMAN;F5GXQ0_HUMAN;Q5VW33_HUMAN	-4.14	7.06E-02	3.92E+01
B8ZZK2_HUMAN	Gamma-glutamylcyclotransferase	GGCT_HUMAN;B8ZZR8_HUMAN;B8ZZN4_HUMAN;B8ZZK2_HUMAN;H7BZK5_HUMAN	-0.20	4.99E-01	1.63E+02	GGCT_HUMAN	Gamma-glutamylcyclotransferase	GGCT_HUMAN;B8ZZR8_HUMAN;B8ZZK2_HUMAN;M0QZK8_HUMAN;B8ZZN4_HUMAN;H7BZK5_HUMAN	-3.39	1.28E-01	7.08E+01
BASP1_HUMAN	Brain acid soluble protein 1	BASP1_HUMAN	-3.96	4.26E-02	1.39E+01	BASP1_HUMAN	Brain acid soluble protein 1	BASP1_HUMAN	-4.06	7.95E-02	4.41E+01
BPI_HUMAN	Bactericidal permeability-increasing protein	BPI_HUMAN;H0Y738_HUMAN	0.00	8.48E-01	2.77E+02	BPI_HUMAN	Bactericidal permeability-increasing protein	BPI_HUMAN;H0Y738_HUMAN	0.77	8.57E-01	4.76E+02
C9J592_HUMAN	Ras-related protein Rab-7a (Fragment)	RAB7A_HUMAN;C9J592_HUMAN;C9J8S3_HUMAN;C9IZZ0_HUMAN;FR1L6_HUMAN;OTOF_HUMAN;C9J7D1_HUMAN;C9J4V0_HUMAN;C9J4S4_HUMAN	-5.35	4.72E-03	1.54E+00	RAB7A_HUMAN	Ras-related protein Rab-7a	RAB7A_HUMAN;C9J7D1_HUMAN;C9J4V0_HUMAN;C9J4S4_HUMAN;C9J592_HUMAN;C9J8S3_HUMAN;C9IZZ0_HUMAN;FR1L6_HUMAN;OTOF_HUMAN	-6.99	6.00E-03	3.33E+00
C9JC60_HUMAN	Nicotinate phosphoribosyltransferase	PNCB_HUMAN;G5E977_HUMAN;C9J8U2_HUMAN;C9JC60_HUMAN;H0YF31_HUMAN;H0YDA6_HUMAN	-4.18	1.77E-04	5.77E-02	PNCB_HUMAN	Nicotinate phosphoribosyltransferase	PNCB_HUMAN;G5E977_HUMAN;C9JC60_HUMAN;C9J8U2_HUMAN; H0YDA6_HUMAN;H0YF31_HUMAN	-3.70	1.98E-02	1.10E+01
C9JIF9_HUMAN	Acylamino-acid-releasing enzyme	ACPH_HUMAN;H7C1U0_HUMAN;H0YFE5_HUMAN;C9JIF9_HUMAN;C9JLK2_HUMAN;H7C393_HUMAN	-3.82	1.40E-02	4.58E+00	C9JIF9_HUMAN	Acylamino-acid-releasing enzyme	ACPH_HUMAN;C9JLK2_HUMAN;H7C1U0_HUMAN;H7C393_HUMAN; C9JIF9_HUMAN;H0YFE5_HUMAN; F8WEH5_HUMAN	-2.54	2.44E-03	1.36E+00
C9JIS1_HUMAN	Guanine nucleotide-binding protein G(I)/G(S)/G(T) subunit beta-2 (Fragment)	GBB1_HUMAN;GBB2_HUMAN;GBB3_HUMAN;GBB4_HUMAN;E7EP32_HUMAN;C9JZN1_HUMAN;B1AKQ8_HUMAN;C9JXA5_HUMAN;F6X3N5_HUMAN;F5H8J8_HUMAN;F5H100_HUMAN;E9PCP0_HUMAN;F5H0S8_HUMAN;C9JD14_HUMAN;F6UT28_HUMAN;C9JIS1_HUMAN	-2.85	1.68E-01	5.49E+01	GBB1_HUMAN	Guanine nucleotide-binding protein G(I)/G(S)/G(T) subunit beta-1	GBB1_HUMAN;B3KVK2_HUMAN;F6X3N5_HUMAN;F6UT28_HUMAN	0.61	8.77E-01	4.86E+02
						C9JIS1_HUMAN	Guanine nucleotide-binding protein G(I)/G(S)/G(T) subunit beta-2 (Fragment)	GBB2_HUMAN;GBB4_HUMAN;B3KPU1_HUMAN;E7EP32_HUMAN;C9JZN1_HUMAN;C9JXA5_HUMAN;H7C5J5_HUMAN;C9JIS1_HUMAN	-3.81	1.20E-03	6.63E-01
CAH1_HUMAN	Carbonic anhydrase 1	CAH1_HUMAN;E5RG43_HUMAN;E5RGU8_HUMAN;H0YBE2_HUMAN;E5RIF9_HUMAN;E5RFL2_HUMAN;E5RFE7_HUMAN;E5RHP7_HUMAN;E5RH81_HUMAN;E5RJI8_HUMAN;E5RG81_HUMAN;E5RJF6_HUMAN;E5RII2_HUMAN	-1.41	1.51E-02	4.94E+00	CAH1_HUMAN	Carbonic anhydrase 1	CAH1_HUMAN;H0YBE2_HUMAN;E5RJI8_HUMAN;E5RFE7_HUMAN;E5RHP7_HUMAN;E5RH81_HUMAN;E5RJF6_HUMAN;E5RG43_HUMAN;E5RGU8_HUMAN;E5RIF9_HUMAN;E5RFL2_HUMAN;E5RII2_HUMAN;E5RG81_HUMAN	-2.20	2.58E-01	1.43E+02
CAH2_HUMAN	Carbonic anhydrase 2	CAH2_HUMAN;E5RID5_HUMAN;E5RK37_HUMAN	-1.41	2.49E-02	8.10E+00	CAH2_HUMAN	Carbonic anhydrase 2	CAH2_HUMAN;E5RID5_HUMAN;E5RK37_HUMAN	-2.54	1.24E-01	6.85E+01
CALR_HUMAN	Calreticulin	CALR_HUMAN	-3.78	1.60E-05	5.23E-03	CALR_HUMAN	Calreticulin	CALR_HUMAN;K7EJB9_HUMAN	-2.44	3.24E-03	1.80E+00
CAN1_HUMAN	Calpain-1 catalytic subunit	CAN1_HUMAN;E9PRM1_HUMAN;E9PL37_HUMAN	-4.61	7.61E-05	2.48E-02	CAN1_HUMAN	Calpain-1 catalytic subunit	CAN1_HUMAN;E9PJA6_HUMAN;E9PLC9_HUMAN;E9PLQ6_HUMAN;E9PRM1_HUMAN;E9PIA9_HUMAN;E9PLX0_HUMAN;E9PQB3_HUMAN;E9PSA6_HUMAN;E9PJJ3_HUMAN;E9PMC6_HUMAN;E9PL37_HUMAN	-3.90	4.24E-04	2.35E-01
CAP1_HUMAN	Adenylyl cyclase-associated protein 1	CAP1_HUMAN;Q5T0R4_HUMAN;Q5T0R3_HUMAN;Q5T0R9_HUMAN;Q5T0R2_HUMAN;Q5T0R7_HUMAN;Q5T0R6_HUMAN;Q5T0R1_HUMAN;Q5T0R5_HUMAN;Q5T0S3_HUMAN	-4.22	2.28E-05	7.42E-03	CAP1_HUMAN	Adenylyl cyclase-associated protein 1	CAP1_HUMAN;Q5T0R4_HUMAN;Q5T0R3_HUMAN;Q5T0R2_HUMAN;Q5T0R7_HUMAN;Q5T0R6_HUMAN;Q5T0R1_HUMAN;Q5T0R5_HUMAN;CAP2_HUMAN;B7Z1C4_HUMAN;B7Z214_HUMAN;B7Z385_HUMAN;E9PDI2_HUMAN;Q5T0S3_HUMAN	-2.71	1.89E-02	1.05E+01
CAP7_HUMAN	Azurocidin	CAP7_HUMAN;REVERSED_F86B1_HUMAN;REVERSED_F86B2_HUMAN;REVERSED_E9PLC7_HUMAN;REVERSED_E9PLW5_HUMAN;REVERSED_E9PN63_HUMAN;REVERSED_E9PRJ7_HUMAN;REVERSED_H0YDM8_HUMAN;REVERSED_H7BXI9_HUMAN;REVERSED_E9PM45_HUMAN;REVERSED_E9PQV7_HUMAN;REVERSED_E9PNH4_HUMAN;REVERSED_E9PPT9_HUMAN;REVERSED_H0YD24_HUMAN;REVERSED_E9PJ39_HUMAN	5.35	2.19E-05	7.15E-03	CAP7_HUMAN	Azurocidin	CAP7_HUMAN	6.37	2.84E-03	1.58E+00
CATA_HUMAN	Catalase	CATA_HUMAN	-4.26	2.09E-05	6.82E-03	CATA_HUMAN	Catalase	CATA_HUMAN	-4.00	1.78E-03	9.89E-01
CATG_HUMAN	Cathepsin G	CATG_HUMAN	5.55	2.69E-07	8.77E-05	CATG_HUMAN	Cathepsin G	CATG_HUMAN	5.86	2.50E-03	1.39E+00
CAZA1_HUMAN	F-actin-capping protein subunit alpha-1	CAZA1_HUMAN;CAZA2_HUMAN;B4DG50_HUMAN;C9JUG7_HUMAN;F8W9N7_HUMAN	-5.18	4.54E-03	1.48E+00	CAZA1_HUMAN	F-actin-capping protein subunit alpha-1	CAZA1_HUMAN	-3.01	1.56E-02	8.68E+00
					1.48E+00	CAZA2_HUMAN	F-actin-capping protein subunit alpha-2	CAZA2_HUMAN;B4DG50_HUMAN;C9JUG7_HUMAN;F8W9N7_HUMAN	-1.77	7.68E-02	4.26E+01
CDC42_HUMAN	Cell division control protein 42 homolog	CDC42_HUMAN;E7ETU3_HUMAN	-0.73	8.32E-02	2.71E+01	CDC42_HUMAN	Cell division control protein 42 homolog	CDC42_HUMAN;E7ETU3_HUMAN;Q5JYX0_HUMAN	-0.62	7.90E-01	4.39E+02
CDD_HUMAN	Cytidine deaminase	CDD_HUMAN	-5.59	5.58E-03	1.82E+00	CDD_HUMAN	Cytidine deaminase	CDD_HUMAN	-6.18	2.52E-03	1.40E+00

CEAM8_HUMAN	Carcinoembryonic antigen-related cell adhesion molecule 8	CEAM1_HUMAN;CEAM5_HUMAN;CEAM8_HUMAN;H9KVA7_HUMAN;E7EUB1_HUMAN	-1.84	6.62E-03	2.16E+00	CEAM8_HUMAN	Carcinoembryonic antigen-related cell adhesion molecule 8	CEAM8_HUMAN;CEAM1_HUMAN;CEAM5_HUMAN;H9KVA7_HUMAN;E7EUB1_HUMAN	-1.45	2.11E-01	1.17E+02
CH3L1_HUMAN	Chitinase-3-like protein 1	CH3L1_HUMAN;H0Y3U8_HUMAN;ZN423_HUMAN;F5H7S1_HUMAN	-2.90	9.32E-03	3.04E+00	CH3L1_HUMAN	Chitinase-3-like protein 1	CH3L1_HUMAN;H0Y3U8_HUMAN	-5.73	7.95E-04	4.41E-01
CLH1_HUMAN	Clathrin heavy chain 1	CLH1_HUMAN;J3KS13_HUMAN;J3KRF5_HUMAN;K7EJJ5_HUMAN;CLH2_HUMAN;J3KR87_HUMAN;J3KSQ2_HUMAN;J3QL20_HUMAN	-3.22	4.25E-04	1.38E-01	CLH1_HUMAN	Clathrin heavy chain 1	CLH1_HUMAN;J3KS13_HUMAN;J3KRF5_HUMAN;K7EJJ5_HUMAN;CLH2_HUMAN;J3KR87_HUMAN;J3KSQ2_HUMAN;F5H5N6_HUMAN	-2.43	4.21E-02	2.34E+01
CLIC1_HUMAN	Chloride intracellular channel protein 1	CLIC1_HUMAN;CLIC2_HUMAN;CLIC4_HUMAN;CLIC5_HUMAN;A6PVS0_HUMAN	-3.82	1.12E-02	3.64E+00	CLIC1_HUMAN	Chloride intracellular channel protein 1	CLIC1_HUMAN;CLIC2_HUMAN;CLIC4_HUMAN;CLIC5_HUMAN;A6PVS0_HUMAN	-3.38	4.59E-02	2.55E+01
COR1A_HUMAN	Coronin-1A	COR1A_HUMAN;H3BRY3_HUMAN;DDX46_HUMAN;D6RJA6_HUMAN;H3BTU6_HUMAN;H3BNA2_HUMAN;H3BU76_HUMAN;H3BSL1_HUMAN;H3BRJ0_HUMAN	-3.51	1.94E-03	6.33E-01	COR1A_HUMAN	Coronin-1A	COR1A_HUMAN;H3BRY3_HUMAN;H3BTU6_HUMAN;H3BRJ0_HUMAN;DDX46_HUMAN;D6RJA6_HUMAN;H3BNA2_HUMAN;H3BU76_HUMAN;H3BSL1_HUMAN	-2.44	4.45E-02	2.47E+01
COTL1_HUMAN	Coactosin-like protein	COTL1_HUMAN;H3BT58_HUMAN	-4.91	5.36E-03	1.75E+00	COTL1_HUMAN	Coactosin-like protein	COTL1_HUMAN;H3BT58_HUMAN	-4.45	3.15E-02	1.75E+01
CPNE3_HUMAN	Copine-3	CPNE3_HUMAN;CPNE2_HUMAN;CPNE4_HUMAN;CPNE5_HUMAN;CPNE6_HUMAN;CPNE7_HUMAN;CPNE8_HUMAN;CPNE9_HUMAN;Q86VY2_HUMAN;Q719H8_HUMAN;Q7Z6C8_HUMAN;E7ENV7_HUMAN;F5GXN1_HUMAN	-1.64	1.04E-02	3.38E+00	CPNE3_HUMAN	Copine-3	CPNE3_HUMAN;CPNE2_HUMAN;CPNE4_HUMAN;CPNE5_HUMAN;CPNE6_HUMAN;CPNE7_HUMAN;CPNE8_HUMAN;CPNE9_HUMAN;Q86VY2_HUMAN;Q719H8_HUMAN;Q7Z6C8_HUMAN;E7ENV7_HUMAN;F5GXN1_HUMAN	-3.71	1.19E-01	6.60E+01
CPPED_HUMAN	Calcineurin-like phosphoesterase domain-containing protein 1	CPPED_HUMAN;B4DQ68_HUMAN	-3.25	8.90E-03	2.90E+00	CPPED_HUMAN	Calcineurin-like phosphoesterase domain-containing protein 1	CPPED_HUMAN;B4DQ68_HUMAN	-4.82	1.64E-03	9.08E-01
D6R9A6_HUMAN	High mobility group protein B2 (Fragment)	HMGB2_HUMAN;D6R9A6_HUMAN	-3.84	6.16E-03	2.01E+00	HMGB2_HUMAN	High mobility group protein B2	HMGB2_HUMAN;D6R9A6_HUMAN	-0.32	5.54E-01	3.08E+02
D6RAU8_HUMAN	Calnexin (Fragment)	CALX_HUMAN;B4DGP8_HUMAN;D6RB85_HUMAN;D6RHJ3_HUMAN;D6RAQ8_HUMAN;D6RDP7_HUMAN;D6RD16_HUMAN;H0Y9Q7_HUMAN;D6RAU8_HUMAN	-0.51	9.74E-01	3.18E+02	B4DGP8_HUMAN	Calnexin	CALX_HUMAN;B4DGP8_HUMAN;D6RB85_HUMAN;D6RAQ8_HUMAN;D6RDP7_HUMAN;H0Y9Q7_HUMAN;D6RAU8_HUMAN;B4E2T8_HUMAN	-3.42	3.11E-02	1.73E+01
D6REY1_HUMAN	Chitotriosidase-1	CHIT1_HUMAN;G5EAS1_HUMAN;D6REY1_HUMAN	-5.23	1.97E-04	6.42E-02	CHIT1_HUMAN	Chitotriosidase-1	CHIT1_HUMAN;G5EAS1_HUMAN;D6REY1_HUMAN	-6.82	1.42E-02	7.90E+00
D6RFM0_HUMAN	Ubiquitin-conjugating enzyme E2 D2 (Fragment)	UB2D2_HUMAN;UB2D3_HUMAN;D6RAH7_HUMAN;H9KV45_HUMAN;D6RFM0_HUMAN;D6RAW0_HUMAN;D6RA11_HUMAN;D6RIZ3_HUMAN	-4.64	1.17E-04	3.80E-02	UB2D3_HUMAN	Ubiquitin-conjugating enzyme E2 D3	UB2D2_HUMAN;UB2D3_HUMAN;D6RAH7_HUMAN;D6RA11_HUMAN;D6RIZ3_HUMAN;H9KV45_HUMAN;D6RAW0_HUMAN;D6RFM0_HUMAN;D6R933_HUMAN;D6R9F6_HUMAN;D6R980_HUMAN;D6RGD0_HUMAN	-4.77	2.58E-03	1.43E+00
DEF3_HUMAN	Neutrophil defensin 3	DEF1_HUMAN;DEF3_HUMAN	-2.10	1.06E-03	3.44E-01	DEF1_HUMAN	Neutrophil defensin 1	DEF1_HUMAN;DEF3_HUMAN	-1.81	6.21E-01	3.45E+02
E5RK69_HUMAN	Annexin	ANXA6_HUMAN;A6NN80_HUMAN;E5RK69_HUMAN;E7EMC6_HUMAN;E5RJF5_HUMAN;E5RIU8_HUMAN;E5RFF0_HUMAN;E5RIO5_HUMAN;E5RK63_HUMAN;E5RJR0_HUMAN	-2.84	5.15E-02	1.68E+01	E5RK69_HUMAN	Annexin	ANXA6_HUMAN;A6NN80_HUMAN;E7EMC6_HUMAN;E5RK69_HUMAN;E5RJF5_HUMAN;E5RIU8_HUMAN;E5RFF0_HUMAN;E5RIO5_HUMAN;E5RK63_HUMAN;E5RJR0_HUMAN	-0.13	8.20E-01	4.55E+02
E7EMB3_HUMAN	Calmodulin	CALM_HUMAN;M0QZ52_HUMAN;H0Y7A7_HUMAN;G3V479_HUMAN;E7ETZ0_HUMAN;E7EMB3_HUMAN;F8WBR5_HUMAN;Q96HY3_HUMAN;G3V361_HUMAN;G3V226_HUMAN	-1.21	6.55E-01	2.13E+02	E7EMB3_HUMAN	Calmodulin	CALL3_HUMAN;CALM_HUMAN;TNNC2_HUMAN;M0QZ52_HUMAN;C9J7T9_HUMAN;H0Y7A7_HUMAN;G3V479_HUMAN;E7ETZ0_HUMAN;E7EMB3_HUMAN;F8WBR5_HUMAN;Q96HY3_HUMAN;G3V361_HUMAN	4.43	3.94E-01	2.18E+02
E7EMG9_HUMAN	Lymphocyte-specific protein 1 (Fragment)	LSP1_HUMAN;C9JDV1_HUMAN;C9JU59_HUMAN;E7EMG9_HUMAN;E9PBD8_HUMAN;C9JKF7_HUMAN;C9J9B9_HUMAN;C9JNQ1_HUMAN	-6.38	7.40E-03	2.41E+00	E7EMG9_HUMAN	Lymphocyte-specific protein 1 (Fragment)	LSP1_HUMAN;C9JDV1_HUMAN;C9JU59_HUMAN;E7EMG9_HUMAN;E9PBD8_HUMAN;C9JKF7_HUMAN	-0.37	2.28E-01	1.27E+02
E7ENQ5_HUMAN	Annexin	ANXA5_HUMAN;E9PHT9_HUMAN;E7ENQ5_HUMAN;D6RBL5_HUMAN;D6RBE9_HUMAN	-2.51	4.97E-01	1.62E+02	ANXA5_HUMAN	Annexin A5	ANXA5_HUMAN;E9PHT9_HUMAN;E7ENQ5_HUMAN;D6RBL5_HUMAN;D6RBE9_HUMAN;D6RCN3_HUMAN	0.67	7.14E-01	3.96E+02
E7ERI3_HUMAN	Threonine--tRNA ligase, cytoplasmic	SYTC_HUMAN;G3XAN9_HUMAN;E7ERI3_HUMAN	5.47	1.45E-01	4.73E+01	E7ERI3_HUMAN	Threonine--tRNA ligase, cytoplasmic	SYTC_HUMAN;G3XAN9_HUMAN;E7ERI3_HUMAN	-1.89	1.35E-01	7.48E+01
E7ERL0_HUMAN	Nucleoside diphosphate kinase A	NDKA_HUMAN;NDKB_HUMAN;E5RHP0_HUMAN;Q32Q12_HUMAN;J3KPD9_HUMAN;C9K028_HUMAN;E7ERL0_HUMAN	-6.45	4.14E-03	1.35E+00	Q32Q12_HUMAN	Nucleoside diphosphate kinase	NDKB_HUMAN;F6XY72_HUMAN;Q32Q12_HUMAN;NDK8_HUMAN	-3.42	3.18E-02	1.76E+01
E7EU23_HUMAN	Rab GDP dissociation inhibitor beta	GDIB_HUMAN;Q5SX90_HUMAN;Q5SX86_HUMAN;E7EU23_HUMAN;Q5SX87_HUMAN;Q5SX91_HUMAN	-4.97	2.90E-03	9.45E-01	E7EU23_HUMAN	Rab GDP dissociation inhibitor beta	GDIB_HUMAN;E7EU23_HUMAN;Q5SX90_HUMAN;Q5SX86_HUMAN;Q5SX87_HUMAN;Q5SX91_HUMAN	-5.03	2.48E-03	1.38E+00
E7EUC7_HUMAN	UTP--glucose-1-phosphate uridylyltransferase	UGPA_HUMAN;E7EUC7_HUMAN;C9JNZ1_HUMAN;C9JQU9_HUMAN;C9JVG3_HUMAN;C9JUW1_HUMAN;C9JWG0_HUMAN;C9JTZ5_HUMAN	-2.04	1.70E-03	5.54E-01	E7EUC7_HUMAN	UTP--glucose-1-phosphate uridylyltransferase	UGPA_HUMAN;C9JQU9_HUMAN;F2Z3H1_HUMAN;C9JVG3_HUMAN;E7EUC7_HUMAN;C9JUW1_HUMAN;C9JWG0_HUMAN;C9JNZ1_HUMAN;C9JTZ5_HUMAN	-3.03	2.88E-02	1.60E+01
E9PCY7_HUMAN	Heterogeneous nuclear ribonucleoprotein H	HNRH1_HUMAN;HNRPF_HUMAN;G8JLB6_HUMAN;H0YBD7_HUMAN;F5GZT4_HUMAN;E9PCY7_HUMAN;H0YB39_HUMAN;H0YBG7_HUMAN;HNRH2_HUMAN;E5RGV0_HUMAN;H0YAQ2_HUMAN;D6R9T0_HUMAN;D6RIU0_HUMAN;E7EQJ0_HUMAN;D6RBM0_HUMAN;D6RJ04_HUMAN;D6RIH9_HUMAN;E5RGH4_HUMAN;D6RAM1_HUMAN;D6RFM3_HUMAN;D6RIT2_HUMAN;D6RDU3_HUMAN	-4.80	6.36E-04	2.07E-01	E9PCY7_HUMAN	Heterogeneous nuclear ribonucleoprotein H	HNRH1_HUMAN;HNRH2_HUMAN;G8JLB6_HUMAN;E5RGV0_HUMAN;H0YAQ2_HUMAN;D6R9T0_HUMAN;D6RIU0_HUMAN;E7EQJ0_HUMAN;E9PCY7_HUMAN;D6RBM0_HUMAN;D6RJ04_HUMAN;D6RIH9_HUMAN;E5RGH4_HUMAN;D6RAM1_HUMAN;D6RFM3_HUMAN;D6RIT2_HUMAN;D6RDU3_HUMAN;E7EN40_HUMAN;H0YB39_HUMAN	-3.96	1.37E-02	7.61E+00
E9PDB2_HUMAN	Malate dehydrogenase, mitochondrial	MDHM_HUMAN;G3XAL0_HUMAN;E9PDB2_HUMAN	-2.30	2.20E-03	7.16E-01	MDHM_HUMAN	Malate dehydrogenase, mitochondrial	MDHM_HUMAN;E9PDB2_HUMAN;G3XAL0_HUMAN	-1.24	1.65E-01	9.14E+01
E9PK25_HUMAN	Cofilin-1	COF1_HUMAN;G3V1A4_HUMAN;E9PLJ3_HUMAN;E9PP50_HUMAN;E9PK25_HUMAN;E9PS23_HUMAN;E9PQB7_HUMAN;COF2_HUMAN;G3V5P4_HUMAN;F8WDN3_HUMAN;G3V2U0_HUMAN;DEST_HUMAN;F6RFD5_HUMAN	-4.40	1.81E-05	5.89E-03	E9PK25_HUMAN	Cofilin-1	COF1_HUMAN;G3V1A4_HUMAN;E9PLJ3_HUMAN;E9PP50_HUMAN;E9PK25_HUMAN;E9PS23_HUMAN;E9PQB7_HUMAN;COF2_HUMAN;G3V5P4_HUMAN;F8WDN3_HUMAN;G3V2U0_HUMAN;DEST_HUMAN;F6RFD5_HUMAN	-3.18	3.88E-02	2.15E+01
E9PLD0_HUMAN	Ras-related protein Rab-1B	RAB1A_HUMAN;RAB1B_HUMAN;RAB1C_HUMAN;B7Z8M7_HUMAN;E7END7_HUMAN;E9PLD0_HUMAN;RAB8A_HUMAN;RAB8B_HUMAN;B4DEK7_HUMAN;H0YNE9_HUMAN;F5GY21_HUMAN;H0YMN7_HUMAN;E7E	-4.81	4.24E-03	1.38E+00	E9PLD0_HUMAN	Ras-related protein Rab-1B	RAB1B_HUMAN;RAB1C_HUMAN;E9PLD0_HUMAN	-3.92	5.74E-02	3.18E+01
						RAB8A_HUMAN	Ras-related protein Rab-8A	RAB8A_HUMAN;B4DEK7_HUMAN	-4.18	1.46E-02	8.10E+00
						H0YNE9_HUMAN	Ras-related protein Rab-8B (Fragment)	RAB8B_HUMAN;H0YNE9_HUMAN;F5GY21_HUMAN	-1.75	5.72E-01	3.18E+02
ECP_HUMAN	Eosinophil cationic protein	ECP_HUMAN	1.29	5.44E-02	1.77E+01	ECP_HUMAN	Eosinophil cationic protein	ECP_HUMAN	2.18	1.19E-02	6.61E+00
EF2_HUMAN	Elongation factor 2	EF2_HUMAN	-2.55	5.99E-04	1.95E-01	EF2_HUMAN	Elongation factor 2	EF2_HUMAN;U5S1_HUMAN;K7EJ74_HUMAN;K7EJ81_HUMAN;K7EP67_HUMAN	-2.89	1.01E-02	5.58E+00
EFHD2_HUMAN	EF-hand domain-containing protein D2	EFHD2_HUMAN;H0Y4Y4_HUMAN	-6.50	4.79E-04	1.56E-01	EFHD2_HUMAN	EF-hand domain-containing protein D2	EFHD2_HUMAN;H0Y4Y4_HUMAN;EFHD1_HUMAN;Q8WYH2_HUMAN;C9JTV4_HUMAN	-5.92	6.53E-02	3.62E+01
ELNE_HUMAN	Neutrophil elastase	ELNE_HUMAN	2.99	5.18E-04	1.69E-01	ELNE_HUMAN	Neutrophil elastase	ELNE_HUMAN	4.51	2.70E-03	1.50E+00
ENOA_HUMAN	Alpha-enolase	ENOA_HUMAN;K7EM90_HUMAN;K7EN23_HUMAN;K7EQF3_HUMAN;K7ERS8_HUMAN	-4.22	1.03E-04	3.35E-02	ENOA_HUMAN	Alpha-enolase	ENOA_HUMAN;K7EM90_HUMAN;K7EN23_HUMAN;K7EQF3_HUMAN;K7ERS8_HUMAN	-2.88	1.27E-02	7.06E+00
F2Z2Y4_HUMAN	Pyridoxal kinase	PDXK_HUMAN;F2Z2Y4_HUMAN	-3.34	3.15E-04	1.03E-01	PDXK_HUMAN	Pyridoxal kinase	PDXK_HUMAN;F2Z2Y4_HUMAN;A8MV33_HUMAN	-2.56	1.01E-01	5.58E+01

F5GXR5_HUMAN	NAD kinase	NADK_HUMAN;Q5QPS4_HUMAN;Q5QPS5_HUMAN;J3KSP9_HUMAN;F5GXR5_HUMAN;J3KTI3_HUMAN	-3.01	4.99E-04	1.63E-01	F5GXR5_HUMAN	NAD kinase	NADK_HUMAN;Q5QPS4_HUMAN;F5GXR5_HUMAN;REVERSED_ABCA4_HUMAN;Q5QPS5_HUMAN;REVERSED_F5H6E5_HUMAN;J3KSP9_HUMAN;J3KTI3_HUMAN	-4.43	4.02E-03	2.23E+00
F5H1A8_HUMAN	Gelsolin	GELS_HUMAN;Q5T0H8_HUMAN;Q5T0H7_HUMAN;F5H1A8_HUMAN;Q5T0H9_HUMAN	-4.18	2.54E-03	8.27E-01	F5H1A8_HUMAN	Gelsolin	GELS_HUMAN;Q5T0H8_HUMAN;Q5T0H7_HUMAN;F5H1A8_HUMAN	-3.06	3.22E-03	1.79E+00
F5H1J5_HUMAN	Septin-6	SEPT6_HUMAN;B1AMS2_HUMAN;B4E049_HUMAN;F5H1J5_HUMAN;SEP11_HUMAN;SEPT8_HUMAN;D6RGI3_HUMAN;C9JV02_HUMAN;A6NMH6_HUMAN;F8W8I8_HUMAN;A6NFQ9_HUMAN;D6RER5_HUMAN;D6RDU5_HUMAN;F6W7K9_HUMAN	-0.07	7.24E-01	2.36E+02	D6RDU5_HUMAN	Septin-11 (Fragment)	SEP11_HUMAN;SEPT6_HUMAN;SEPT8_HUMAN;D6RGI3_HUMAN;B1AMS2_HUMAN;B4E049_HUMAN;C9JV02_HUMAN;A6NMH6_HUMAN;F8W8I8_HUMAN;A6NFQ9_HUMAN;D6RER5_HUMAN;F5H1J5_HUMAN;D6RDU5_HUMAN;F6W7K9_HUMAN;D6R9Y6_HUMAN;D6RDP1_HUMAN	-1.11	1.69E-01	9.40E+01
F5H6I0_HUMAN	Beta-2-microglobulin form pI 5.3	B2MG_HUMAN;F5H6I0_HUMAN;H0YLF3_HUMAN	-4.31	6.40E-07	2.09E-04	F5H6I0_HUMAN	Beta-2-microglobulin form pI 5.3	B2MG_HUMAN;F5H6I0_HUMAN;H0YLF3_HUMAN	-3.65	1.37E-02	7.62E+00
F5H6Q2_HUMAN	Polyubiquitin-C (Fragment)	RL40_HUMAN;RS27A_HUMAN;UBB_HUMAN;UBC_HUMAN;B4DV12_HUMAN;F5H041_HUMAN;Q96C32_HUMAN;F5GXK7_HUMAN;J3QS39_HUMAN;M0R1V7_HUMAN;J3QKN0_HUMAN;F5GYU3_HUMAN;M0R1M6_HUMAN;F5H7Y5_HUMAN;F5H7K6_HUMAN;F5H4D8_HUMAN;F5H388_HUMAN;F5H2Z3_HUMAN;J3QTR3_HUMAN;F5H265_HUMAN;F5H747_HUMAN;F5H6Q2_HUMAN;M0R2S1_HUMAN;J3QSA3_HUMAN;F5GZ39_HUMAN;J3KSM4_HUMAN;J3QLP7_HUMAN;J3QRK5_HUMAN;K7EMA8_HUMAN	-1.61	1.59E-04	5.17E-02	F5H6Q2_HUMAN	Polyubiquitin-C (Fragment)	RL40_HUMAN;RS27A_HUMAN;UBB_HUMAN;UBC_HUMAN;B4DV12_HUMAN;F5H041_HUMAN;Q96C32_HUMAN;J3KSM4_HUMAN;F5GXK7_HUMAN;J3QS39_HUMAN;M0R1V7_HUMAN;J3QKN0_HUMAN;F5GYU3_HUMAN;J3QLP7_HUMAN;M0R1M6_HUMAN;F5H7Y5_HUMAN;F5GZ39_HUMAN;F5H7K6_HUMAN;F5H4D8_HUMAN;F5H388_HUMAN;J3QRK5_HUMAN;F5H2Z3_HUMAN;J3QTR3_HUMAN;F5H265_HUMAN;F5H747_HUMAN;F5H6Q2_HUMAN;M0R2S1_HUMAN;K7EMA8_HUMAN;J3QSA3_HUMAN	-0.66	7.77E-02	4.31E+01
F8VW92_HUMAN	Tubulin beta chain	TBB2A_HUMAN;TBB2B_HUMAN;TBB4A_HUMAN;TBB4B_HUMAN;TBB5_HUMAN;TBB6_HUMAN;TBB8L_HUMAN;TBB8_HUMAN;YI016_HUMAN;Q5SQY0_HUMAN;F8VYX6_HUMAN;E7EWR1_HUMAN;Q5JP53_HUMAN;Q5ST81_HUMAN;F8VUJ7_HUMAN;F5H0I4_HUMAN;K7ESM5_HUMAN;I3L2F9_HUMAN;F8VW92_HUMAN;C9JAA5_HUMAN;E9PBJ4_HUMAN;TBB3_HUMAN;A8K8S4_HUMAN;TBB1_HUMAN;G3V2A3_HUMAN;M0R2D3_HUMAN;M0QYM7_HUMAN;M0R042_HUMAN;G3V2R8_HUMAN;G3V2N6_HUMAN;G3V3R4_HUMAN;G3V5W4_HUMAN	3.54	3.90E-03	1.27E+00	F8VW92_HUMAN	Tubulin beta chain	TBB4A_HUMAN;TBB4B_HUMAN;TBB5_HUMAN;F8VYX6_HUMAN;E7EWR1_HUMAN;Q5JP53_HUMAN;Q5ST81_HUMAN;F8VUJ7_HUMAN;F8VW92_HUMAN;TBB2A_HUMAN;TBB2B_HUMAN;TBB6_HUMAN;TBB8L_HUMAN;TBB8_HUMAN;YI016_HUMAN;Q5SQY0_HUMAN;F5H0I4_HUMAN;K7ESM5_HUMAN;I3L2F9_HUMAN;C9JAA5_HUMAN;TBB3_HUMAN;A8K8S4_HUMAN;E9PBJ4_HUMAN	2.70	1.46E-01	8.13E+01
F8W1A4_HUMAN	Adenylate kinase 2, mitochondrial	KAD2_HUMAN;F8VYV4_HUMAN;F8W1A4_HUMAN;G3V213_HUMAN;F8VZG5_HUMAN	-2.66	1.62E-02	5.27E+00	F8W1A4_HUMAN	Adenylate kinase 2, mitochondrial	KAD2_HUMAN;G3V213_HUMAN;F8VZG5_HUMAN;F8W1A4_HUMAN;F8VYV4_HUMAN;F8VPP1_HUMAN	-5.50	3.93E-02	2.18E+01
F8W8N6_HUMAN	CD177 antigen	CD177_HUMAN;F8W8N6_HUMAN	-2.35	4.06E-02	1.32E+01	CD177_HUMAN	CD177 antigen	CD177_HUMAN;F8W8N6_HUMAN;H7BYC5_HUMAN	-3.96	4.92E-03	2.73E+00
F8WCF6_HUMAN	Actin-related protein 2/3 complex subunit 4	ARPC4_HUMAN;F6TTL5_HUMAN;H7C0A3_HUMAN;F8WCF6_HUMAN;F8WDD7_HUMAN;F8WE39_HUMAN	-3.63	5.90E-05	1.92E-02	ARPC4_HUMAN	Actin-related protein 2/3 complex subunit 4	ARPC4_HUMAN;H7C0A3_HUMAN;F8WDD7_HUMAN;F8WCF6_HUMAN;F6TTL5_HUMAN;F8WE39_HUMAN;F8WDW3_HUMAN	-4.36	2.12E-01	1.18E+02
FA49B_HUMAN	Protein FAM49B	FA49B_HUMAN;E5RGI7_HUMAN;E5RI16_HUMAN;E5RJE1_HUMAN;E5RFS4_HUMAN;E5RIR8_HUMAN;E5RJL8_HUMAN;E5RHU5_HUMAN;E5RK61_HUMAN;Q9NW21_HUMAN;FA49A_HUMAN	-5.57	2.96E-06	9.64E-04	FA49B_HUMAN	Protein FAM49B	FA49A_HUMAN;FA49B_HUMAN;Q9NW21_HUMAN;E5RI16_HUMAN;E5RJE1_HUMAN;E5RIR8_HUMAN;E5RJL8_HUMAN;E5RGI7_HUMAN	-3.43	7.28E-02	4.04E+01
FKB1A_HUMAN	Peptidyl-prolyl cis-trans isomerase FKBP1A	FKB1A_HUMAN;Q5W0X3_HUMAN;Q1JUQ5_HUMAN;TM163_HUMAN;Q5VVH2_HUMAN;A8MSS1_HUMAN	-4.18	1.24E-04	4.03E-02	FKB1A_HUMAN	Peptidyl-prolyl cis-trans isomerase FKBP1A	FKB1A_HUMAN;Q5W0X3_HUMAN;Q5VVH2_HUMAN;Q1JUQ5_HUMAN;A8MSS1_HUMAN	-5.90	2.22E-03	1.23E+00
FLNA_HUMAN	Filamin-A	FLNA_HUMAN;F8WE98_HUMAN;Q5HY54_HUMAN;E9PHF0_HUMAN;H0Y5C6_HUMAN;FLNC_HUMAN;FLNB_HUMAN;H0Y5F3_HUMAN	-3.88	1.42E-04	4.62E-02	FLNA_HUMAN	Filamin-A	FLNA_HUMAN;Q5HY54_HUMAN;F8WE98_HUMAN;E9PHF0_HUMAN;H0Y5C6_HUMAN;FLNB_HUMAN;H7C5L4_HUMAN;E7EN95_HUMAN;H0Y5F3_HUMAN;H7C2E7_HUMAN;FLNC_HUMAN	-3.17	1.12E-02	6.22E+00
G3P_HUMAN	Glyceraldehyde-3-phosphate dehydrogenase	G3P_HUMAN;E7EUT5_HUMAN;E7EUT4_HUMAN;G3PT_HUMAN	-2.71	6.64E-04	2.16E-01	G3P_HUMAN	Glyceraldehyde-3-phosphate dehydrogenase	G3P_HUMAN;E7EUT5_HUMAN;E7EUT4_HUMAN;G3PT_HUMAN	-1.41	1.25E-01	6.92E+01
G3V2F7_HUMAN	HCG2044781	UB2V1_HUMAN;UB2V2_HUMAN;G3V113_HUMAN;G3V2F7_HUMAN;E5RGE2_HUMAN;J3KNL8_HUMAN;H0YBP9_HUMAN	-0.51	6.13E-01	2.00E+02	G3V2F7_HUMAN	HCG2044781	UB2V1_HUMAN;G3V2F7_HUMAN	-4.71	4.85E-04	2.69E-01
						UB2V2_HUMAN	Ubiquitin-conjugating enzyme E2 variant 2	UB2V2_HUMAN;G3V113_HUMAN;H0YBP9_HUMAN;H0YBX6_HUMAN	-6.47	4.35E-04	2.42E-01
G3V5V7_HUMAN	Heterogeneous nuclear ribonucleoproteins C1/C2 (Fragment)	HNRPC_HUMAN;B4DY08_HUMAN;G3V576_HUMAN;G3V2D6_HUMAN;G3V2Q1_HUMAN;G3V4C1_HUMAN;G3V4W0_HUMAN;G3V5V7_HUMAN;HNRCL_HUMAN	-1.64	1.09E-01	3.55E+01	G3V5V7_HUMAN	Heterogeneous nuclear ribonucleoproteins C1/C2 (Fragment)	HNRCL_HUMAN;HNRPC_HUMAN;B4DY08_HUMAN;G3V576_HUMAN;G3V2D6_HUMAN;G3V2Q1_HUMAN;G3V4C1_HUMAN;G3V4W0_HUMAN;G3V5V7_HUMAN	-0.12	6.37E-01	3.53E+02
G3V5Z7_HUMAN	Proteasome subunit alpha type	PSA6_HUMAN;B4DXJ9_HUMAN;G3V3U4_HUMAN;G3V295_HUMAN;G3V5Z7_HUMAN;G3V3I1_HUMAN;B4DQR4_HUMAN	-2.99	2.26E-03	7.36E-01	G3V5Z7_HUMAN	Proteasome subunit alpha type	PSA6_HUMAN;B4DXJ9_HUMAN;G3V3U4_HUMAN;G3V295_HUMAN;G3V5Z7_HUMAN;G3V3I1_HUMAN;B4DQR4_HUMAN;G3V4S5_HUMAN;G3V2S7_HUMAN	-2.04	6.97E-02	3.87E+01
G6PD_HUMAN	Glucose-6-phosphate 1-dehydrogenase	G6PD_HUMAN;E9PD92_HUMAN;E7EMS7_HUMAN;E7EUI8_HUMAN	-5.12	5.48E-09	1.79E-06	G6PD_HUMAN	Glucose-6-phosphate 1-dehydrogenase	G6PD_HUMAN;E9PD92_HUMAN	-3.96	1.31E-02	7.27E+00
G6PI_HUMAN	Glucose-6-phosphate isomerase	G6PI_HUMAN;K7EIL4_HUMAN;K7EP41_HUMAN;K7ERK8_HUMAN;K7ERC6_HUMAN;K7ELR7_HUMAN;K7ENR8_HUMAN;K7ESF4_HUMAN;SIX5_HUMAN	-4.07	3.54E-05	1.15E-02	G6PI_HUMAN	Glucose-6-phosphate isomerase	G6PI_HUMAN;K7EP41_HUMAN;K7ELR7_HUMAN;K7ENR8_HUMAN;K7ERK8_HUMAN;K7ERC6_HUMAN;K7EIL4_HUMAN;SIX5_HUMAN	-3.46	1.43E-02	7.94E+00
G8JLA2_HUMAN	Myosin light polypeptide 6	MYL6_HUMAN;G3V1V0_HUMAN;B7Z6Z4_HUMAN;G3V1Y7_HUMAN;F8VZU9_HUMAN;F8VZV5_HUMAN;G8JLA2_HUMAN;F8W1R7_HUMAN;J3KND3_HUMAN;F8VPF3_HUMAN;F8W180_HUMAN;F8VXL3_HUMAN;H0YI43_HUMAN;MYL6B_HUMAN;F8W1I5_HUMAN	-3.65	5.62E-03	1.83E+00	G8JLA2_HUMAN	Myosin light polypeptide 6	MYL6_HUMAN;G3V1V0_HUMAN;B7Z6Z4_HUMAN;G3V1Y7_HUMAN;F8VZU9_HUMAN;F8VZV5_HUMAN;G8JLA2_HUMAN;F8W1R7_HUMAN;J3KND3_HUMAN;F8VPF3_HUMAN;F8W180_HUMAN;MYL6B_HUMAN;F8W1I5_HUMAN;H0YI43_HUMAN;F8VXL3_HUMAN	-4.17	4.36E-02	2.42E+01
G8JLH9_HUMAN	Signal transducer and activator of transcription 3	STAT3_HUMAN;K7ENL3_HUMAN;G8JLH9_HUMAN	-2.46	7.46E-02	2.43E+01	G8JLH9_HUMAN	Signal transducer and activator of transcription 3	STAT3_HUMAN;K7ENL3_HUMAN;G8JLH9_HUMAN	-4.93	6.27E-02	3.48E+01
GDIR1_HUMAN	Rho GDP-dissociation inhibitor 1	GDIR1_HUMAN;A8MXW0_HUMAN;J3KTF8_HUMAN;J3KRY1_HUMAN;J3QQX2_HUMAN;J3KRE2_HUMAN	-5.72	9.54E-03	3.11E+00	GDIR1_HUMAN	Rho GDP-dissociation inhibitor 1	GDIR1_HUMAN;J3KTF8_HUMAN;J3QQX2_HUMAN;A8MXW0_HUMAN;J3KRY1_HUMAN;J3KRE2_HUMAN;J3KS60_HUMAN	-3.11	2.49E-02	1.38E+01
GDIR2_HUMAN	Rho GDP-dissociation inhibitor 2	GDIR2_HUMAN;H0YGX7_HUMAN;F5H3P3_HUMAN;F5H2R5_HUMAN;F5H6Q0_HUMAN	-3.60	1.06E-03	3.45E-01	GDIR2_HUMAN	Rho GDP-dissociation inhibitor 2	GDIR2_HUMAN;H0YGX7_HUMAN;F5H3P3_HUMAN;F5H2R5_HUMAN;F5H6Q0_HUMAN	-3.28	4.02E-03	2.23E+00
GLGB_HUMAN	1,4-alpha-glucan-branching enzyme	GLGB_HUMAN;E9PGM4_HUMAN	-5.88	3.82E-05	1.25E-02	GLGB_HUMAN	1,4-alpha-glucan-branching enzyme	GLGB_HUMAN;E9PGM4_HUMAN	-4.31	1.76E-02	9.79E+00
GLRX1_HUMAN	Glutaredoxin-1	GLRX1_HUMAN	-5.52	9.92E-05	3.23E-02	GLRX1_HUMAN	Glutaredoxin-1	GLRX1_HUMAN	-4.72	6.64E-04	3.68E-01
GRP78_HUMAN	78 kDa glucose-regulated protein	GRP78_HUMAN	-2.22	9.74E-03	3.18E+00	GRP78_HUMAN	78 kDa glucose-regulated protein	GRP78_HUMAN	-2.50	9.86E-03	5.47E+00
GSHR_HUMAN	Glutathione reductase, mitochondrial	GSHR_HUMAN;E5RIO6_HUMAN;H0YBD4_HUMAN	-3.95	2.16E-04	7.05E-02	GSHR_HUMAN	Glutathione reductase, mitochondrial	GSHR_HUMAN;E5RIO6_HUMAN;H0YBD4_HUMAN;H0YC68_HUMAN	-4.04	1.51E-02	8.36E+00
GSTP1_HUMAN	Glutathione S-transferase P	GSTP1_HUMAN;A8MX94_HUMAN	-5.47	4.83E-06	1.57E-03	GSTP1_HUMAN	Glutathione S-transferase P	GSTP1_HUMAN;A8MX94_HUMAN	-4.82	2.31E-02	1.28E+01
GYS1_HUMAN	Glycogen [starch] synthase, muscle	GYS1_HUMAN;B7Z806_HUMAN;M0QYU1_HUMAN;F5H1N8_HUMAN;F5H3S3_HUMAN	-3.80	7.62E-04	2.48E-01	GYS1_HUMAN	Glycogen [starch] synthase, muscle	GYS1_HUMAN;B7Z806_HUMAN;F5H1N8_HUMAN;F5H3S3_HUMAN;M0QYU1_HUMAN	-2.54	1.89E-01	1.05E+02

H0YN26_HUMAN	Acidic leucine-rich nuclear phosphoprotein 32 family member A	AN32A_HUMAN;AN32C_HUMAN;AN32D_HUMAN;H0YN26_HUMAN	-4.67	5.26E-03	1.71E+00	H0YN26_HUMAN	Acidic leucine-rich nuclear phosphoprotein 32 family member A	AN32A_HUMAN;H7BZ09_HUMAN;H0YN26_HUMAN;AN32C_HUMAN;AN32D_HUMAN	-5.78	9.97E-02	5.53E+01
H2AJ_HUMAN	Histone H2AJ	H2A1D_HUMAN;H2A1H_HUMAN;H2A1J_HUMAN;H2A1_HUMAN;H2A2A_HUMAN;H2A2C_HUMAN;H2AJ_HUMAN;H0YFX9_HUMAN;H2A1A_HUMAN;H2A1B_HUMAN;H2A1C_HUMAN;H2A3_HUMAN;H2AX_HUMAN	7.17	6.61E-10	2.16E-07	H0YFX9_HUMAN	Histone H2A (Fragment)	H2A1D_HUMAN;H2A1H_HUMAN;H2A1J_HUMAN;H2A1_HUMAN;H2A2A_HUMAN;H2A2C_HUMAN;H2AJ_HUMAN;H0YFX9_HUMAN	7.77	3.30E-03	1.83E+00
						H2A3_HUMAN	Histone H2A type 3	H2A1B_HUMAN;H2A1C_HUMAN;H2A3_HUMAN	7.46	4.74E-03	2.63E+00
H2AY_HUMAN	Core histone macro-H2A.1	H2AY_HUMAN;B4DJC3_HUMAN;D6RCF2_HUMAN;H2AW_HUMAN;Q5SQT3_HUMAN	-4.36	3.08E-03	1.00E+00	H2AY_HUMAN	Core histone macro-H2A.1	H2AY_HUMAN;B4DJC3_HUMAN;H2AW_HUMAN;D6RCF2_HUMAN	-5.35	1.03E-02	5.73E+00
H3BSC1_HUMAN	Ras-related protein Rab-11A	RB11A_HUMAN;RB11B_HUMAN;B4DMK0_HUMAN;B4DT13_HUMAN;H3BMH2_HUMAN;J3KQP6_HUMAN;H3BSC1_HUMAN;RAB25_HUMAN	-4.96	9.86E-05	3.22E-02	H3BSC1_HUMAN	Ras-related protein Rab-11A	RB11A_HUMAN;RB11B_HUMAN;B4DMK0_HUMAN;B4DT13_HUMAN;H3BMH2_HUMAN;J3KQP6_HUMAN;H3BSC1_HUMAN;B4DQU5_HUMAN;M0R377_HUMAN;M0R2D0_HUMAN;H3BN38_HUMAN	-5.35	3.57E-02	1.98E+01
H4_HUMAN	Histone H4	H4_HUMAN	7.47	3.90E-07	1.27E-04	H4_HUMAN	Histone H4	H4_HUMAN	8.42	1.60E-02	8.87E+00
H7BXD5_HUMAN	Grancalcin	GRAN_HUMAN;H7BXD5_HUMAN;H7C2Z6_HUMAN;C9JIZ3_HUMAN;C9JWQ8_HUMAN;C9JV47_HUMAN	-4.72	1.59E-05	5.20E-03	H7BXD5_HUMAN	Grancalcin	GRAN_HUMAN;H7BXD5_HUMAN;H7C2Z6_HUMAN;C9JIZ3_HUMAN;C9JWQ8_HUMAN;C9JV47_HUMAN	-5.09	1.72E-02	9.53E+00
H7BZJ3_HUMAN	Thioredoxin (Fragment)	PDIA3_HUMAN;G5EAS2_HUMAN;H7BZJ3_HUMAN	0.34	9.40E-01	3.06E+02	G5EAS2_HUMAN	Protein disulfide isomerase family A, member 3, isoform CRA_b	PDIA3_HUMAN;G5EAS2_HUMAN;H7BZJ3_HUMAN	0.86	1.84E-01	1.02E+02
H7BZT7_HUMAN	S-formylglutathione hydrolase (Fragment)	ESTD_HUMAN;H7BZT7_HUMAN	-5.40	6.39E-04	2.08E-01	ESTD_HUMAN	S-formylglutathione hydrolase	ESTD_HUMAN;H7BZT7_HUMAN	-4.63	1.56E-03	8.68E-01
H9KV70_HUMAN	Neutrophil gelatinase-associated lipocalin	NGAL_HUMAN;H9KV70_HUMAN	-6.17	3.18E-03	1.04E+00	H9KV70_HUMAN	Neutrophil gelatinase-associated lipocalin	NGAL_HUMAN;H9KV70_HUMAN	-6.09	2.76E-03	1.53E+00
HBA_HUMAN	Hemoglobin subunit alpha	HBA_HUMAN	-0.14	4.27E-01	1.39E+02	HBA_HUMAN	Hemoglobin subunit alpha	HBA_HUMAN	-0.45	4.77E-01	2.65E+02
HBB_HUMAN	Hemoglobin subunit beta	HBB_HUMAN;F8W6P5_HUMAN	-0.74	1.32E-01	4.31E+01	HBB_HUMAN	Hemoglobin subunit beta	HBB_HUMAN;F8W6P5_HUMAN	-1.02	2.82E-01	1.56E+02
HBD_HUMAN	Hemoglobin subunit delta	HBD_HUMAN;E9PEW8_HUMAN;E9PFT6_HUMAN;C9JRG0_HUMAN	-0.80	1.32E-01	4.31E+01	HBD_HUMAN	Hemoglobin subunit delta	HBD_HUMAN;E9PEW8_HUMAN;E9PFT6_HUMAN;C9JRG0_HUMAN	-1.09	2.86E-01	1.58E+02
HBG2_HUMAN	Hemoglobin subunit gamma-2	HBG1_HUMAN;HBG2_HUMAN;E9PBW4_HUMAN	-0.05	6.59E-01	2.15E+02	HBG1_HUMAN	Hemoglobin subunit gamma-1	HBG1_HUMAN;HBG2_HUMAN;E9PBW4_HUMAN;F8WB96_HUMAN	0.98	9.12E-01	5.06E+02
HEBP2_HUMAN	Heme-binding protein 2	HEBP2_HUMAN;Q5THN1_HUMAN	-4.54	7.96E-03	2.60E+00	HEBP2_HUMAN	Heme-binding protein 2	HEBP2_HUMAN;Q5THN1_HUMAN	0.56	3.44E-01	1.91E+02
HPRT_HUMAN	Hypoxanthine-guanine phosphoribosyltransferase	HPRT_HUMAN	-4.20	1.21E-04	3.93E-02	HPRT_HUMAN	Hypoxanthine-guanine phosphoribosyltransferase	HPRT_HUMAN;PRDC1_HUMAN	-3.44	1.56E-02	8.64E+00
HS90A_HUMAN	Heat shock protein HSP 90-alpha	HS90A_HUMAN;Q86U12_HUMAN;HS904_HUMAN;G3V2J8_HUMAN;HS905_HUMAN;HS902_HUMAN	-4.10	3.50E-06	1.14E-03	HS90A_HUMAN	Heat shock protein HSP 90-alpha	HS90A_HUMAN;Q86U12_HUMAN;HS904_HUMAN;G3V2J8_HUMAN;HS905_HUMAN	-3.48	3.77E-02	2.09E+01
HS90B_HUMAN	Heat shock protein HSP 90-beta	H90B2_HUMAN;HS90B_HUMAN;H0Y5S7_HUMAN;H0Y6E4_HUMAN;H0Y598_HUMAN	-3.89	6.57E-04	2.14E-01	HS90B_HUMAN	Heat shock protein HSP 90-beta	H90B3_HUMAN;HS90B_HUMAN;H0Y6E4_HUMAN;H0Y5S7_HUMAN;H0Y598_HUMAN;H90B2_HUMAN	-3.50	6.67E-02	3.70E+01
HSP71_HUMAN	Heat shock 70 kDa protein 1A/1B	HSP71_HUMAN;F8VZJ4_HUMAN;E7EP11_HUMAN;Q5SP16_HUMAN;E7EP94_HUMAN;HS71L_HUMAN;Q53FA3_HUMAN;B4DXY3_HUMAN;F8W1P1_HUMAN	-4.47	2.00E-03	6.51E-01	HSP71_HUMAN	Heat shock 70 kDa protein 1A/1B	HSP71_HUMAN;Q5SP16_HUMAN;E7EP94_HUMAN;F8VZJ4_HUMAN;E7EP11_HUMAN	-4.30	1.03E-02	5.69E+00
HSP7C_HUMAN	Heat shock cognate 71 kDa protein	HSP72_HUMAN;HSP7C_HUMAN;E9PQQ4_HUMAN;E9PKE3_HUMAN;E9PN25_HUMAN;E9PK54_HUMAN;E9PLF4_HUMAN;E9PN89_HUMAN;E9PQK7_HUMAN;E9PPY6_HUMAN;E9PNE6_HUMAN;A8K7Q2_HUMAN;E9PM13_HUMAN;E9PS65_HUMAN;E9PI65_HUMAN;E9PSH5_HUMAN;GRP75_HUMAN	-5.44	5.76E-05	1.88E-02	HSP7C_HUMAN	Heat shock cognate 71 kDa protein	HSP7C_HUMAN;A8K7Q2_HUMAN;E9PKE3_HUMAN;E9PN89_HUMAN;E9PNE6_HUMAN;E9PQQ4_HUMAN;E9PN25_HUMAN;E9PK54_HUMAN;E9PLF4_HUMAN;E9PQK7_HUMAN;E9PPY6_HUMAN;E9PS65_HUMAN;GRP75_HUMAN;HSP72_HUMAN;E9PI65_HUMAN;E9PM13_HUMAN;E9PSH5_HUMAN	-3.80	2.74E-03	1.52E+00
HXK3_HUMAN	Hexokinase-3	HXK3_HUMAN;H0Y8U9_HUMAN;H0Y9N6_HUMAN;HXK1_HUMAN;HXK2_HUMAN;E9PB90_HUMAN;E7ENR4_HUMAN	-4.75	3.14E-03	1.02E+00	HXK3_HUMAN	Hexokinase-3	HXK3_HUMAN;H0Y8U9_HUMAN;H0Y9N6_HUMAN	-3.74	1.37E-02	7.59E+00
						E7ENR4_HUMAN	Hexokinase-1	HXK1_HUMAN;E7ENR4_HUMAN;HXK2_HUMAN;E9PB90_HUMAN	-3.05	3.31E-01	1.84E+02
I3L0K2_HUMAN	Thioredoxin domain-containing protein 17	TXD17_HUMAN;I3L3M7_HUMAN;I3L0K2_HUMAN	-6.92	9.83E-04	3.20E-01	TXD17_HUMAN	Thioredoxin domain-containing protein 17	TXD17_HUMAN;I3L3M7_HUMAN;I3L0K2_HUMAN;I3L2R6_HUMAN	-5.22	9.88E-03	5.48E+00
I3L2P8_HUMAN	Protein disulfide-isomerase	PDIA1_HUMAN;F5H8J2_HUMAN;H7BZ94_HUMAN;I3L398_HUMAN;I3L2P8_HUMAN;H0Y3Z3_HUMAN;I3L3U6_HUMAN;I3NI03_HUMAN;I3L0S0_HUMAN	1.14	7.31E-02	2.38E+01	I3L2P8_HUMAN	Protein disulfide-isomerase	PDIA1_HUMAN;F5H8J2_HUMAN;I3L3U6_HUMAN;H7BZ94_HUMAN;I3L2P8_HUMAN;I3NI03_HUMAN;I3L398_HUMAN;I3L312_HUMAN;I3L514_HUMAN;I3L1Y5_HUMAN;I3L0S0_HUMAN;I3L3P5_HUMAN;I3L4M2_HUMAN;H0Y3Z3_HUMAN	-0.97	2.31E-01	1.28E+02
I3L2U8_HUMAN	Platelet-activating factor acetylhydrolase IB subunit alpha	LIS1_HUMAN;I3L2U8_HUMAN;B4DF38_HUMAN;I3L3N5_HUMAN	-4.98	3.40E-03	1.11E+00	LIS1_HUMAN	Platelet-activating factor acetylhydrolase IB subunit alpha	LIS1_HUMAN;I3L2U8_HUMAN;B4DF38_HUMAN;I3L3N5_HUMAN;I3L495_HUMAN	-5.02	1.25E-02	6.94E+00
I3L3Q4_HUMAN	Glyoxalase domain-containing protein 4 (Fragment)	GLOD4_HUMAN;B7Z403_HUMAN;I3L3Q4_HUMAN;I3L1F4_HUMAN	-4.30	8.78E-03	2.86E+00	GLOD4_HUMAN	Glyoxalase domain-containing protein 4	GLOD4_HUMAN;B7Z403_HUMAN;I3L1I0_HUMAN	-1.67	3.23E-02	1.80E+01
IDHC_HUMAN	Isocitrate dehydrogenase [NADP] cytoplasmic	IDHC_HUMAN;C9J4N6_HUMAN	-4.20	1.78E-04	5.79E-02	IDHC_HUMAN	Isocitrate dehydrogenase [NADP] cytoplasmic	IDHC_HUMAN;IDHP_HUMAN;B4DSZ6_HUMAN;B4DFL2_HUMAN;C9J4N6_HUMAN;C9JJE5_HUMAN;C9JLU6_HUMAN	-4.57	5.30E-03	2.94E+00
IGHA1_HUMAN	Ig alpha-1 chain C region	IGHA1_HUMAN;IGHA2_HUMAN	-4.56	9.42E-03	3.07E+00	IGHA1_HUMAN	Ig alpha-1 chain C region	IGHA1_HUMAN;IGHA2_HUMAN	-4.77	1.55E-02	8.62E+00
IGHG1_HUMAN	Ig gamma-1 chain C region	IGHG1_HUMAN;IGHG2_HUMAN;IGHG3_HUMAN;IGHG4_HUMAN	-5.95	1.09E-06	3.57E-04	IGHG1_HUMAN	Ig gamma-1 chain C region	IGHG1_HUMAN	-4.40	2.82E-02	1.57E+01
						IGHG2_HUMAN	Ig gamma-2 chain C region	IGHG2_HUMAN	-3.99	2.84E-02	1.58E+01
IGKC_HUMAN	Ig kappa chain C region	IGKC_HUMAN	-6.33	5.67E-08	1.85E-05	IGKC_HUMAN	Ig kappa chain C region	IGKC_HUMAN	-4.73	7.54E-02	4.19E+01
ILEU_HUMAN	Leukocyte elastase inhibitor	ILEU_HUMAN;B4DNT0_HUMAN	-2.97	2.28E-05	7.42E-03	ILEU_HUMAN	Leukocyte elastase inhibitor	ILEU_HUMAN;B4DNT0_HUMAN	-3.32	2.81E-02	1.56E+01
IMB1_HUMAN	Importin subunit beta-1	IMB1_HUMAN;J3QR48_HUMAN;B7ZAV6_HUMAN	-4.30	6.14E-05	2.00E-02	IMB1_HUMAN	Importin subunit beta-1	IMB1_HUMAN;J3QR48_HUMAN;B7ZAV6_HUMAN;F5H4R7_HUMAN;J3KTM9_HUMAN	-3.34	2.56E-02	1.42E+01
IQGA1_HUMAN	Ras GTPase-activating-like protein IQGAP1	IQGA1_HUMAN;IQGA3_HUMAN;H0YLE8_HUMAN;F2Z2E2_HUMAN	-4.77	1.26E-06	4.12E-04	IQGA1_HUMAN	Ras GTPase-activating-like protein IQGAP1	IQGA1_HUMAN;H0YLE8_HUMAN;IQGA3_HUMAN;F2Z2E2_HUMAN;IQGA2_HUMAN;E7EWC2_HUMAN;F5H7S7_HUMAN;J3KR91_HUMAN	-4.53	4.51E-02	2.51E+01
ITAM_HUMAN	Integrin alpha-M	ITAM_HUMAN	-3.45	3.18E-06	1.04E-03	ITAM_HUMAN	Integrin alpha-M	ITAM_HUMAN;H3BMV4_HUMAN;ITAD_HUMAN;ITAX_HUMAN;H3BN02_HUMAN	-2.17	3.20E-02	1.78E+01
J3KNB4_HUMAN	Cathelicidin antimicrobial peptide	CAMP_HUMAN;J3KNB4_HUMAN	-4.73	1.41E-04	4.59E-02	J3KNB4_HUMAN	Cathelicidin antimicrobial peptide	CAMP_HUMAN;J3KNB4_HUMAN;REVERSED_AMZ1_HUMAN	-4.62	3.24E-03	1.80E+00
J3KPA1_HUMAN	Cysteine-rich secretory protein 3	CRIS3_HUMAN;J3KPA1_HUMAN;I3L0A1_HUMAN;J3KQX0_HUMAN	-6.89	3.55E-04	1.16E-01	J3KPA1_HUMAN	Cysteine-rich secretory protein 3	CRIS3_HUMAN;J3KPA1_HUMAN;I3L0A1_HUMAN;CRIS2_HUMAN;J3KQX0_HUMAN	-9.04	3.78E-04	2.10E-01
J3KQE5_HUMAN	GTP-binding nuclear protein Ran (Fragment)	RAN_HUMAN;B5MDF5_HUMAN;H0YFC6_HUMAN;F5H018_HUMAN;J3KQE5_HUMAN;B4DV51_HUMAN	-2.56	7.60E-04	2.48E-01	J3KQE5_HUMAN	GTP-binding nuclear protein Ran (Fragment)	RAN_HUMAN;B5MDF5_HUMAN;H0YFC6_HUMAN;F5H018_HUMAN;J3KQE5_HUMAN;B4DV51_HUMAN	-3.07	6.62E-03	3.67E+00
J3QKR3_HUMAN	Proteasome subunit beta type-3 (Fragment)	PSB3_HUMAN;J3KRR2_HUMAN;J3QKR3_HUMAN;J3KSM3_HUMAN	-4.52	2.59E-02	8.43E+00	J3QKR3_HUMAN	Proteasome subunit beta type-3 (Fragment)	PSB3_HUMAN;J3KRR2_HUMAN;J3QKR3_HUMAN;J3KSM3_HUMAN	-1.09	5.78E-01	3.21E+02
J3QLI9_HUMAN	Small nuclear ribonucleoprotein Sm D1	SMD1_HUMAN;J3QLI9_HUMAN	-2.11	1.94E-03	6.31E-01	SMD1_HUMAN	Small nuclear ribonucleoprotein Sm D1	SMD1_HUMAN;J3QLI9_HUMAN;J3QLR7_HUMAN	-1.70	4.65E-02	2.58E+01
J3QR68_HUMAN	Haptoglobin (Fragment)	HPTR_HUMAN;HPT_HUMAN;Q0VAC5_HUMAN;H0Y300_HUMAN;J3KTC3_HUMAN;J3QR68_HUMAN;H3BS21_HUMAN;J3QLC9_HUMAN;J3KRH2_HUMAN	-6.15	2.08E-05	6.79E-03	HPT_HUMAN	Haptoglobin	HPTR_HUMAN;HPT_HUMAN;Q0VAC5_HUMAN;H3BS21_HUMAN;J3QR68_HUMAN;J3QLC9_HUMAN;J3KRH2_HUMAN;H0Y300_HUMAN;J3KTC3_HUMAN;J3QQI8_HUMAN;H3BMJ7_HUMAN;J3KSV1_HUMAN	-8.69	4.43E-04	2.46E-01
J3QRS3_HUMAN	Myosin regulatory light chain 12A	ML12A_HUMAN;ML12B_HUMAN;MYL9_HUMAN;J3QRS3_HUMAN	-4.46	8.24E-03	2.69E+00	J3QRS3_HUMAN	Myosin regulatory light chain 12A	ML12A_HUMAN;ML12B_HUMAN;J3QRS3_HUMAN;MYL9_HUMAN;J3KTJ1_HUMAN	-5.06	1.38E-02	7.68E+00
K7ELW0_HUMAN	Protein DJ-1	PARK7_HUMAN;K7ELW0_HUMAN;K7EN27_HUMAN	-2.08	8.18E-03	2.67E+00	PARK7_HUMAN	Protein DJ-1	PARK7_HUMAN;K7ELW0_HUMAN;K7EN27_HUMAN	-3.74	4.50E-03	2.50E+00

KPYM_HUMAN	Pyruvate kinase isozymes M1/M2	KPYM_HUMAN;KPYR_HUMAN;Q504U3_HUMAN;H3BTN5_HUMAN;H3BSU3_HUMAN;H3BQ34_HUMAN;H3BTJ2_HUMAN;H3BT25_HUMAN;H3BUW1_HUMAN;H3BQZ3_HUMAN;H3BU13_HUMAN;H3BN34_HUMAN	-2.09	3.36E-04	1.10E-01	KPYM_HUMAN	Pyruvate kinase isozymes M1/M2	KPYM_HUMAN	-3.33	8.10E-02	4.50E+01
LDHA_HUMAN	L-lactate dehydrogenase A chain	LDHA_HUMAN;F5H308_HUMAN;F5GWW2_HUMAN;F5GXC7_HUMAN;F5GXU1_HUMAN;F5H8H6_HUMAN;F5GZQ4_HUMAN;F5GXY2_HUMAN;F5GXH2_HUMAN;F5GYU2_HUMAN;F5H5J4_HUMAN;F5H6W8_HUMAN	-4.22	1.18E-03	3.84E-01	LDHA_HUMAN	L-lactate dehydrogenase A chain	LDHA_HUMAN;F5H308_HUMAN;F5GXY2_HUMAN;F5GXH2_HUMAN;F5GYU2_HUMAN;F5H5J4_HUMAN;F5H6W8_HUMAN;LDH6A_HUMAN;F5GWW2_HUMAN;F5GXC7_HUMAN;F5GXU1_HUMAN;F5H8H6_HUMAN;F5GZQ4_HUMAN	-3.32	3.49E-02	1.94E+01
LDHB_HUMAN	L-lactate dehydrogenase B chain	LDHB_HUMAN;A8MW50_HUMAN;C9J7H8_HUMAN;F5H793_HUMAN	-3.67	5.20E-04	1.69E-01	LDHB_HUMAN	L-lactate dehydrogenase B chain	LDHB_HUMAN;A8MW50_HUMAN;C9J7H8_HUMAN;F5H793_HUMAN	-1.13	7.48E-02	4.15E+01
LEG3_HUMAN	Galectin-3	LEG3_HUMAN;G3V3R6_HUMAN	-4.98	2.58E-04	8.41E-02	LEG3_HUMAN	Galectin-3	LEG3_HUMAN;G3V3R6_HUMAN	-3.85	2.16E-02	1.20E+01
LKHA4_HUMAN	Leukotriene A-4 hydrolase	LKHA4_HUMAN;B4DEH5_HUMAN	-4.61	1.90E-03	6.20E-01	LKHA4_HUMAN	Leukotriene A-4 hydrolase	LKHA4_HUMAN;B4DEH5_HUMAN	-3.42	1.74E-02	9.66E+00
LMNB1_HUMAN	Lamin-B1	LMNB1_HUMAN;E9PBF6_HUMAN	-2.57	5.16E-04	1.68E-01	LMNB1_HUMAN	Lamin-B1	LMNB1_HUMAN;E9PBF6_HUMAN	-5.57	1.26E-02	7.02E+00
LPPL_HUMAN	Eosinophil lysophospholipase	LPPL_HUMAN	-5.00	9.19E-04	3.00E-01	LPPL_HUMAN	Eosinophil lysophospholipase	LPPL_HUMAN;LEG16_HUMAN	-5.10	3.77E-05	2.09E-02
LYSC_HUMAN	Lysozyme C	LYSC_HUMAN;F8VV32_HUMAN	-3.35	8.83E-04	2.88E-01	LYSC_HUMAN	Lysozyme C	LYSC_HUMAN;F8VV32_HUMAN	-2.08	4.08E-02	2.27E+01
M0QYG8_HUMAN	Glia maturation factor gamma	GMFG_HUMAN;M0QYJ8_HUMAN;M0R0C1_HUMAN;M0R1D2_HUMAN;M0QYG8_HUMAN;M0QXC2_HUMAN;GMFB_HUMAN;G3V4P8_HUMAN	-1.70	2.16E-03	7.05E-01	GMFG_HUMAN	Glia maturation factor gamma	E41L5_HUMAN;GMFG_HUMAN;M0R0C1_HUMAN;M0R1D2_HUMAN;M0QX47_HUMAN;M0QYG8_HUMAN;M0QYJ8_HUMAN;M0QXC2_HUMAN;GMFB_HUMAN;G3V4P8_HUMAN	-3.68	5.97E-02	3.31E+01
M0R192_HUMAN	Flavin reductase (NADPH)	BLVRB_HUMAN;M0R192_HUMAN;M0QZL1_HUMAN	-3.69	2.00E-05	6.53E-03	BLVRB_HUMAN	Flavin reductase (NADPH)	BLVRB_HUMAN;M0R192_HUMAN;M0QZL1_HUMAN	-3.29	1.01E-01	5.61E+01
MDHC_HUMAN	Malate dehydrogenase, cytoplasmic	MDHC_HUMAN;B9A041_HUMAN;C9JF79_HUMAN;B8ZZ51_HUMAN;C9JRL4_HUMAN;C9JLV6_HUMAN;C9IZI0_HUMAN;F8WFC2_HUMAN	-4.35	5.53E-05	1.80E-02	MDHC_HUMAN	Malate dehydrogenase, cytoplasmic	MDHC_HUMAN;B9A041_HUMAN;B8ZZ51_HUMAN;C9JF79_HUMAN;C9JRL4_HUMAN	-1.97	9.82E-03	5.45E+00
MIF_HUMAN	Macrophage migration inhibitory factor	MIF_HUMAN	-6.10	9.56E-03	3.12E+00	MIF_HUMAN	Macrophage migration inhibitory factor	MIF_HUMAN	-1.56	1.51E-02	8.37E+00
MMP8_HUMAN	Neutrophil collagenase	MMP8_HUMAN;H7C1M3_HUMAN	-6.54	5.72E-05	1.86E-02	MMP8_HUMAN	Neutrophil collagenase	MMP8_HUMAN;H7C1M3_HUMAN;MMP10_HUMAN	-7.59	2.22E-03	1.23E+00
MMP9_HUMAN	Matrix metalloproteinase-9	MMP9_HUMAN	-7.21	1.32E-03	4.30E-01	MMP9_HUMAN	Matrix metalloproteinase-9	MMP9_HUMAN	-9.79	7.54E-03	4.18E+00
MNDA_HUMAN	Myeloid cell nuclear differentiation antigen	MNDA_HUMAN;H0Y6P3_HUMAN	3.85	7.66E-05	2.50E-02	MNDA_HUMAN	Myeloid cell nuclear differentiation antigen	MNDA_HUMAN;H0Y6P3_HUMAN	4.50	1.62E-03	8.98E-01
MOES_HUMAN	Moesin	MOES_HUMAN	-3.72	5.58E-04	1.82E-01	MOES_HUMAN	Moesin	MOES_HUMAN;RADI_HUMAN;A7YIJ8_HUMAN;F5H1A7_HUMAN	-2.07	4.26E-02	2.36E+01
MTPN_HUMAN	Myotrophin	MTPN_HUMAN;C9JL85_HUMAN	-2.40	3.18E-02	1.04E+01	MTPN_HUMAN	Myotrophin	MTPN_HUMAN;C9JL85_HUMAN	-1.07	2.80E-01	1.55E+02
MVP_HUMAN	Major vault protein	MVP_HUMAN;H3BNF6_HUMAN;H3BRL2_HUMAN;H3BUK7_HUMAN;H3BP76_HUMAN;H3BQK6_HUMAN	0.00	9.50E-01	3.10E+02	MVP_HUMAN	Major vault protein	MVP_HUMAN;H3BNF6_HUMAN;H3BRL2_HUMAN;H3BUK7_HUMAN;H3BP76_HUMAN;H3BQK6_HUMAN;J3L155_HUMAN	-0.40	6.73E-01	3.73E+02
MYH9_HUMAN	Myosin-9	MYH9_HUMAN;MYH10_HUMAN;MYH11_HUMAN;MYH14_HUMAN;Q5BKV1_HUMAN;G8JL19_HUMAN;F2Z2U8_HUMAN;F8W6L6_HUMAN;M0QY43_HUMAN;E7ERA5_HUMAN;B1AH99_HUMAN;MYH13_HUMAN;MYH1_HUMAN;MYH2_HUMAN;MYH3_HUMAN;MYH4_HUMAN;MYH6_HUMAN;MYH7B_HUMAN;MYH7_HUMAN;MYH8_HUMAN;REVERSED_ZMY12_HUMAN;REVERSED_E9PFV0_HUMAN	-2.97	1.46E-03	4.76E-01	MYH9_HUMAN	Myosin-9	MYH10_HUMAN;MYH9_HUMAN;F8W6L6_HUMAN;Q5BKV1_HUMAN;REVERSED_MAP2_HUMAN;REVERSED_TTLL6_HUMAN;REVERSED_F8W9N0_HUMAN;REVERSED_E7EV03_HUMAN;MYH11_HUMAN;MYH14_HUMAN;G8JL19_HUMAN;F2Z2U8_HUMAN;B1AH99_HUMAN;M0QY43_HUMAN;MYH7B_HUMAN;E7ERA5_HUMAN;REVERSED_ZMY12_HUMAN;REVERSED_E9PFV0_HUMAN	-1.92	8.47E-02	4.70E+01
NAGK_HUMAN	N-acetyl-D-glucosamine kinase	NAGK_HUMAN;E9PPU6_HUMAN;C9JEV6_HUMAN;H7C3G9_HUMAN;H7C1L7_HUMAN;H0YEB7_HUMAN;H0YC94_HUMAN	-3.90	4.82E-04	1.57E-01	NAGK_HUMAN	N-acetyl-D-glucosamine kinase	NAGK_HUMAN;E9PPU6_HUMAN;C9JEV6_HUMAN;H7C3G9_HUMAN;H7C1L7_HUMAN;H0YEB7_HUMAN;H0YC94_HUMAN;H0YF44_HUMAN	-5.34	2.92E-03	1.62E+00
NAMPT_HUMAN	Nicotinamide phosphoribosyltransferase	NAMPT_HUMAN;Q5SYT8_HUMAN;F5H246_HUMAN;C9JG65_HUMAN	-4.95	3.39E-06	1.11E-03	NAMPT_HUMAN	Nicotinamide phosphoribosyltransferase	NAMPT_HUMAN;F5H246_HUMAN;Q5SYT8_HUMAN;C9JG65_HUMAN;C9JF35_HUMAN	-4.99	2.18E-02	1.21E+01
NCF1_HUMAN	Neutrophil cytosol factor 1	NCF1B_HUMAN;NCF1C_HUMAN;NCF1_HUMAN;C9J155_HUMAN;H7C1S1_HUMAN	-4.31	1.57E-05	5.13E-03	NCF1_HUMAN	Neutrophil cytosol factor 1	NCF1B_HUMAN;NCF1_HUMAN;C9J155_HUMAN;NCF1C_HUMAN;H7C1S1_HUMAN	-3.85	1.63E-01	9.04E+01
NCF2_HUMAN	Neutrophil cytosol factor 2	NCF2_HUMAN;B1ALB7_HUMAN	-3.02	2.80E-02	9.11E+00	NCF2_HUMAN	Neutrophil cytosol factor 2	NCF2_HUMAN;B1ALB7_HUMAN;B1ALB6_HUMAN	-4.32	1.74E-01	9.66E+01
NIT2_HUMAN	Omega-amidase NIT2	NIT2_HUMAN;H7C579_HUMAN;F8WF70_HUMAN	-3.89	1.22E-04	3.99E-02	NIT2_HUMAN	Omega-amidase NIT2	NIT2_HUMAN;H7C579_HUMAN;F8WF70_HUMAN	-5.67	2.00E-03	1.11E+00
NPM_HUMAN	Nucleophosmin	NPM_HUMAN;E5RI98_HUMAN	-1.31	1.76E-01	5.72E+01	NPM_HUMAN	Nucleophosmin	NPM_HUMAN;E5RGW4_HUMAN	-3.99	9.35E-02	5.19E+01
OLFM4_HUMAN	Olfactomedin-4	OLFM4_HUMAN;REVERSED_DQX1_HUMAN	-5.47	2.58E-04	8.40E-02	OLFM4_HUMAN	Olfactomedin-4	OLFM4_HUMAN;REVERSED_DQX1_HUMAN	-2.30	1.90E-01	1.05E+02
OSTF1_HUMAN	Osteoclast-stimulating factor 1	OSTF1_HUMAN	-0.73	4.94E-01	1.61E+02	OSTF1_HUMAN	Osteoclast-stimulating factor 1	OSTF1_HUMAN	0.60	7.08E-01	3.93E+02
PDC6I_HUMAN	Programmed cell death 6-interacting protein	PDC6I_HUMAN;F8WDK9_HUMAN	0.31	5.40E-01	1.76E+02	PDC6I_HUMAN	Programmed cell death 6-interacting protein	PDC6I_HUMAN;F8WDK9_HUMAN;C9IZF9_HUMAN;F8WBR8_HUMAN;F8WEQ7_HUMAN	-1.82	3.41E-02	1.89E+01
PEBP1_HUMAN	Phosphatidylethanolamine-binding protein 1	PEBP1_HUMAN	-3.81	1.39E-02	4.52E+00	PEBP1_HUMAN	Phosphatidylethanolamine-binding protein 1	PEBP1_HUMAN	-2.32	1.26E-02	7.00E+00
PERE_HUMAN	Eosinophil peroxidase	PERE_HUMAN	3.50	4.44E-03	1.45E+00	PERE_HUMAN	Eosinophil peroxidase	PERE_HUMAN	1.96	1.14E-01	6.32E+01
PERM_HUMAN	Myeloperoxidase	PERM_HUMAN;J3QSF7_HUMAN	4.38	4.87E-06	1.59E-03	PERM_HUMAN	Myeloperoxidase	PERM_HUMAN;J3QSF7_HUMAN	4.64	2.62E-03	1.46E+00
PGAM1_HUMAN	Phosphoglycerate mutase 1	PGAM1_HUMAN;PGAM4_HUMAN;PGAM2_HUMAN	-4.45	1.72E-05	5.62E-03	PGAM1_HUMAN	Phosphoglycerate mutase 1	PGAM1_HUMAN;PGAM2_HUMAN;PGAM4_HUMAN	-4.70	2.33E-02	1.29E+01
PGK1_HUMAN	Phosphoglycerate kinase 1	PGK1_HUMAN;PGK2_HUMAN;E7ERH5_HUMAN;B7Z7A9_HUMAN	-3.84	2.72E-06	8.85E-04	PGK1_HUMAN	Phosphoglycerate kinase 1	PGK1_HUMAN;B7Z7A9_HUMAN;E7ERH5_HUMAN;PGK2_HUMAN;REVERSED_KIT_HUMAN;REVERSED_CCAR1_HUMAN;REVERSED_F5H1H2_HUMAN;REVERSED_F5H2E6_HUMAN	-2.89	8.90E-03	4.94E+00
PGM1_HUMAN	Phosphoglucomutase-1	PGM1_HUMAN	-4.93	1.55E-07	5.07E-05	PGM1_HUMAN	Phosphoglucomutase-1	PGM1_HUMAN;CP1B1_HUMAN;REVERSED_UQCC_HUMAN;REVERSED_B7Z1C6_HUMAN;REVERSED_H7BYA2_HUMAN;REVERSED_B7Z314_HUMAN;REVERSED_B7Z7J8_HUMAN;REVERSED_B1AKV3_HUMAN;REVERSED_B1AKV4_HUMAN	-4.18	1.60E-02	8.90E+00
PGM2_HUMAN	Phosphoglucomutase-2	PGM2_HUMAN;E7ENQ8_HUMAN;E9PD70_HUMAN;F5H6V2_HUMAN;B4E0G8_HUMAN	-4.99	2.40E-05	7.83E-03	PGM2_HUMAN	Phosphoglucomutase-2	PGM2_HUMAN;F5H6V2_HUMAN;E7ENQ8_HUMAN;E9PD70_HUMAN;B4E0G8_HUMAN;H0Y921_HUMAN	-3.79	4.69E-02	2.60E+01
PGRP1_HUMAN	Peptidoglycan recognition protein 1	PGRP1_HUMAN	-6.71	2.74E-03	8.94E-01	PGRP1_HUMAN	Peptidoglycan recognition protein 1	PGRP1_HUMAN	-7.96	1.42E-03	7.91E-01
PLEC_HUMAN	Plectin	PLEC_HUMAN;E9PMV1_HUMAN	7.73	1.19E-01	3.86E+01	PLEC_HUMAN	Plectin	PLEC_HUMAN;E9PMV1_HUMAN;E9PKG0_HUMAN	-4.15	4.67E-02	2.59E+01
PLSI_HUMAN	Plastin-1	PLSI_HUMAN	-4.72	1.58E-05	5.14E-03	PLSI_HUMAN	Plastin-1	PLSI_HUMAN	-2.95	1.49E-02	8.27E+00
PLSL_HUMAN	Plastin-2	PLSL_HUMAN;Q5TBN3_HUMAN;B4DUA0_HUMAN;Q5TBN5_HUMAN;PLST_HUMAN;B4DGB4_HUMAN;B7Z6M1_HUMAN;F8W8D8_HUMAN;B4DI60_HUMAN;H7C4N2_HUMAN	-5.32	2.00E-05	6.52E-03	PLSL_HUMAN	Plastin-2	PLSL_HUMAN;PLST_HUMAN;B4DGB4_HUMAN;B7Z6M1_HUMAN;F8W8D8_HUMAN;Q5TBN3_HUMAN;B4DUA0_HUMAN;Q5TBN5_HUMAN;B4DI60_HUMAN;H7C4N2_HUMAN	-3.29	2.63E-02	1.46E+01
PNPH_HUMAN	Purine nucleoside phosphorylase	PNPH_HUMAN;G3V5M2_HUMAN;G3V2H3_HUMAN;G3V308_HUMAN;G3V393_HUMAN	-4.73	1.23E-04	4.00E-02	PNPH_HUMAN	Purine nucleoside phosphorylase	PNPH_HUMAN;G3V5M2_HUMAN;G3V2H3_HUMAN;G3V393_HUMAN;G3V308_HUMAN	-2.81	1.67E-02	9.28E+00

PPIA_HUMAN	Peptidyl-prolyl cis-trans isomerase A	PAL4A_HUMAN;PPIA_HUMAN;F8WE65_HUMAN;C9J5S7_HUMAN;Q567Q0_HUMAN;E5RIZ5_HUMAN;PAL4D_HUMAN;PAL4G_HUMAN;PPID_HUMAN;PPIF_HUMAN;PPIH_HUMAN;RBP2_HUMAN;Q2YDB7_HUMAN;A6NM32_HUMAN;E9PGT0_HUMAN;C9JQD4_HUMAN;H0Y548_HUMAN	-4.36	1.94E-05	6.32E-03	PPIA_HUMAN	Peptidyl-prolyl cis-trans isomerase A	PPIA_HUMAN;Q567Q0_HUMAN;F8WE65_HUMAN;C9J5S7_HUMAN;PAL4A_HUMAN;PAL4D_HUMAN;PAL4G_HUMAN;E5RIZ5_HUMAN	-2.14	4.78E-03	2.65E+00
PPIB_HUMAN	Peptidyl-prolyl cis-trans isomerase B	PPIB_HUMAN	-2.68	8.74E-02	2.85E+01	PPIB_HUMAN	Peptidyl-prolyl cis-trans isomerase B	PPIB_HUMAN	-3.39	2.31E-02	1.28E+01
PRDX2_HUMAN	Peroxiredoxin-2	PRDX2_HUMAN;A6NIW5_HUMAN	-1.39	3.66E-02	1.19E+01	PRDX2_HUMAN	Peroxiredoxin-2	PRDX2_HUMAN;A6NIW5_HUMAN	-0.90	4.61E-01	2.56E+02
PRDX6_HUMAN	Peroxiredoxin-6	PRDX6_HUMAN	-3.59	1.00E-03	3.26E-01	PRDX6_HUMAN	Peroxiredoxin-6	PRDX6_HUMAN	-1.39	1.45E-01	8.03E+01
PROF1_HUMAN	Profilin-1	PROF1_HUMAN;K7EJ44_HUMAN;J3L3D5_HUMAN;PROF2_HUMAN;C9JQJ7_HUMAN;G5E9Q6_HUMAN;C9J712_HUMAN;C9J2N0_HUMAN;C9JQ45_HUMAN	-5.05	1.44E-03	4.68E-01	PROF1_HUMAN	Profilin-1	PROF1_HUMAN;K7EJ44_HUMAN;J3L3D5_HUMAN;PROF2_HUMAN;C9JQJ7_HUMAN;G5E9Q6_HUMAN;C9J712_HUMAN;C9J2N0_HUMAN;C9JQ45_HUMAN	-3.18	1.35E-02	7.47E+00
PRTN3_HUMAN	Myeloblastin	PRTN3_HUMAN	-3.19	3.64E-04	1.19E-01	PRTN3_HUMAN	Myeloblastin	PRTN3_HUMAN	-3.58	2.66E-03	1.48E+00
PSA1_HUMAN	Proteasome subunit alpha type-1	PSA1_HUMAN;B4DEV8_HUMAN;F5GX11_HUMAN	-3.22	1.42E-03	4.62E-01	PSA1_HUMAN	Proteasome subunit alpha type-1	PSA1_HUMAN;F5GX11_HUMAN;B4DEV8_HUMAN	-2.06	4.83E-02	2.68E+01
PSA2_HUMAN	Proteasome subunit alpha type-2	PSA2_HUMAN;C9JCK5_HUMAN;Q6MZI6_HUMAN;H3BT36_HUMAN;H7C402_HUMAN	-3.64	1.71E-02	5.57E+00	PSA2_HUMAN	Proteasome subunit alpha type-2	PSA2_HUMAN;H3BT36_HUMAN;H7C402_HUMAN;C9JCK5_HUMAN;Q6MZI6_HUMAN	-1.80	5.06E-02	2.81E+01
PSA3_HUMAN	Proteasome subunit alpha type-3	PSA3_HUMAN;G3V5N4_HUMAN;G3V3W4_HUMAN	-2.09	2.16E-03	7.03E-01	PSA3_HUMAN	Proteasome subunit alpha type-3	PSA3_HUMAN;G3V4X5_HUMAN;G3V5N4_HUMAN;G3V3W4_HUMAN;H0YJO3_HUMAN	-1.99	7.95E-02	4.41E+01
PSA5_HUMAN	Proteasome subunit alpha type-5	PSA5_HUMAN	-3.46	1.56E-03	5.10E-01	PSA5_HUMAN	Proteasome subunit alpha type-5	PSA5_HUMAN	-3.23	2.39E-02	1.33E+01
PSA7_HUMAN	Proteasome subunit alpha type-7	PSA7_HUMAN;H0Y586_HUMAN;PSA7L_HUMAN;Q5JXJ2_HUMAN;F5GY34_HUMAN	-6.13	8.75E-04	2.85E-01	PSA7_HUMAN	Proteasome subunit alpha type-7	PSA7_HUMAN;H0Y586_HUMAN;Q5JXJ2_HUMAN;PSA7L_HUMAN;F5GY34_HUMAN	-2.22	1.03E-01	5.69E+01
PSB10_HUMAN	Proteasome subunit beta type-10	PSB10_HUMAN;J3QQN1_HUMAN;J3QL48_HUMAN	1.49	5.71E-02	1.86E+01	PSB10_HUMAN	Proteasome subunit beta type-10	PSB10_HUMAN;J3QQN1_HUMAN	-1.79	2.31E-01	1.28E+02
PSB2_HUMAN	Proteasome subunit beta type-2	PSB2_HUMAN	-2.39	1.30E-02	4.25E+00	PSB2_HUMAN	Proteasome subunit beta type-2	PSB2_HUMAN	-1.86	3.95E-01	2.19E+02
PSB4_HUMAN	Proteasome subunit beta type-4	PSB4_HUMAN	-3.97	1.76E-04	5.73E-02	PSB4_HUMAN	Proteasome subunit beta type-4	PSB4_HUMAN	-1.72	3.43E-02	1.90E+01
PSB6_HUMAN	Proteasome subunit beta type-6	PSB6_HUMAN;I3L3X7_HUMAN	-2.68	1.88E-03	6.12E-01	PSB6_HUMAN	Proteasome subunit beta type-6	PSB6_HUMAN;I3L3X7_HUMAN	-1.98	1.85E-02	1.03E+01
PSB8_HUMAN	Proteasome subunit beta type-8	PSB8_HUMAN;Q5JNW7_HUMAN;B0UZC1_HUMAN	-1.38	2.93E-02	9.54E+00	PSB8_HUMAN	Proteasome subunit beta type-8	PSB8_HUMAN;Q5JNW7_HUMAN;B0UZC1_HUMAN	-2.15	1.31E-01	7.26E+01
PSME1_HUMAN	Proteasome activator complex subunit 1	PSME1_HUMAN;A6NJG9_HUMAN;H0YNE3_HUMAN;H0YLU2_HUMAN;H0YKK6_HUMAN	-3.79	1.81E-02	5.89E+00	H0YNE3_HUMAN	Proteasome activator complex subunit 1	PSME1_HUMAN;A6NJG9_HUMAN;H0YNE3_HUMAN;H0YLU2_HUMAN;H0YKK6_HUMAN	-2.07	7.25E-02	4.02E+01
PTN6_HUMAN	Tyrosine-protein phosphatase non-receptor type 6	PTN6_HUMAN;F5GY79_HUMAN;F5H0N8_HUMAN;F5H5H9_HUMAN;F5GZM7_HUMAN;F5H1Z8_HUMAN	-3.34	1.43E-02	4.66E+00	PTN6_HUMAN	Tyrosine-protein phosphatase non-receptor type 6	PTN6_HUMAN;F5GY79_HUMAN;F5H0N8_HUMAN;F5GZM7_HUMAN;F5H1Z8_HUMAN;F5H1V7_HUMAN;F5GXD4_HUMAN;F5H4Z1_HUMAN;F5H5H9_HUMAN;PTN11_HUMAN	-3.51	1.52E-03	8.45E-01
PTX3_HUMAN	Pentraxin-related protein PTX3	PTX3_HUMAN	-4.64	6.70E-03	2.18E+00	PTX3_HUMAN	Pentraxin-related protein PTX3	PTX3_HUMAN	-4.65	1.69E-02	9.36E+00
PURA2_HUMAN	Adenylosuccinate synthetase isozyme 2	PURA2_HUMAN	-5.12	8.24E-03	2.69E+00	PURA2_HUMAN	Adenylosuccinate synthetase isozyme 2	PURA2_HUMAN;PURA1_HUMAN;G3V2N1_HUMAN;G3V232_HUMAN;G3V5D8_HUMAN	-4.74	7.06E-03	3.92E+00
PYGL_HUMAN	Glycogen phosphorylase, liver form	PYGL_HUMAN;E9PK47_HUMAN;E9PMM6_HUMAN;PYGB_HUMAN;PYGM_HUMAN;H0Y4Z6_HUMAN	-4.7	1.60E-05	5.23E-03	PYGL_HUMAN	Glycogen phosphorylase, liver form	PYGL_HUMAN;E9PK47_HUMAN;E9PMM6_HUMAN;PYGM_HUMAN;REVERSED_ADIP_HUMAN;REVERSED_J3KR02_HUMAN	-4.12	1.35E-02	7.49E+00
						PYGB_HUMAN	Glycogen phosphorylase, brain form	PYGB_HUMAN;H0Y4Z6_HUMAN	-0.16	5.30E-01	2.94E+02
Q5T123_HUMAN	SH3 domain-binding glutamic acid-rich-like protein 3	SH3L3_HUMAN;Q5T123_HUMAN	-3.35	6.24E-04	2.03E-01	Q5T123_HUMAN	SH3 domain-binding glutamic acid-rich-like protein 3	SH3L3_HUMAN;Q5T123_HUMAN	-2.06	1.82E-01	1.01E+02
Q5T6W1_HUMAN	Heterogeneous nuclear ribonucleoprotein K	HNRPK_HUMAN;Q5T6W2_HUMAN;Q5T6W5_HUMAN;Q5T6W1_HUMAN	-0.43	8.44E-01	2.75E+02	Q5T6W5_HUMAN	Heterogeneous nuclear ribonucleoprotein K	HNRPK_HUMAN;Q5T6W2_HUMAN;Q5T6W5_HUMAN;Q5T6W1_HUMAN	2.24	4.72E-02	2.62E+01
Q5TA02_HUMAN	Glutathione S-transferase omega-1 (Fragment)	GSTO1_HUMAN;Q5TA02_HUMAN;Q5TA01_HUMAN	-3.75	1.66E-03	5.40E-01	Q5TA02_HUMAN	Glutathione S-transferase omega-1 (Fragment)	GSTO1_HUMAN;Q5TA02_HUMAN;Q5TA01_HUMAN	-2.86	7.96E-02	4.42E+01
Q5VU66_HUMAN	Tropomyosin alpha-3 chain	Q5VU59_HUMAN;Q5VU63_HUMAN;J3KN67_HUMAN;Q5VU61_HUMAN;Q5VU66_HUMAN;Q5VU58_HUMAN;Q5VU72_HUMAN;D6RFM2_HUMAN;D6R904_HUMAN;TPM3_HUMAN;TPM1_HUMAN;TPM2_HUMAN;TPM4_HUMAN;B7Z596_HUMAN;Q6ZN40_HUMAN;D9YZV2_HUMAN;H7BYY1_HUMAN;D9YZV8_HUMAN;D9YZV3_HUMAN;Q5TCU8_HUMAN;H0YNC7_HUMAN;Q5TCU3_HUMAN;F5H7S3_HUMAN;H0YK48_HUMAN;H0YL80_HUMAN;H0YL52_HUMAN;H0YKP3_HUMAN;H0YKX5_HUMAN;K7ENT6_HUMAN;K7ERG3_HUMAN;K7EP68_HUMAN	-0.97	7.49E-01	2.44E+02	Q5VU59_HUMAN	Tropomyosin alpha-3 chain	Q5VU59_HUMAN;Q5VU58_HUMAN;Q5VU72_HUMAN;D6RFM2_HUMAN;D6R904_HUMAN;Q5VU61_HUMAN;Q5VU66_HUMAN	-0.22	3.92E-01	2.18E+02
QSOX1_HUMAN	Sulfhydryl oxidase 1	QSOX1_HUMAN;A8MXT8_HUMAN	-3.02	2.22E-03	7.24E-01	QSOX1_HUMAN	Sulfhydryl oxidase 1	QSOX1_HUMAN;A8MXT8_HUMAN	-4.94	2.50E-03	1.39E+00
RAB5C_HUMAN	Ras-related protein Rab-5C	RAB5C_HUMAN;K7ERI8_HUMAN;K7ENY4_HUMAN;K7ERQ8_HUMAN	-3.89	6.24E-03	2.04E+00	RAB5C_HUMAN	Ras-related protein Rab-5C	RAB5C_HUMAN;K7EIP6_HUMAN;K7ERI8_HUMAN;K7ENY4_HUMAN;K7ERQ8_HUMAN	-3.21	4.99E-02	2.77E+01
RAC2_HUMAN	Ras-related C3 botulinum toxin substrate 2	RAC2_HUMAN;B1AH80_HUMAN;B1AH77_HUMAN;B1AH78_HUMAN;RAC1_HUMAN;RAC3_HUMAN;J3KSC4_HUMAN;J3QLK0_HUMAN	-0.05	5.36E-01	1.75E+02	RAC2_HUMAN	Ras-related C3 botulinum toxin substrate 2	RAC2_HUMAN;B1AH80_HUMAN;B1AH78_HUMAN;B1AH77_HUMAN	-1.13	2.99E-01	1.66E+02
RAP1B_HUMAN	Ras-related protein Rap-1b	RAP1A_HUMAN;RAP1B_HUMAN;F5GYH7_HUMAN;F5H077_HUMAN;F5H500_HUMAN;F5H004_HUMAN;F5H491_HUMAN;F5GWU8_HUMAN;F8WBC0_HUMAN;F5GX62_HUMAN;F5H0B7_HUMAN;F5H7Y6_HUMAN;F5H6R7_HUMAN;F5GYB5_HUMAN;F5H4H0_HUMAN;E7ESV4_HUMAN;RP1BL_HUMAN;B7ZB78_HUMAN;F5GZG1_HUMAN;F5H823_HUMAN	-0.57	1.92E-01	6.26E+01	RAP1B_HUMAN	Ras-related protein Rap-1b	RAP1A_HUMAN;RAP1B_HUMAN;RP1BL_HUMAN;B7ZB78_HUMAN;F5GZG1_HUMAN;F5H823_HUMAN;F5GX62_HUMAN;F5H7Y6_HUMAN;E7ESV4_HUMAN;F5GYH7_HUMAN;F5H077_HUMAN;F5H500_HUMAN;F5H004_HUMAN;F5H491_HUMAN;F5GWU8_HUMAN;F8WBC0_HUMAN;F5H0B7_HUMAN;F5H6R7_HUMAN;F5GYB5_HUMAN;F5H4H0_HUMAN	-0.58	5.80E-01	3.22E+02
RETN_HUMAN	Resistin	RETN_HUMAN;Q76B53_HUMAN	-4.36	5.56E-05	1.81E-02	RETN_HUMAN	Resistin	RETN_HUMAN;Q76B53_HUMAN	-6.21	2.33E-02	1.30E+01
RHG01_HUMAN	Rho GTPase-activating protein 1	RHG01_HUMAN;H0YE29_HUMAN;E9PNR6_HUMAN	-5.30	5.22E-03	1.70E+00	RHG01_HUMAN	Rho GTPase-activating protein 1	RHG01_HUMAN;H0YE29_HUMAN;E9PNR6_HUMAN	-1.27	4.76E-01	2.64E+02
RHG30_HUMAN	Rho GTPase-activating protein 30	RHG30_HUMAN;E9PLT5_HUMAN;RHG32_HUMAN;RHG33_HUMAN;G3V174_HUMAN;A1A5D2_HUMAN;K7EQI6_HUMAN;K7EMC2_HUMAN	-3.75	1.17E-02	3.83E+00	RHG30_HUMAN	Rho GTPase-activating protein 30	RHG30_HUMAN;E9PLT5_HUMAN	-3.30	6.43E-02	3.57E+01
RHOA_HUMAN	Transforming protein RhoA	RHOA_HUMAN;RHOC_HUMAN;Q5JR07_HUMAN;C9JX21_HUMAN;Q5JR08_HUMAN;E9PN11_HUMAN;Q5JR05_HUMAN;C9JNR4_HUMAN;E9PQH6_HUMAN;RHOB_HUMAN;E9PLA2_HUMAN;C9J1T2_HUMAN;Q5JR06_HUMAN;C9JRM1_HUMAN	-1.34	5.32E-03	1.74E+00	RHOA_HUMAN	Transforming protein RhoA	RHOA_HUMAN;RHOC_HUMAN;E9PLA2_HUMAN;Q5JR07_HUMAN;C9JX21_HUMAN;C9J1T2_HUMAN;Q5JR08_HUMAN;E9PN11_HUMAN;Q5JR06_HUMAN;Q5JR05_HUMAN;C9JNR4_HUMAN;C9JRM1_HUMAN;E9PQH6_HUMAN	0.35	2.68E-01	1.49E+02
RINI_HUMAN	Ribonuclease inhibitor	RINI_HUMAN;E9PMJ3_HUMAN;E9PIK5_HUMAN;E9PMA9_HUMAN;E9PIM9_HUMAN;E9PLZ3_HUMAN;E9PMN0_HUMAN;H0YCR7_HUMAN	-4.25	4.77E-04	1.55E-01	RINI_HUMAN	Ribonuclease inhibitor	RINI_HUMAN;E9PMJ3_HUMAN;E9PIK5_HUMAN;E9PMA9_HUMAN;E9PIM9_HUMAN;E9PLZ3_HUMAN;E9PMN0_HUMAN;H0YCR7_HUMAN	-3.71	1.73E-02	9.58E+00
RNAS2_HUMAN	Non-secretory ribonuclease	RNAS2_HUMAN	0.41	3.65E-01	1.19E+02	RNAS2_HUMAN	Non-secretory ribonuclease	RNAS2_HUMAN	1.85	6.24E-02	3.46E+01
ROA2_HUMAN	Heterogeneous nuclear ribonucleoproteins A2/B1	ROA2_HUMAN	-5.24	1.01E-04	3.28E-02	ROA2_HUMAN	Heterogeneous nuclear ribonucleoproteins A2/B1	ROA2_HUMAN	-2.41	6.66E-02	3.70E+01
RPIA_HUMAN	Ribose-5-phosphate isomerase	RPIA_HUMAN	-3.85	1.02E-03	3.33E-01	RPIA_HUMAN	Ribose-5-phosphate isomerase	RPIA_HUMAN	-3.44	2.94E-02	1.63E+01
RSU1_HUMAN	Ras suppressor protein 1	RSU1_HUMAN;F2Z2H2_HUMAN	-4.40	5.98E-04	1.95E-01	RSU1_HUMAN	Ras suppressor protein 1	RSU1_HUMAN;F2Z2H2_HUMAN	-3.65	1.61E-01	8.93E+01
S100P_HUMAN	Protein S100-P	S100P_HUMAN	-3.93	2.63E-04	8.59E-02	S100P_HUMAN	Protein S100-P	S100P_HUMAN	-4.94	2.95E-02	1.64E+01
S10A4_HUMAN	Protein S100-A4	S10A4_HUMAN	-4.72	8.62E-03	2.81E+00	S10A4_HUMAN	Protein S100-A4	S10A4_HUMAN	-3.23	2.30E-02	1.27E+01

S10A6_HUMAN	Protein S100-A6	S10A6_HUMAN	-2.26	9.80E-03	3.19E+00	S10A6_HUMAN	Protein S100-A6	S10A6_HUMAN	-3.56	5.89E-02	3.27E+01
S10A8_HUMAN	Protein S100-A8	S10A8_HUMAN	-3.40	5.02E-04	1.64E-01	S10A8_HUMAN	Protein S100-A8	S10A8_HUMAN	-3.91	1.22E-01	6.78E+01
S10A9_HUMAN	Protein S100-A9	S10A9_HUMAN	-4.92	9.81E-05	3.20E-02	S10A9_HUMAN	Protein S100-A9	S10A9_HUMAN	-2.62	2.06E-01	1.14E+02
S10AB_HUMAN	Protein S100-A11	S10AB_HUMAN	-4.12	9.32E-03	3.04E+00	S10AB_HUMAN	Protein S100-A11	S10AB_HUMAN	-3.29	1.54E-01	8.55E+01
S10AC_HUMAN	Protein S100-A12	S10AC_HUMAN	-3.38	8.17E-05	2.66E-02	S10AC_HUMAN	Protein S100-A12	S10AC_HUMAN	-2.13	2.79E-01	1.55E+02
SAHH_HUMAN	Adenosylhomocysteinase	SAHH_HUMAN	-5.09	3.56E-04	1.16E-01	SAHH_HUMAN	Adenosylhomocysteinase	SAHH_HUMAN	-2.97	4.12E-03	2.29E+00
SH3L1_HUMAN	SH3 domain-binding glutamic acid-rich-like protein	SH3L1_HUMAN	-4.40	2.62E-04	8.53E-02	SH3L1_HUMAN	SH3 domain-binding glutamic acid-rich-like protein	SH3L1_HUMAN	-1.50	1.99E-01	1.10E+02
SODC_HUMAN	Superoxide dismutase [Cu-Zn]	SODC_HUMAN;H7BYH4_HUMAN	-2.08	1.26E-02	4.10E+00	SODC_HUMAN	Superoxide dismutase [Cu-Zn]	SODC_HUMAN;H7BYH4_HUMAN	-2.95	6.31E-02	3.50E+01
SPB10_HUMAN	Serpin B10	SPB10_HUMAN;H7BYS2_HUMAN;H7C004_HUMAN	-4.73	2.58E-04	8.40E-02	SPB10_HUMAN	Serpin B10	SPB10_HUMAN	-5.28	1.06E-02	5.86E+00
SPB6_HUMAN	Serpin B6	SPB6_HUMAN;H0Y3G3_HUMAN	-4.24	2.05E-04	6.68E-02	SPB6_HUMAN	Serpin B6	SPB6_HUMAN;H0Y3G3_HUMAN	-4.42	5.04E-03	2.80E+00
SPTB2_HUMAN	Spectrin beta chain, non-erythrocytic 1	SPTB2_HUMAN;F8W6C1_HUMAN	-3.79	6.12E-03	2.00E+00	SPTB2_HUMAN	Spectrin beta chain, non-erythrocytic 1	SPTB2_HUMAN;F8W6C1_HUMAN;SPTN2_HUMAN	-3.76	2.64E-02	1.47E+01
SYWC_HUMAN	Tryptophan--tRNA ligase, cytoplasmic	SYWC_HUMAN;H0YJP3_HUMAN;G3V3H8_HUMAN;G3V3Y5_HUMAN;G3V3P2_HUMAN;G3V456_HUMAN;G3V227_HUMAN;G3V3X0_HUMAN;G3V5U1_HUMAN;G3V423_HUMAN;G3V277_HUMAN;G3V2Y7_HUMAN	-4.39	1.97E-05	6.43E-03	SYWC_HUMAN	Tryptophan--tRNA ligase, cytoplasmic	SYWC_HUMAN;H0YJP3_HUMAN;G3V3P2_HUMAN;G3V456_HUMAN;G3V227_HUMAN;G3V5U1_HUMAN;G3V423_HUMAN;G3V277_HUMAN;G3V3H8_HUMAN;G3V2Y7_HUMAN;G3V3Y5_HUMAN;G3V3X0_HUMAN;G3V3S7_HUMAN;G3V5W1_HUMAN	-3.76	9.08E-03	5.04E+00
TAGL2_HUMAN	Transgelin-2	TAGL2_HUMAN	-5.33	3.97E-04	1.29E-01	TAGL2_HUMAN	Transgelin-2	TAGL2_HUMAN	-3.78	2.30E-01	1.28E+02
TALDO_HUMAN	Transaldolase	TALDO_HUMAN;F2Z393_HUMAN;E9PKI8_HUMAN;E9PM01_HUMAN	-3.65	2.85E-04	9.29E-02	TALDO_HUMAN	Transaldolase	TALDO_HUMAN;F2Z393_HUMAN;E9PKI8_HUMAN;E9PM01_HUMAN	-3.30	6.24E-02	3.46E+01
TERA_HUMAN	Transitional endoplasmic reticulum ATPase	TERA_HUMAN;C9JUP7_HUMAN;C9IZA5_HUMAN	-3.10	1.11E-02	3.63E+00	TERA_HUMAN	Transitional endoplasmic reticulum ATPase	TERA_HUMAN;C9JUP7_HUMAN;C9IZA5_HUMAN	-2.30	1.93E-02	1.07E+01
THIO_HUMAN	Thioredoxin	THIO_HUMAN	-6.16	3.72E-03	1.21E+00	THIO_HUMAN	Thioredoxin	THIO_HUMAN	-2.79	5.94E-03	3.30E+00
TKT_HUMAN	Transketolase	TKT_HUMAN;B4E022_HUMAN;F8W888_HUMAN;E9PFF2_HUMAN;F8WAX4_HUMAN	-4.45	1.64E-05	5.35E-03	TKT_HUMAN	Transketolase	TKT_HUMAN;B4E022_HUMAN;E9PFF2_HUMAN;F8W888_HUMAN;TKTL1_HUMAN;Q5TYJ8_HUMAN;F8WAX4_HUMAN	-2.43	9.44E-03	5.24E+00
TLN1_HUMAN	Talin-1	TLN1_HUMAN;Q5TCU6_HUMAN;TLN2_HUMAN;H0YMT1_HUMAN	-4.19	2.04E-03	6.65E-01	TLN1_HUMAN	Talin-1	TLN1_HUMAN;Q5TCU6_HUMAN;TLN2_HUMAN;H0YMT1_HUMAN	-3.06	4.19E-02	2.32E+01
TPIS_HUMAN	Triosephosphate isomerase	TPIS_HUMAN	-4.01	8.38E-05	2.73E-02	TPIS_HUMAN	Triosephosphate isomerase	TPIS_HUMAN	-2.65	2.02E-02	1.12E+01
TRFL_HUMAN	Lactotransferrin	TRFL_HUMAN;E7EQB2_HUMAN;E7ER44_HUMAN;C9J0S5_HUMAN;C9JCF5_HUMAN	0.28	2.29E-01	7.46E+01	TRFL_HUMAN	Lactotransferrin	TRFL_HUMAN;E7EQB2_HUMAN;C9J0S5_HUMAN;C9JCF5_HUMAN;E7ER44_HUMAN	-0.03	4.29E-01	2.38E+02
TYB4_HUMAN	Thymosin beta-4	TYB4_HUMAN;Q5T4B6_HUMAN	-3.28	5.34E-01	1.74E+02	TYB4_HUMAN	Thymosin beta-4	TYB4_HUMAN;Q5T4B6_HUMAN	-3.63	6.63E-01	3.68E+02
TYPH_HUMAN	Thymidine phosphorylase	TYPH_HUMAN;C9JGI3_HUMAN	-2.29	1.50E-02	4.90E+00	C9JGI3_HUMAN	Thymidine phosphorylase (Fragment)	TYPH_HUMAN;C9JGI3_HUMAN	-2.08	7.75E-02	4.30E+01
UBA1_HUMAN	Ubiquitin-like modifier-activating enzyme 1	UBA1_HUMAN	-1.58	2.51E-02	8.19E+00	UBA1_HUMAN	Ubiquitin-like modifier-activating enzyme 1	UBA1_HUMAN;Q5JRR6_HUMAN;Q5JRS0_HUMAN;Q5JRS1_HUMAN;Q5JRS2_HUMAN;Q5JRR9_HUMAN;Q5JRS3_HUMAN	-1.31	9.17E-02	5.09E+01
UBE2N_HUMAN	Ubiquitin-conjugating enzyme E2 N	UBE2N_HUMAN;F8VZ29_HUMAN;F8VSD4_HUMAN;F8VV71_HUMAN;UE2NL_HUMAN;F8VQQ8_HUMAN	-4.68	9.52E-03	3.10E+00	UBE2N_HUMAN	Ubiquitin-conjugating enzyme E2 N	UBE2N_HUMAN;F8VQQ8_HUMAN;F8VSD4_HUMAN;F8VV71_HUMAN;UE2NL_HUMAN;F8VZ29_HUMAN	-2.75	4.28E-03	2.37E+00
URP2_HUMAN	Fermitin family homolog 3	URP2_HUMAN;F5H1C6_HUMAN;H0YFT5_HUMAN	-2.92	1.90E-03	6.21E-01	URP2_HUMAN	Fermitin family homolog 3	URP2_HUMAN;F5H1C6_HUMAN;F5H3I6_HUMAN;H0YFT5_HUMAN	-0.75	3.92E-01	2.18E+02
VASP_HUMAN	Vasodilator-stimulated phosphoprotein	VASP_HUMAN;K7EM16_HUMAN;K7EQD0_HUMAN	-2.98	1.10E-02	3.59E+00	VASP_HUMAN	Vasodilator-stimulated phosphoprotein	VASP_HUMAN;K7EM16_HUMAN;K7EQD0_HUMAN;K7ENL7_HUMAN;K7ENR7_HUMAN;K7EIG8_HUMAN	-2.61	2.26E-02	1.25E+01
VAT1_HUMAN	Synaptic vesicle membrane protein VAT-1 homolog	VAT1_HUMAN;B0AZP7_HUMAN;B4DPX4_HUMAN;K7ESA3_HUMAN;K7EM19_HUMAN;K7ENX2_HUMAN;K7ERT7_HUMAN	-3.48	3.92E-02	1.28E+01	VAT1_HUMAN	Synaptic vesicle membrane protein VAT-1 homolog	VAT1_HUMAN;B0AZP7_HUMAN;B4DPX4_HUMAN;K7ESA3_HUMAN;K7ERT7_HUMAN;K7EM19_HUMAN;K7ENX2_HUMAN;SC31B_HUMAN;K7EJM4_HUMAN;K7ER81_HUMAN	-2.32	3.57E-02	1.98E+01
VINC_HUMAN	Vinculin	VINC_HUMAN;Q5JQ13_HUMAN;B4DTM7_HUMAN	-4.49	8.20E-05	2.67E-02	VINC_HUMAN	Vinculin	VINC_HUMAN;B4DTM7_HUMAN;Q5JQ13_HUMAN	-3.89	5.96E-03	3.31E+00
WDR1_HUMAN	WD repeat-containing protein 1	WDR1_HUMAN;D6RD66_HUMAN	-3.63	4.42E-05	1.44E-02	WDR1_HUMAN	WD repeat-containing protein 1	WDR1_HUMAN;D6RD66_HUMAN	-3.41	6.24E-03	3.46E+00
XRCC5_HUMAN	X-ray repair cross-complementing protein 5	XRCC5_HUMAN	-2.50	8.43E-02	2.75E+01	XRCC5_HUMAN	X-ray repair cross-complementing protein 5	XRCC5_HUMAN	1.87	9.32E-02	5.17E+01

Table 8-5 Quantitative comparison of protein levels in SN and D (DNase-I treated NET fraction) fraction

Samples from 4 donors (on the left) were acquired using LTQ Orbitrap Velos ETD and samples from 3 donors (on the right) using Q Exactive MS. The data was subsequently quantified in separate analyses.